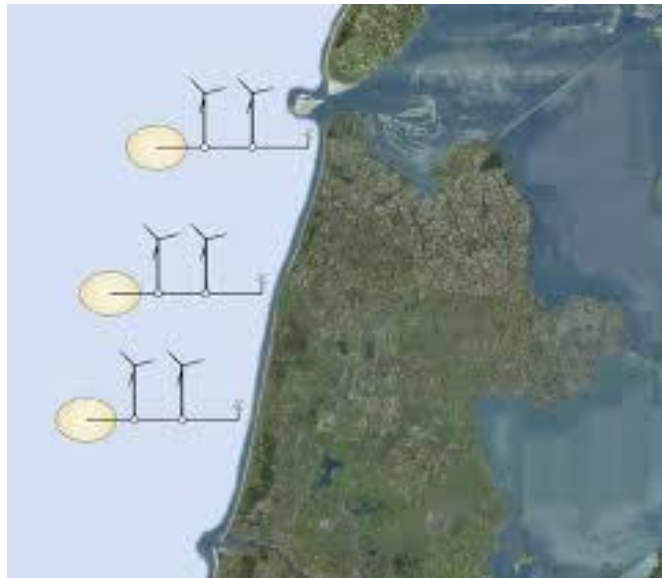


THE EFFECTS OF A CONTINUOUS NOURISHMENT ON THE PHYSICAL BEHAVIOR OF THE DUTCH COASTLINE

*Studying the behavior of a continuous nourishment at the
Delfland coastal stretch in the first year of its lifetime*



MARNIX P VAN HUGTEN

MSC THESIS REPORT

September 18th 2019

The effects of a continuous nourishment on the physical behavior of the Dutch coastline

Studying the behavior of a continuous nourishment at the Delfland coastal stretch in
the first year of its lifetime

By

M.P. van Hugten

In partial fulfilment of the requirements for attaining the degree of

Master of Science in Civil Engineering

At Delft University of Technology

September 18th, 2019

Thesis Committee

Prof. Dr. Ir. S.G.J. Aarninkhof (chairman) TU Delft

Ir. J. Kollen

Sweco NL

Ir. A.P. Luijendijk

TU Delft

Dr. J.E.A. Storms

TU Delft

Dr. S.E. Vos

TU Delft



Summary

The conventional methods of nourishing the Dutch coast are no longer justified as a consequence of the growing awareness of climate change. Therefore a sustainable concept has been developed, in which the process of applying nourishments, by dredging vessels, is replaced by the combination of wind mills at sea and pipelines to the shoreline. Energy is being generated by these wind mills, which drive pumps to transport sediment in suspension from deep sea towards the nearshore zone through pipelines. This method is CO₂-neutral as toxic gases are not exhausted.

An unknown element of this concept is the physical behavior of the nourishment after it is disposed in the nearshore zone. It is questioned whether sediment from this nourishment is able to be redistributed in alongshore direction in a relatively short time since it is not an instantaneous nourishment, but a continuous nourishment. A continuous nourishment is characterized by the principle that sediment is supplied at every moment in time, with a constant mixed sediment-water discharge. If sediment cannot be transported from the nourishment location, extensive accumulation will occur. Therefore the research question is stated:

How does a continuous nourishment along the southern Holland coast develop in the nearshore zone in the first year of its lifetime?

The research question is supported by a set of research elements that are answered. These elements focus on the optimization of this type of nourishment. First the optimal depth to supply a continuous nourishment is investigated. Second, the discharge limit is approached. At last, research to application of the nourishment volume over multiple disposal locations close to each other is performed to gain insight in options to enhance longshore sediment transport.

To answer the research question and the supporting questions, the numerical modelling tool Delft3d has been used. The model that was used to hindcast five years of the Zandmotor at the Delfland coastal stretch, has been applied, including its input settings. With the help of the built-in function 'Discharges', a continuous nourishment has been simulated. This setting has been performed in 7 different configurations, including a reference configuration without nourishments. The standard annual nourishment volume is set to 100'000 m³. The range of depths for this research is set between MSL -3.0 m and MSL -6.0 m.

The configurations have brought insight in the optimization of applying continuous nourishments at the Delfland coastal stretch. The differences in longshore sediment redistribution are significantly large for different depths of nourishing in the range of MSL -3.0 m to MSL -6.0 m. From the reference configuration, a sediment transport belt has been observed between MSL -1.0 and MSL -4.0 m, with significantly large transport magnitudes compared to other depths. Disposing sediment at this range of depths will lead to an enhanced redistribution of sediment. The second part focuses on the maximization of the discharge volume. This is set to 150'000 m³/year at MSL -3.0 m, but provides undesired effects, such as exceedance of the bed level to above Mean Low Water for a large period of time. The bed level of the continuous nourishment may not exceed the Mean Low Water for

Summary

a larger period of time as this requires increased wave forcing to erode sediment. Absence of erosion might eventually lead to the formation of small islands in front of the shoreline, which is not desired for recreational and navigational purposes. The third part focuses on spreading of the disposal locations to enhance sediment redistribution. The annual nourishment volume is then equally divided over these locations. This leads to an increased longshore sediment redistribution as wave forcing is more effective over a larger area due to increased depth. Therefore the longshore currents remain large as well and sediment is more easily transported.

An input reduction of waves has been applied. The assumption for this reduction is that sediment transport is negligibly small for waves under 1.5 m. This assumption has been considered valid after studying the results, as accretion of the bed level occurs during small wave heights. In real time, these waves still occur, which means that disposal of sediment occurs under small waves. This leads to the case that overaccumulation occurs due to a lack of sediment transport capacity. This risk is compensated by an operational limit in wind forcing of the Zandwindmolen and assumes an operational time of 60% in which wind speed is sufficiently large. Overaccumulation is thus not likely to occur during application of a continuous nourishment.

To conclude the results, the nourishment accretes and erodes continuously as a result of varying wave conditions. The nourishment volume of 100'000 m³/year is able to be redistributed and does not exceed mean water level. The optimal configuration of this type of nourishment is a set of disposal locations near each other at a depth between 3 and 4 m, of which the total annual volume is between 100'000 and 150'000 m³.

There are opportunities to further improve this optimal configuration. This requires, however, additional research to the local small-scale behavior (<10 m) of this type of nourishments. The numerical model used is not completely suitable to investigate the morphodynamic behavior. However, the outcomes are promising and the technical feasibility of this innovative concept is likely to be achieved.

Acknowledgement

This thesis report represents the translation of years of education towards a summary of the knowledge that I have gained to complete this research. With executing this thesis, it has been a challenge to create a logical set of coherent pieces that together form a solution or a basis for further research. But even more, personal development has been the largest fulfilment during this phase.

The thesis has been conducted for the purpose of in-depth research to the technical feasibility of the innovative concept Zandwindmolen, which has been invented by Jan Kollen. Several feasibility studies have already been performed, and in the present phase it is needed to define the concept to a higher level of detail. This research has been contributed in order to reach that higher level of detail.

Without a number of people, this process would have been more difficult to fulfil. First, I would like to thank Jan Kollen for giving me the opportunity to do research for this innovative concept that creates a sustainable alternative for coastline development. This is an essential element in the Netherlands and matches my personal interests. It has been a great experience to learn about the innovation Zandwindmolen and to do research for this concept. Because of Jan, I have been able to look behind the scenes of both Sweco and Rijkswaterstaat, by attending the meetings of the Dutch Coastline Challenge, which have given insight my knowledge of how ideas are transformed to actual plans ready for execution and how inventive you have to be with dozens of stakeholders.

Secondly, I thank Sander Vos for his assistance and his feedback he has given me during the several meetings we have had. His support has given me the right structure to continue in this process.

Furthermore, I thank Arjen Luijendijk for providing me the Delft3d model that I have used for conducting the research part of this thesis, as well as for his effort to give me the required technical support and feedback to properly use the model.

Contents

Summary	i
Acknowledgement	iii
Nomenclature	ix
List of abbreviations.....	ix
List of symbols.....	x
Chapter 1: Introduction	1
1.1 Social background	1
1.2 Problem statement	1
1.2.1 Problem description.....	1
1.2.2 Problem analysis	2
1.2.3 Problem definition	3
1.3 Research goal.....	3
1.4 Research sub-questions	4
1.5 Report structure.....	4
Chapter 2: Analysis.....	5
2.1 Historical context of the Dutch coastline.....	5
2.2 Coastal hydrodynamics.....	7
2.2.1 Tidal forcing.....	7
2.2.2 Wave forcing	7
2.2.3 Relative sea level rise	10
2.2.4 Wind forcing.....	10
2.3 Coastal morphodynamics.....	11
2.3.1 Longshore currents and sediment transport	11
2.3.2 Cross-shore currents and sediment transport.....	12
2.3.3 Sediment demand of the coastal zone	13
2.4 Present situation of the Holland coastline.....	14
2.5 Sustainable nourishments: the Sand Engine.....	15
2.5.1 Development of the project ‘Sand Engine’	15
2.5.2 Comparing the Sand Engine with Zandwindmolen.....	16
2.6 Future predictions of hydrodynamic processes.....	16
2.6.1 Longshore sediment transport by tidal and wave forcing	16

Contents

2.6.2	Relative sea level rise and sediment demand.....	16
2.7	Chapter Summary	18
Chapter 3: Research methodology		21
3.1	Research parts.....	21
3.1.1	Part 1: the optimal location in the cross-shore profile.....	21
3.1.2	Part 2: the optimal discharge at the optimal location	21
3.1.3	Part 3: spreading of disposal locations to enhance sediment redistribution	22
3.2	Research conditions.....	22
3.2.1	Continuous supply of sediment in time	22
3.2.2	Fixed location in the coastal domain	22
3.3	Evaluation criteria	23
3.4	Research tool: Delft3D	24
3.5	Model application	25
3.5.1	Model domain.....	26
3.5.2	Input processes	29
3.5.3	Sediment transport under initial conditions.....	32
3.5.4	Reduction of computational effort	33
3.5.5	Discharges as nourishment input.....	34
3.6	Model simulations	36
3.7	Chapter Summary	37
Chapter 4: Results.....		39
4.1	Defining the optimal depth.....	39
4.1.1	Nourishment at MSL -3.0 m	39
4.1.2	Nourishment at MSL -4.0 m	44
4.1.3	Nourishment at MSL -5.0 m	47
4.1.4	Nourishment at MSL -6.0 m	52
4.1.5	Comparison of 4 nourishment depths	56
4.2	Increase of the annual nourishment volume.....	60
4.2.1	Nourishment of 150'000 m ³ /year at 3 m depth	61
4.2.2	Comparison of discharge variations.....	64
4.3	Spreading of the disposal locations	68
4.3.1	Nourishment spread over 5 cells at 5 m depth.....	68
4.3.2	Comparison of spreading variations	74
4.4	Chapter summary.....	79

Chapter 5: Discussion.....	81
5.1 Discussion.....	81
5.2 Limitations of the numerical model.....	82
Chapter 6: Conclusions & recommendations	83
6.1 Conclusion.....	83
6.2 Recommendations	84
6.2.1 Recommendations for further research	84
6.2.2 Recommendations for Engineering & Consultancy firm Sweco NL	85
Bibliography	87
List of Figures	89
List of Tables	96
List of Terms.....	97
List of Appendices	99
A.1 Grid of FLOW and WAVE domain	100
A.2 Grid of FLOW domain	101
A.3 Initial bathymetry	102
B.1 Calculation of Discharge rate and density as input values	103
B.2 Wave data analysis – Year 1	105
C.1 Reference simulation – Summary.....	108
C.2 Reference situation – Monthly development.....	112
D.1 Nourishment at MSL -3.0 m – Summary	116
D.2 Nourishment at MSL -3.0 m – Monthly development	119
E.1 Nourishment at MSL -4.0 m – Summary.....	123
E.2 Nourishment at MSL -4.0 m – Monthly development	126
F.1 Nourishment at MSL -5.0 m – Summary	130
F.2 Nourishment at MSL -5.0 m – Monthly development	133
G.1 Nourishment at MSL -6.0 m – Summary	137
G.2 Nourishment at MSL -6.0 m – Monthly development	140
H.1 Discharge of 150'000 m ³ /year – Summary.....	144
H.2 Discharge of 150'000 m ³ /year – Monthly development.....	147
I.1 Spread of nourishment over 5 locations – Summary	151
I.2 Spread of nourishment over 5 locations – Monthly development.....	154

Nomenclature

List of abbreviations

Below a list of abbreviations used in this report.

Abbreviation	Meaning	Explanation
2D	Two dimensional	
3D	Three dimensional	
BKL	Basiskustlijn	Dutch reference coastline
CO₂	Carbon dioxide	Emission gas
e.g.	For example	
i.e.	That is	
MSL	Mean sea level	Average water level for all seas and oceans
MLW	Mean Low Water	The water level during low tide
IKZ	Innovatie Kustlijnzorg	Program of Rijkswaterstaat to reduce emission on coastal development
NAP	Normaal Amsterdams Peil	Dutch reference level for water and land

List of symbols

Below a list of symbols used in this report.

Symbol	Meaning	Explanation
%	Percent	
½	One half	
⅔	Two third	
<	Smaller than (less than)	
>	Larger than (more than)	
<i>a</i>	Amplitude (tidal)	Expressed in m
<i>α</i>	Phase (tidal)	Expressed in deg
<i>C</i>	Concentration	Expressed in kg/m ³
<i>C_v</i>	Volumetric concentration	
<i>cm</i>	Centimeter	
<i>deg</i>	degree	
<i>hr</i>	hour	
<i>kg</i>	kilogram	
<i>km</i>	Kilometer	
<i>l</i>	liter	
<i>M</i>	First coordinate of grid cell in Delft3D	
<i>m</i>	Meter	
<i>m²</i>	Square meter	
<i>m³</i>	Cubic meter	
<i>M2</i>	Semi-diurnal tidal constituent forced by the moon	
<i>M_s</i>	Sediment particle mass	Expressed in kg
<i>M_{s,sec}</i>	Sediment particle mass	Expressed in kg
<i>M_w</i>	Water mass	Expressed in kg
<i>N</i>	Second coordinate of grid cell in Delft3D	
<i>η</i>	Tidal elevation	Expressed in m
<i>p</i>	porosity	
<i>ρ_m</i>	Density of mixture	Expressed in kg/m ³
<i>ρ_s</i>	Density of sediment particles	Expressed in kg/m ³
<i>ρ_w</i>	Density of water	Expressed in kg/m ³
<i>Q</i>	Discharge of mixture	Expressed in m ³ /s
<i>Q_{real}</i>	Discharge of mixture	Expressed in m ³ /s
<i>t</i>	Time step	Expressed in
<i>T</i>	Time	Expressed in
<i>V_{s,dry}</i>	In situ sediment volume per year	Expressed in m ³
<i>V_w</i>	Volume of water	Expressed in m ³
<i>ω</i>	Frequency (tidal)	Expressed in deg/hr
<i>X</i>	First coordinate in location	
<i>Y</i>	Second coordinate in location	

Chapter 1: Introduction

The Zandwindmolen is an innovation first introduced by Sweco in 2008. The concept is designed to transport sediment from deeper areas in the North Sea towards the nearshore zone of the Dutch coast, without the use of dredging vessels that produce CO₂. The concept works as follows: windmills drive pumps that dredge sediment from the bottom of the sea and transport this sediment to the coast through pipelines. At a predetermined location in the nearshore zone or at the beach, sediment is disposed (see Figure 1). The volume of sediment is then redistributed in alongshore and cross-shore direction by wave-induced and tide-induced currents. Using this concept, the coastline is maintained and strengthened in a sustainable way. An important mechanism in this innovation is the continuous supply of sediment that is generated because of continuously operating wind mills.

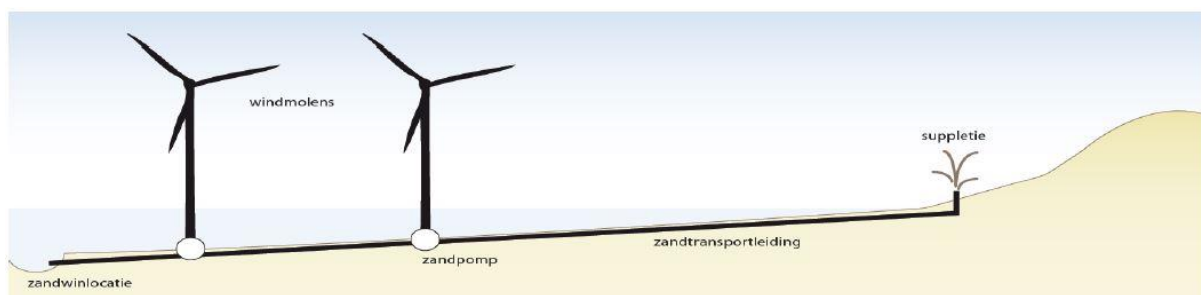


Figure 1 The concept Zandwindmolen as how it works. (Image source: Dekker (2013))

1.1 Social background

The conventional method of supplying sediment at the Dutch coast is by dredging vessels that produce CO₂. The emission of CO₂ is one of the driving mechanisms of climate change. The Dutch government is aware of this social problem and is therefore reconsidering the conventional method, which is done in the Program Innovatie Kustlijn zorg (IKZ; Innovation Coastline Care). The aim of this program is to develop sustainable alternatives for applying nourishments at the Dutch coast where the most important requirement is the reduction of CO₂-emission. The Zandwindmolen fulfils this requirement.

1.2 Problem statement

1.2.1 Problem description

The Zandwindmolen assumes a continuous supply of sediment in time. This differs from the conventional method, where a volume of sediment is placed at one location at once. The Zandwindmolen considers that the amount of sediment is equally being distributed to this location through the time that it takes for the coastal system to redistribute the sediment. The discharge rate of the pipeline is therefore depending on the sediment transport capacity of the coastal stretch.

Chapter 1: Introduction

There are also limits in the application of the concept along the Dutch coastline. The investment costs are considerable, which leads to an economically minimum discharge volume per year. The annual nourishment volume for which the concept is economic feasible, is found between 1 and 2 million m³ of sediment. Only a few parts of the Dutch coastline require this order of volume (Dekker, 2013):

- The 'Kop van Noord-Holland': 1.75 million m³/year
- Texel Island: 2.25 million m³/year
- Marsdiep Inlet: 3.86 million m³/year
- Ameland Island: 1.69 million m³/year

The required annual volumes of sediment represent expected annual volumes when a relative sea level rise of 85 cm is expected in the year 2100. The volumes are much larger than for other coastal stretches. The southern Holland coast, between Hoek van Holland and IJmuiden only requires 0.5 million m³/year (Dekker, 2013).

1.2.2 Problem analysis

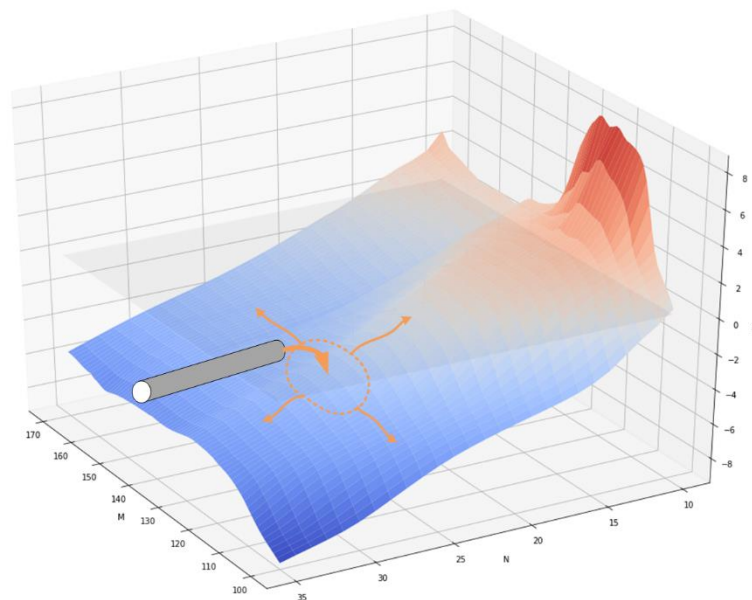


Figure 2 Visualization of the problem analysis: the behavior of sediment particles after being disposed near the shoreline.

The effects of instantaneous supply of sediment on the Dutch coastal system have been extensively investigated and these type of nourishments are applied in practice. However, research regarding a continuous supply has not been conducted yet. It is important to know how sediment behaves after disposal (see Figure 2), in which direction sediment is transported and what the driving mechanisms are of redistribution of sediment around a continuous nourishment location to get an overview on the effects of the Dutch coastal system.

It is also important to include the operational characteristics of the Zandwindmolen, such as minimum and maximum discharge through pipelines and the expected operational time in a year. These factors form the boundary conditions for the applicability of the Zandwindmolen in the coastal system.

1.2.3 Problem definition

It is not known what the behavior of a continuous nourishment is in a specific domain of the Dutch coastal system and what the effects of a continuous supply of sediment are on the behavior of the overall Dutch coastal system. The innovative method differs significantly from the conventional method, and therefore requires more research to the effects. The problem definition holds the uncertainty of the behavior of the continuous nourishment in a specific domain of the Dutch coastal system. Key question is the possibility of redistribution of sediment by hydrodynamic forcing mechanisms.

1.3 Research goal

The aim of this research is to develop boundary conditions for the application of a continuous nourishment. These boundary conditions are the location of disposal, the annual volume of sediment particles that can be disposed and the configuration of disposal locations. Variation in these conditions will give constraints in which a continuous nourishment is optimally behaving. This then leads to an overview of how such a nourishment will develop in time. Therefore, the following research question is stated:

How does a continuous nourishment along the southern Holland coast develop in the nearshore zone in the first year of its lifetime?

In this research, the southern Holland coast is considered, as a fully calibrated, detailed model is available for this coastal stretch. This model includes representative data of waves, tide and sediment properties. The small spatio-temporal scale is chosen, because the local effects are most important and these are best evaluated in the first period of the lifetime of the nourishment.

The research is performed using the numerical Delft3D model of the Sand Engine, developed by (Luijendijk, et al., 2017). The model is fully calibrated for hindcasting of the Sand Engine. The evaluation from that research have almost fully matched the observations and measures in the field, which confirms the reliability of the model for research to behavior of continuous nourishments. The coastal stretches in paragraph 1.2.1 are likely to be of more interest due to the larger required annual volume. However, this research will focus on the initial behavior of a continuous nourishment, to define the limitations of the concept in general.

1.4 Research sub-questions

The concept brings a relatively new concept of execution of nourishments. Instead of a large instantaneous disposal volume, a smaller continuous volume is disposed over a longer period of time. It is not known whether the coastal area is able to deal with this continuous supply of sediment. Therefore four sub-questions help answering the research question:

1. What are the governing hydrodynamic and morphodynamic processes that drive sediment transport and control behavior of a nourishment?
2. What is the optimal depth to apply a continuous nourishment?
3. What are the changes in behavior when the annual nourishment volume increases?
4. What changes in the behavior of a continuous nourishment when the annual nourishment volume is spread over multiple, adjacent disposal locations?

Sub-question 1 is answered using the theoretical background given in chapter 2. The sub-questions 2 to 4 are answered in chapter 4, with the results of several nourishment configurations.

1.5 Report structure

This report consists of five chapters. Chapter 2 gives an overview of the analysis that is performed for the research. Coastal hydrodynamic and morphodynamic processes that occur at the Holland coast, as well as the development of the Holland coast in time is elaborated to motivate the relation to the need of applying nourishments. The chapter concludes with future predictions of hydrodynamic processes. In Chapter 3, the research methodology is explained, containing the research parts, research the tool and how the tool is used to provide the results given in chapter 4. The results are further discussed in chapter 5. Conclusions and recommendations for further research are given in chapter 6.

Chapter 2: Analysis

This chapter starts with a short description of the characteristics of the Dutch coastline. Then the hydrodynamic and morphodynamic processes that cause modifications of the Dutch coastline and that are still present at the coastline, are elaborated. These processes explain how the coastline behaves nowadays and what the visible effects are at the coastline. After this part, a comparative analysis between the Zandwindmolen and the Sand Engine is given, which relates the effects of the Sand Engine in general, and in what way the Zandwindmolen is similar to these effects. The chapter ends with a list of future predictions regarding the hydrodynamic processes that are assumed to be relevant for the research. The information given in this chapter is summarized in the last paragraph.

The knowledge provided in this chapter is used to understand the phenomena visualized in chapter 4. The conclusions given in chapter 6 are motivated by this knowledge. The processes that are elaborated in paragraphs 2.2 and 2.3 are used in the formulation of the research parts, the research conditions and the evaluation criteria to present clear boundaries for the research.

2.1 Historical context of the Dutch coastline

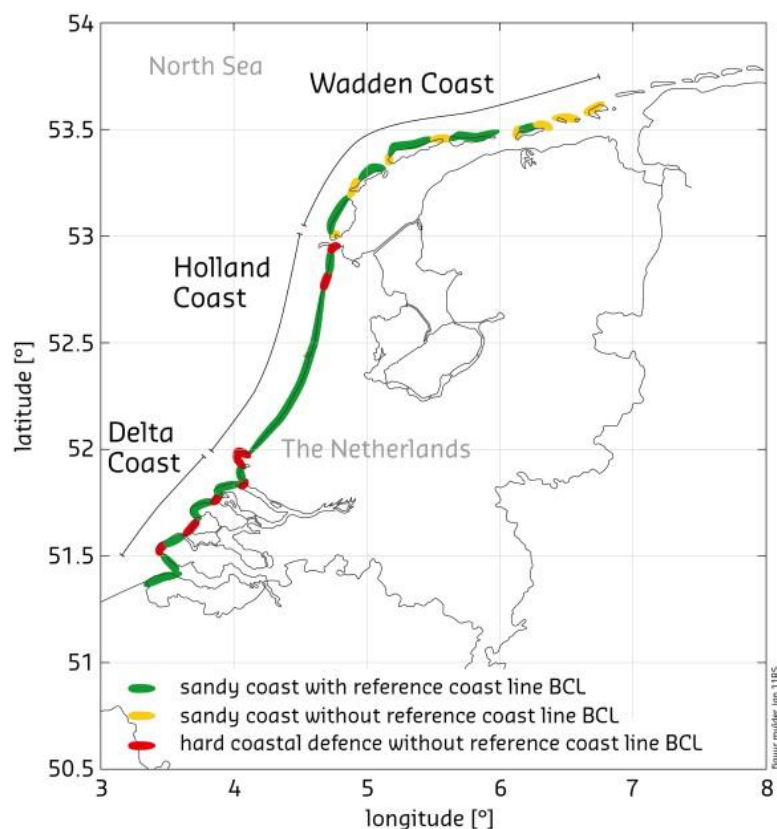


Figure 3 The Dutch coast separated in three coastal sections. The Holland coast is located between Hoek van Holland and Den Helder, where IJmuiden separates the northern part from the southern part. (Image source: Mulder, Hommes, & Horstman (2011))

The Dutch coastline consists of three stretches: The Wadden coast in the north, the Holland coast in the middle, and the Delta coast in the southwest of the Netherlands. Figure 3 shows the location of the coastal stretches. In this research, the focus is on the southern part of the Holland coast, located between Hoek van Holland and IJmuiden.

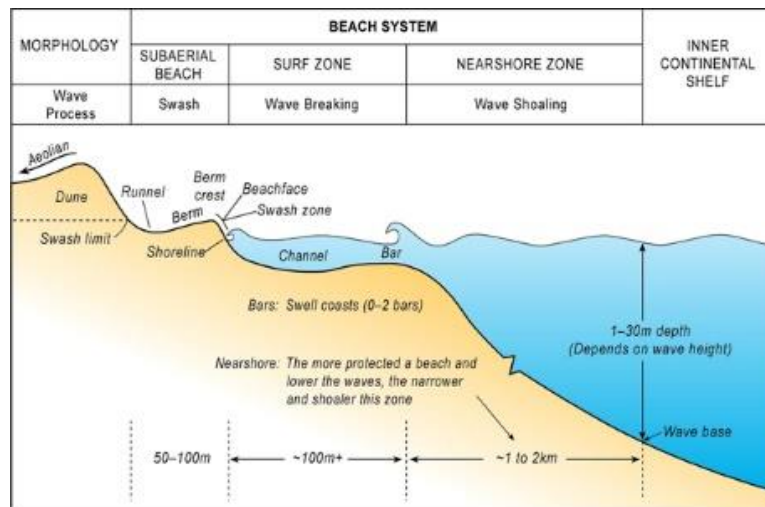


Figure 4 The beach system as is known for the Holland coast. The deep water line is located at the MSL -20.0 m depth contour. Several sand bars function as wave breaker. (Image source: Short (2012))

The cross-shore profile of the Dutch coast is characterized by a shallow surf zone and a deeper nearshore zone, as visualized in Figure 4. The coastline consists of several sand bars, which are located alongshore. These bars function as wave breakers and are highly dynamic: their location varies in time due to morphodynamic processes. The offshore boundary, which is called the deep water line, is located at the 20 meter depth contour. This is the offshore boundary for the research domain.

The Dutch coast has been subject to a set of transformations, starting from the end of the last ice age, about 11'700 years ago (Van der Spek, et al., 1999). Around this time, the North Sea bed was almost dry. Large glaciers from the north covered parts of the North Sea and the Netherlands. When the glacial period ended, these glaciers melted and the sea level raised quickly. This caused a landward retreat of the coastline, because the sediment demand was larger than the supply from the sea bed and rivers. The coastline retreat stabilized after a couple of thousands of years. The supply of sediment increased and the sea level rise decreased. This caused a net seaward extension of the coastline. The most seaward position has been reached during the Roman period. After this, coastline retreat is occurring up to now.

Human interference has contributed to the coastline retreat in the last 2000 years. The damming of rivers and the building of structures has decreased the net contribution of sediment from rivers and has disturbed sediment transport along the coastline. Besides that, the supply from the North Sea bed has decreased. Sediment transport along the Holland coast is partially blocked by breakwaters, harbors and piers. This causes erosion at specific locations along the coastline. The aim of these structures is to protect the hinterland, but the counter effect is valid: erosion of the coastline destabilizes the strength and stability of the coastline (Van der Spek, et al., 1999).

To mitigate erosion, nourishments are applied at several locations along the Dutch coastline (Van Rijn, 1997). These are mostly applied at erosion-extensive locations. The volume of the nourishments depends on the degree of erosion relative to its direct environmental morphodynamic conditions. The rate of applications of nourishments is depending on the degree of erosion and the applied volume. A small nourishment volume requires more frequent applications to maintain strength and stability.

The processes that are involved in erosion and sedimentation patterns, are elaborated in paragraphs 2.2 and 2.3. The effects of these processes on the Holland coast are further explained in paragraph 2.4.

2.2 Coastal hydrodynamics

Within the range of hydrodynamic processes, three relevant processes are elaborated: tidal forcing, wave forcing and relative sea level rise. A fourth process, wind forcing, is briefly mentioned, because sediment transport driven by wind forcing is not considered in this research.

2.2.1 Tidal forcing

The tide occurring along the Holland coast is a dominant M2-tide, driven by the moon. The tidal fluctuations, ebb and flood, happen twice a day. The tidal cycle has a duration of 12 hours and 25 minutes (Bosboom & Stive, 2015).

The tide is a long wave. The flood component represents the crest of the tidal wave, and the ebb component is the trough of the wave. The ebb component experiences more bottom friction, which leads to an asymmetric tidal cycle: the flood duration (4 hours) is smaller than the ebb duration (8 hours). The velocity of the flood is thus larger. Besides that, the magnitude of the flood current is larger than the magnitude of the ebb current. This causes a net northward directed longshore tidal current, which is in the direction of the flood current (Giardino, Santinelli, & Vuik, 2014).

2.2.2 Wave forcing

Waves propagate towards the coast and reduce in wave height and wave energy near the coastline. The generation of currents and wave breaking are key processes in this part of the coast. These processes contribute to the transport of sediment.

Wave propagation in shallow water

Waves propagate towards the coast in the nearshore zone. Due to a decrease in depth, waves experience bottom friction. The bottom friction affects the stability of the wave. Then the wave breaks causing a decrease of the wave energy.

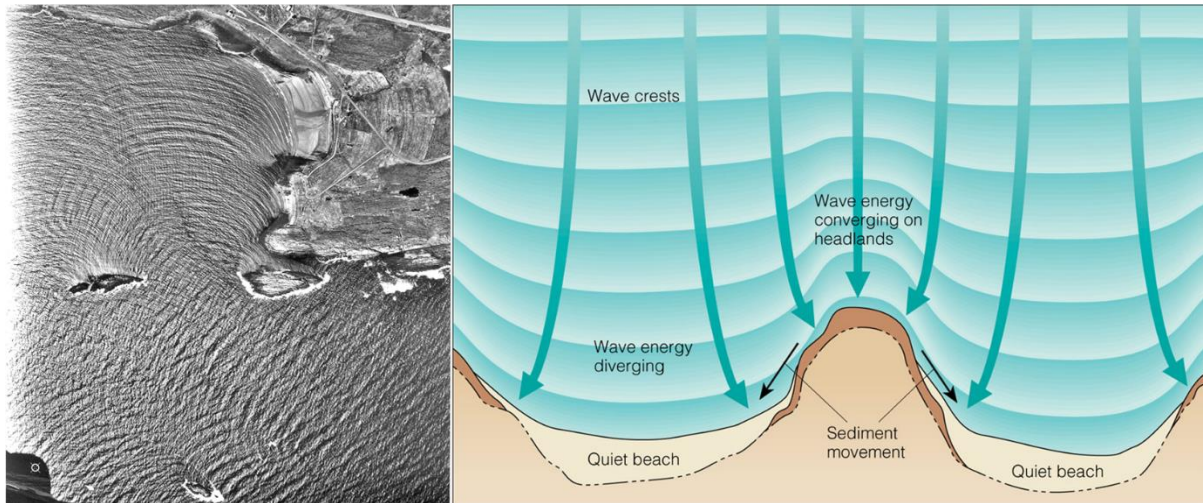


Figure 5 Diffraction (left) and refraction (right). Diffraction occurs due to obstacle in the path of the wave. Refraction is caused by changing orientation of depth contours, as the wave direction is perpendicular to the depth contours. (Images source: Kennesaw State University (n.d.))

The wave direction depends on the bottom profile (Holthuijsen, 2007). The wave direction is perpendicular to the depth contours. Changing orientation of the depth contours changes the wave direction. This phenomenon is called refraction: wave energy converges on headlands, or convex coastlines, and diverges on hollow coastlines. A second phenomenon is called diffraction: obstacles cause divergence of wave energy and semi-circular wave patterns are visible. This is likely to occur at emerged sand bars. Figure 5 visualizes these phenomena. This theory has proven to be important in order to understand the direction of waves and currents around nourishments.

Return current

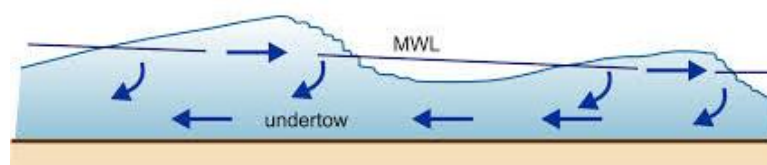
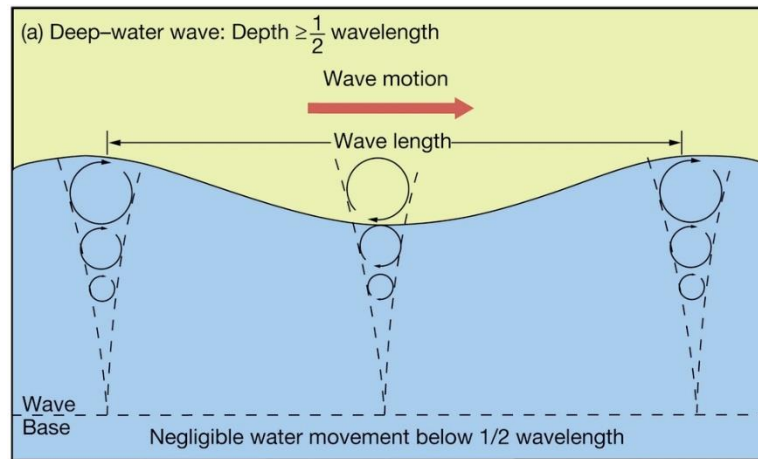


Figure 6 Undertow underneath waves. The orbital motions cause this return current. (Image source: University of Florida (2014))

Underneath the wave, a return current is present. This return current is in opposed direction to the wave direction. The return current is known as undertow (University of Florida, 2014). The mechanism is shown in Figure 6.



Copyright © 2004 Pearson Prentice Hall, Inc.

Figure 7 Orbital motions underneath waves. In deeper layers, the effect of the waves is negligibly small. This line is marked as the wave base and is equal to $\frac{1}{2}$ of the wave length. (Image source: GoSurf Perth (2016))

The circular movement of the current underneath the wave is caused by the orbital motions driven by wave forcing. The orbital motions are forced by the variation in water level. The water level changes with the crest and trough of the wave. Underneath the wave, the orbital motions are changing in magnitude and direction. Under the crest, the motions are in the direction of the wave, but under the trough the motions are opposed to the wave direction. The effect of the motions decreases with increasing depth. Below a certain depth, these motions are negligibly small and therefore no effect on currents is measured. This line is called the wave base and is equal to $\frac{1}{2}$ of the wave length as can be seen in Figure 7 (GoSurf Perth, 2016).

Wave breaking

Wave breaking occurs due to a decrease in depth. This is caused by a relatively fast propagation velocity of the wave crest compared to the velocity of the wave trough. The velocity depends on the depth: a larger depth provides a larger velocity. When the wave crest velocity becomes too large, the stability of the wave is no longer valid and the wave breaks (Holthuijsen, 2007).



Figure 8 Plunging wave breaking is the most common type of breaking at the Holland coast. A lot of wave energy is released which causes an increased sediment transport gradient. (Image source: Holthuijsen (2007))

There are four types of breaking waves, of which one type is most common at the Holland coast: plunging breaking waves. This type of breaking wave causes a large degree of turbulence in the

breaking zone, because of the sudden release of a lot of wave energy. Figure 8 shows the development of a plunging breaking wave. The sediment is stirred in the water column and transported with the current.

Infra-gravity waves

Wave propagation and breaking is mainly valid for short waves: waves with a small period and wave length, and a relatively large wave height. Another type of waves are long waves, which have a large period and wave length with a relatively small wave height. These long waves are also called infra-gravity waves.

Long waves are bounded in wave groups and are released when the short waves break. This makes the long waves free to propagate towards the coast. Different from short waves is the increase of wave height of long waves when the depth decreases. Bottom friction does not play a role as the wave height is significantly small (Bosboom & Stive, 2015).

Long waves cause a large run-up, which causes an increase of erosion at the shoreline (line between water and land at mean sea level (MSL)) and at the dune face. They increase the rate of overwash. The reflection coefficient is large and causes a large outgoing wave height and wave energy (De Bakker, Tissier, & Ruessink, 2014).

2.2.3 Relative sea level rise

Relative sea level rise is the sum of absolute sea level rise and land subsidence. Absolute sea level rise is the raise of the water level at sea compared to a reference water level. Land subsidence is the lowering of the ground level relative to that same reference water level. The reference water level in the Netherlands is Normaal Amsterdams Peil, or NAP. Relative sea level rise contributes to the sediment demand in the coastal zone.

Instead of relative sea level rise, the absolute sea level rise can be considered. However, the Dutch coastal zone suffers from significant lowering of the ground level. This is caused by settlement of clay soil and gas mining in the North Sea. Therefore, the relative sea level rise provides a more reliable prospect.

The small temporal scale used in the research is too small to consider relative sea level rise. The expected sea level rise in one year does not significantly contribute to an increased sediment demand. This process is therefore not used for analyzing sediment transport, sediment demand and bed level changes.

2.2.4 Wind forcing

Wind forcing is dominant at the beach and in the dunes. The wind predominantly comes from the southwest and the north-northwest at the southern Holland coast. The wind causes wave forcing and set-up of the water level in the nearshore zone (Luijendijk, et al., 2017).

Transport of sediment by wind is interesting in case of beach nourishments. These nourishments are emerged (above mean sea level) and therefore under influence of wind forcing.

During strong winds, a large volume of sediment can be redistributed towards the beach and the dunes. Dunes are namely a consequence of wind-induced sediment transport. Submerged nourishments (below mean sea level), which are placed in the foreshore, are not under influence of wind. Then wind-induced sediment transport is not included.

2.3 Coastal morphodynamics

Sediment transport and the subsequent changes in the bottom profile are caused by the forcing mechanisms elaborated in the previous paragraph. These processes generate currents that are able to transport sediment in both longshore and cross-shore direction. The maximum amount of sediment that is transported with the currents, is called the transport capacity.

2.3.1 Longshore currents and sediment transport

Longshore currents are driven by the oblique incidence of the tidal wave and short waves. The currents are predominantly driven by wave forcing.

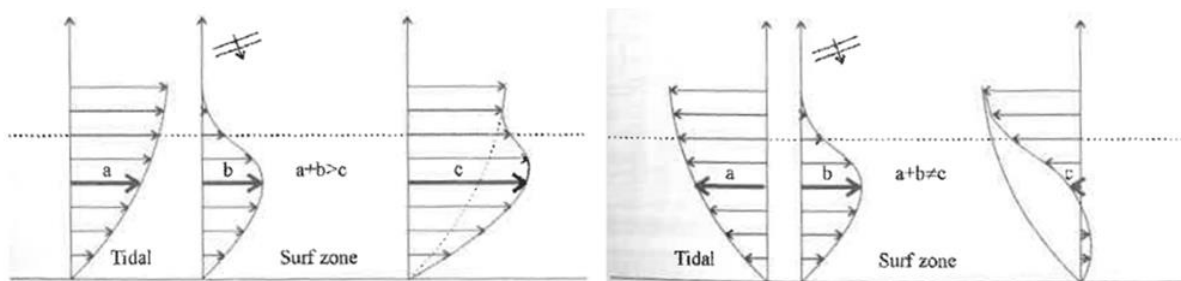


Figure 9 Cross-shore horizontal profile of the longshore current in the surf zone. Profile C is the sum of the tidal current (A) and the wave-induced current (B). The tidal current changes direction for flood (left) and ebb (right), which changes the net direction and magnitude of the longshore current. (Image source: Bosboom & Stive (2015))

The wave-induced current increases when the wave height increases. The larger the angle of incoming waves with the shore normal, the larger the magnitude of the longshore current. The magnitude and direction of the wave-induced current is then varying in time. The wave-induced current is maximum at the location of breaking.

The tide-induced current is relatively small compared to the wave-induced current and is net directed towards the northeast (Giardino, Santinelli, & Vuik, 2014). The tidal current is increasing in magnitude as the depth increases. Figure 9 shows the profiles of the tide-induced and wave-induced currents and their combination for both a flood tidal current and an ebb tidal current.

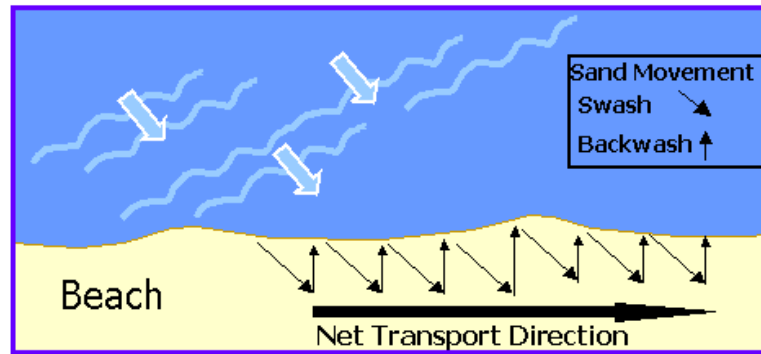


Figure 10 The occurrence of erosion at the beach. The run-up (swash) by waves generates a run-down (backwash) that transports sediment to the surf zone. The net transport direction is then to the north (right in the figure). (Image source: Texas A&M University at Corpus Christi (n.d.))

The longshore sediment transport magnitude is proportional to the magnitude of the longshore current. The angle of incidence and the wave height determine the magnitude. A larger wave height causes more wave energy dissipation and thus stirring of sediment. Also the swash onto the beach contributes to the longshore sediment transport volume, as this amount of sediment is brought to the location of the longshore current, see Figure 10 (Texas A&M University at Corpus Christi, n.d.).

Although the direction of the longshore current changes regularly because of changing wave directions, the net sediment transport gradient is directed to the northeast. The estimated magnitude of the transport gradient is 250'000 m³/year for the southern Holland coastline (Bosboom & Stive, 2015).

2.3.2 Cross-shore currents and sediment transport

The cross-shore current is generated by wave propagation, wave run-up and breaking of waves. A return current is offshore directed and transports sediment from the shallow surf zone and the beach towards the deeper nearshore zone. The transport of sediment as shown in Figure 10 is a result of backwash. This sediment is locally redistributed in cross-shore direction.

Wave breaking forces sediment to stir up from the bed and then brought into suspension. The cross-shore current transports sediment either onshore or offshore. In the outer surf zone, undertow is dominant and sediment transport is offshore directed. In shallow areas in the surf zone, where the wave energy is more or less constant, waves can prevail longer and this generates a small onshore directed transport gradient. More close to the beach, the return current is forced by wave breaking and offshore directed.

The appearance of storms increases the cross-shore sediment transport gradient due to larger waves and strong winds. Erosion occurs at the beach and dune face and more sediment is transport to the deeper nearshore zone. The gross volume that erodes from the beach and dunes remains in the surf zone. This contributes to a larger sediment transport gradient in alongshore direction (Tonnon, Huisman, Stam, & Van Rijn, 2018).

2.3.3 Sediment demand of the coastal zone

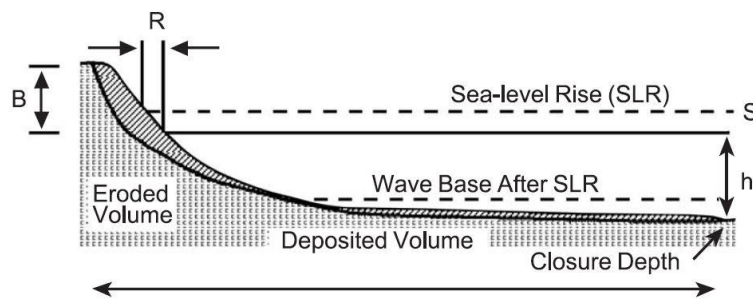


Figure 11 Visualization of the effect of sea level rise on the sediment demand in the nearshore zone. The Bruun Rule is developed to motivate this. (Image source: Cooper & Pilkey (2004))

The sediment demand is depending on the horizontal distance between the shoreline, the deep water line and the rise of the sea level. This is explained by the Bruun Rule as shown in Figure 11. This rule has been developed to determine the sediment transport gradient in offshore direction, as a consequence of sea level rise.

A higher water level causes more erosion of the beach, dunes and surf zone. The sediment is transported to the nearshore zone. As the volume of the nearshore zone increases, more sediment is needed to maintain the position of the coastline. By supplying sediment, the coastal foundation is able to grow with sea level rise (Stronkhorst, Van Rijn, & De Vroeg, 2010).

The beach slope of the Holland coast is a mild slope. The distance between the shoreline and the deep water line is significantly large compared to the depth difference. A small increase of the water level creates a large increase of the horizontal distance. This increases the sediment demand of the Holland coast.

2.4 Present situation of the Holland coastline

The processes discussed in the previous paragraphs help understanding the behavior of the Holland coast, as it is nowadays. The coastline is moving in cross-shore direction: erosion and accretion occur at several locations. A review is given on these locations.



Figure 12 Annual measurements of the coastline position for the year 2018. The measurements are relative to the BKL. The left part shows the southern Holland coast between Hoek van Holland and IJmuiden. The right part shows the coastline between IJmuiden and Den Helder. (Image source: Rijkswaterstaat (n.d.))

Erosion and accretion occur due to varying transport gradients in alongshore direction. The position of the coastline is measured annually by Rijkswaterstaat. The differences in position help determining the need and amount of nourishments for the locations that need to be strengthened. A reference coastline has been determined, which is the Basiskustlijn (Momentary Coastline, or BKL) (Rijkswaterstaat, n.d.). This line is used to define the minimum required position to guarantee strength and stability of the coastal zone. All measured positions are relative to this reference coastline. Figure 12 shows the measurements of the year 2018. For each measurement location, the position gives two important characteristics: whether erosion or accretion takes place, and whether the position is landward or seaward of the reference coastline. These measurements are used to plan nourishments for the coast.

2.5 Sustainable nourishments: the Sand Engine

From Figure 12, it is concluded that the southern Holland coast is slightly accreting, mainly because of application of nourishments. Remarkable locations are the erosion sensitive area in the southwest. Here the project ‘Sand Engine’ has been constructed. This mega nourishment is applied to investigate the efficiency of larger nourishment volumes at the Dutch coastline, in order to develop a more sustainable method of applying nourishments. The aim at this project is to investigate whether it is possible to strengthen the coast at once with a large volume of sediment instead of supplying small volumes every couple of years.

2.5.1 Development of the project ‘Sand Engine’

The Sand Engine is an instantaneous mega nourishment, containing 21 million m³ of sediment (Luijendijk, et al., 2017). The nourishment has been constructed as beach nourishment. The coastline has been extended seaward, up to the initial MSL -8.0 m depth contour.

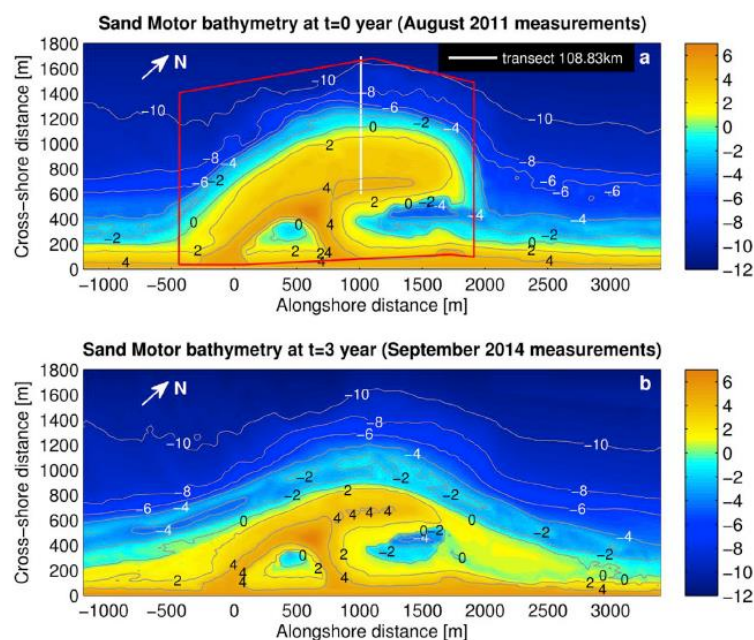


Figure 13 Morphological development of the Sand Engine in the first three years of its lifetime. The nourishment is flattened at the seaside, mainly due to oblique wave forcing. (Image source: Tonnon, Huisman, Stam, & Van Rijn (2018))

The morphological development of the Sand Engine in the first three years of its lifetime are shown in Figure 13. The seaward extension of the nourishment has been flattened and the cross-shore bottom profile has become more steep at the alongshore distance of 1000 m. The MSL -2.0 m depth and the MSL +2.0 m depth are located closer to each other in the lower figure. The dominant sediment transport direction is northward (to the right in the figure), as can be derived from the increase of sediment supply at the right part of the nourishment (at alongshore distance of 2000-2500 m).

The fast morphological response is explained by the fact that the difference with the equilibrium situation is largest. The impact of waves from the southwest is large and almost

perpendicular to the nourishment. This increases the transformation towards a more flattened coastline. The theory of converging wave energy on headlands, as described in paragraph 2.2.2, is applicable in this situation. The Sand Engine functions as a headland on a coastline that is overall a straight line. The energy around this nourishment is then larger compared to its environment, and therefore the impact of waves and subsequent longshore currents is large as well.

2.5.2 Comparing the Sand Engine with Zandwindmolen

There are similarities between the Sand Engine and the Zandwindmolen. Both assume a large volume of sediment per period of time. With the Sand Engine, this amount has been placed instantaneous. The Zandwindmolen assumes sediment supply gradients that are in this order of magnitude, and larger. As no nourishments are required for this coastal section, it is likely that the Sand Engine functions as a continuous nourishment for a large period of time.

This assumption forms a basis for the expected results in chapter 4. It is likely that small humps of sediment are generated when applying the Zandwindmolen in the coastal system. The location and discharge rate are therefore important to optimize the effect. The Sand Engine provides reliable expectations regarding the effect of longshore currents and transport patterns, in order to define the best location in the cross-shore profile.

2.6 Future predictions of hydrodynamic processes

The relevant hydrodynamic processes discussed in paragraph 2.2 are likely to change in the next decades. The predictions of these processes is briefly explained.

2.6.1 Longshore sediment transport by tidal and wave forcing

It is not likely that the tidal forcing will change in the next 100 years. The tide is forced by the moon and this force will not change.

There is little to no reliable information available to predict wave height in the next 100 years. Moreover, there is also a lack of data in the prediction of wind speed and frequency, which is used to predict the intensity and frequency of storms. Storms cause large erosion and are therefore important to consider in erosion of nourishments. The absence of reliable data therefore increases the uncertainty of future development in erosion mechanisms. However, it is likely that due to climate change, the frequency or intensity of storms will increase. According to the IPCC, the frequency of storms will change with fractions of 1-2% (Klein Tank, et al., 2014).

2.6.2 Relative sea level rise and sediment demand

Relative sea level rise for the Holland coast is expected to be between 25 and 100 cm in the year 2100, with a most likely value of 80 cm (Giardino, Santinelli, & Vuik, 2014). The sediment demand is then increasing.

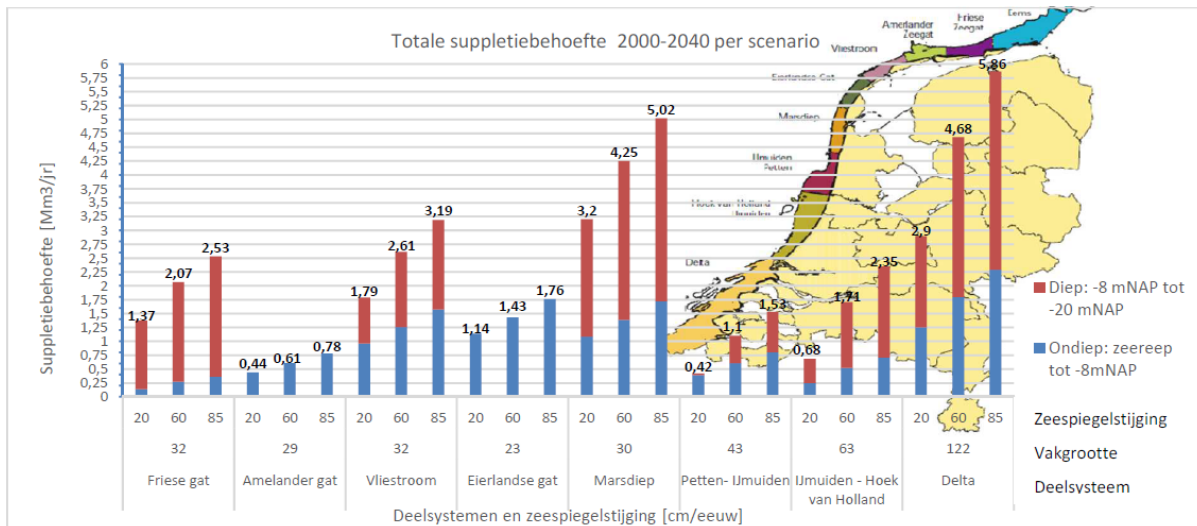
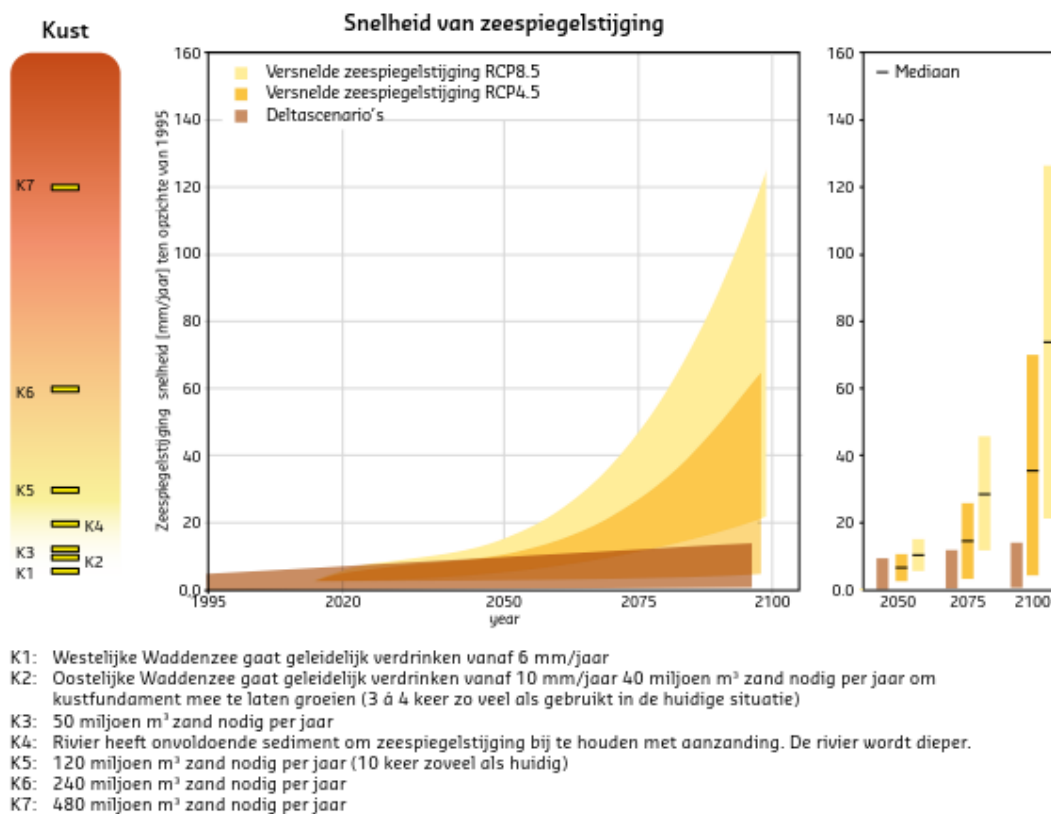


Figure 14 Expected sediment volume for several coastal stretches of the Dutch coast. The southern Holland coast is expected to have a shortage of 2.35 million m³ per year for the case with 80 cm sea level rise in the year 2100. From this volume, 750'000 m³ is required between the shoreline and the MSL -8.0 m depth contour. (Image source: Dekker (2013))



- K1: Westelijke Waddenzee gaat geleidelijk verdrinken vanaf 6 mm/jaar
- K2: Oostelijke Waddenzee gaat geleidelijk verdrinken vanaf 10 mm/jaar 40 miljoen m³ zand nodig per jaar om kustfundament mee te laten groeien (3 à 4 keer zo veel als gebruikt in de huidige situatie)
- K3: 50 miljoen m³ zand nodig per jaar
- K4: Rivier heeft onvoldoende sediment om zeespiegelstijging bij te houden met aanzanding. De rivier wordt dieper.
- K5: 120 miljoen m³ zand nodig per jaar (10 keer zoveel als huidige)
- K6: 240 miljoen m³ zand nodig per jaar
- K7: 480 miljoen m³ zand nodig per jaar

Figure 15 Possible accelerating sea level rise up to the year 2100. The worst-case scenario (RCP8.5) predicts a rise of over 120 cm within one century, which is twice the rising height of the second scenario (RCP4.5). (Image source: Deltares (2018))

Research has been performed to the annual sediment demand for several coastal stretches (Dekker, 2013). For the most likely value of 80 cm rise, the southern Holland coast is expected to have a shortage of 2.35 million m³ per year in the year 2100, which must be supplied by nourishments to maintain the strength and stability of the coastline. This is shown in Figure 14. The amount of sediment that is required is valid for the entire nearshore zone up to the deep water line. The sediment demand in the zone between the shoreline and the MSL -8.0 m depth contour is assumed to be 750'000 m³/year in the year 2100.

A recent study of Deltares has brought insight in a possible accelerated sea level rise (Deltares, 2018). The findings are summarized in Figure 15. The worst-case scenario predicts a rise of 120 cm in the year 2100, while the second worst-case scenario only predicts a rise of 60 cm. The worst-case scenario therefore expects an acceleration of 20%. This has large consequences for the Dutch coastline, its strength and the need for maintenance. It is also larger than the predictions in Figure 14, which means that these values will increase as well.

2.7 Chapter Summary

This chapter discussed the relevant hydrodynamic and morphodynamic processes that explain sediment transport and morphological behavior of the coastline in general and with nourishments. The research sub-question to answer is stated as follows:

What are the governing hydrodynamic and morphodynamic processes that drive sediment transport and control behavior of a nourishment?

The governing hydrodynamic processes are forcing of currents by waves and tide on the short-term and relative sea level rise on the long-term. Wave forcing is the dominant mechanism at the Dutch coastline. In the surf zone, wave breaking results in energy dissipation in the water column and forces sediment to stir up from the bottom. Large energy dissipation causes more stirring and increases the degree of turbulence. Sediment in suspension is more easily being transported by currents. Therefore wave breaking is the dominant mechanism in sediment redistribution. The longshore redistribution is forced by longshore currents. These currents are generated by wave breaking and energy dissipation. The magnitude of a longshore current is also determined by the angle of incidence of the waves on the shoreline. The larger the angle with the shore normal, the larger the longshore component of the resulting current.

The governing morphodynamic processes are predominantly longshore sediment transport, generated by longshore currents. Cross-shore, shoreward directed sediment transport is caused by incoming waves. Besides that, cross-shore transport due to undertow underneath waves forces sediment to move seaward. The degree of wave breaking at nourishments and in the surf zone determines the net shoreward directed sediment transport and the net longshore component of sediment transport. The net longshore sediment transport component is directed northeast for the southern Dutch coastline.

The relevant processes form the bridge between the historical development of the Dutch coast and the present situation of the coast. This adds to the need of nourishments, why they are applied and how this is usually done.

A brief elaboration about the Sand Engine has been given, in combination with the link to the Zandwindmolen. Similarities in the type of nourishment have been explained, which are helpful in predicting the behavior of the continuous nourishment in the Holland coastal stretch.

Future predictions regarding relevant processes have been elaborated. The most important process that is likely to affect the local coastal system is relative sea level rise. This process increases the sediment demand significantly. Multiple studies have been performed to determine the sea level rise in the year 2100. It is possible that the rise is faster than expected, causing an increase in the sediment demand of the Dutch coastline. Research has been performed to the sediment demand for several coastal stretches along the Dutch coastline, as well as for a range of expected sea level rises. The value for 80 cm rise is most likely, which gives a net sediment demand of 2.35 million m³/year in the year 2100 for the southern Holland coastal stretch between the shoreline and the MSL -20.0 m depth contour line.

The prediction of wave forcing is uncertain. A lack of data causes large uncertainties regarding wave height and frequency and duration of storms, from which wave forcing depends on. It is likely that the intensity of wave forcing due to storms will increase in the future, but it cannot be stated with full certainty.

Chapter 3: Research methodology

In this chapter, the research set-up is explained. The set-up consists of three elements. These elements are treated in the first three paragraphs of this chapter. The evaluation criteria are used to adequately compare the observations in the results.

To perform the research, a numerical modelling tool is used, called Delft3D. This tool is elaborated on its contents, application range and specific functions in the fourth paragraph. The last paragraph of this chapter deals with the practical application of the model in the research. The model domain is explained, as well as hydrodynamic and morphodynamic input parameters. The interaction between the processes is explained and the output parameters are briefly discussed to explain the possible results.

3.1 Research parts

The goal of this research is to investigate the spread of sediment around the nourishment location. This research goal can be divided into three parts to reach this goal. First is to find the optimal location for a continuous nourishment, second to find the optimal or maximum nourishment volume for the southern Holland coast, and third to investigate the effects of spreading over multiple disposal locations. The three parts are further explained in this paragraph.

3.1.1 Part 1: the optimal location in the cross-shore profile

Supplying sediment is possible at all locations in the cross-shore profile, defined by the depth in which it is executed. The appearance of currents and breaking points of waves determine the optimal location. The optimal location is defined as: “the location with a specific depth for which the sediment redistribution is largest in alongshore direction”.

As has been elaborated in paragraph 2.3.1, the largest transport gradients occur in the surf zone and just seaward of this zone. For the southern Holland coast, this zone is located between the shoreline and the MSL -8.0 m depth contour. The discharges on the depth contours that are to be investigated, are discussed in paragraph 3.6.

3.1.2 Part 2: the optimal discharge at the optimal location

When the optimal location is determined, the sediment discharge is maximized. The Zandwindmolen assumes a minimum yearly discharge, for which the concept is economic beneficial. Besides that, the operational discharge volume depends on the technical characteristics of the pumps, pipelines and windmills.

The aim of this part of research is to find the sediment discharge rate for which the local coastal system is able to redistribute the sediment volume in alongshore and cross-shore direction. The limitations as described above will not be decisive for the outcome of this part of research.

3.1.3 Part 3: spreading of disposal locations to enhance sediment redistribution

Supplying the complete volume of sediment at one location might bring issues, such as transport limitations. This third and last research part investigates the advantages and disadvantages of applying multiple disposal locations near each other, on which the focus is on the transport intensity in the coastal domain, the development of the bed level and the total alongshore distance in redistribution.

3.2 Research conditions

The research parts are bounded by a set of conditions. These are discussed below.

3.2.1 Continuous supply of sediment in time

The Zandwindmolen assumes a continuous supply of sediment. The principle states that a constant volume of sediment per time step is discharged into the local coastal system. The supply rate depends on the annual required sediment volume and the assumed operational time of the wind mills per year. For this research, the operational time of the concept equals one year (365 days). The sediment is in suspension through the pipeline and is discharged in this composition.

3.2.2 Fixed location in the coastal domain

The discharge location is best applicable at the locations where the transport capacity is largest. Three directional positions are considered: alongshore position, cross-shore position, and position in vertical. These positions are discussed below.

Alongshore position

The location in alongshore direction is best at erosion-sensitive stretches. Sediment at these locations is transported away due to increased transport capacity. Supplying at these stretches adds extra sediment to minimize the erosion rate.

Cross-shore position

The applicability of the Zandwindmolen in the surf zone is difficult, as the system is present all the time. Supplying at the zone between the shoreline and the MSL -2.0 m depth contour is practically not desired as this is dangerous for swimmers. The continuous morphodynamic modifications (i.e. the bed profile) cause steering of currents and different breaking points of waves, which can create strong return currents. Discharging at these depths is therefore not considered in the determination of the optimal location in the cross-shore profile.

Vertical position

The discharge location is also effective in the vertical water column. When discharging in the top layers of the water, wave motions are stronger and redistribution of sediment occurs quicker.

Disposing near the bed is more effective for longshore distribution as the longshore currents are stronger near the bed. Deposition near the bed is also practical for the system as it is easier to keep pipelines at the bed.

The vertical position is not further discussed as the modelling tool applied in this research is not able to distinct the different positions in the vertical for the discharge function. However, it is likely to have different behavior of sediment when supplied at the bottom or at the water level. For the latter, sediment must settle down through the water column, which increases the degree of turbulence and the ratio of suspended sediment transport. When supplying at the bottom, the vertical distance is smaller and the effect of currents might be less.

3.3 Evaluation criteria

The research parts are evaluated on the basis of a set of physical elements. These elements are as follows:

- Bed level at different moments in time, to map the development of the nourishment on size and spread;
- Cumulative erosion and sedimentation patterns, used to define the spread of sediment over the entire period of time;
- Mean total transport magnitudes, which are used to define the net direction of sediment;
- Temporal development of the significant wave height at the nourishment location, to gain insight in the wave energy dissipation relative to the behavior of the nourishment.

Both moments in time as well as temporal development are used to explain the results. For any random moment in time, the elements above can be explained in one view. These elements help to investigate the spread of sediment around the nourishment. The results of the reference simulation are explained by these elements in appendix C.1 and C.2.

The evaluation criteria are set as follows:

1. The maximum height of the nourishment may not exceed a water level equal to MSL -1.0 m, which is equal to the water level during low tide. It is not desired to have small islands visible during large parts of the day. Besides the aesthetic point of view, the nourishment is likely to be less eroding when its top is above water for a longer time. waves will break on it, but wave-induced currents have less effect over the nourishment and flow around it, without erosion of the top.
2. The transport gradients must remain sufficiently large, in order to keep initial transport patterns in a larger domain. The initial nourishment applied at one cell is the minimum requirement on which the nourishment settings are evaluated.
3. The alongshore distance of redistributed sediment must be as large as possible to enhance coastal strengthening. The distance over which sediment has been redistributed is used to define the applicability of the nourishment on the specified depth.

3.4 Research tool: Delft3D

The numerical modelling tool Delft3D is an integrated process-based model, which simulates 2D and 3D flow, sediment transport and morphological behavior, waves, water quality and ecology. It is able to interact between these processes, which are programmed in modules. The different modules are shown in Table 1 (Deltares, 2014). The modules FLOW and WAVE are used in the MOR module to investigate morphological behavior due to waves and currents. The MOR module is designed to simulate wave propagation, currents, sediment transport, morphological behavior and development in coastal, riverine and estuarine areas.

Table 1 Modules available in the Delft3D software package (Source: Deltares (2014))

Module	Functions
FLOW	Calculates the non-steady flow and transport resulting from tidal and meteorological forcing on a curvilinear, boundary-fitted grid.
SED	Calculates sediment transport of both cohesive and non-cohesive material, and is able to study the spreading of dredged material, and sedimentation/erosion patterns.
WAVE	To study the evolution of random, short-crested wind-generated waves in coastal waters. It computes wave propagation, wave generation by wind, non-linear wave-wave interactions and dissipation for a given bottom topography, wind field, water level, and current fields in deep, intermediate and finite water depth. The SWAN model is implemented in this module to transform waves from offshore to nearshore waves.
MOR	Combination of FLOW, SED, and WAVE module
WAQ	Water quality module, not relevant for this research.
ECO	Ecology module, not relevant for this research.
PART	Particle tracking module, not relevant for this research.

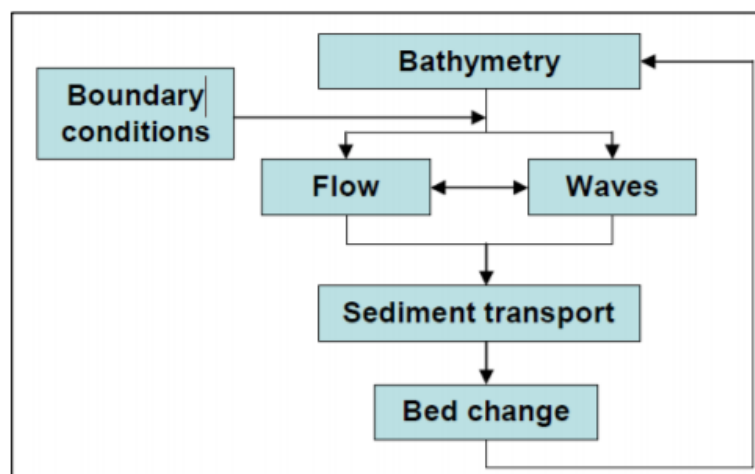


Figure 16 Schematization of the performed steps in the MOR-module in Delft3D. The morphological scale factor is built in the step from 'Sediment transport' to 'Bed change'. (Image source: Hillen (2009))

Delft3D is a tool that requires significant computational effort. This was a limiting factor in this research as it costs much time to get results. However, most of the cases require processes that cannot be modelled with other tools. The morphological scale factor helps with this issue (Tonnon, Huisman, Stam, & Van Rijn, 2018). The scale factor performs multiple morphodynamic calculations for each hydrodynamic time step. The morphological behavior and development is then accelerated compared to the hydrodynamic processes. However, there is a remark: the hydrodynamic data, such as wave data, must not be significantly changing over time. This is to avoid loss of data and loss of reliable predictions of the morphological development (Luijendijk, et al., 2017). The morphological scale factor is built in in the step from sediment transport to bed change, as is shown in Figure 16.

The computation of wave characteristics in the WAVE module is performed by the SWAN application. This tool computes offshore wave characteristics to nearshore wave characteristics, defined by the bathymetry, wave conditions and wind conditions. The results from the WAVE and FLOW computations are combined and used to determine the required changes in morphology. This is performed 'online', which states that Delft3D computes WAVE conditions first. These conditions are used to determine the FLOW conditions, after which both sets of conditions are implemented in the computation of the morphological behavior and development. The results from this part are coupled back to the WAVE and FLOW modules, after which the cycle repeats. The results are now determined per time step, instead of a non-changing set of wave data used for all time steps.

3.5 Model application

This paragraph elaborates on the application of the model in this research. Firstly, the model domain is explained, including the grid, bathymetry and boundaries. Secondly, the input processes are given, such as tidal and wave forcing and sediment characteristics.

The model application that is used is derived from the Sand Engine Model, developed by Deltares, to hindcast the initial morphological development of the Sand Engine in the first years of its lifetime. This model application is a state-of-the-art Delft3D model, which is calibrated for the Delfland coastal stretch. Several hydrodynamic processes have been used to predict the morphological response of the Sand Engine.

The model application is now used to predict morphological response of a continuous nourishment along this coastal stretch. The hydrodynamic processes that are implemented remain equal. The nourishment is implemented as a discharge, which is found in the FLOW module under 'Operations'. In paragraph 3.5.5, the input values for Discharges is discussed.

3.5.1 Model domain

The model domain consists of grid, depth and boundaries. These parts are explained below.

Grid

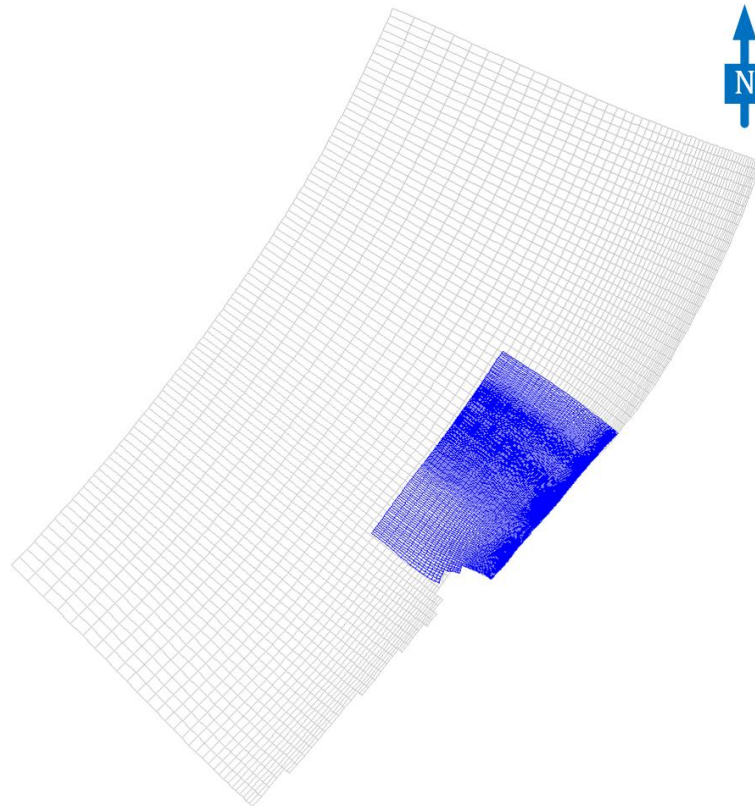


Figure 17 FLOW grid (blue) and WAVE grid (grey). The WAVE domain is much larger in order to accurately predict wave characteristics for the FLOW domain.

The grid is divided in two parts: a FLOW grid and a WAVE grid. These are visualized in Figure 17. The figure is shown at full-size in appendix A.1. The FLOW domain itself is shown in appendix A.2.

The WAVE domain (grey) is much larger than the FLOW domain. This is done in order to accurately predict wave characteristics for the FLOW domain. The boundary at the upper left is at the seaside. At the left corner of the WAVE domain the ‘Europlatform’ is located, which is a measurement station offshore from the Port of Rotterdam. At the northern corner the measurement station IJmuiden ‘Munitiestortplaats I’ is located. The distance between these corners is over 80 km.

The FLOW domain is located between Hoek van Holland and Scheveningen, over a longshore distance of 20 km. The seaside edge is at the MSL -20.0 m depth contour line. The grid cell sizes in the FLOW domain vary between 10 and 1100 m in cross-shore direction, and between 25 and 385 m in alongshore direction. The number of cells counts 83 in cross-shore direction and 223 in alongshore direction.

Bathymetry

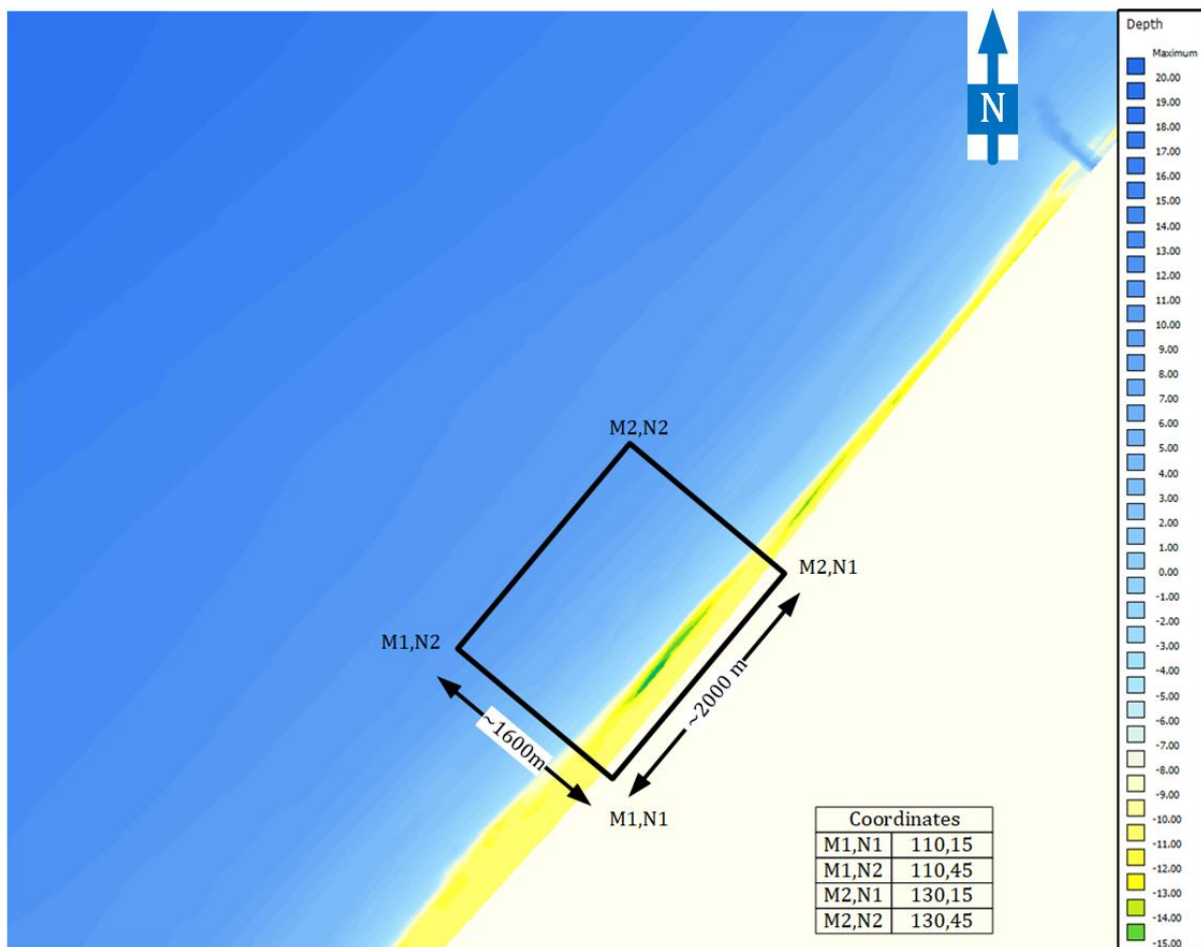


Figure 18 Area of interest for the research. This area is bounded by the dunes and the 10 m depth contour, and the initial location of the Sand Engine in the southwest and the port entrance of Scheveningen in the northeast.

The bathymetry is derived from measurements in August 2010 (Luijendijk, et al., 2017). The bathymetry for the full FLOW domain is found in appendix A.3.

The area of interest used for application of a continuous nourishment is only a small part of the FLOW domain. The domain as defined in Figure 18 is used: an area of 2000 by 1800 m, located between MSL +2.0 m and MSL -10.0 m. The coordinates of the four corners are cell coordinates as defined in the model grid and do not represent actual locations along the coastline. For reference, this area is located just northeast of the initial location of the Sand Engine. This part of the domain has been chosen because of nearly parallel depth contours and a fairly rectangular grid. Moreover, a strong transport zone is present (see appendix C.1, Figure 76). This transport zone is expected to enhance sediment transport from the nourishment location.

Boundary conditions

The FLOW domain is bounded at four sides: land, sea, north and south. The land side consists of dunes with a maximum height of 18 m, and is considered as non-permeable for processes at this

side. The seaside boundary is located near the MSL -20.0 m depth contour line. This boundary is at 15 km offshore, measured from the shoreline. The southern boundary is located at the Maasgeul, the deep entrance waterway of the Port of Rotterdam. The northern boundary is perpendicular to the coastline at Scheveningen.

Table 2 Boundary conditions in the model. The Nieuwe Waterweg represents a discharge, which is the river output.

Boundary	Type of Open Boundary	Forcing type
South01	Neumann	Harmonic
Sea01	Water level	Harmonic
Sea02	Water level	Harmonic
Sea03	Water level	Harmonic
Sea04	Water level	Harmonic
Sea05	Water level	Harmonic
North01	Neumann	Harmonic
Nieuwe Waterweg	Total discharge	Harmonic

Frequency [deg/h]	Amplitude Begin [m]	Phase Begin [deg]	Amplitude End [m]	Phase End [deg]
0	0	0	0	0
29.032	1.0508	267.46	1.0181	270.93
58.065	0.29586	166.5	0.30074	169.2
87.097	0.074896	272.42	0.067792	276.53
116.129	0.040369	212.25	0.04291	220.9
145.161	0.02155	14.37	0.021429	20.39
174.194	0.0073183	242.25	0.0075789	252.2
203.226	0.0068821	36.55	0.0062584	43.68
232.258	0.004157	227.15	0.0039601	238.14

Figure 19 Boundary conditions for Sea03. The fluctuations represent the tidal cycle in the North Sea. For every boundary at sea, the values are slightly different.

In the model Delft3D, the boundary conditions are implemented as in Table 2. The sea boundaries are set up as water level types. The water level is representing the tidal forcing, which fluctuates every tidal cycle. The values for boundary Sea03 are shown in Figure 19. The five seaside boundaries, sea01 to sea05, are found at the edge of the FLOW domain between the west corner and the north corner. They represent the incoming tidal elevation and have slightly different input values. They are divided into 5 separate boundary conditions, as the distance of this boundary is too large to apply only one tidal condition. These five conditions predict the elevation in the nearshore zone more accurately.

3.5.2 Input processes

The following processes are elaborated: wind set-up, tidal forcing, wave forcing and sediment transport characteristics.

Wind set-up

Although wind forcing is not considered regarding sediment transport, wind fields contribute to wave generation and propagation, and to water level set-up. These two mechanisms are included in the WAVE domain.

Tidal forcing

The tidal cycle as discussed in paragraph 2.2.1 is implemented. This is done in the boundary conditions given in Table 2. The boundaries Sea01 to Sea05 are representing water levels, which change every cycle. The frequency (= 29.032 deg/hr.) given in the second line of Figure 19 represents the M2-tidal cycle.

The water level at a specific time step is determined by summing up all amplitudes of the frequencies in Figure 19. This is done using the formula below:

$$\eta(t) = a_0 + \sum_{k=1}^K a_n * \cos(\omega_n t - \alpha_n)$$

In the formula, 'a' represents the amplitude, 'ω' represents the frequency, 'α' represents the phase and 'K' the number of frequencies used to calculate the total elevation 'η' on time step 't' (Bosboom & Stive, 2015).

The time series for tidal forcing is not accelerated in this model, because compressing of tidal water level variations and horizontal tidal currents may lead to unrealistic behavior of tidal velocities. It is therefore assumed that the time scale of the tide can be decoupled from the time scale of waves and morphology.

Wave forcing

Wave data from two measurement stations is used to predict reliable wave characteristics in the FLOW domain. The southwest corner of the WAVE domain is at the 'Europlatform' and the northwest corner uses data from the Ijmuiden 'Munitiestortplaats I'.

The initial wave data represents five years of waves, from august 2011 till august 2016. However, the amount of data is significantly large. Therefore, this data is compressed. Two steps have been applied to achieve this (Luijendijk, De Schipper, & Ranasinghe, 2019):

1. All waves with a wave height below 1.5 m have been deleted from the time series, as these waves will not sufficiently contribute to sediment transport and morphological behavior;
2. The other waves are compressed in a smaller time series, which causes different waves to occur closer after each other, meant to reduce computational effort.

The effect of this reduction on computational effort is further explained in paragraph 3.5.4.

Reference date	<input type="text" value="01 08 2011"/>	[dd mm yyyy]
Simulation start time	<input type="text" value="01 08 2011 00 00 00"/>	[dd mm yyyy hh mm ss]
Simulation stop time	<input type="text" value="18 05 2012 06 17 00"/>	[dd mm yyyy hh mm ss]
Time step	<input type="text" value="0.25"/>	[min]

Figure 20 Time frame for the simulations. The duration between start and end time is 291 days.

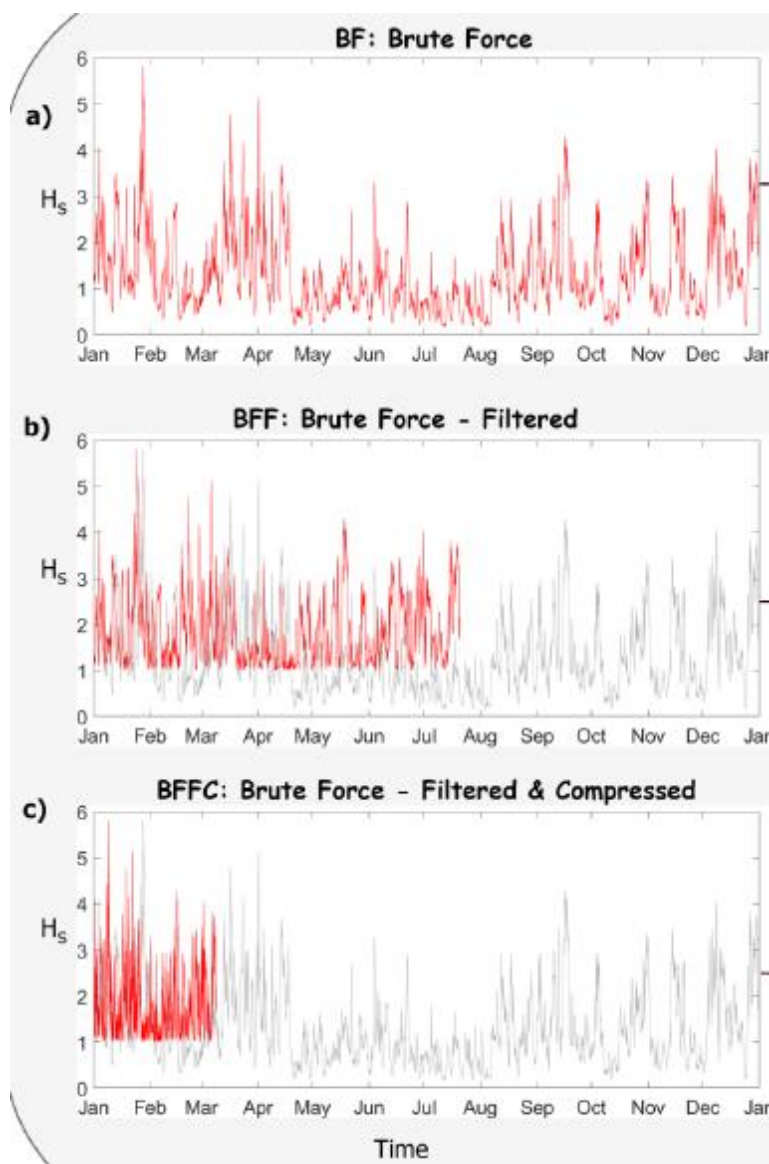


Figure 21 Morphodynamic acceleration on the wave data. The Brute Force Filtered and Brute Force Filtered & Compressed have been used to reduce the time series and after that the series has been compressed. (Image source: Luijendijk, De Schipper, & Ranasinghe (2019))

The wave data initially represents a time series of 5 years, which are 1827 days (2012 and 2016 were leap years). The reduction of the first step removed 52% of the wave data, which resulted in a reduced time series of 874 days. The compressing of the reduced time series with a factor equal to the morfac, provides a net time series of 291 days with wave data. This period of time is equal to the initial time input values in the model (see Figure 20). Figure 21 shows the two steps of input reduction of waves. The methods used are the Brute Force Filtered and Brute Force Filtered & Compressed (Luijendijk, De Schipper, & Ranasinghe, 2019).

The model simulations will not complete the entire time scale. Only data representing 1 year is used to evaluate initial development of the nourishments. The wave data representing the first year has therefore been analyzed. A summary of this analysis can be found in appendix B.2.

Origin of waves and statistics

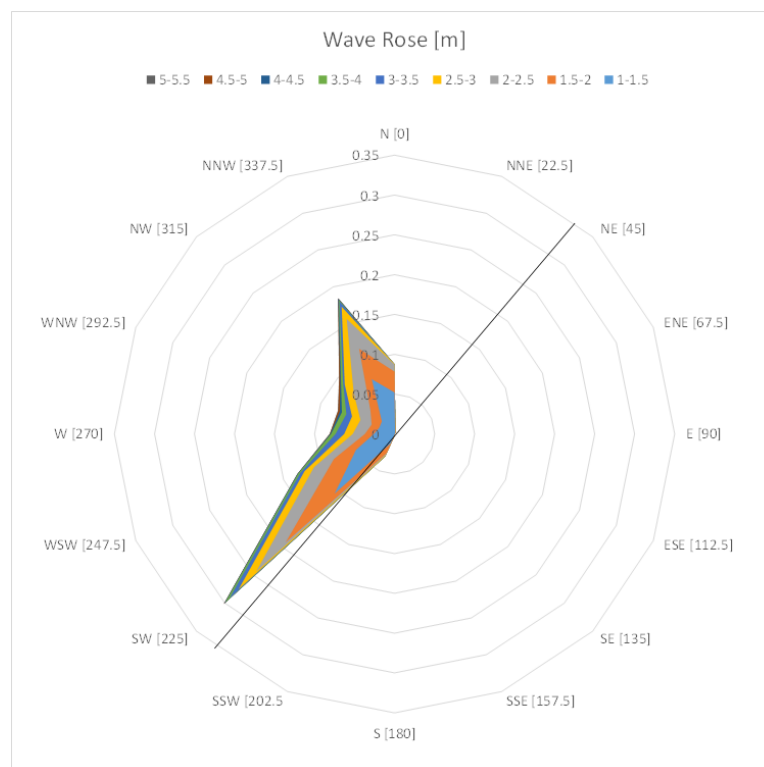


Figure 22 Wave rose representing the input wave data for the first year of the model simulation time scale. An analysis of this wave data is elaborated in appendix B.2.

Figure 22 represents the wave data for year 1, visualized in a wave rose. The two dominant wave directions are southwest and north-northwest. The largest waves originate mostly from the southwest. The black line represents the coastline. Waves that originate at the right side of this line are theoretically propagating from the land. In the model, these waves will not have influence on the coastal dynamics, as they travel away from the coastal domain.

Sediment transport characteristics

Table 3 Input values for model

Input parameter	Value	Unit
Density Sediment (dry)	2650	Kg/m ³
Density Water	1025	Kg/m ³
Grain diameter	0.300	mm

The sediment characteristics that are applied, are summarized in Table 3. The transport formula that is used to calculate sediment transport gradients is the Van Rijn 2004 transport formula. To avoid crashes of the model, the layer thickness is set to 20 m. This will avoid that erosion rates remove more sediment than the domain is giving: the thickness of the layer is smaller than the amount of sediment eroded.

3.5.3 Sediment transport under initial conditions

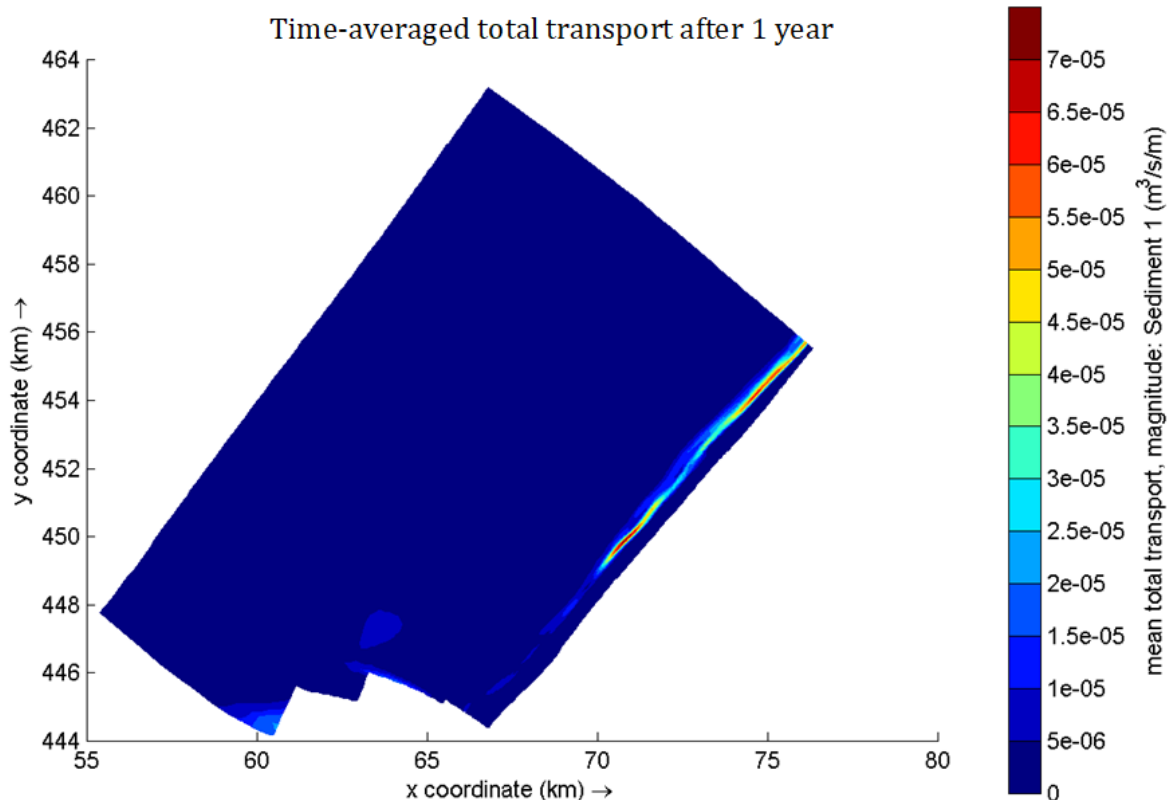


Figure 23 Mean total transport after 1 year (= time-averaged total transport). The red zone located at coordinates X,Y = [70,449] represents a transport belt with significantly large transport magnitudes.

The Delfland coastal stretch has been used to apply the Sand Engine. Its location has been determined on the basis of likely sediment transport patterns. The location of this nourishment is at the southern tip of the red zone, shown in Figure 23. This zone is located between MSL -1.0 m and MSL -4.0 m and is generated by wave breaking and wave-induced currents. This zone is not located over the entire coastal stretch, as waves from the southwest are blocked by the pier of Hoek van Holland/Maasgeul and the structure of the Maasvlakte 2. These structures are visible in the lower part of the FLOW domain in Figure 23. Due to this blocking, waves from the southwest reach the shoreline at the southern end of this transport belt. From this location towards the northeast, all waves are able to enter the surf zone and thus sediment transport increases from here. This zone is highly suitable for applying continuous nourishments, because of its large transport magnitudes. The net transport direction of this belt is towards the northeast.

3.5.4 Reduction of computational effort

Two methods have been applied to reduce the computational effort, without losing significant data and reliability of results: the morphological acceleration factor and input reduction of waves.

Morphological acceleration factor

The morphological acceleration factor is applied to calculate morphodynamic behavior more quickly, without losing substantial data and quality of results. The factor is set to 3. Therefore the morphodynamic time scale will present results over a period that is three times larger than the period of the hydrodynamic time scale.

Hydrodynamic acceleration factor

Besides the application of a morphological acceleration factor, the computational effort has been reduced by input reduction of waves. The amount of wave data has been reduced to 48% of its initial amount. The input reduction of wave data reduced the time period with a factor of $\frac{100\%}{48\%} = 2.09$.

Total acceleration factor

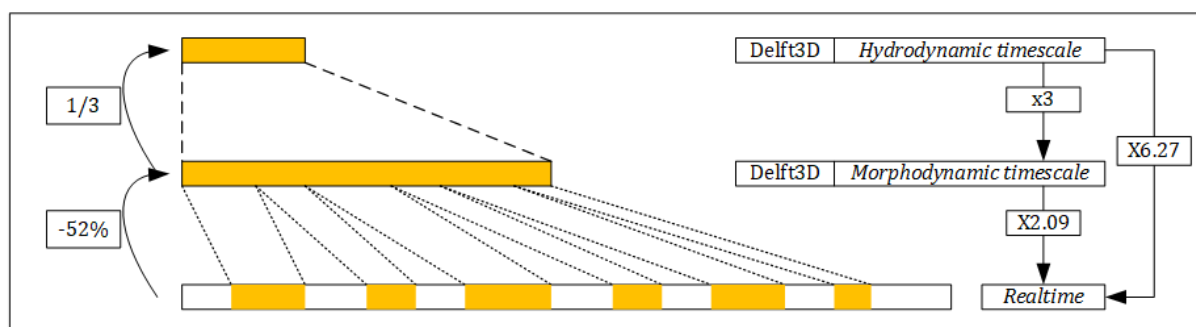


Figure 24 Relation between different timescales in the model and results. The reduction of wave data and the morphological acceleration factor lead to an increase of computation of 6.27, which is the factor for multiplying the morphological time in the results.

The representation of results is depending on both the morphological acceleration factor and the reduction of wave data. The results that are shown represent a situation that is 6.27 times the simulation time. For a simulation time of 1 day, the morphological development in real-time represents 6.27 days. The steps in Figure 24 clarify the relation between the observed results and the real time they occur in.

This has consequences for other input parameters, such as discharges. The morphological acceleration factor adequately deals with the discharge input: a discharge rate is calculated three times per hydrodynamic time step. The morphological development responds well to this.

The other factor, input reduction, must be applied manually. The product of discharge and concentration must be multiplied with the factor 2.09, in order to represent the morphological development over the actual real-time time series.

3.5.5 Discharges as nourishment input

Discharge: M,N						
Type: Normal						
Interpolation: Linear						
Time			Flow	Sediment 1		
dd	mm	yyyy	hh mm ss	[m ³ /s]	[kg/m ³]	
01	08	2011	00 00 00	0	0	
18	05	2012	06 17 00	0	0	

Figure 25 Discharges input screen.

To apply continuous nourishments, the option Discharges is used. For this element, a set of input variables is required: a location, a start and end time, a discharge rate (of a mixture of sediment and water) and a concentration of the sediment particles in the discharge (see Figure 25).

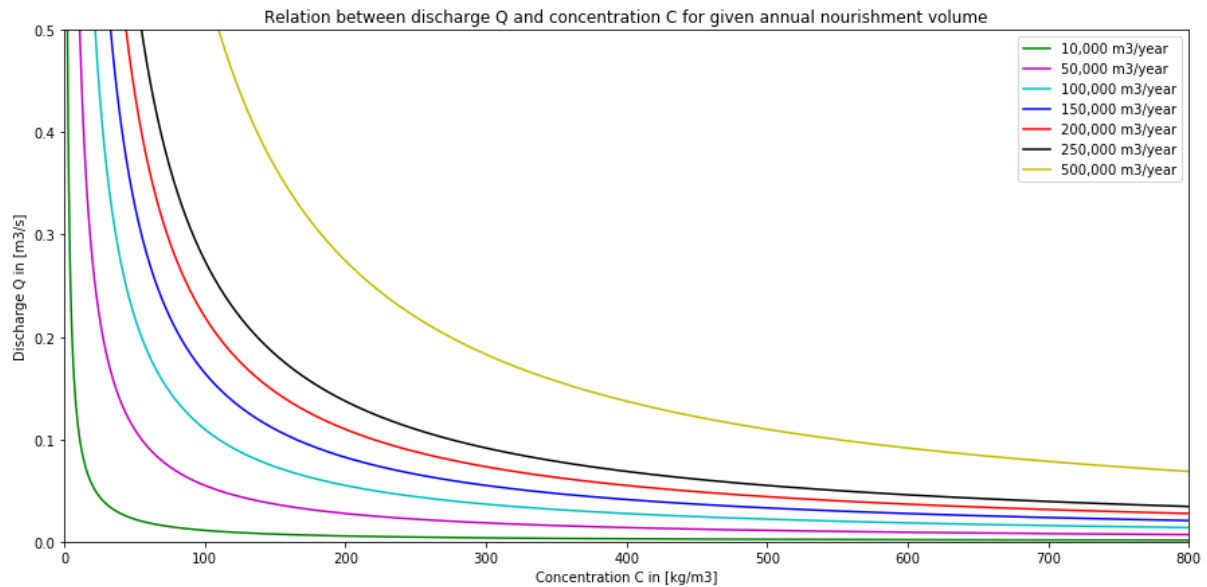


Figure 26 Relation between concentration of sediment particles (in kg/m^3) and discharge rate (in m^3/s), for several annual nourishment volumes. The calculation of this graph is shown in appendix B.1. The variable is the added volume of water: more water decreases the concentration and thus increases the discharge rate, for a constant sediment particle discharge.

The relation between the discharge rate and the concentration of sediment particles is given in Figure 26, for several annual nourishment volumes. The calculation of this graph is summarized in appendix B.1. The values represent a discharge of a mixture of water and sediment disposed out of a pipeline.

A larger discharge rate leads to a smaller density, as more water is added in the pipeline. Adding a small volume of water to the volume of sediment will cause problems regarding settlement of sediment in the pipeline. A large velocity in the pipeline is desired to avoid settlement of sediment particles, which is achieved by a large volume of added water. This decreases the density of the mixture, but the net production remains equal.

In the next paragraph, the simulations are set up and for each simulation a discharge rate and density is applied.

3.6 Model simulations

Table 4 Input values for simulations. Simulation 101 represents the reference situation, without a nourishment.

Simulation-ID	M	N	Depth [m]	Annual nourishment volume [m3]	Discharge rate [m3/s]	Concentration [kg/m3]	Appendix
101	N.A.	N.A.	N.A.	N.A.	N.A.	N.A.	C
502	119	28	3	100'000	0.02071	530	D
503	119	30	4	100'000	0.02071	530	E
501	119	32	5	100'000	0.02071	530	F
504	119	36	6	100'000	0.02071	530	G
301	119	28	3	150'000	0.03107	530	H
401	118	32					
	119	31		100'000	0.02071		
	119	32	5	(per cell: 20'000)	(per cell: 0.004142)	530	I
	119	33					
	120	32					

The simulations that are applied for this research are shown in Table 4. For each simulation, the location in the domain is defined, as well as the depth on which the nourishment is applied. The discharge rate and density are given. The simulations run for 50 days on the simulation time scale. The hydrodynamic time scale then equals 105 days, and the morphodynamic time scale is 314 days. The selection for discharge rate and concentration is done in order to achieve a volumetric concentration of 20%. More information about these parameters is found in appendix B.1.

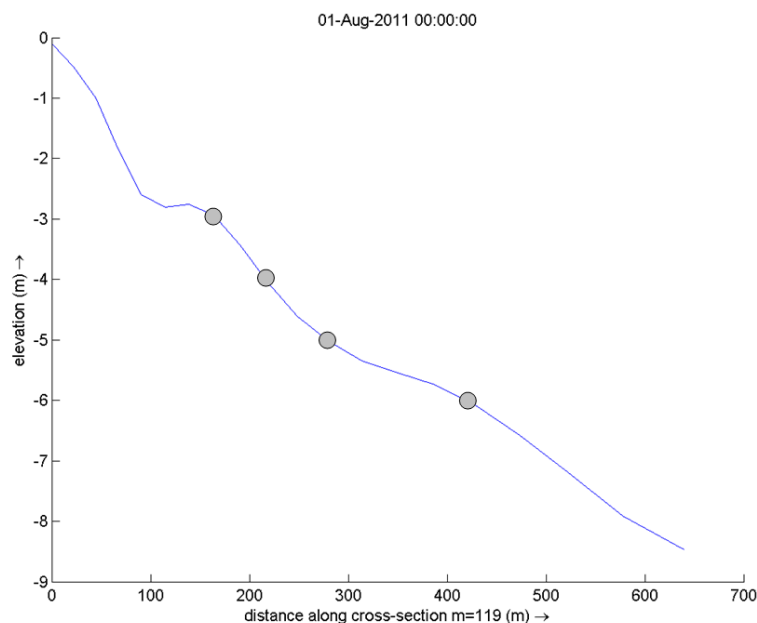


Figure 27 Discharge locations for research part 1. The distance from the shoreline is also visualized.

Figure 27 shows the four discharge locations that are investigated for part 1. The locations are shown as the distance to the shoreline. This distance varies between 150 m and 410 m.

3.7 Chapter Summary

This chapter dealt with the research set-up, the tools that are used and the evaluation criteria that define the optimal configurations of research parameters. The research is divided in three parts: definition of the optimal depth to nourish continuously, the optimal (maximum) nourishment volume that can be supplied at a single location, and research to spreading over multiple disposal locations to enhance sediment transport.

The results are evaluated on the basis of three components: bed level development, mean total transport magnitudes, and redistribution of sediment (erosion and sedimentation patterns). Bed level development is used to investigate the maximum bed levels and possible dry bed levels. The transport magnitudes are used to optimize the amount of redistributed sediment volumes. Erosion and sedimentation patterns help understanding the spatio-temporal redistribution of nourished sediment, which determine the effectivity of the nourishment at a specific depth.

The numerical model Delft3D is used to compute hydrodynamic and morphodynamic processes and morphological behavior under influence of continuous nourishments. The specific model is derived from the Sand Engine prediction model and has been adapted to correctly simulate behavior as a consequence of continuous discharge of sediment into the system. The parameters as used in the initial model are also implemented in this research. The bathymetry measured in August 2011 is used as initial depth. The Delfland coastal stretch is used as research area.

The wave data has been reduced in order to reduce computational time. A reduction of 52% has performed. A morphological acceleration factor equal to 3 is applied, which reduces the computational time even more. The total reduction is a factor 6.27, of which a factor equal to 2.09 is due to wave reduction.

The input parameters under 'Discharges' are set up by achieving a volumetric concentration of 20%, which is commonly used in practice. This leads to a net input value of 530 kg/m^3 for the concentration of the discharge mix. The flow parameter varies with the required annual nourishment volume. The reduction factor of 2.09 is used to multiply the input values of the flow, in order to get the realistic nourishment volume into the model and morphological changes in the model that correspond to the real-time timescale.

Chapter 4: Results

This chapter elaborates on the findings of the different performed simulations and their relation and interaction. The simulations have been analyzed and described in appendices C to I. The research parts as described in paragraph 3.1 are discussed separately. An overall summary concludes this chapter.

Research part 1 explains the observations of the temporal development of bed level, transport magnitudes and alongshore sediment redistribution as a result of nourishing at different depths. A continuous nourishment of $100'000 \text{ m}^3/\text{year}$ is applied at MSL -3.0 m, MSL -4.0 m, MSL -5.0 m, and MSL -6.0 m. The individual observations are elaborated in appendices D, E, F, and G. The evaluation is done on the maximum bed level, mean total alongshore transport magnitudes, and the maximum alongshore spread of sediment after 1 year.

Research part 2 elaborates on the observations of applying a larger annual nourishment volume at MSL -3.0 m, used to define the effects on the maximum bed level and spreading of sediment. Appendix H describes the observations of the nourishment with increased volume.

Research part 3 investigates the change in behavior when disposing the nourishment volume over 5 locations close to each other. Especially the change in longshore sediment redistribution is interesting, as this would lead to an optimization tool for the application of a continuous nourishment.

4.1 Defining the optimal depth

This paragraph discusses the impact of the nourishments applied at four different depths in shallow water. A comparison is made between each individual nourishment and the reference situation (no nourishment applied). This results in a clear view of changes that helps defining the optimal depth. First the four individual nourishments are elaborated, after which a comparative analysis is provided of the four types of nourishments.

4.1.1 Nourishment at MSL -3.0 m

The development in bed level, mean total transport and wave height are discussed in this paragraph. Additional visualizations of the nourishment are summarized in appendix D.1. Appendix D.2 shows the monthly changes in the spatial domain for bed level and mean total transport.

Chapter 4: Results

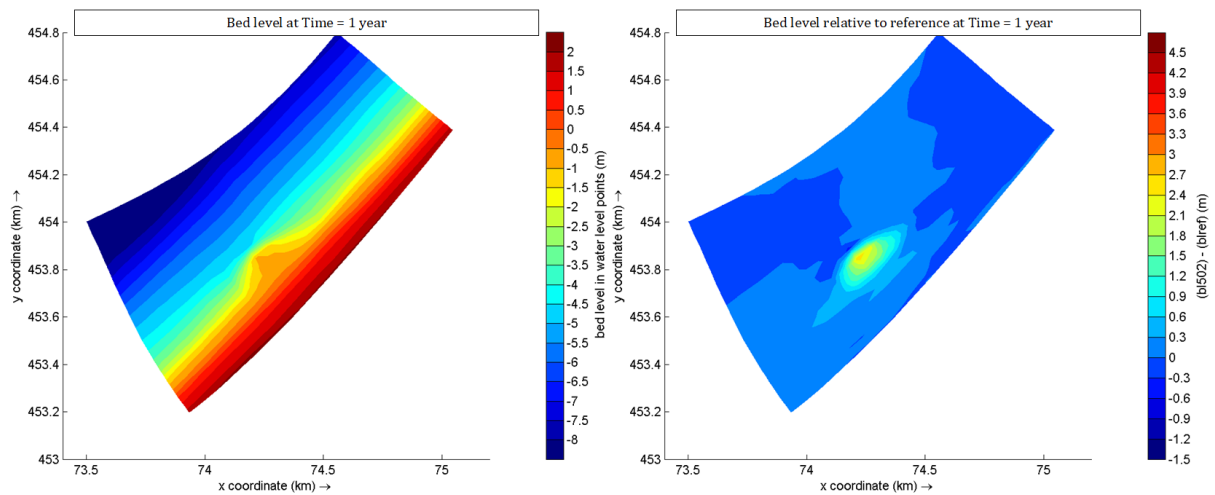


Figure 28 Bed level after 1 year for MSL -3.0 m (left) and relative difference to reference (right). The nourishment develops as a bell-shaped extension of the beach. The relative increase is around the nourishment only, the differences in the rest of the domain are minimal.

The bed level after 1 year, visualized in Figure 28, shows a beach extension with a length of 300 m. The nourishment is bell-shaped, which is logical when considering the initial transport pattern in the surf zone: between MSL -1.0 m and MSL -4.0 m a large longshore transport zone is located. The net difference in bed level relative to the reference situation (right figure in Figure 28) shows this effect as well. Most sediment has been redistributed towards the southwest and northeast, so parallel to the shoreline. The net cross-shore distribution of sediment is smaller, which is caused by the presence of the shoreline close to the nourishment. The volume of sediment redistributed to above the mean water level is significantly small. The shoreline functions as a barrier for cross-shore sediment transport: the cross-shore transport component is negligibly small for bed levels above MSL, which results in minimal volumes of sediment that is transport from the nourishment to the beach.

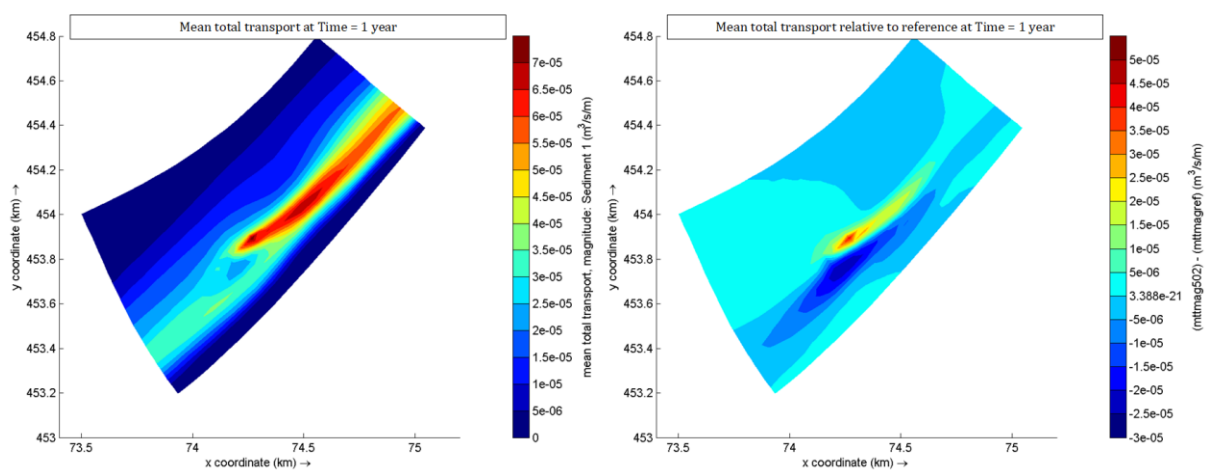


Figure 29 Mean total transport (time-averaged total sediment transport) after 1 year for MSL -3.0 m (left) and relative difference to reference (right). The nourishment causes an increase in transport just downstream in northeast direction. At the transport zone, the magnitude decreases as a result of shadowing.

The mean total transport magnitude (time-averaged total transport magnitude) clearly shows a large transport zone developing just downstream of the nourishment location. Initially a large transport zone was located over the entire domain from southwest to northeast, between MSL -1.0 m and MSL -4.0 m. The transport zone has decreased in magnitude south and east from the nourishment (dark blue colored section in right figure of Figure 29). This is caused by the decrease in wave height and thus wave energy. Waves break earlier at the seaside of the nourishment due to a sudden decrease in depth. The bed slope is relatively steep, which causes this sudden decrease in depth. Waves either break or (partly) reflect on this slope. Wave energy dissipation increases and the significant wave height on and behind the nourishment becomes smaller. These waves generate less turbulence and smaller longshore currents, which reduce the transport capacity of the currents and thus the mean total transport magnitude in the surf zone.

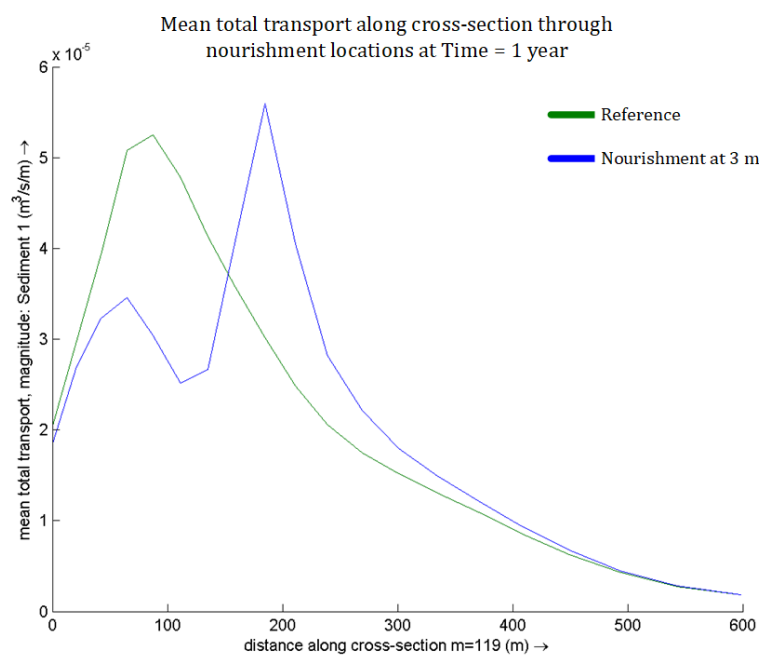


Figure 30 Mean total transport along cross-section of nourishment location at 3 m depth, measured from the shoreline. The blue peak is located at the nourishment location and shows a seaward shift of the transport pattern.

In Figure 30, the cross-shore profile of the time-averaged transport magnitude for nourishing at 3 m depth is shown. The maximum value is shifted seaward due to the disposal of sediment. At a depth of MSL -8.0 m (at 600 m), the transport magnitude is negligibly small. The total transport magnitude for the nourishment case (blue line) is estimated to be 372'000 m³/year.

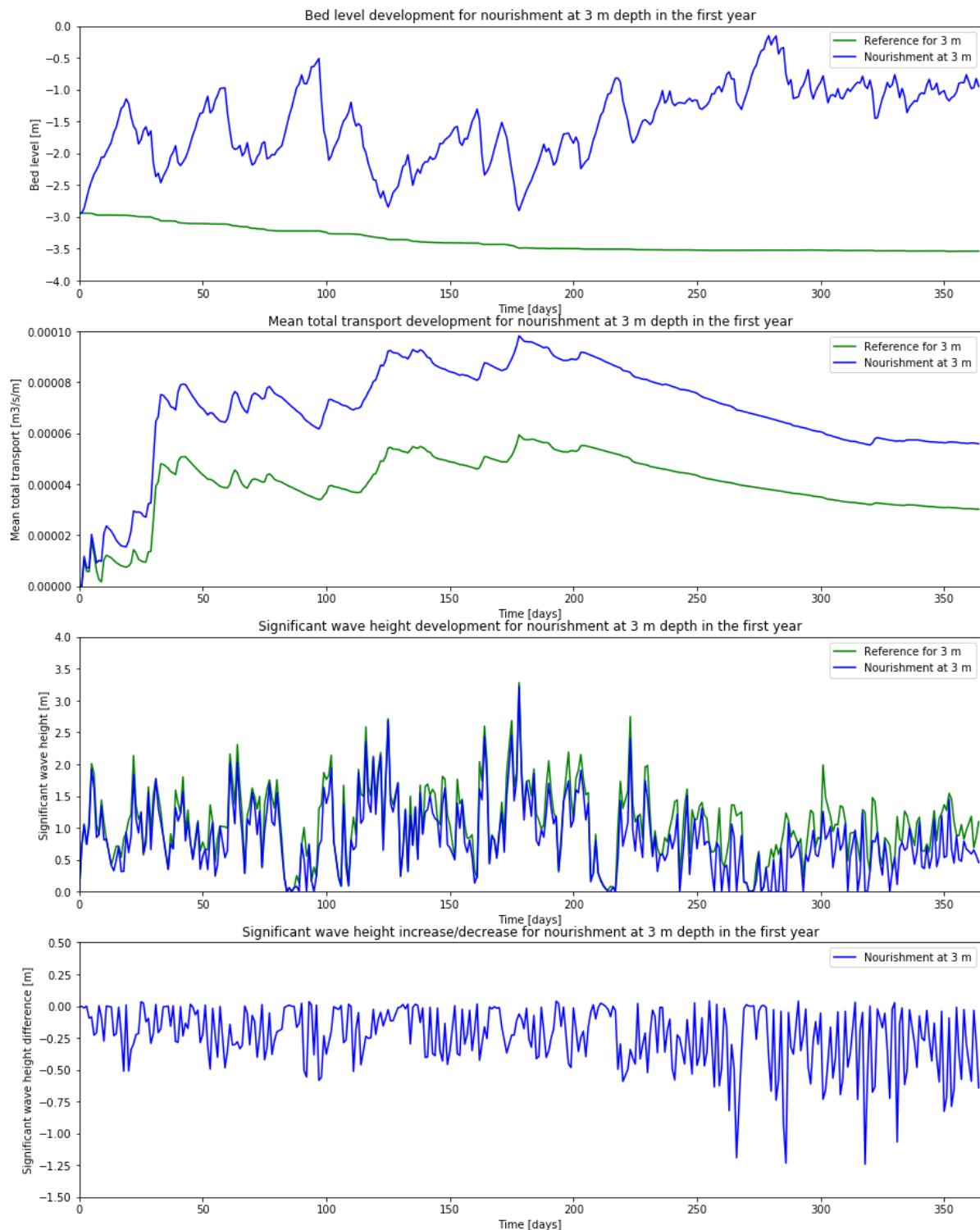


Figure 31 Temporal development of bed level (top), mean total transport (middle) and significant wave height (bottom), measured at the nourishment location. The bed level and transport magnitude increase as a result of the nourishment. The wave height decreases due to the decrease in depth.

The bed level increases to an average height of MSL -1.2 m after 1 year (see Figure 31). Its maximum height is reached after 270 days, at MSL -0.20 m. Sediment transport is around 1.4 l/s, or 44'000 m³/year from the nourishment location. The mean total transport magnitude has increased

with over 70%, due to the presence of the nourishment. The wave height has decreased at the nourishment location, due to a decrease in depth. The decrease is between 0.20 and 0.50 m. Especially waves between 1.0 and 2.5 m decrease in height, the larger waves occurring after 175 days show a smaller decrease. At this moment in time, the bed level equals MSL -2.8 m, and a wave height of over 3.0 m is then less affected by bottom friction.

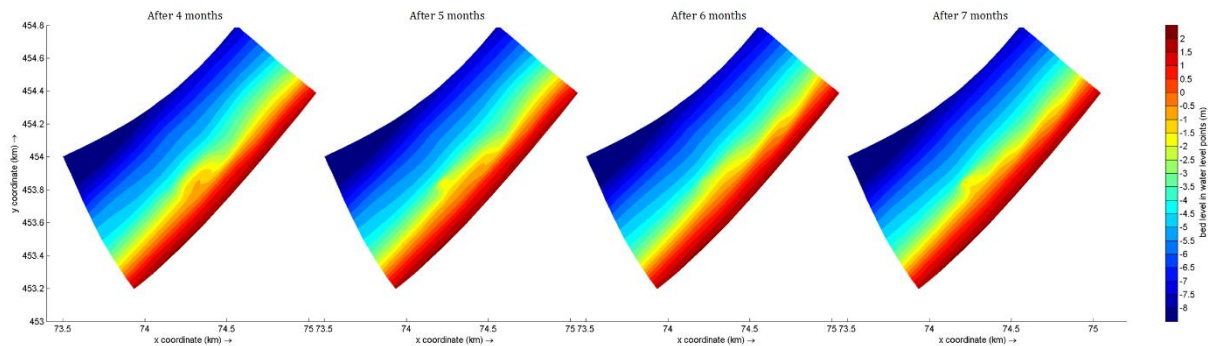


Figure 32 Bed level development after 4, 5, 6, and 7 months for nourishing at 3 m depth. The storm causes significant erosion of the nourishment and flattens the nourishment over a larger area. Appendix D.2 visualizes both bed level and mean total transport after each month.

The monthly situation shown in Figure 32 shows similar development for the spatial domain. Sedimentation of the nourishment location leads to an increase of the nourishment area. Due to large waves, the area is being eroded and flattened. A shoreward distribution of sediment is noticed for every time that this occurs. After 6 months, a large storm occurs and the nourishment has been significantly eroded. The mean total transport magnitude in the domain has significantly increased northeast from the nourishment location. In the second half of the year, wave forcing decreases, which is visible in the redevelopment of the nourishment and in the decrease of the mean total transport magnitude in the domain.

There is a direct relation visible between bed level change, development of the mean total transport magnitude and the significant wave height (see Figure 31). Large wave heights, such as the waves at day 175, cause increased transport. As a result, erosion occurs and the bed level decreases. Calmer wave climates, after 300 days, do not produce large transport magnitudes. Therefore the bed level grows and approaches an equilibrium. An average wave height of 1.0 m will give a fairly constant mean total transport magnitude and thus a fairly constant bed level around MSL -1.2 m.

4.1.2 Nourishment at MSL -4.0 m

The development in bed level, mean total transport and wave height are discussed in this paragraph. Additional visualizations of the nourishment are summarized in appendix E.1. Appendix E.2 shows the monthly changes in the spatial domain for bed level and mean total transport.

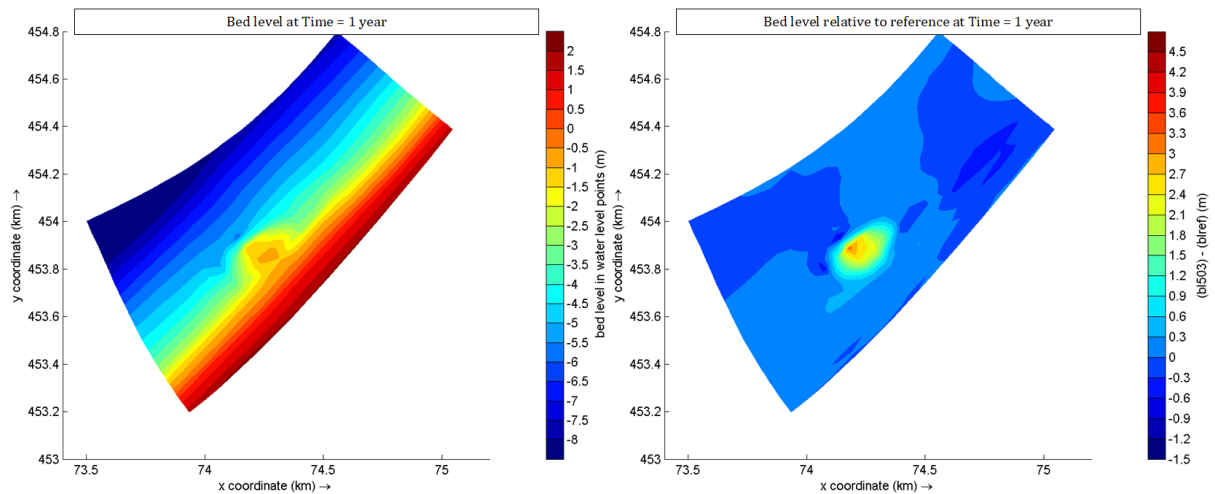


Figure 33 Bed level after 1 year for MSL -4.0 m (left) and relative difference to reference (right). The nourishment develops as an oval-shaped island, connected to the beach. The relative increase is around the nourishment only, the differences in the rest of the domain are minimal.

The nourishment applied at 4 m depth is developing as a small island in front of the shoreline (see Figure 33). The island is connected to the beach over its entire length (= 200 m). The nourishment is oval-shaped. The redistribution of sediment takes place towards the southeast (onshore directed) and northeast (longshore directed). The effect to the rest of the domain are negligible: the depth contours are not affected upstream and downstream of the nourishment. The effect of the nourishment is therefore considered locally within 500 m of the nourishment location.

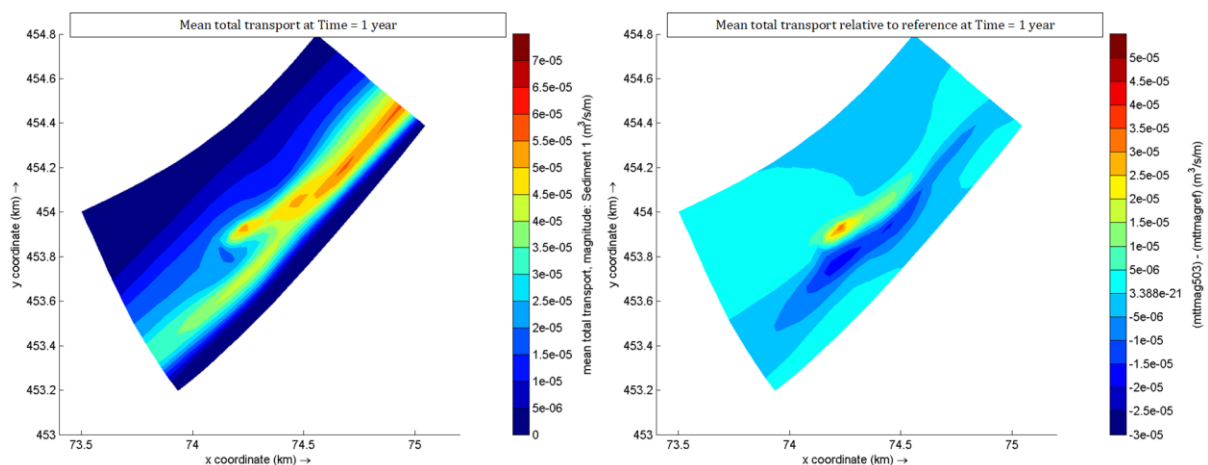


Figure 34 Mean total transport after 1 year for MSL -4.0 m (left) and relative difference to reference (right). The nourishment causes an increase in transport just downstream in northeast direction, although this increase is not significantly large. At the transport zone, the magnitude decreases as a result of shadowing.

There is a large transport magnitude downstream of the nourishment location. The transport zone south and east of the nourishment has decreased in magnitude with 20%, as is visible in Figure 34 (right figure), compared to the reference situation. This is a result of shadowing due to decreased wave breaking, as is already explained in paragraph 4.1.1.

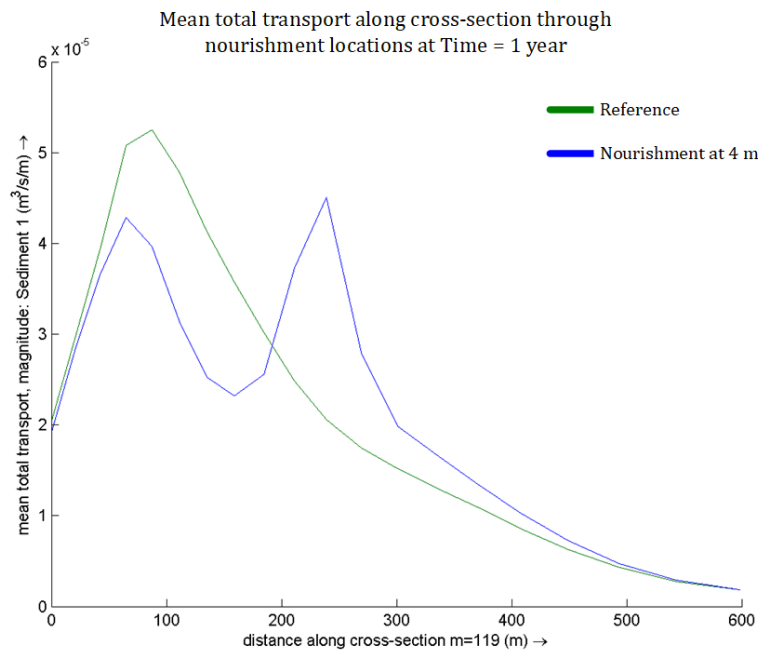


Figure 35 Mean total transport along cross-section of nourishment location at 4 m depth, measured from the shoreline. The blue peaks are almost equal in magnitude.

In Figure 35, the cross-shore profile of the time-averaged transport magnitude for nourishing at 4 m depth is shown. The maximum value is shifted seaward due to the disposal of sediment. A second peak, which is almost equal to the peak at the nourishment location, is found at the peak of the reference simulation. At a depth of MSL -8.0 m (at 600 m), the transport magnitude is negligibly small. The total transport magnitude for the nourishment case (blue line) is estimated to be 375'000 m³/year.

Chapter 4: Results

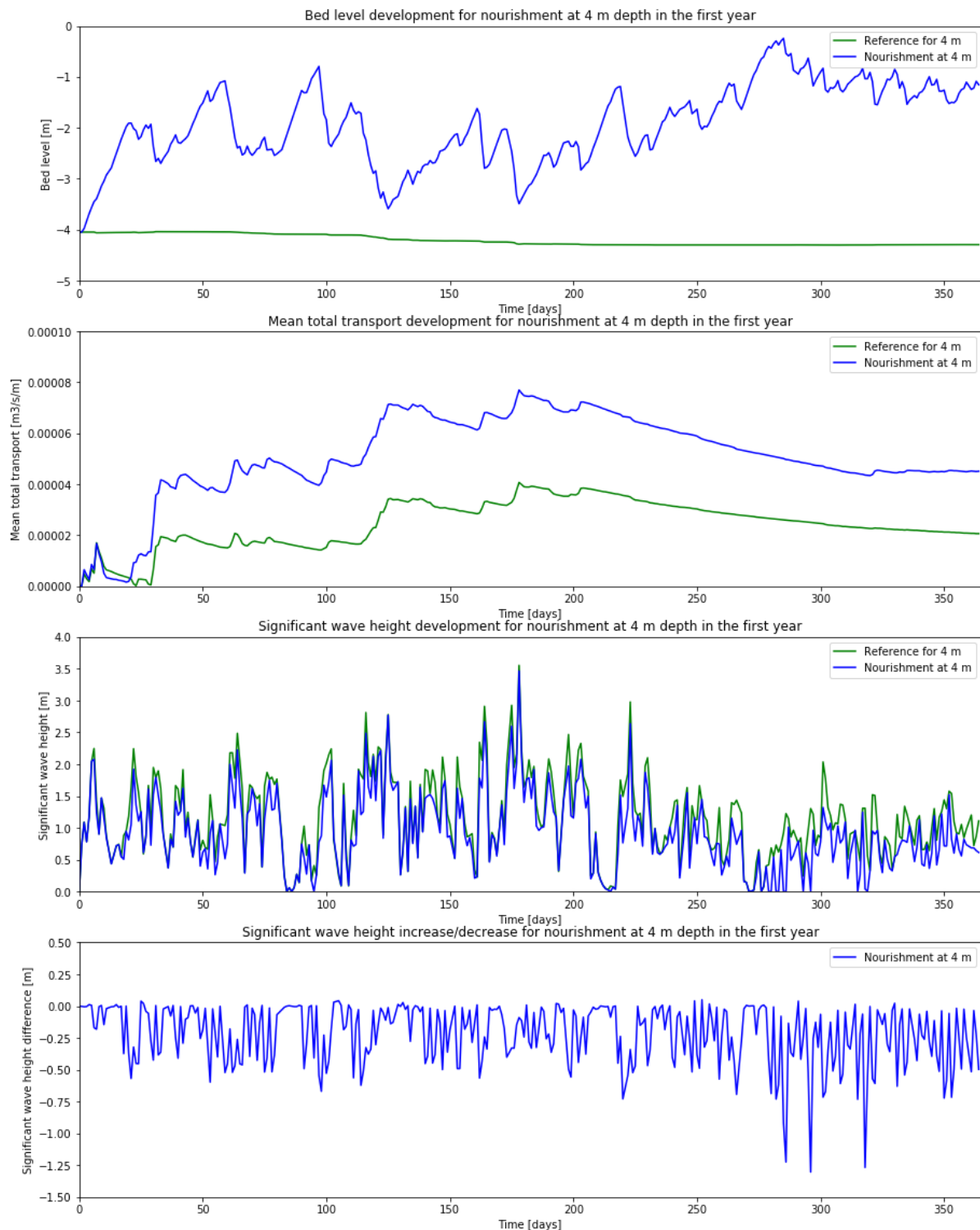


Figure 36 Temporal development of bed level (top), mean total transport (middle) and significant wave height (bottom), measured at the nourishment location. The bed level and transport magnitude increase as a result of the nourishment. The wave height decreases due to the decrease in depth.

The bed level reaches an average height of MSL -1.2 m after 1 year (see Figure 36). The maximum measured value is MSL -0.20 m at day 280. The development in bed level, transport and wave height is similar to that for a nourishment at MSL -3.0 m. The mean total transport magnitude

increased with 140% to a value of 1.2 l/s, or 38'000 m³/year. The wave height decreases for most waves under 2.5 m, due to the decrease in depth.

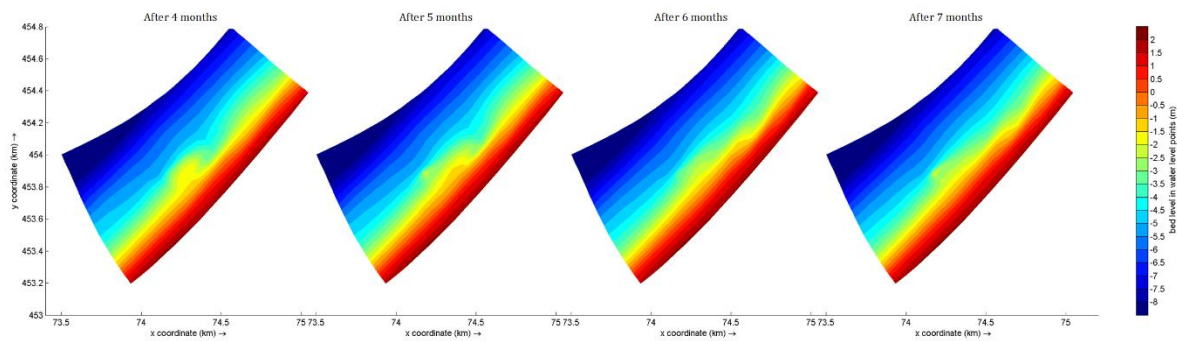


Figure 37 Bed level development after 4, 5, 6, and 7 months for nourishing at 4 m depth. The storm causes significant erosion of the nourishment and flattens the nourishment over a larger area. Appendix E.2 visualizes both bed level and mean total transport after each month.

The monthly situation shown in Figure 37 shows the development for the spatial domain. The nourishment location is located at the edge of the large transport zone. The effect of the large storm halfway the year on the nourishment is less than for the nourishment at MSL -3.0 m, but the nourishment is still flattened significantly. The nourishment initially develops as a small island, but connects to the beach in the last 4 months. It increases in height and forms an island again, where the connection remains at a lower level than the nourishment level. It is likely that in a longer period of time this connection reaches an equal level with the nourishment and eventually causes a beach extension, if the wave climate remains calm as in the last 4 months.

While at the nourishment at MSL -3.0 m the transport magnitude still slightly decreased, the transport magnitude for this nourishment (at 4 m) is stable after 320 days. This occurs as the significant wave height is a bit larger in this period of time, compared to the previous nourishment.

4.1.3 Nourishment at MSL -5.0 m

The development in bed level, mean total transport and wave height are discussed in this paragraph. Additional visualizations of the nourishment are summarized in appendix F.1. Appendix F.2 shows the monthly changes in the spatial domain for bed level and mean total transport.

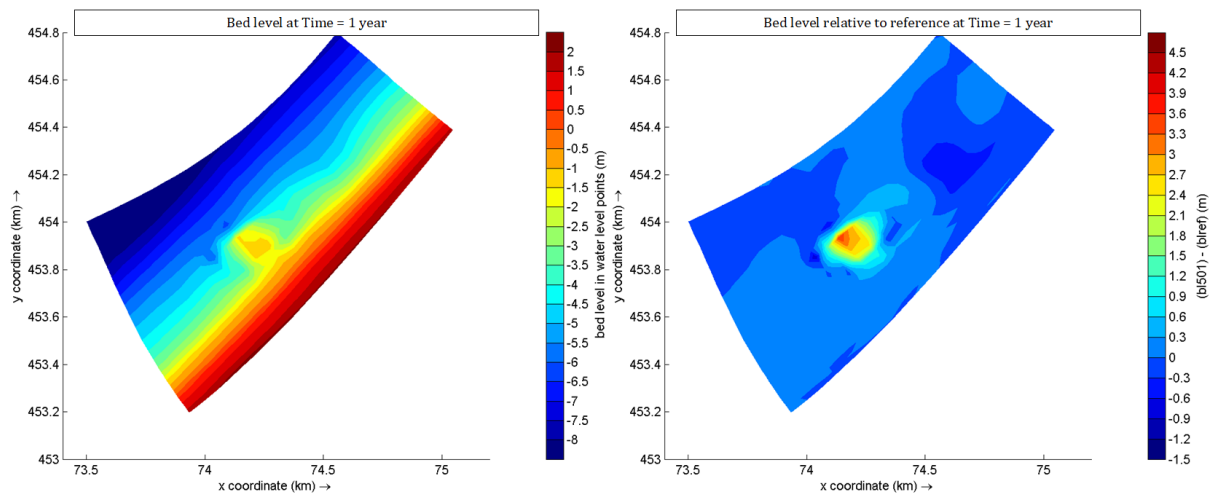


Figure 38 Bed level after 1 year for MSL -5.0 m (left) and relative difference to reference (right). The nourishment develops as a small circular island in front of the shoreline. The depth between the nourishment and the shoreline has slightly decreased. A small extension of the beach near the nourishment is noticed, which can mean that the beach will eventually be connected to the nourishment (e.g. as a tombolo).

The nourishment at MSL -5.0 m develops as an island. The nourishment location is located outside the transport zone and is therefore less influenced by the longshore currents. The alongshore redistribution distance is equal to the cross-shore distance, forced by waves coming from the west-southwest (see also Figure 22). The beach is extending a number of meters towards the nourishment, which is visible in Figure 38 at coordinates X; Y = 74.4; 453.85. The decrease in transport between the nourishment and the shoreline causes this sedimentation. Such an extension will likely form a tombolo: a sand bar which connects the nourishment with the beach.

Different than for the previous two nourishment depths, the depth contours are not parallel northeast from the nourishment. A shoreward shift is noticed around coordinates X;Y = 74.5;454.2. The location of the nourishment in deeper water prevents longshore currents and sediment transport from equalizing the depth to parallel contours.

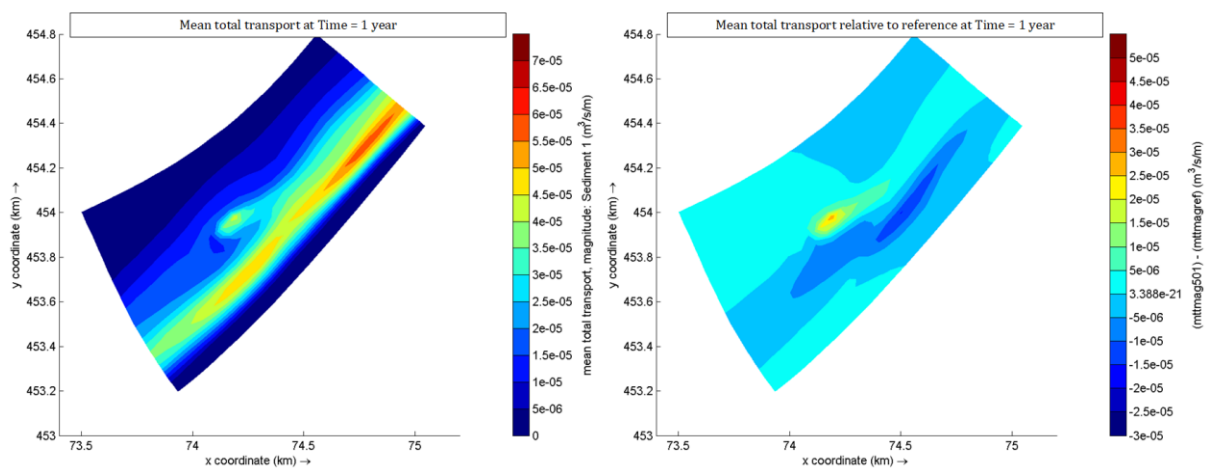


Figure 39 Mean total transport after 1 year for MSL -5.0 m (left) and relative difference to reference (right). The nourishment causes an increase in transport just downstream in northeast direction. At the transport zone, the magnitude decreases as a result of shadowing.

The mean total transport magnitude is large downstream of the nourishment (see Figure 39). The transport zone between the nourishment and the shoreline is decreasing in magnitude as a result of shadowing, with a fraction of 20%. The decrease is not significantly large, because waves are able to redevelop over the fetch behind the nourishment.

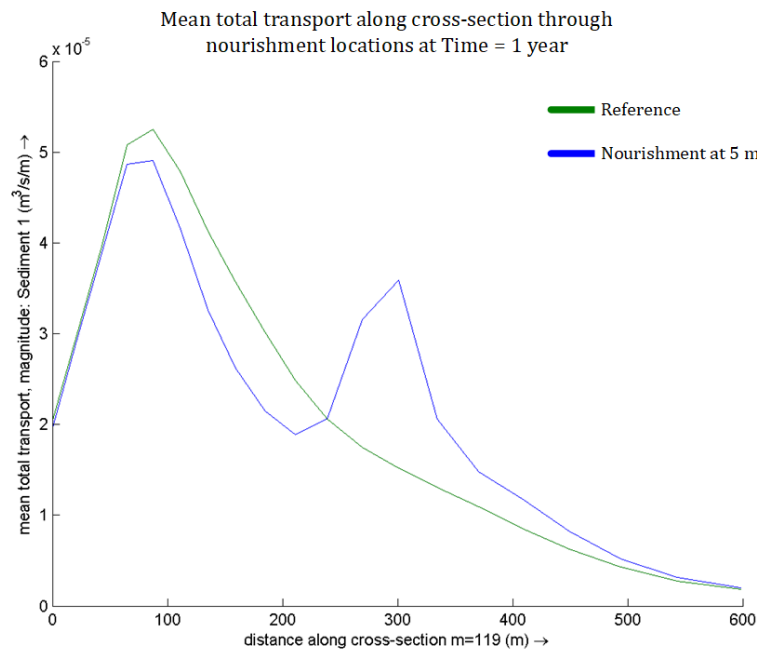


Figure 40 Mean total transport along cross-section of nourishment location at 5 m depth, measured from the shoreline. The blue peak at 100 m is almost equal to the reference transport peak, while the second peak at 300 m is caused by the nourishment. It is likely that the effect of the nourishment on the transport belt at 3 m depth decreases when nourishing in deeper water.

In Figure 40, the cross-shore profile of the time-averaged transport magnitude for nourishing at 5 m depth is shown. The maximum value is found at the location of the transport belt. A second large transport peak is found at the nourishment location. The effect of the nourishment depth on the transport belt is less for this nourishment depth than for 3 and 4 m depth. The total transport magnitude for the nourishment case (blue line) is estimated to be 402'000 m³/year, which is a significant increase. This increase is caused by the transport magnitude at 5 m depth, which is an addition of the transport belt at 3 m depth.

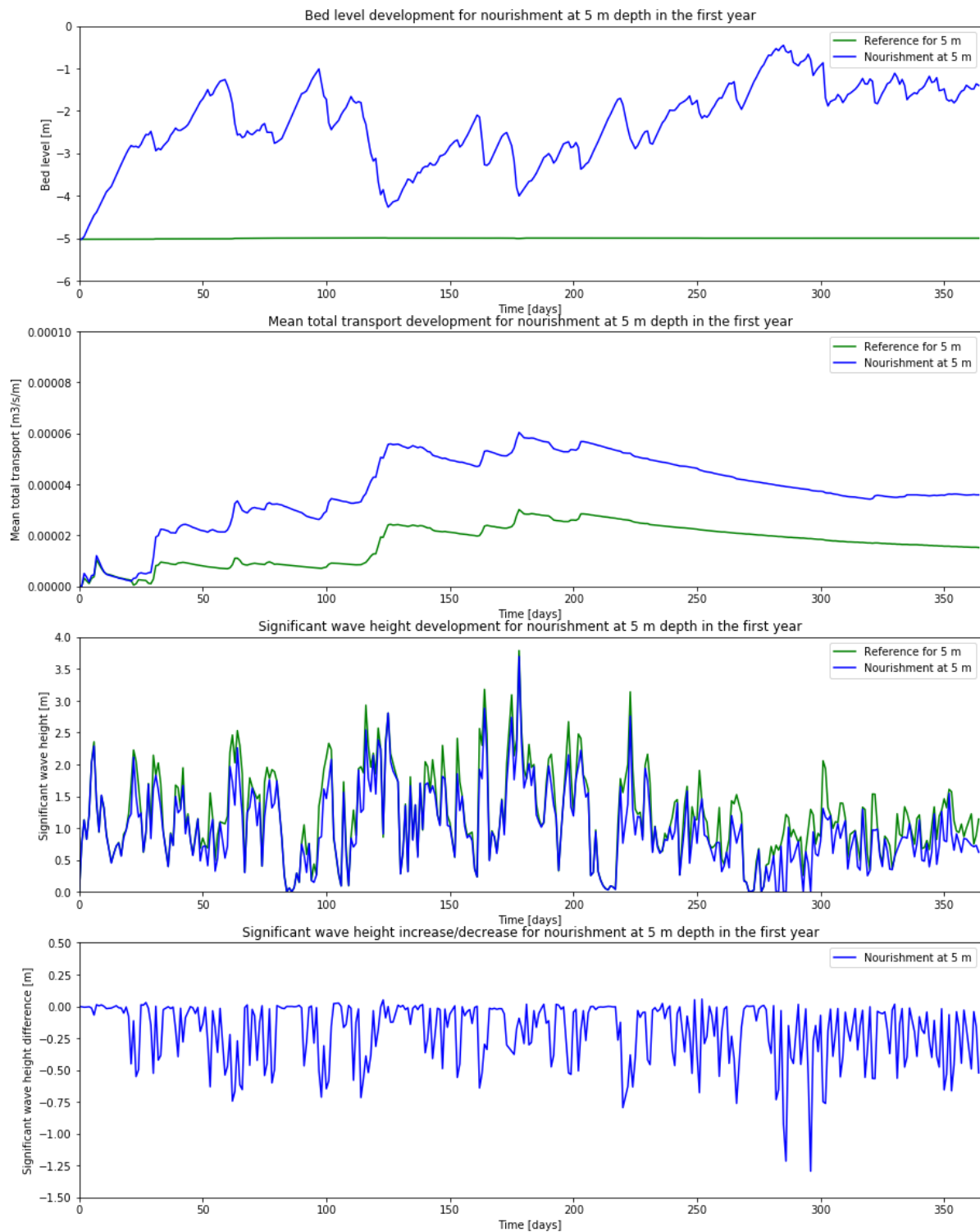


Figure 41 Temporal development of bed level (top), mean total transport (middle) and significant wave height (bottom), measured at the nourishment location. The bed level and transport magnitude increase as a result of the nourishment. The wave height decreases due to the decrease in depth.

The bed level is MS -1.4 m after 1 year (see Figure 41). The maximum height stays just below a level of MSL -0.4 m. The mean total transport magnitude shows similar values for a nourishment at MSL -5.0 m as for MSL -4.0 m, which is 38'000 m³/year.

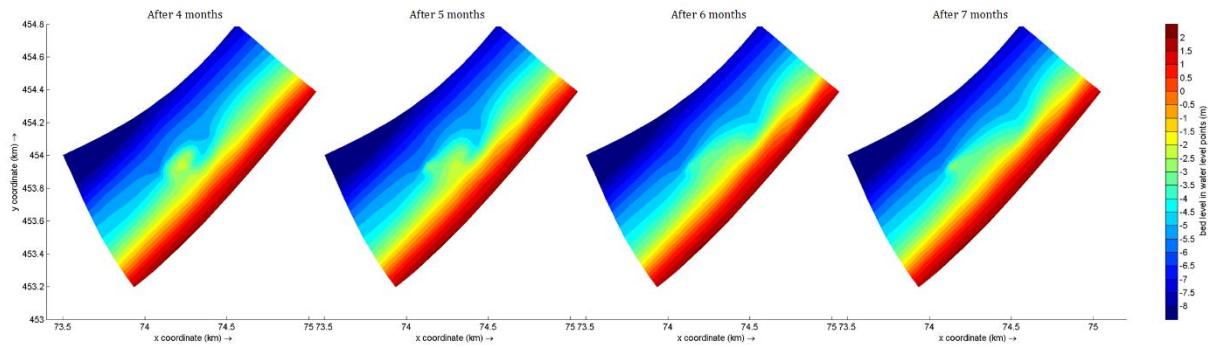


Figure 42 Bed level development after 4, 5, 6, and 7 months for nourishing at 5 m depth. The storm causes significant erosion of the nourishment and flattens the nourishment over a larger area. Appendix F.2 visualizes both bed level and mean total transport after each month.

The monthly situation shown in Figure 42 shows the development in bed level and mean total transport for the spatial domain. The effect of the nourishment on the shoreline is much smaller, mainly because the nourishment is located outside the transport zone. This transport zone remains large for the first months as the nourishment does not have a large effect on wave breaking in this first period of time. That occurs halfway the year, when the large storm causes redistribution of the nourishment towards the shoreline. A part of the nourishment area is now located in the transport zone, which increases the transport magnitude of the transport zone (see 'Mean total transport after 6 months'). In the last months, a spatial development towards an island-shaped nourishment is visible, due to partial absence of large wave forcing and thus a lack of significant erosion.

The temporal pattern is similar to the other two nourishments. This means that wave forcing is the dominant factor for nourishment development. Also for this case, a wave height of 1.5 m causes a stable mean total transport magnitude and bed level.

4.1.4 Nourishment at MSL -6.0 m

The development in bed level, mean total transport and wave height are discussed in this paragraph. Additional visualizations of the nourishment are summarized in appendix G.1. Appendix G.2 shows the monthly changes in the spatial domain for bed level and mean total transport.

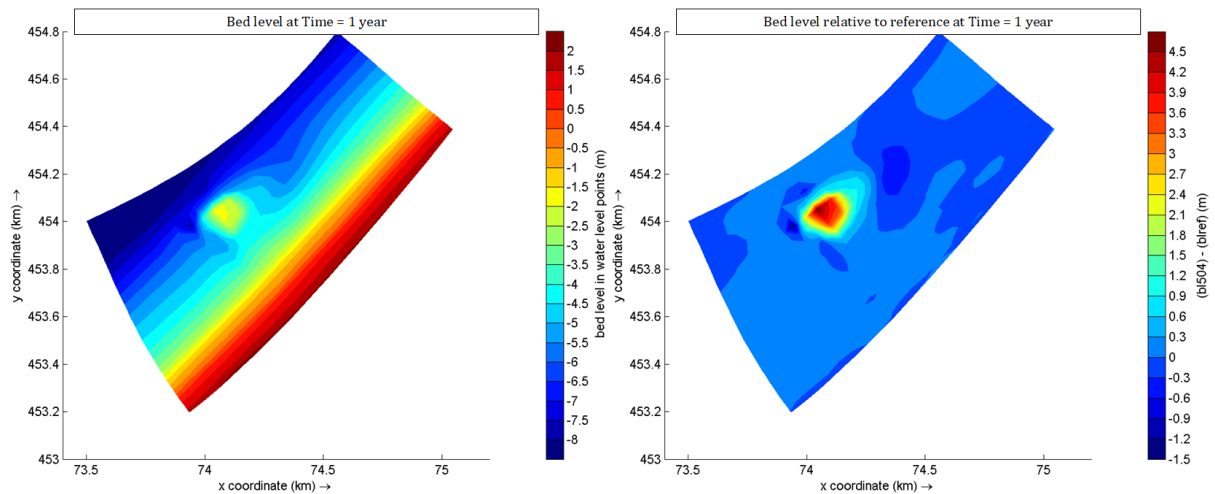


Figure 43 Bed level after 1 year for MSL -6.0 m (left) and relative difference to reference (right). The bed level differences are centered on the nourishment. The nourishment seems not to affect the zone between the nourishment and the shoreline.

The nourishment develops as a circular island. It does not affect the surrounding domain. The bed level differences shown in the right figure of Figure 43 are less than 0.5 m for the entire domain except the nourishment location. The effects of wave forcing are significantly small at this depth: waves do not break yet, which does not generate strong currents near the nourishment. As most waves are below 2.5 m height, a depth of 6 m will prevent waves to break due to bottom friction.

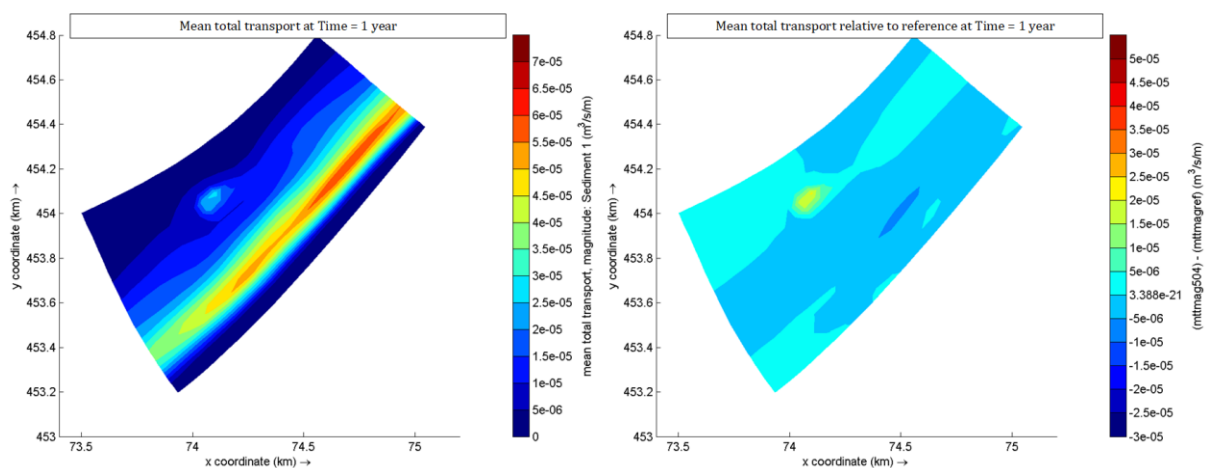


Figure 44 Mean total transport after 1 year for MSL -6.0 m (left) and relative difference to reference (right). Transport from the nourishment is small compared to the magnitudes in the transport zone between MSL -1.0 m and MSL -4.0 m. The differences with the reference situation are negligibly small.

The mean total transport magnitude near the nourishment is pretty small compared to the transport magnitudes of the other 3 nourishment depths (see Figure 44). The transport zone between MSL -1.0 m and MSL -4.0 m is hardly affected, compared to the reference situation. The effect of the nourishment is therefore mainly bounded around the depth of 6 m. In alongshore direction there is hardly any difference noticed as well.

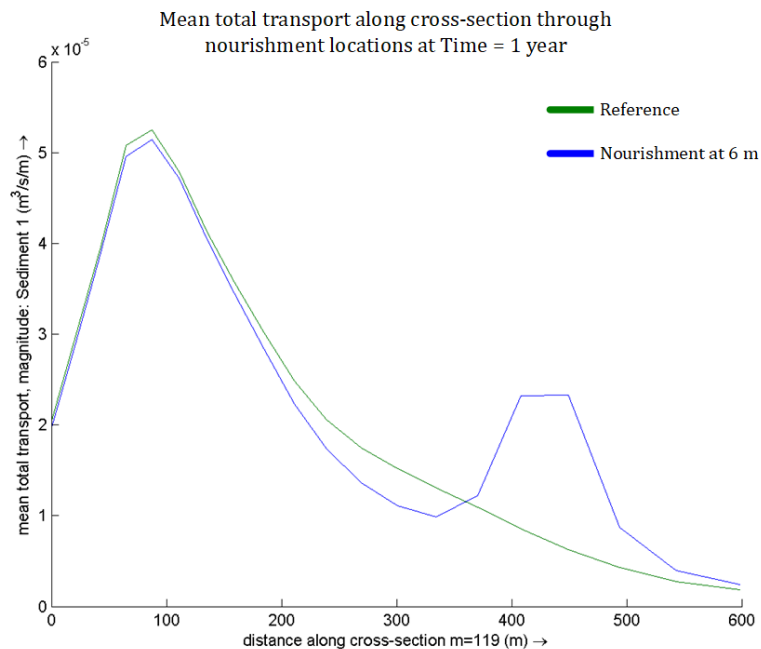


Figure 45 Mean total transport along cross-section of nourishment location at 6 m depth, measured from the shoreline. The blue peak at 100 m is equal in magnitude. A second peak at the nourishment location shows an increase of 200%.

In Figure 45, the cross-shore profile of the time-averaged transport magnitude for nourishing at 6 m depth is shown. The maximum value is found at the location of the transport belt and is equal to the reference value. A second large transport peak is found at the nourishment location. The effect of the nourishment depth on the transport belt is less for this nourishment depth than for shallower depths. The total transport magnitude for the nourishment case (blue line) is estimated to be 413'000 m³/year, which is a significant increase.

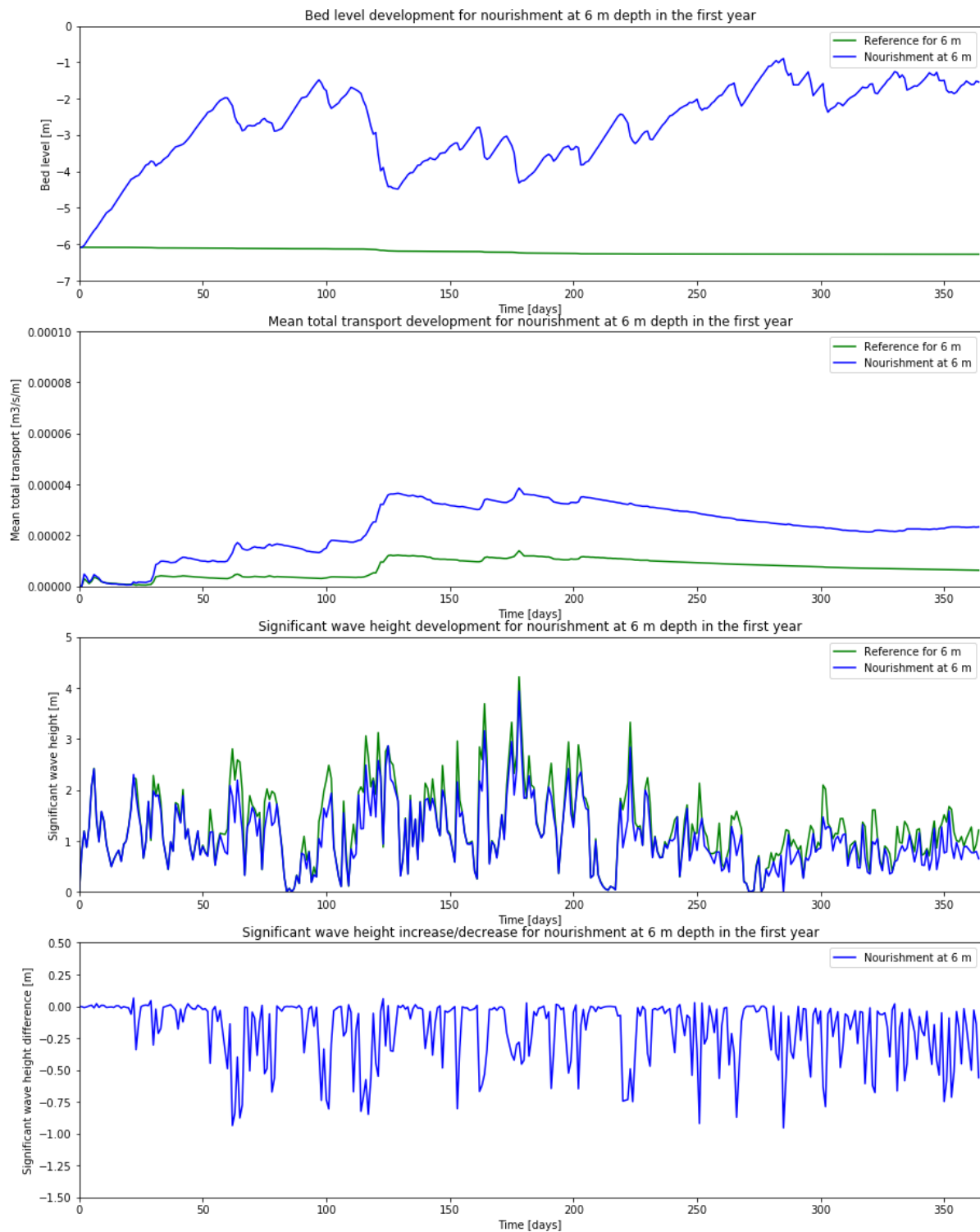


Figure 46 Temporal development of bed level (top), mean total transport (middle) and significant wave height (bottom), measured at the nourishment location. The bed level and transport magnitude increase as a result of the nourishment. The wave height decreases due to the decrease in depth.

The bed level reaches a level of MSL -1.5 m after 1 year (see Figure 46). The transport magnitude is on average 1.0 l/s (= 31'000 m³/year) and has increased with 200%. Although the effect of wave forcing at a depth of 6 m is minimal, the decreased depth at the nourishment still reduces the

significant wave height with 0.5 m at maximum. The temporal behavior of the bed level, transport magnitude and wave height is similar to that of the previous three nourishment depths.

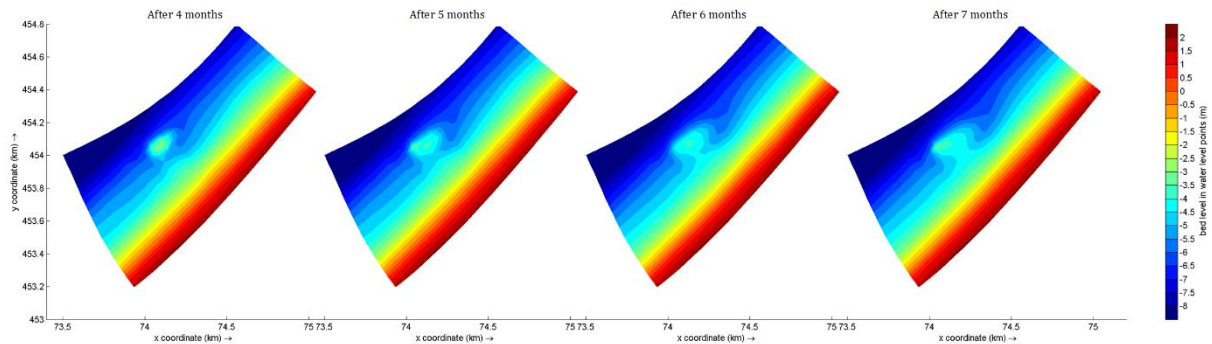


Figure 47 Bed level development after 4, 5, 6, and 7 months for nourishing at 6 m depth. The storm causes significant erosion of the nourishment and flattens the nourishment towards the shoreline. Appendix G.2 visualizes both bed level and mean total transport after each month.

The monthly situation shown in Figure 47 shows the development for the spatial domain. It is confirmed that the nourishment has hardly an effect on the shallow surf zone. The large storm after 6 months shows an onshore shift of the nourishment, which has a small influence on the morphological behavior in the shallow parts of the domain. The large volume of sediment eventually occurs a seaward shift of the depth contour at MSL -4.0 m, which curves around the seaside of the nourishment after 1 year. However, the effect of the nourishment of the coastline is significantly small: it can be concluded that at a depth of MSL -6.0 m and deeper a nourishment is not effective on the short-term.

Chapter 4: Results

4.1.5 Comparison of 4 nourishment depths

The four nourishment depths are compared on the development of bed level, mean total transport magnitude and significant wave height. Their individual results have been described in paragraphs 4.1.1 to 4.1.4.

Differences in time

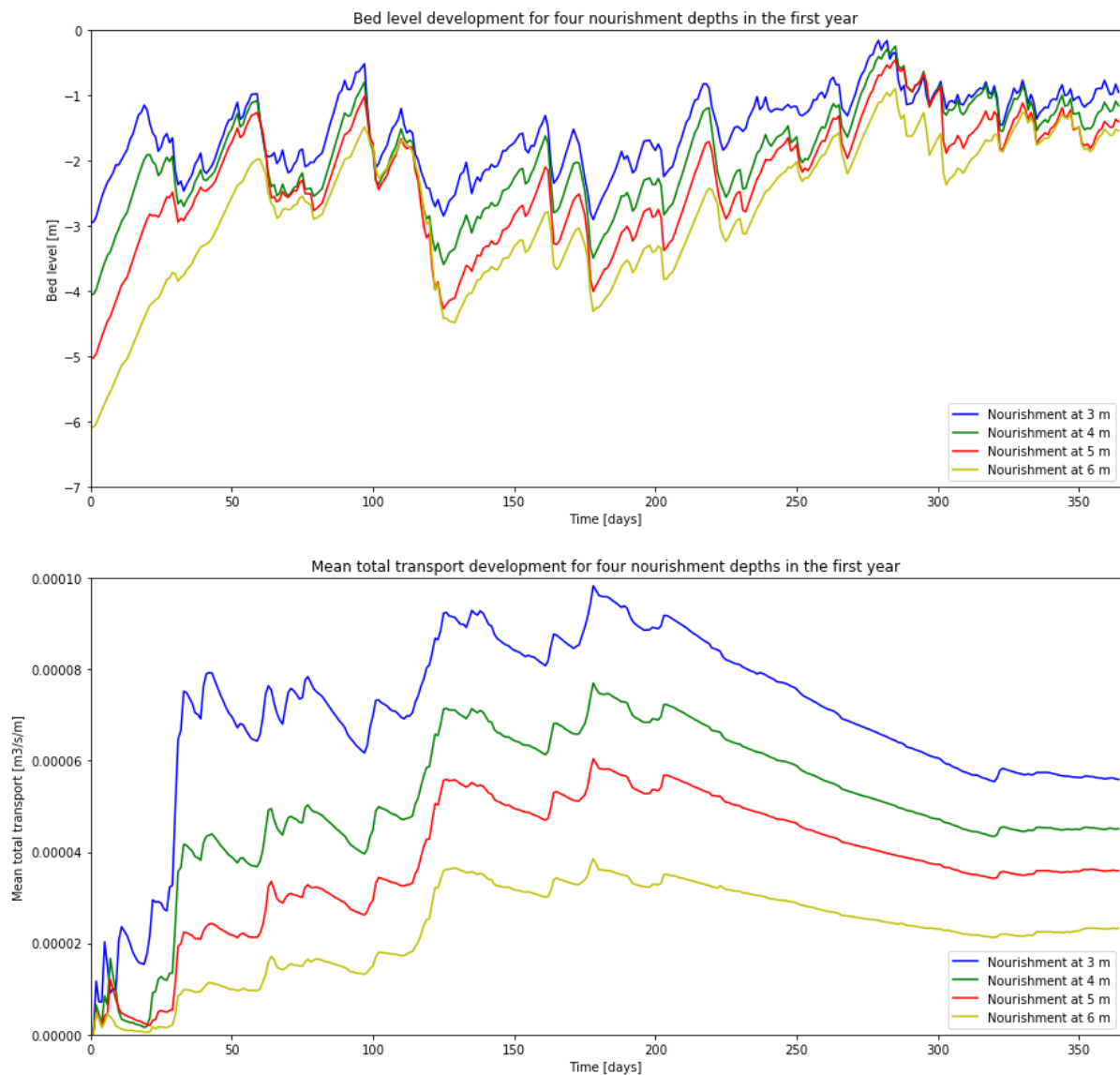


Figure 48 Temporal development of bed level and mean total transport magnitude for the four nourishment depths.

The temporal behavior is equal for all four depths, which is a result from the used wave climate (see Figure 48). The wave height is largest for the nourishment at MSL -6.0 m, as this nourishment is located in the deepest water. The mean total transport magnitudes respond to the wave climate. The depth is an important factor in determining the height of the transport magnitude. In shallow water,

most waves break, while in deeper water only the largest waves break due to bottom friction. This explains the maximum transport magnitude at 3 m considering all depths.

In the transport zone between MSL -1.0 m and MSL -4.0 m, most waves break which causes energy dissipation and turbulence and therefore longshore currents with a larger transport capacity (due to dissipation). The transport intensity at MSL -3.0 m is therefore larger than at the other three depths.

The bed level instantly responds to varying transport magnitudes. When the transport magnitude increases, erosion occurs and the bed level decreases, and vice versa. The bed level at 3 m is largest in time, although the differences are small. The quick raise of the bed level is due to the large supply rate of sediment for the nourishment. Large waves, mostly occurring during storms, cause erosion which reduces the bed level with 3.5 m at maximum for the nourishment at MSL -6.0 m after 120 days. The effect for the nourishment at MSL -3.0 m is smaller, as this nourishment is more covered by the surrounding area. The maximum erosion level is determined by the maximum depth of the area around the nourishment: erosion occurs up to MSL -3.0 m.

The degree of erosion is thus dependent on the available volume of sediment, the wave height over the nourishment, the bed slope of the nourishment and the bed level of the surrounding area. If all four criteria are large, then the erosion degree is large as well. A steep bed slope is an indication of a high nourishment bed level relative to the surrounding area. Waves reflect more on this steep slope, which causes a smaller transport magnitude than for cases with a more fluent bed slope. In the latter case, waves propagate more easily over the nourishment and then break due to a decrease in depth and increased bottom friction. This increases the local transport magnitude.

Differences in spatial domain

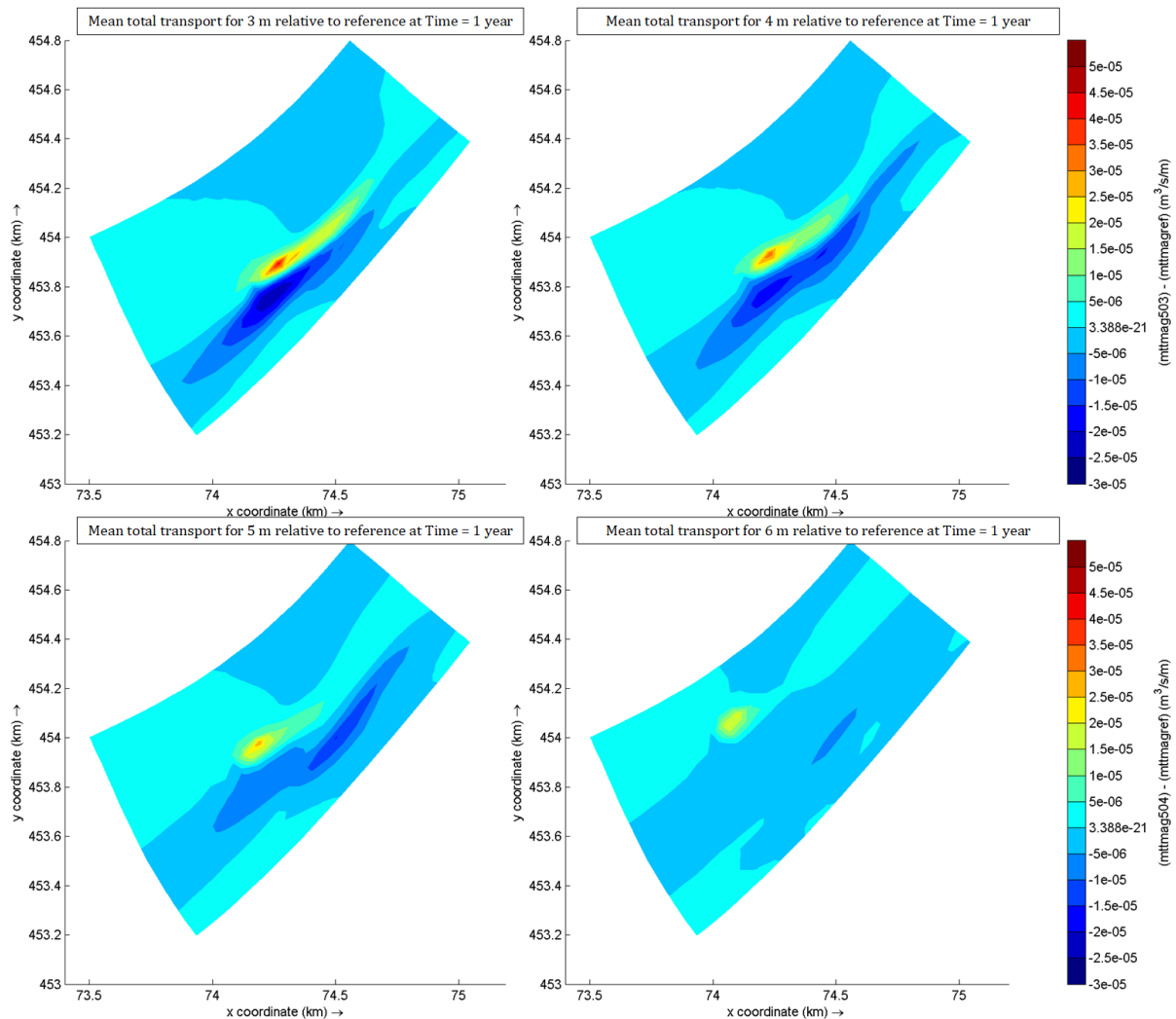


Figure 49 Mean total transport relative to reference situation for the 4 nourishment depths.

There are differences in the spreading of sediment of the nourishments (see Figure 49). The nourishment at 3 m is partially blocked by the shoreline, as there is no cross-shore sediment transport onto the beach measured. The spreading of sediment of the nourishment at MSL -6.0 m is relatively small compared to the other three nourishments. The nourishments at MSL -3.0 m and MSL -4.0 m show similar behavior in spreading (see Figure 49). The relative decrease in magnitude is smaller for the nourishment at MSL -5.0 m, compared to the MSL -3.0 m and MSL -4.0 m.

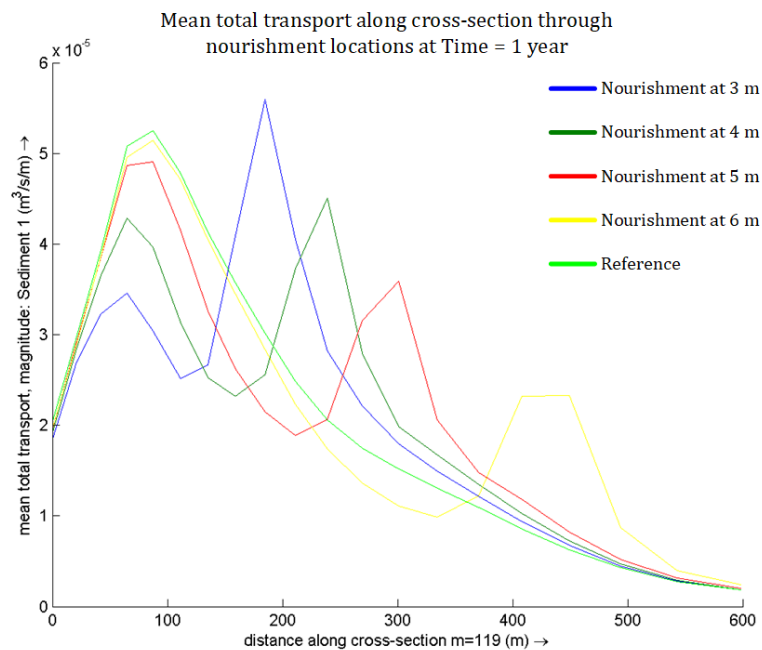


Figure 50 Mean total transport along cross-section of all nourishment locations, measured from the shoreline. The influence on the transport belt of the nourishment at 3 m and 4 m depth is large. The maximum transport magnitude at the nourishment location decreases with increasing depth.

Figure 50 shows the cross-shore distribution of the mean total transport magnitude for all four nourishment depths and the reference simulation. The influence of the nourishments at 3 m and 4 m depth on the transport belt are large. The shadow-effect as was already visible in the spatial figures is clearly present. Remarkable is the decrease in transport magnitude when nourishing in deeper water (6 m). This occurs due to a decrease in wave forcing at that location, in combination with large height differences between the nourishment and the surrounding area, which generates more reflection of waves instead of shoreward propagation and breaking of waves. The reference transport magnitude over this cross-section equals 386'000 m³/year. The order of magnitudes for the four nourishment simulations are listed below:

- 3 m: 372'000 m³/year
- 4 m: 375'000 m³/year
- 5 m: 402'000 m³/year
- 6 m: 413'000 m³/year

As was already shown in Figure 50, deeper located nourishments do less affect the transport belt and therefore add to the transport intensity over the cross-section. The transport intensity has decreased for the nourishment simulations at MSL -3.0 m and MSL -4.0 m, mainly as a result of the shadow-effect of wave forcing.

Table 5 Sediment redistribution distance in alongshore and cross-shore direction for the 4 nourishment depths. The values are retrieved from the bed level figures in paragraphs 4.1.1 to 4.1.4.

Depth [m]	Total alongshore distance [m]	Of which northeast directed (downstream) [m]	Total cross-shore distance [m]	Of which shoreward directed [m]
3	580	260	210	150
4	360	220	240	170
5	330	210	280	210
6	360	260	250	180

The effect of a nourishment is partly determined by the maximum redistribution distance of sediment in alongshore direction. As retrieved from Table 5, the alongshore redistribution distance is largest for a nourishment at MSL -3.0 m, around 500 m, which is explained by the presence of this nourishment in the transport zone. The alongshore distance decreases with increasing depth, as the longshore current decreases in magnitude with increasing depth. The nourishments of 4 m and 5 m are partly affected by the transport zone, because the cross-shore redistribution reaches into the transport zone. This enhances the longshore redistribution of the two nourishments. The nourishment at 6 m is almost isolated from the transport patterns. The redistribution distances are smallest for this nourishment.

The effect of the nourishments on the transport zone is different as well. The nourishment at MSL -3.0 m affects this transport zone significantly: the magnitude reduces south and east from the nourishment and increases northeast, most of all nourishments. The deeper the nourishment is located, the less affected the transport zone is. Up to a nourishment at MSL -5.0 m, differences in magnitude still occur. The nourishment at MSL -6.0 m hardly affects the transport zone.

The relatively large cross-shore redistribution in the first year is mainly caused by strong cross-shore currents. An earlier study has shown similar results in the behavior of nourishments in the foreshore (Huisman, 2019). This study has shown that due to the abrupt change in environment, wave velocities become more asymmetric, which increases the rate of erosion in onshore direction. This phenomenon explains the onshore redistribution for the four nourishment depths.

4.2 Increase of the annual nourishment volume

This paragraph discusses the change in behavior of the nourishment when the annual volume is increased to 150'000 m³/year. The definition of the transport capacity is now governing, as the nourishment volume is closer to the annual transported volume of sediment along the Delfland coastal stretch (= 250'000 m³/year). The limitations that occur here give insight in the maximum volume of sediment that can be disposed at a single location. First the individual nourishment with increased volume is elaborated. Subsequently, the similarities and differences with the smaller volume (100'000 m³/year) is discussed.

4.2.1 Nourishment of 150'000 m³/year at 3 m depth

The development in bed level, mean total transport and wave height are discussed in this paragraph. Additional visualizations of the nourishment are summarized in appendix H.1. Appendix H.2 shows the monthly changes in the spatial domain for bed level and mean total transport.

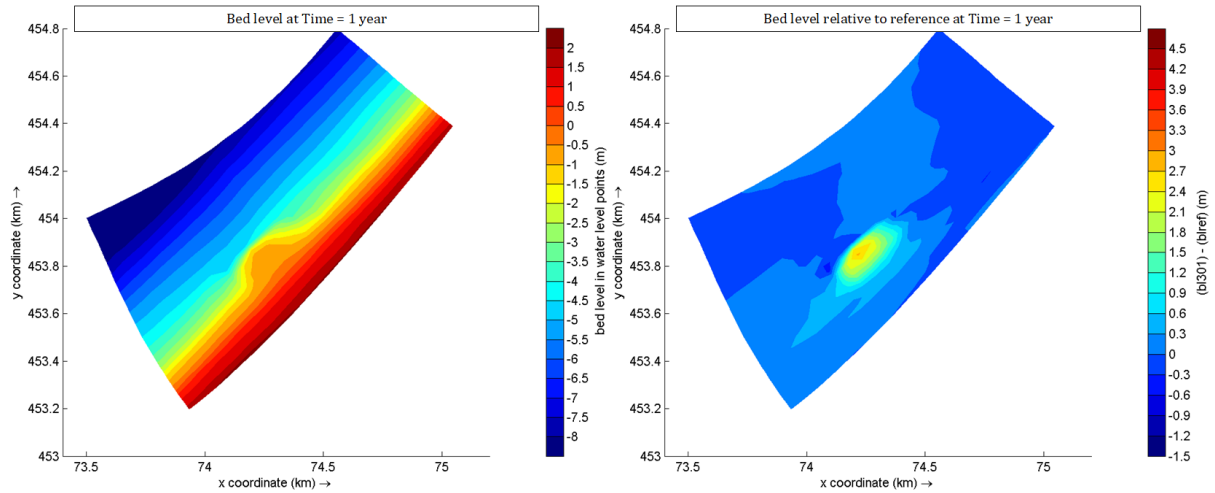


Figure 51 Bed level after 1 year for a discharge of 150'000 m³/year (left) and relative difference to reference (right). The nourishment develops as a bell-shaped extension of the beach. The relative increase is around the nourishment only, the differences in the rest of the domain are minimal. A shallow plume is travelling to the southwest.

The bed level around 3 m depth visualizes a significant extension of the beach (see Figure 51). The seaside of the nourishment reaches to the MSL -4.0 m depth contour. The nourishment is developing as a bell-shaped extension. The redistribution of sediment has increased in southwest direction in the shape of a shallow plume. Erosion has occurred seaward of the nourishment as a result of wave energy dissipation.

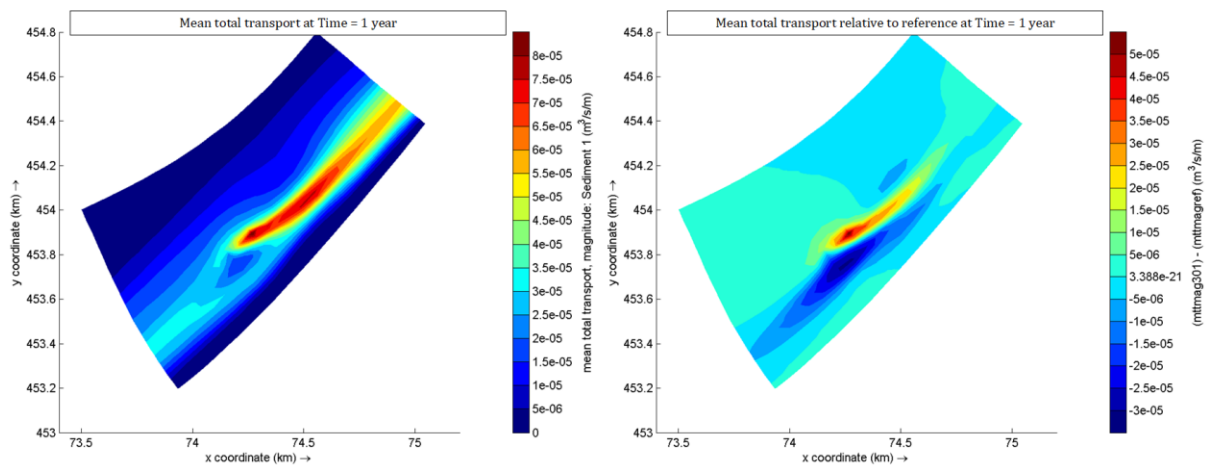


Figure 52 Mean total transport after 1 year for a discharge of 150'000 m³/year (left) and relative difference to reference (right). The nourishment causes an increase in transport just downstream in northeast direction. At the transport zone, the magnitude decreases as a result of shadowing.

The mean total transport magnitude has increased due to the nourishment (see Figure 52). South from the nourishment, the relative decrease is significantly large. The nourishment has become significantly large, which has caused more wave energy dissipation. Therefore the transport magnitude has decreased relative to the reference situation.

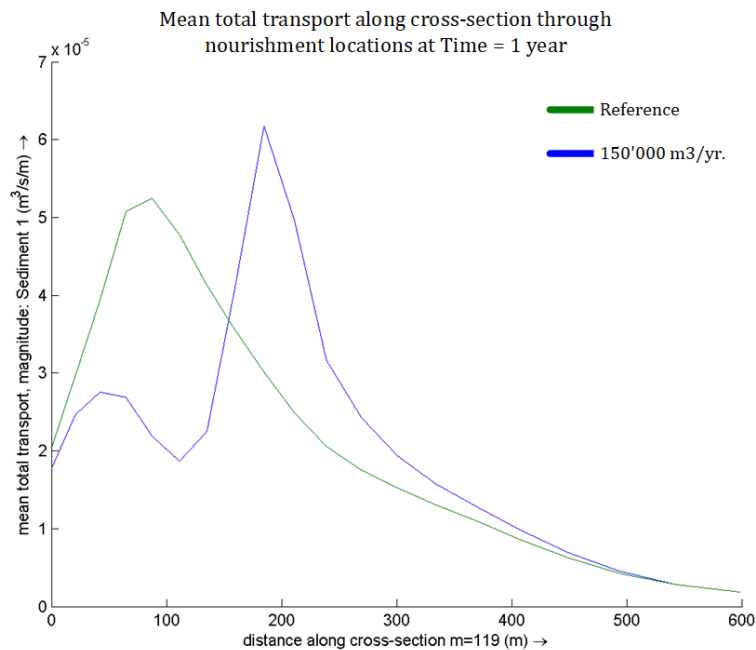


Figure 53 Mean total transport along cross-section of nourishment location at 3 m depth with increased nourishment volume, measured from the shoreline. The transport peak at 3 m depth is significantly larger than the reference peak at 2 m depth.

Figure 53 shows the cross-shore profile of the time-averaged transport magnitude for nourishing of 150'000 m³/year at 3 m depth. The maximum value is found at the nourishment location and is significantly larger than the reference transport peak. The shadow-effect is clearly visible as the transport magnitude at the transport belt has decreased significantly. The total transport magnitude for the nourishment case (blue line) is estimated to be 323'000 m³/year, which is a significant decrease relative to the reference magnitude (i.e. 386'000 m³/year).

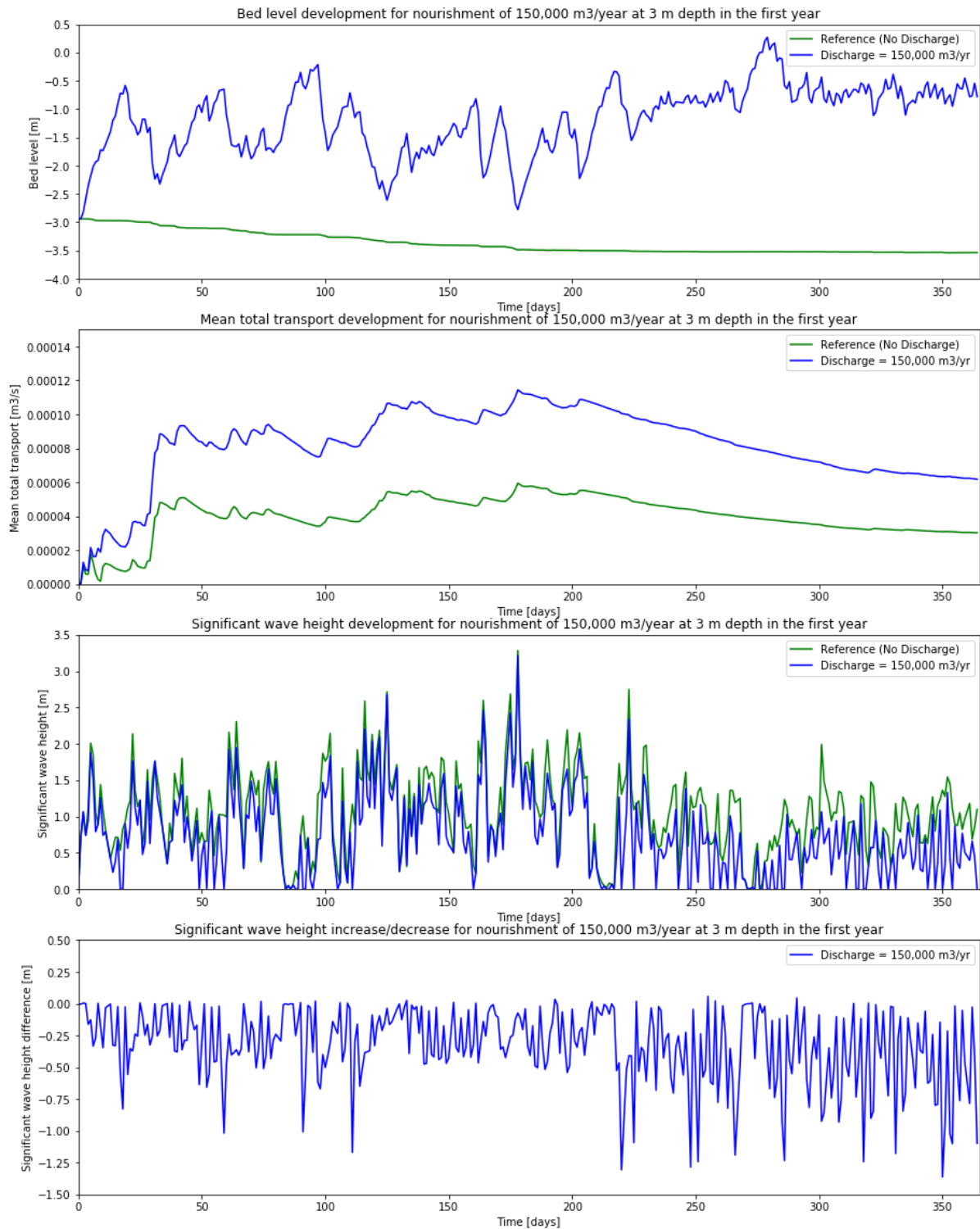


Figure 54 Temporal development of bed level (top), mean total transport (middle) and significant wave height (bottom), measured at the nourishment location. The bed level and transport magnitude increase as a result of the nourishment. The wave height decreases due to the decrease in depth.

The bed level has developed to a value of MSL -0.7 m (see Figure 54). The bed level has exceeded the mean water level for a couple of days after 280 days. The mean total transport magnitude at the nourishment location is significantly larger than for the reference situation. The year-

averaged transport magnitude is 1.5 l/s, or 47'000 m³/year, which is an increase of 80% of the reference transport magnitude. The wave height has decreased due to the presence of the nourishment.

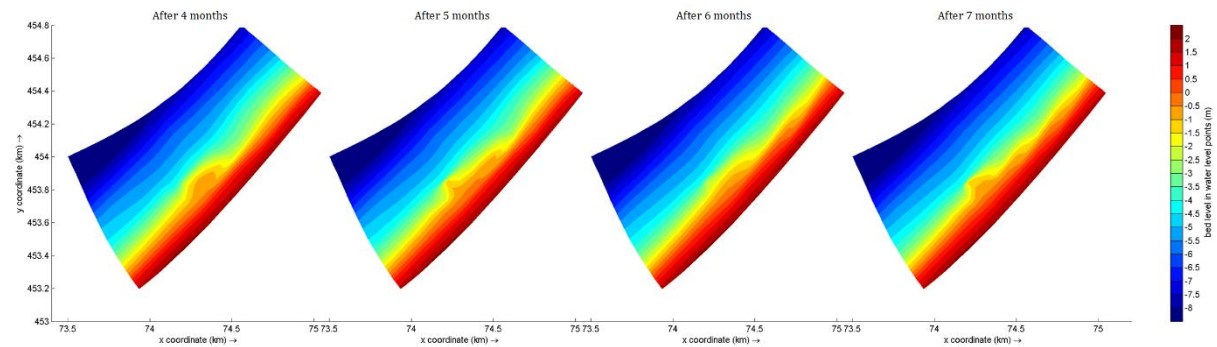


Figure 55 Bed level development after 4, 5, 6, and 7 months for nourishing at 3 m depth. The storm causes significant erosion of the nourishment and flattens the nourishment over a larger area. Appendix H.2 visualizes both bed level and mean total transport after each month.

The monthly situation shown in Figure 55 shows similar development for the spatial domain as for a smaller nourishment volume. The maximum values are larger, however. The behavior of the bed level and mean total transport magnitude in the domain is similar: after the storm at 6 months flattens the nourishment extensively. The mean total transport magnitude, however, is much larger, which was already derived from Figure 52 and Figure 54. The temporal development of the alongshore spread of sediment is larger for this nourishment volume in the last 4 months.

The increase of the bed level to above mean water level occurs when the wave height is almost zero. This has happened for all nourishments. However, the relatively large supply rate of sediment causes bed levels that become too large in periods of smaller waves. The occurrence of this effect is not desired.

4.2.2 Comparison of discharge variations

The nourishment of 150'000 m³/year is compared with the nourishment of 100'000 m³/year. The differences in bed level, mean total transport and significant wave height are explained.

Differences in time

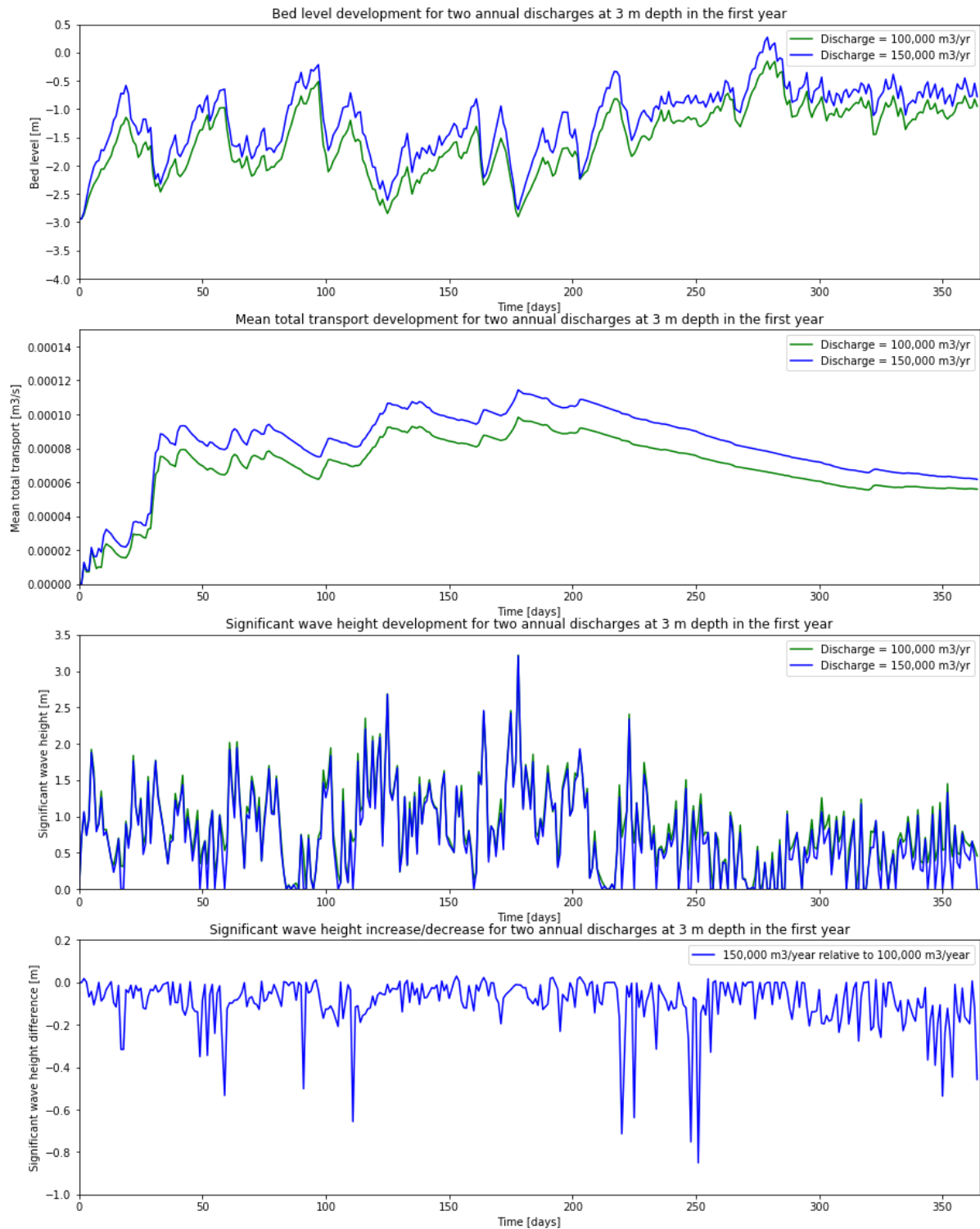


Figure 56 Temporal development of bed level, mean total transport magnitude and significant wave height for two annual discharge volumes at MSL -3.0 m.

The nourishment of 150'000 m³/year results in the same temporal development (see Figure 56). However, the values are larger. On average, the bed level is 0.5 m higher than for the nourishment of 100'000 m³/year at the same location. The mean total transport magnitude is larger as well. After 1 year, the year-averaged magnitude is around 3000 m³/year larger. This is a relative increase of 7%, while the nourishment volume has increased with 50%. More sediment remains at the nourishment location and is not redistributed in alongshore direction.

The significant wave height has decreased with the increased nourishment volume. The bed level has increased, which results in more wave energy dissipation and therefore smaller waves over the nourishment. The increased wave energy dissipation has resulted in larger transport magnitudes at the seaside of the nourishment.

Differences in spatial domain

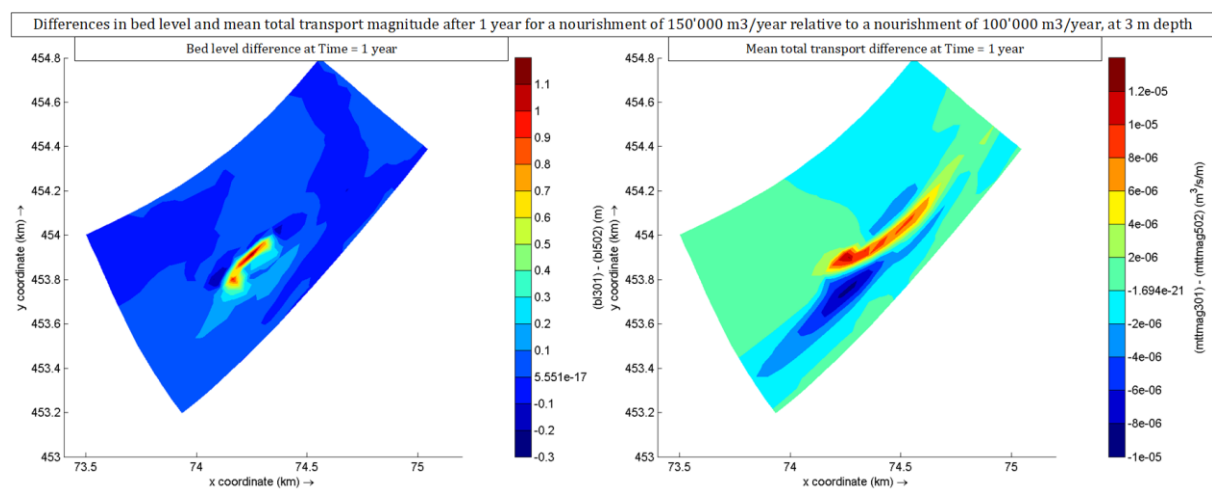


Figure 57 Difference in bed level and mean total transport magnitude of nourishment of 150'000 m³/year relative to 100'000 m³/yr.

The increase of the nourishment volume increases the size of the nourishment, both in horizontal direction and vertical direction. The maximum height is 0.50 m larger. The alongshore spread has increased as well. The relative increase of the bed level is visualized in Figure 57 (left figure). At the seaside of the nourishment, more accretion takes place. This was already visible in the previous paragraph, where it was noticed that the nourishment has extended to the MSL -4.0 m depth contour.

The increased volume also has effect on the transport magnitude. From the nourishment location, the transported volume towards the northeast has increased. The transport zone at the south side has decreased even more relative to the annual volume of 100'000 m³. As less sediment is transported in this part of the domain, more sediment is accreted and the nourishment extends towards the southwest.

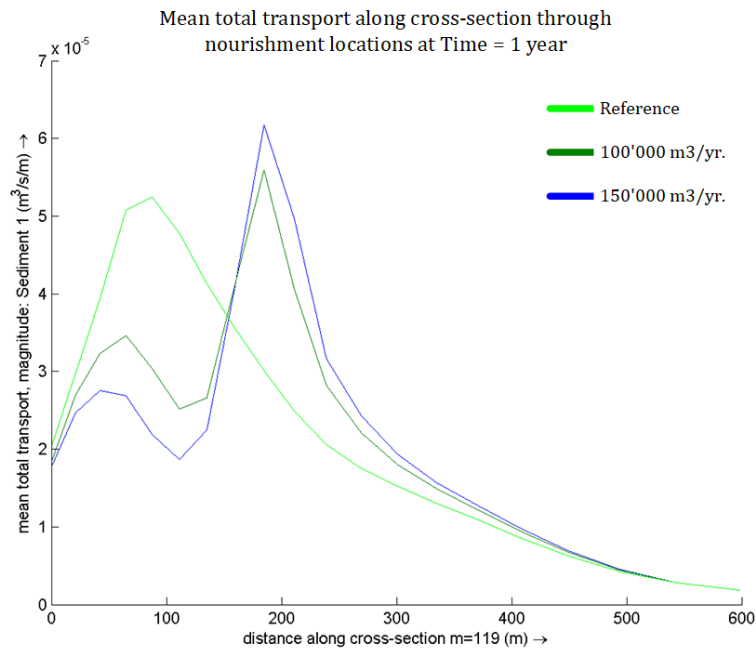


Figure 58 Mean total transport along cross-section of for the three nourishment volumes at 3 m, measured from the shoreline: no volume, 100'000 and 150'000 m³/year. The increase of the volume leads to a small increase of transport at the nourishment location and a decrease in transport at the transport belt as a result of shadowing.

Figure 58 shows the differences of transport magnitudes as a result of increasing the nourishment volume. The transport peak at the nourishment location shows a small increase due to the increased volume. At the transport belt, a decrease is measured, due to shadowing. The area of the nourishment has increased, which leads to increased wave breaking and energy dissipation. This causes a decrease in energy and currents at the transport belt. In total, an increase of the nourishment volume causes a decrease in total transport over the entire cross-section between MSL 0.0 m and MSL -8.0 m, at 600 m distance (i.e. the surface below the blue graph is smaller than the dark green surface). A conclusion that can be drawn from this data, is that a larger nourishment volume increases the effect of shadowing on the transport belt, which leads to an overall decrease in transport capacity. Thus an increase of the nourishment volume has a negative effect on the redistribution of sediment at the location of the transport belt.

Table 6 Sediment redistribution distance in alongshore and cross-shore direction for the two annual nourishment volumes. The values are retrieved from paragraph 4.1.1 and 4.2.1.

Annual Nourishment volume [m ³ /year]	Total alongshore distance [m]	Of which northeast directed (downstream) [m]	Total cross-shore distance [m]	Of which shoreward directed [m]
100'000	580	260	210	150
150'000	740	280	240	170

The plume to the southwest as a result of the increased discharge volume causes a significant increase in alongshore sediment redistribution to this direction (see Table 6). The redistribution distance to the northeast, however, is fairly equal for both cases, which means that the net effect of the volume increase does not significantly increase longshore redistribution of sediment.

The sediment redistribution in cross-shore direction has increased towards the shoreline. This increase of the bed level functions as a barrier for the longshore transport zone. It causes a decrease in transport magnitude and thus a bed level increase. Therefore the increase of the nourishment volume increases the alongshore accretion at the upstream side of the nourishment location.

4.3 Spreading of the disposal locations

This paragraph discusses the impact of an equal nourishment volume that is applied over 5 adjacent disposal locations. It is elaborated whether the spread of disposal locations has influence on the bed level development, transport intensity and the longshore redistribution distance. The individual nourishment is elaborated, followed by a comparison with a single-location nourishment.

4.3.1 Nourishment spread over 5 cells at 5 m depth

The development in bed level, mean total transport and wave height are discussed in this paragraph. Additional visualizations of the nourishment are summarized in appendix I.1. Appendix I.2 shows the monthly changes in the spatial domain for bed level and mean total transport.

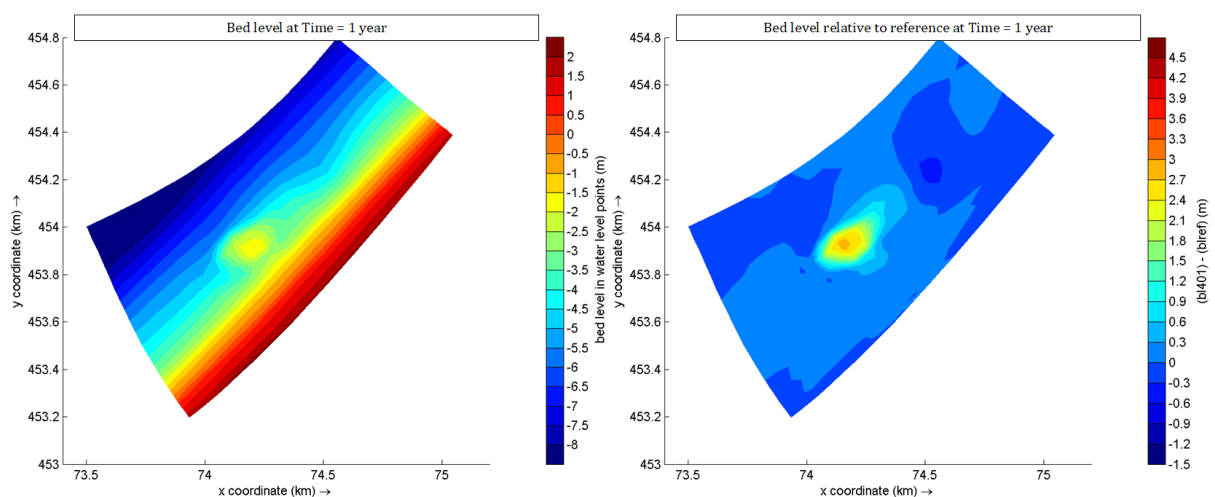


Figure 59 Bed level after 1 year for a nourishment spread over 5 cells (left) and relative difference to reference (right) around 5 m depth. The nourishment develops significantly in northeast direction.

Disposing the nourishment volume over 5 locations close to each other, provides a bed level that has a value of MSL -2.0 m after 1 year around 5 m depth (see Figure 59). The relative increase is just 3 m. The spread of sediment is predominantly northeast directed. A fraction is shoreward directed. An erosion spot is noticed northeast of the nourishment. The nourishment is blocking sediment transport at MSL -5.0 m, which prevents the coast from smoothing the depth contours.

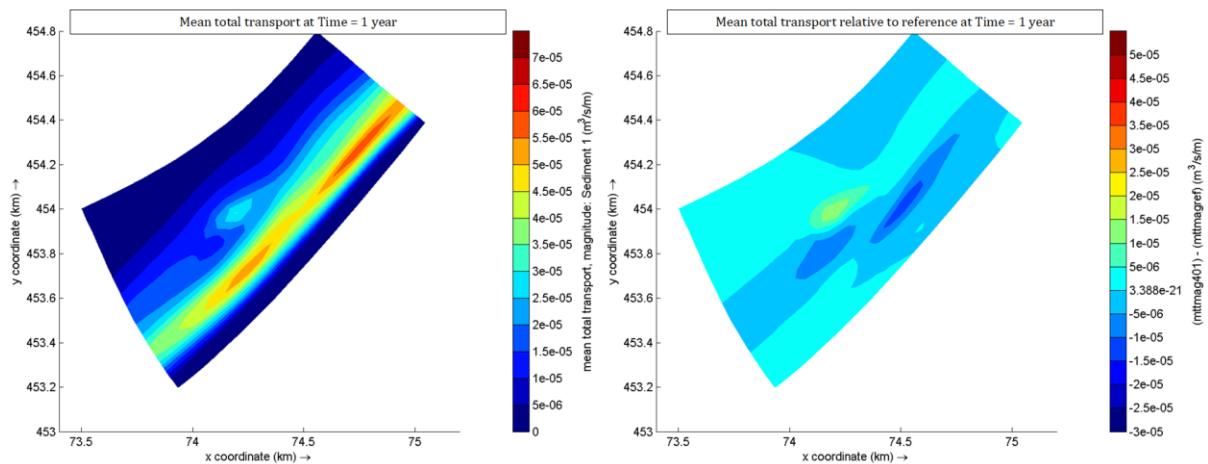


Figure 60 Mean total transport after 1 year for a nourishment spread over 5 cells (left) and relative difference to reference (right). The effect on the transport zone is small.

The transport zone is not affected (see Figure 60). The transport magnitude from the nourishment is small compared to the transport zone. Overall the influence of the nourishment on the transport pattern in the domain is not significantly large. Spreading an equal volume over multiple locations is in favor of the transport pattern and bed level development.

Just as with the other two research parts, the nourishment locations have been analyzed in time to define the mechanisms that give a net northeast directed redistribution pattern. The locations are shaped in a cross and indicated as C2, C4, C5, C6, and C8. The four adjacent cells in the corners have been added, indicated as C1, C3, C7 and C9. The 9 cells in Figure 61, Figure 62 and Figure 64 to Figure 67 are orientated 45 degrees counter-clockwise to fit in the spatial domain of Figure 59 and Figure 60. The dominant wave direction in this domain is directed from the upper left cell towards the lower right cell. The longshore transport zone is travelling from left to right.

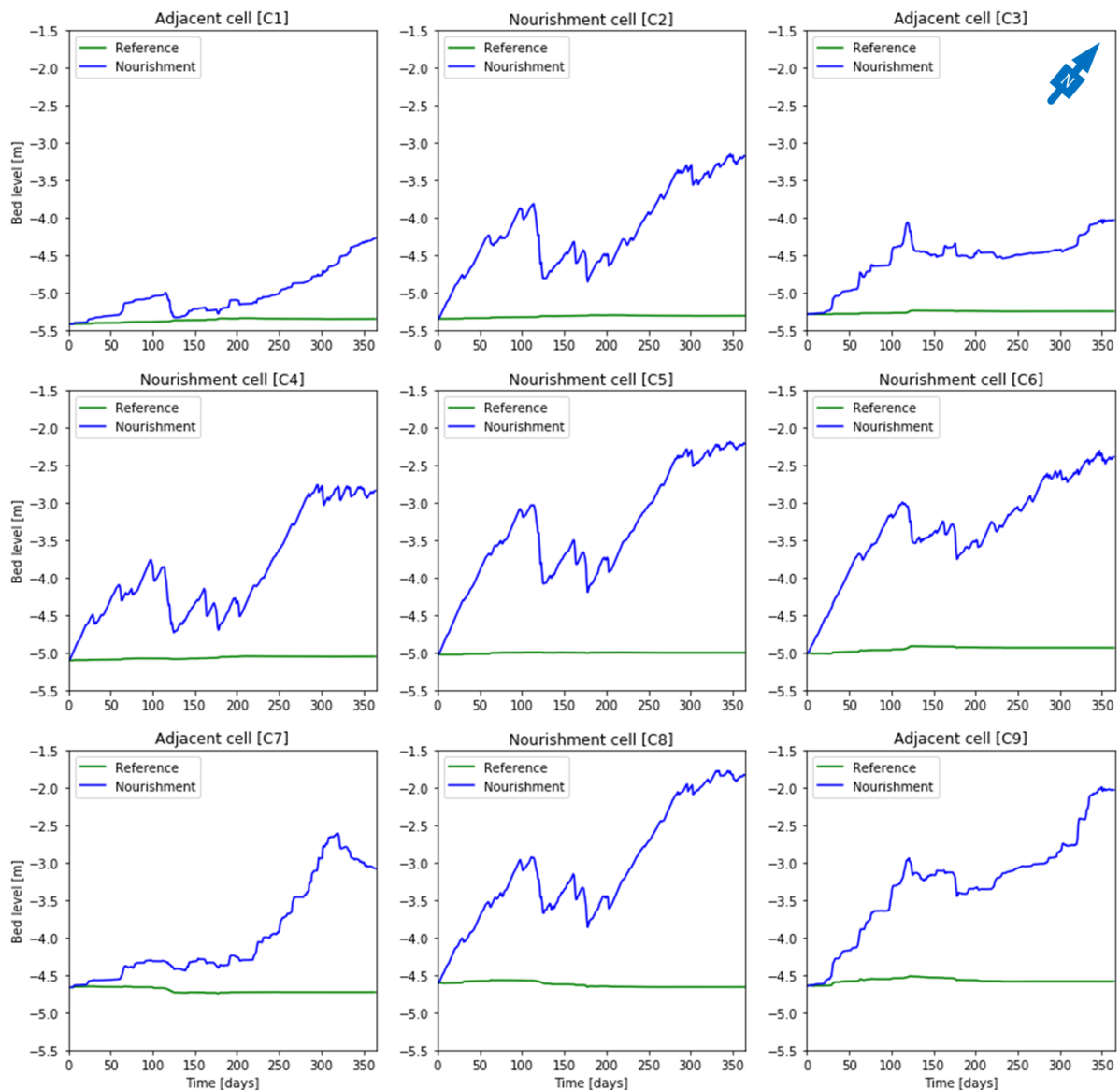


Figure 61 Temporal development of the bed level, measured at the nourishment locations. The four adjacent cells (in the corners) give the effects of the nourishments in a rectangular domain. The bed levels in the adjacent cells increase as well due to the nourishments.

The bed level increases due to the nourishment (see Figure 61). The increase is largest in the nourishment cells and downstream of the nourishment (cells C7, C9). At the seaside (C1, C3) of the nourishment, only a small increase of the bed level is measured, which is a result of small cross-shore transport gradients in time. The temporal development is similar due to the wave climate. The maximum bed level after 1 year is MSL -1.8 m, measured in the nourishment cell located most shoreward (C8). It is also the maximum bed level that is reached in the full year.

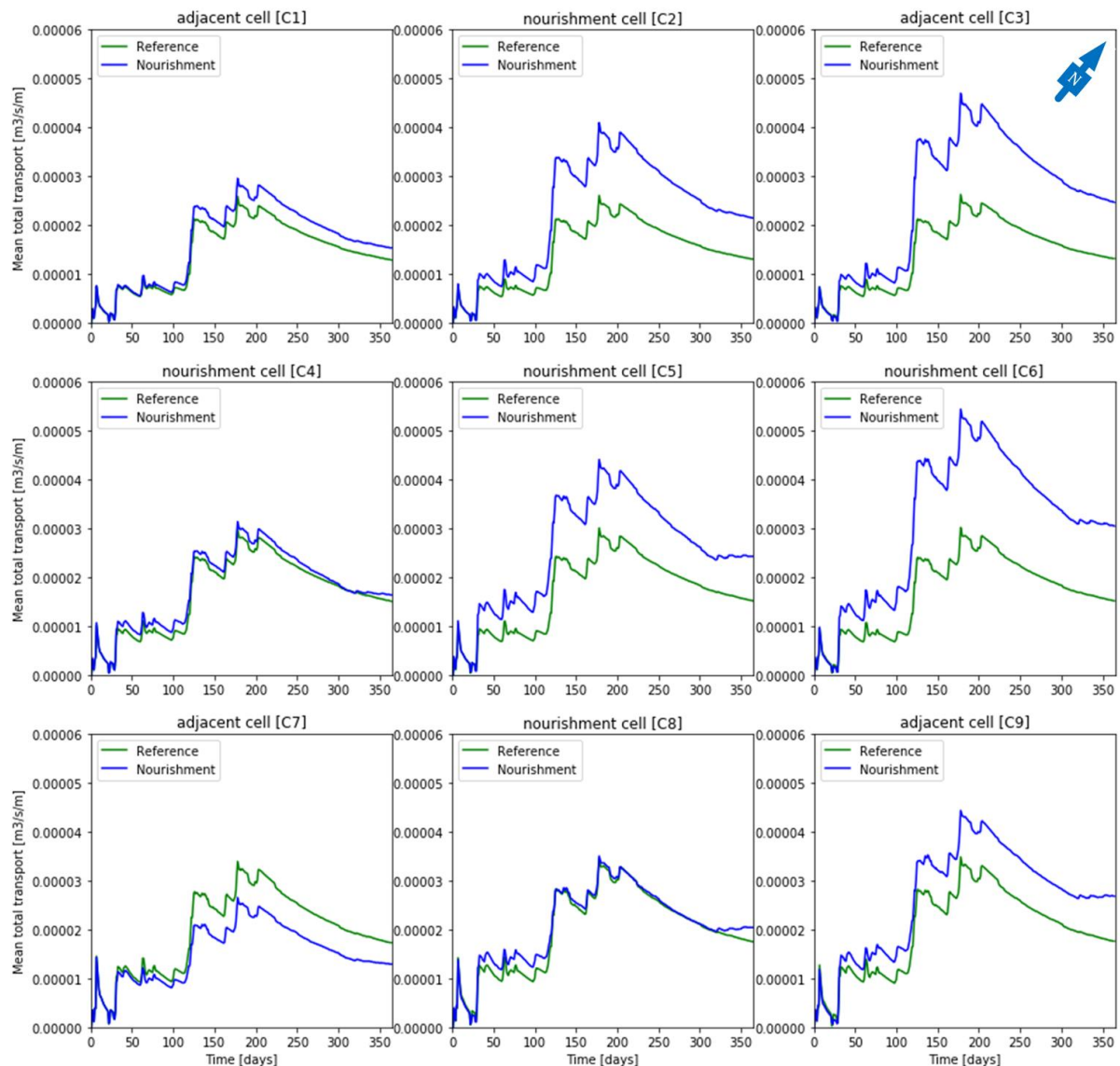


Figure 62 Temporal development of the mean total transport magnitude, measured at the nourishment locations. In most cells, the transport magnitude has increased due to the nourishment.

The transport magnitude increases significantly at the nourishment center (C5) and downstream of this center (C5, C6, C7) (see Figure 62). The dominant transport direction is therefore in the direction of the waves. Transport increases at the southwest of the nourishment (C1), due to breaking of waves in front of the nourishment. The year-averaged transport magnitude increases at the beach side of the nourishment (C8), due to the disposal of sediment. Because of the increase in bed level at the beach side of the nourishment, sediment transport from the southwest is partially blocked and causes a decrease in transport upstream from the nourishment, as is visible in cell C7.

Although sediment is disposed at location C4, the transport magnitude remains fairly equal. The volume of sediment is likely to be in equilibrium with the transport capacity at this particular depth. The significantly small increase in transport (<5%) still causes a bed level increase of more than 3.0 m.

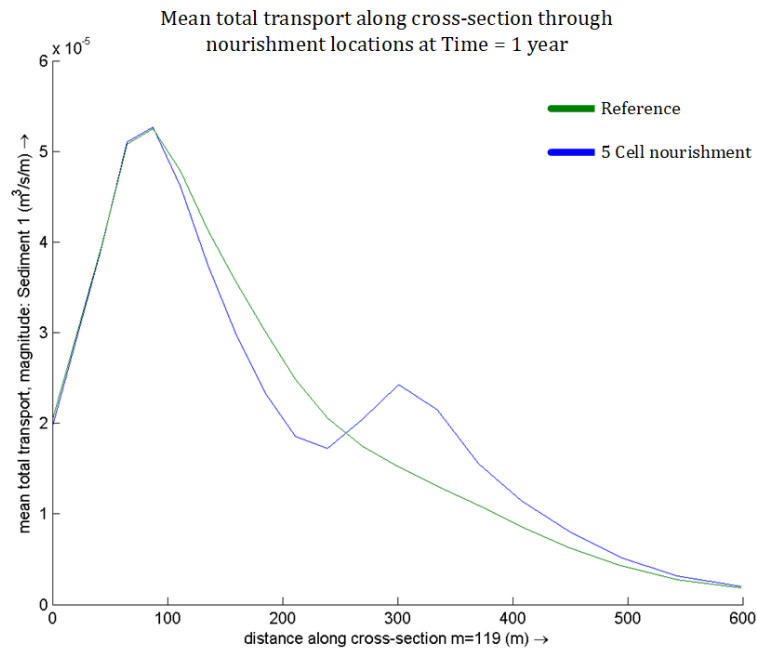


Figure 63 Mean total transport along cross-section of nourishment location at 5 m depth with spreading over multiple cells, measured from the shoreline. Due to the spreading, the transport magnitude at the nourishment locations is spread as well.

In Figure 63, the cross-shore profile of the time-averaged transport magnitude for nourishing at multiple cells around 5 m depth is shown. The maximum value is found at the nourishment location. The spread of transport in cross-shore direction is larger than for single cell nourishments. The maximum value is smaller due to spreading. The maximum value is found at the transport belt, which is hardly influenced by this nourishment. The total transport magnitude for the nourishment case (blue line) is estimated to be 390'000 m³/year, which is a small increase relative to the reference volume (i.e. 386'000 m³/year).

In appendix I.2, Figure 116, the monthly development of the larger domain is shown. For the entire year, the bed level remains low, around the depth contour of MSL -2.0 m. It is clearly visible that the alongshore distribution of sediment increases in the last 4 months. The effect of spreading disposal locations on the domain is therefore larger. Besides, the mean total transport magnitude in the transport zone is not extensively affected, because less waves are breaking on the nourishment.

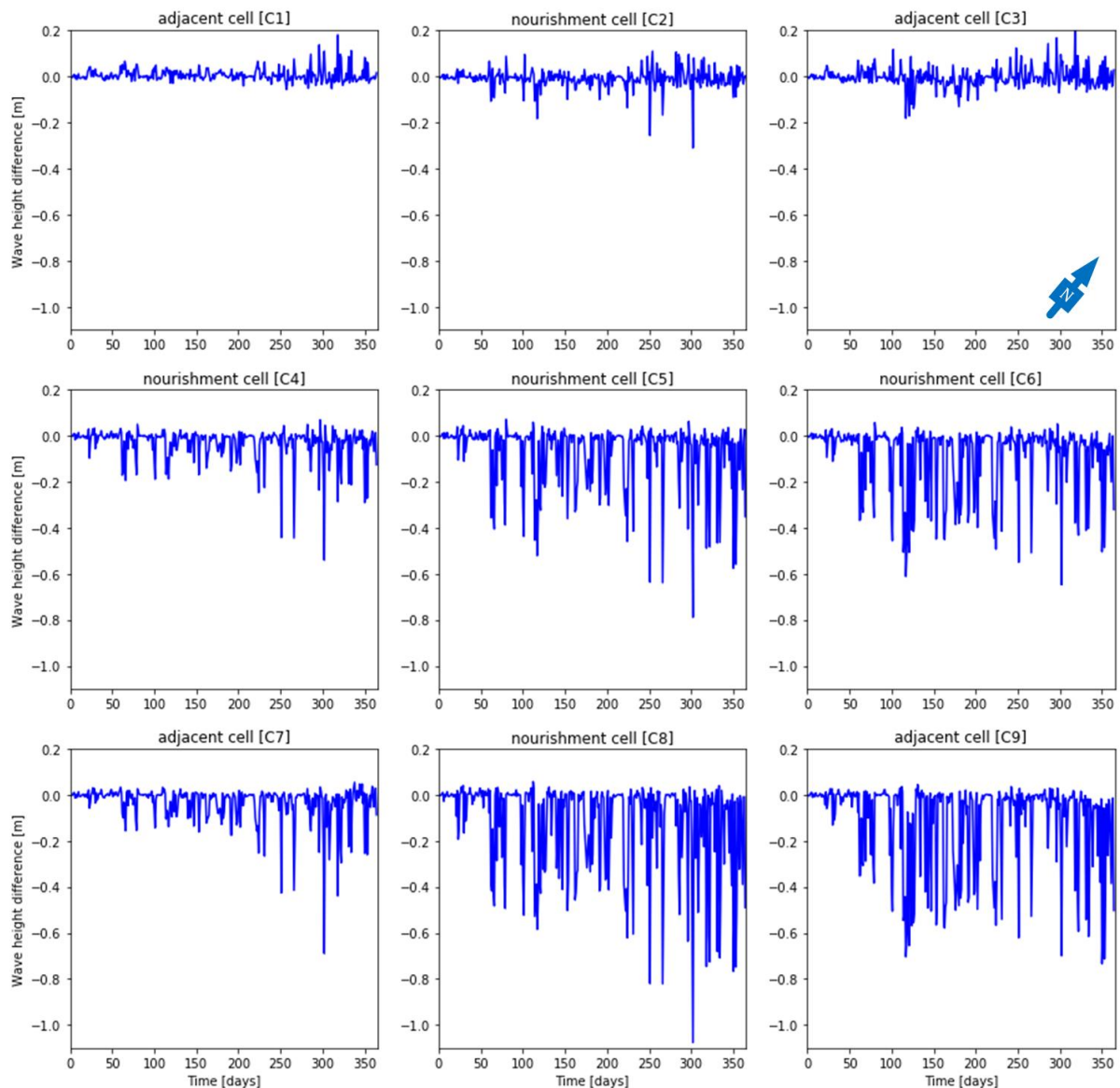


Figure 64 Temporal development of the difference in significant wave height between the nourishment simulation and the reference simulation, measured at the nourishment locations. The wave height has decreased due to a decrease in bed level, except for the adjacent cell at the seaside, where small increases are measured.

The increase of bed level in this domain causes a decrease in wave height (see Figure 64). At the seaside this decrease is small, but at the beach side the decrease is up to 0.5 m. almost all waves that are initially larger than 1.0 m, are partially dissipated due to the nourishment.

Moreover, the area of the nourishment has increased. The distance of the nourishment over which the waves travel has increased, which enforces waves to dissipate more energy and therefore become smaller.

4.3.2 Comparison of spreading variations

The nourishment with spreading over 5 locations is compared with the nourishment with a single supply location. The differences in bed level, mean total transport and significant wave height are explained.

Differences in time

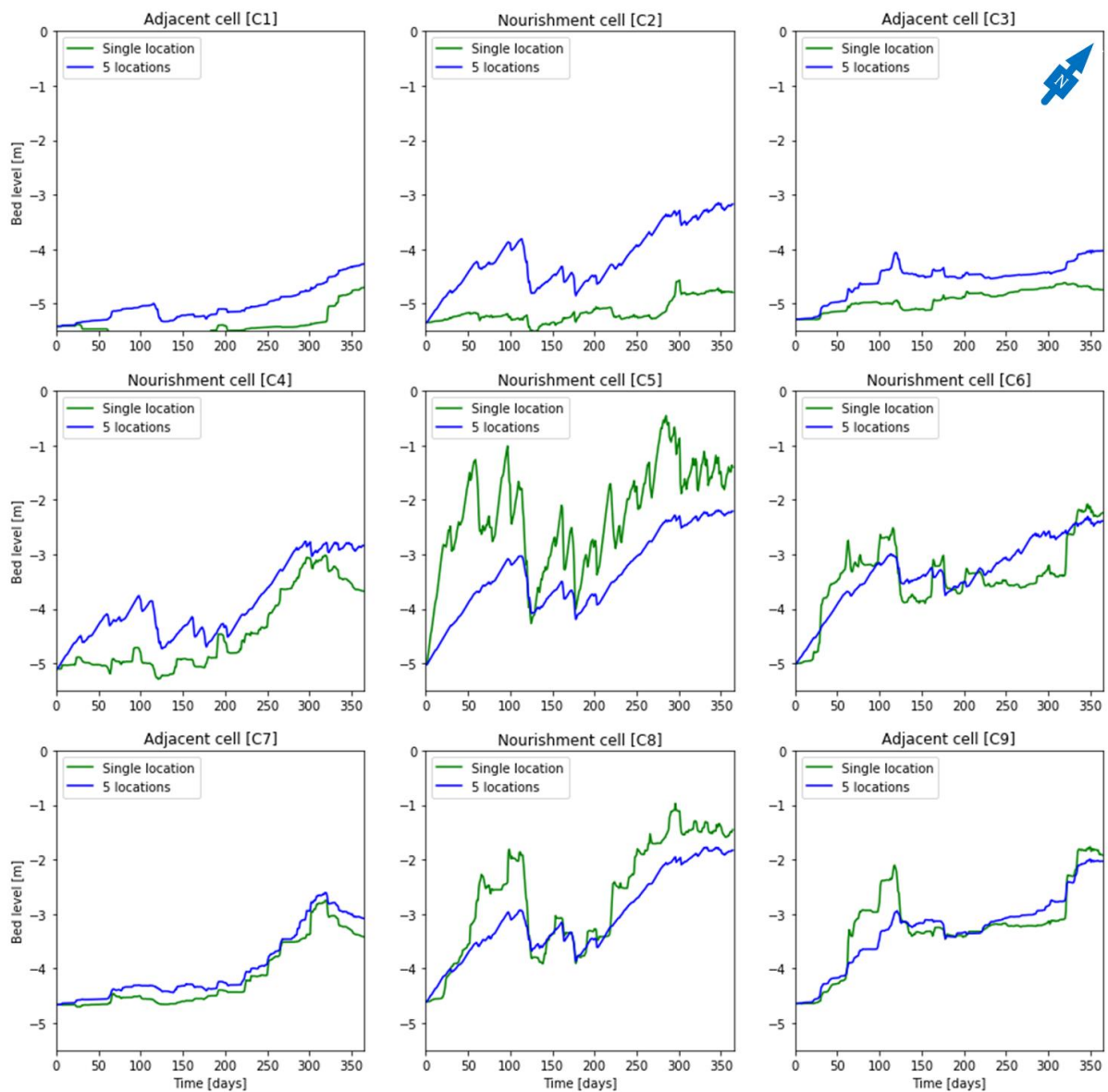


Figure 65 Temporal development of bed level, for single-location (green) and 5-cell nourishment (blue).

The nourishment cell (C5) is the nourishment cell for the single-location nourishment and the center for the 5-cell nourishment (see Figure 65). For both cases, the bed level has increased. The cells at the upstream side of the center (C1, C2, C3, C4, C7) have a larger bed level increase for the 5-cell

nourishment as sediment is actively supplied in this part of the domain. The downstream cells show similar development in bed level for both cases. Only the center is significantly different.

The net transport direction is northeast, which is into the direction of cell C6. The cross-shore component of sediment transport is clearly visible in cell C8, where the bed level increase is larger for the single-location nourishment. Although no sediment is supplied here, the volume in the nourishment center is too large to keep in cell C5.

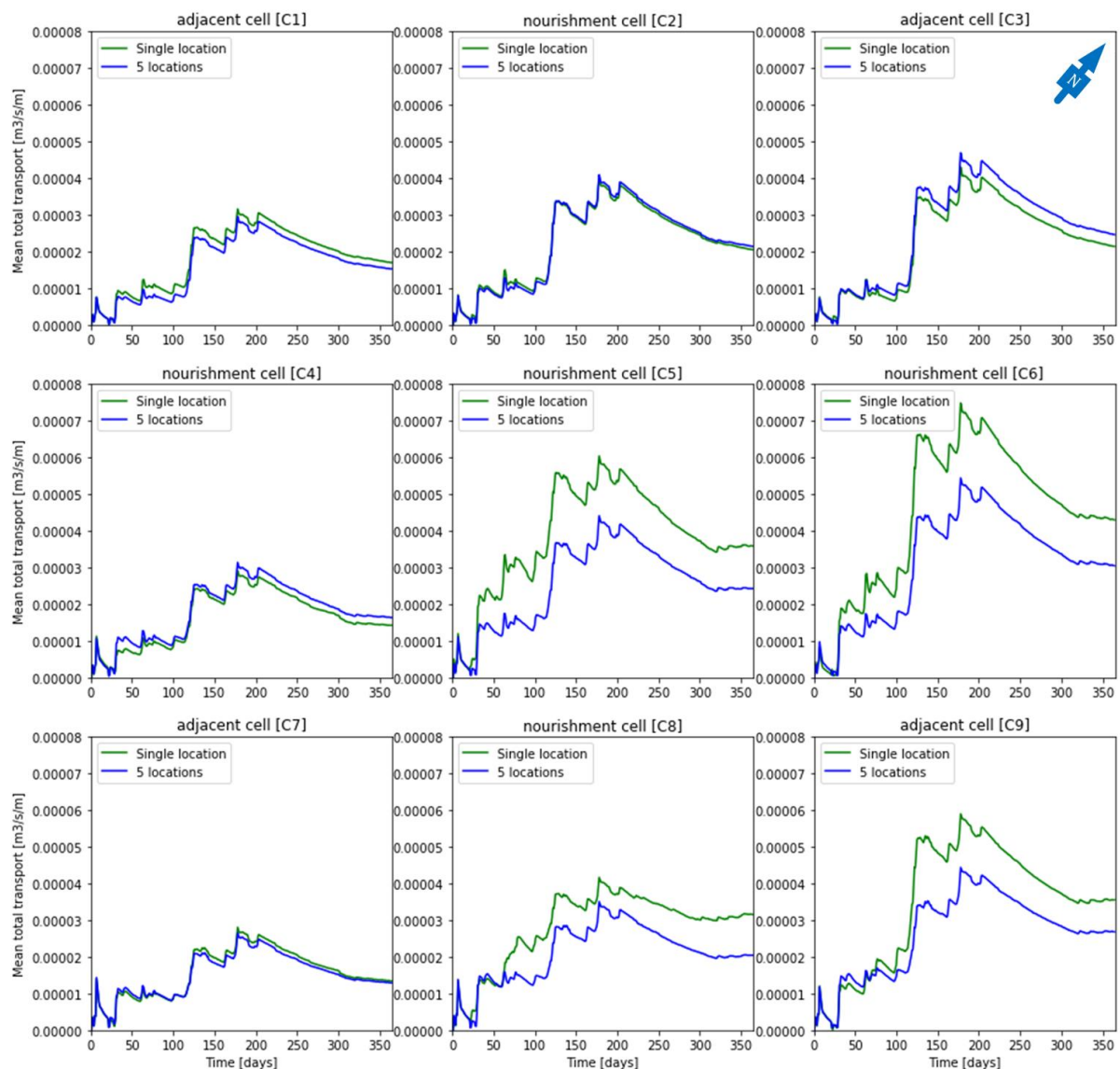


Figure 66 Temporal development of mean total transport magnitude, for single-location (green) and 5-cell nourishment (blue).

For the upstream cells, the transport magnitude is fairly equal for both cases for the entire year (see Figure 66). The single-location nourishment generates larger transport magnitudes for the center and the downstream cells, which is a consequence of a large disposal volume at one location,

instead of spread over multiple locations. The temporal behavior of the transport magnitudes of both nourishments are equal, as a result of the wave climate.

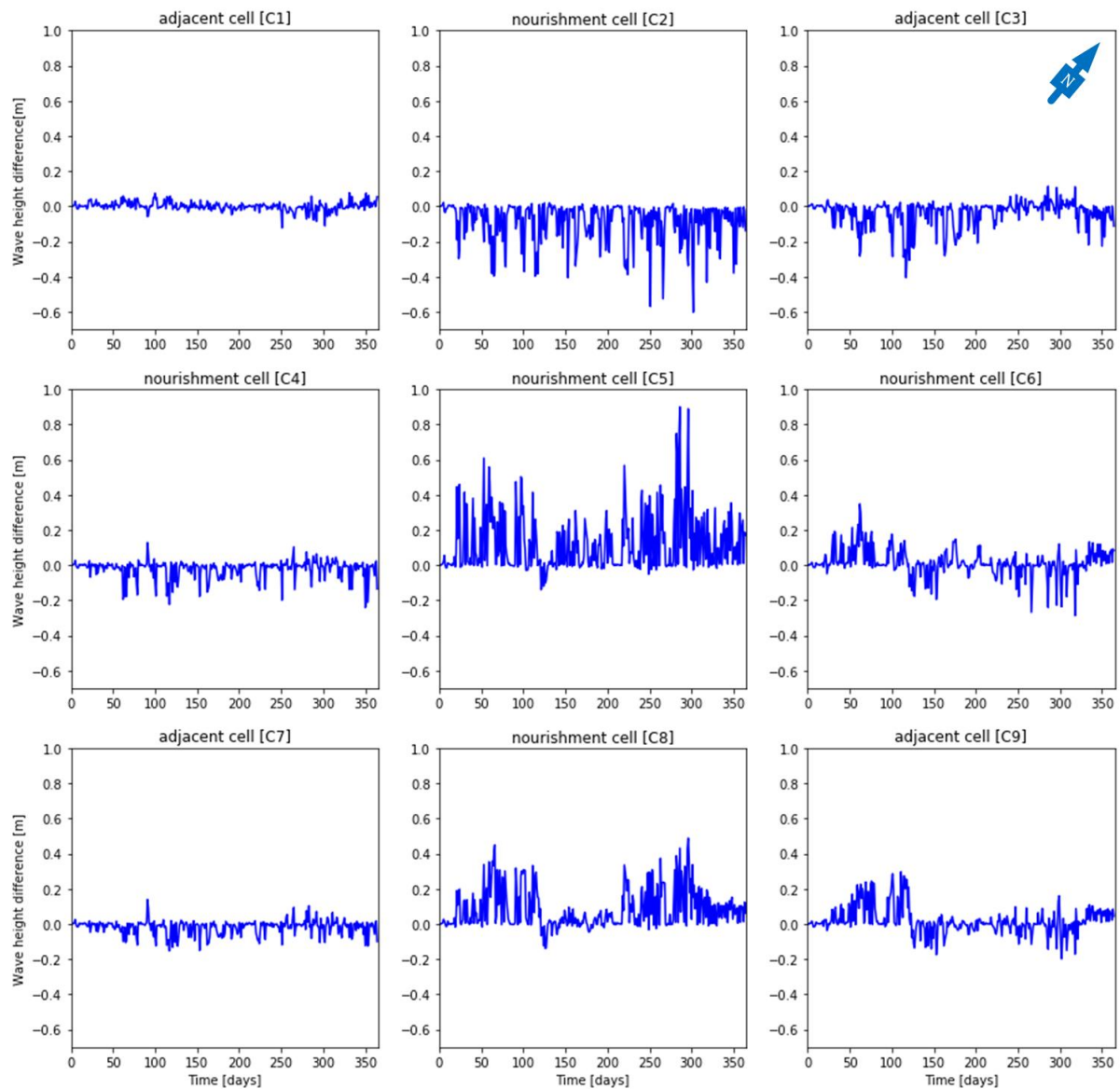


Figure 67 Temporal development of wave height, for single-location (green) and 5-cell nourishment (blue). The figures have switched layouts for cells C5, C6, C8, and C9. This is to present the differences better.

The wave height varies with depth (see Figure 67). As the 5-cell nourishment produces lower bed levels relative to the single-location nourishment, most waves will dissipate less energy or propagate without breaking. The significant wave height then increases. For most waves in the domain downstream of the nourishment center (C5, C6, C8, and C9), this is valid. The wave height upstream is larger in case of the single-location nourishment, as the bed level is lower (see Figure 65). The decrease in wave height causes a relative increase in mean total transport and a decrease in bed level, and is visible in the adjacent cells of the nourishment as well.

Differences in spatial domain

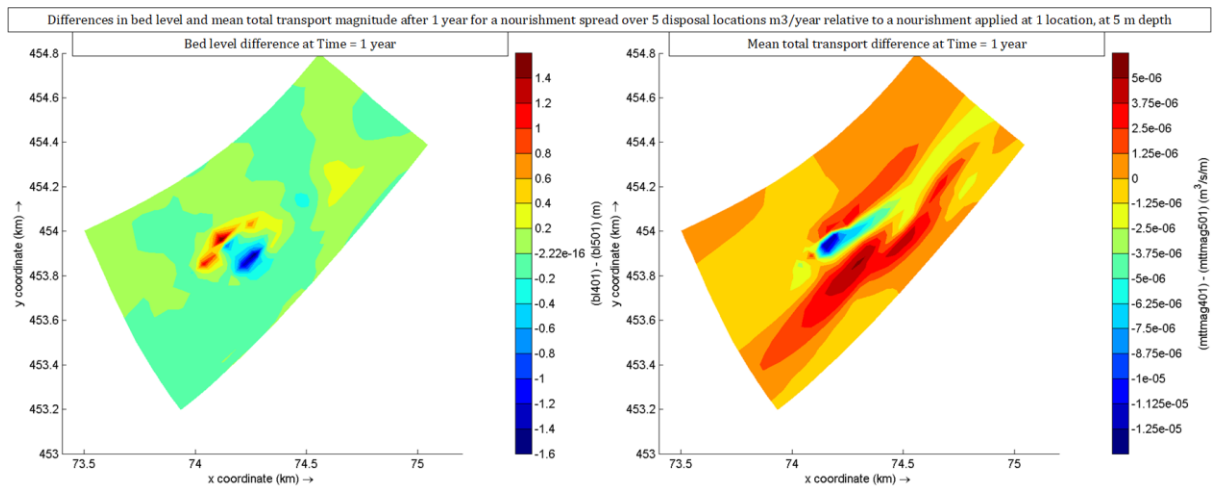


Figure 68 Difference in bed level and mean total transport magnitude of 5-cell nourishment relative to single-location nourishment.

As was already derived from Figure 65, the bed level is lower at the beach side of the nourishment and increases at the seaside of the nourishment due to disposal of sediment at these sides. At the upstream and downstream side, a small relative increase is occurring. The longshore redistribution is therefore larger for a nourishment spread over a larger domain. Because of the lower bed levels, the depth remains large enough to maintain the transport zone between MSL -1.0 m and MSL -4.0 m. Relative to the single-location nourishment, the magnitude in this zone has increased and is closer to its reference magnitude. The supply of sediment is divided over 5 cells, which results in a smaller transport magnitude right downstream of the nourishment. The downstream transport zone reaches further northeast, however.

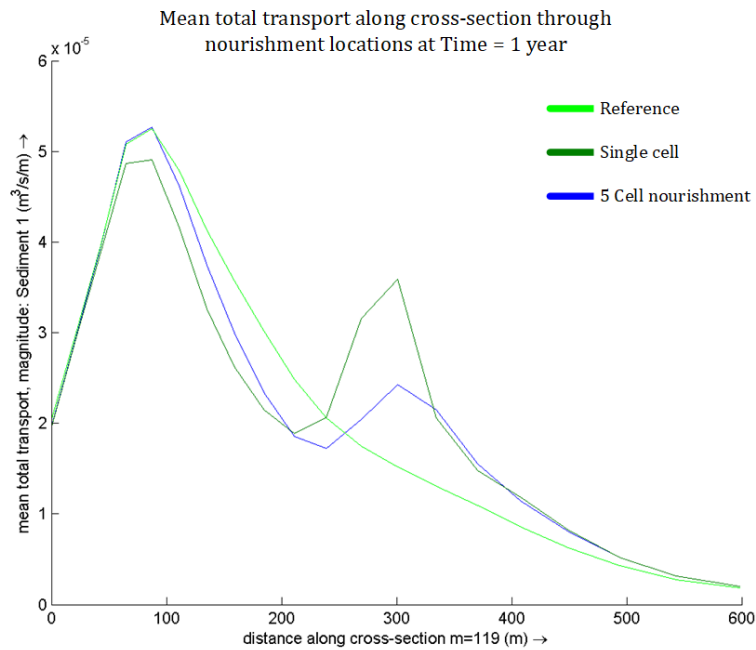


Figure 69 Mean total transport along cross-section of nourishment location at 5 m depth with spreading over multiple cells, measured from the shoreline. Due to the spreading, the transport magnitude at the nourishment locations is spread as well. The single cell nourishment shows a significantly larger peak at the nourishment area than the 5-cell nourishment.

Figure 69 shows the relation between the reference simulation, the single cell nourishment and the 5-cell nourishment. The single cell nourishment generates a larger total transport than the 5-cell nourishment, due to the larger increase in bed level of the nourishment. As a consequence, the shadow-effect at the transport belt is larger, causing a small decrease in the transport magnitude. Overall, the single cell nourishment transports more sediment over this cross-section.

Table 7 Sediment redistribution distance in alongshore and cross-shore direction for the two spreading configurations. The values are retrieved from paragraph 4.1.3 and 4.3.1.

Annual Nourishment volume [m³/year]	Total alongshore distance [m]	Of which northeast directed (downstream) [m]	Total cross-shore distance [m]	Of which shoreward directed [m]
Single location	330	210	280	210
5 locations	490	330	280	190

The longshore redistribution distance has increased with 48%, and the net northeast distance has increased with 57%, mainly due to a larger spread of sediment, as is shown in Table 7. The longshore currents are stronger due to decreased wave breaking at the nourishment. Their transport capacity is therefore larger.

The cross-shore redistribution is fairly equal for both cases. The net effect of a larger spread on the cross-shore redistribution of sediment is still unknown.

4.4 Chapter summary

The results of three research parts have been described in this chapter. These three parts are part of the research sub-questions 2, 3, and 4 as stated in paragraph 1.4. These sub-questions are:

2. *What is the optimal depth to apply a continuous nourishment?*
3. *What are the changes in behavior when the annual nourishment volume increases?*
4. *What changes in the behavior of a continuous nourishment when the annual nourishment volume is spread over multiple, adjacent disposal locations?*

The answer to sub-question 2 was given in paragraph 4.1. The optimal depth is found between MSL -3.0 m and MSL -4.0 m. At these depths the longshore transport of sediment is largest as this zone is located in the breaker zone of a majority of the short waves. Due to breaking, a significant amount of sediment is brought into suspension and transported alongshore. As sediment is in suspension, it is more easily being transported. The strong longshore currents contribute to a relatively quick redistribution of nourished sediment, compared to the disposal locations at MSL -5.0 m and MSL -6.0 m. At these depths, the effect of wave breaking and energy dissipation is much smaller, which reduces the amount of erodible sediment volume. The differences in temporal development of bed level and the maximum bed level are within 0.5 m for the four depths. The development over the year are similar, which is a consequence of the applied wave climate. The wave climate determines this development in time.

The transport magnitude is largest for the nourishment at MSL -3.0 m and decreases with increasing depth. This is due to the presence of the transport zone. The alongshore redistribution distance (i.e. the spread to which sediment from the nourishment has reached) is largest for smaller depths. For MSL -3.0 m, this distance is 500 m, which is significantly large. The cross-shore distance is almost equal for all four nourishment depths, and is between 210 and 280 m. The largest distance is at MSL -5.0 m, because at this depth the larger waves start to break. These waves dissipate relatively much energy which increases the capacity of the cross-shore current significantly. The cross-shore distance at MSL -3.0 m is smaller as most waves have already been dissipated.

The answer to sub-question 3 has been explained in paragraph 4.2. An increase of 50% of the annual nourishment volume, from 100'000 to 150'000 m³/year, was applied at MSL -3.0 m. The relative increase of transport was just less than 10%. The maximum likely nourishment volume for a single cell is found between these annual volumes. The bed level exceeded MSL for a couple of days. The temporal development pattern does not differ from the initial nourishment volume, only the values are larger. The bed level increase occurs over a larger domain. The bell shaped nourishment has exceeded in alongshore direction, both in northeast and southwest direction, and a small part in seaward direction, as relatively less sediment has been redistributed. An increase of the nourishment volume causes a decrease in the overall sediment transport capacity for the zone between the shoreline and the MSL -8.0 m depth contour, which is not desired for maximizing the alongshore distribution of sediment.

An increase of the annual nourishment volume does not bring significant changes in alongshore transport. The transport capacity has been exceeded, as more sediment was supplied than redistributed for a nourishment volume of 150'000 m³/year. The transport capacity has not exceeded for an annual nourishment volume of 100'000 m³/year, as the redistributed volume was of similar

magnitude for the nourishment area. The transport capacity is therefore found between these annual nourishment volumes.

The answer to the last sub-question has been given in paragraph 4.3. A spread of the disposal locations, in this case 5 adjacent locations, was applied at MSL -5.0 m with a total volume of 100'000 m³/year, equally divided over all locations. The spread of disposal locations has given positive differences in alongshore sediment redistribution. The transport intensity has not changed, as the total nourishment volume equals 100'000 m³. The alongshore redistribution distance, however, has increased with 50%. The breaking of waves is smaller as the depth does not increase much relative to a single-location nourishment. As the bed level was more than 1.0 m lower, more waves are able to propagate further and break later at the shoreside of the nourishment, instead of at the seaside. The maximum transport magnitude therefore shifts to the shoreline as well. This leads to a wider transport zone and thus increased transport volume. The spread of sediment is increased, especially the longshore component in northeast direction.

Chapter 5: Discussion

In this chapter, the results of the research are discussed in to what extent they are in accordance with the findings from the literature study, and how they determine the value of the outcomes of this research. Besides that, the limitations that were found during the execution of this research are explained, as well as the consequences these limitations have for the research outcomes.

5.1 Discussion

The concept of applying nourishments in a continuous manner has not yet been investigated. Therefore no comparison can be made with similar types of nourishments. The results from the research show a strong dependence between sediment redistribution, erosion and accretion, and the applied wave climate. The Dutch coast is a wave-dominated coast, which motivates this dependence to wave forcing. A detailed wave climate, has been applied for all configurations to investigate the differences in behavior of sedimentation and erosion, in both temporal and spatial development. For optimization of the research, the used wave data has been reduced to compensate the computational effort of the model (Luijendijk, et al., 2017). The waves that are smaller than 1.0 m are neglected in this research, initially performed under the assumption of negligible impact on sediment transport. This assumption is confirmed valid by the temporal development of bed level and wave height: when waves are smaller than 1.5 m, accretion of nourishment occurs. However, this also is a consequence of the large supply rate. A wave height around 1.5 m shows a balanced temporal development of sediment transport and thus bed level. Larger waves will cause erosion, and smaller waves will cause accretion. This has been visualized in the time series in Figure 31, Figure 36, Figure 41 and Figure 46.

The input reduction of waves gives a prerequisite to the validity of the resulting temporal development of the bed level. The waves under 1.5 m have been neglected, under the assumption that they have negligible influence on sediment transport. However, the concept Zandwindmolen assumes a continuous constant discharge of sediment. This means that sediment is still disposed when waves under 1.5 m occur. This occurs for 48% of the time (i.e. the time of occurrence of waves under 1.5 m). This means that in calm wave periods the nourishment is able to grow to above Mean Low Water and possibly above Mean Sea Level. Fortunately, this is less likely to occur as the Zandwindmolen has an operational limit. The Zandwindmolen is assumed not to be operational in cases of weak wind forcing. It is assumed that for 40% of the time, wind fields are too weak to generate power for the system. And as there is a correlation between wave height and wind forcing, the relation between operational time and used time for disposal of sediment is valid as well. Therefore, the resulting temporal development of bed levels is reliable.

Sediment redistribution is for a large part shoreward directed in the year that was simulated. Especially for nourishments applied at deeper water (4 m, 5 m, 6 m), the cross-shore distance is large relative to the alongshore distance (see Table 5). This has previously been confirmed in research: in the first years of the lifetime of a nourishment, there is a relatively large cross-shore transport volume (Huisman, 2019).

At the seaside of all simulated nourishments, a relatively steep slope is generated. On this slope, incoming waves are partly reflected, which reduces wave propagation over the nourishment

towards the shoreline. Moreover, wave breaking at the nourishment is less, which results in a decrease of sediment transport between the nourishment and the shoreline. This is especially valid for nourishments at MSL -3.0 m and MSL -4.0 m depth. The generation of this steep slope is possibly a numerical response of the model calculations, caused by the relatively large grid cells applied in the model domain.

The mean total transport direction is northeast directed. This is in line with the transport patterns that currently are present along the Dutch coast. The magnitude of the longshore transport intensity for the reference situation in the model is equal to 386'000 m³/year. The annual nourishment volume is disposed at a small section over which this transport intensity is measured and is equal to 26% of the initial transport intensity along the Delfland coastal stretch. The transport intensity increases when a nourishment is applied, except for the nourishments applied at MSL -3.0 m and MSL -4.0 m. At these depths, the interruption of the transport belt, and thus decrease of transport, is larger than the increase of the transport magnitude at the nourishment location. The local increase at the nourishment location is limited and is referred to as the transport capacity. In this thesis, the transport capacity cannot be determined on the basis of the applied nourishment volumes.

5.2 Limitations of the numerical model

The results presented in this chapter show promising perspectives for the technical feasibility of a continuous nourishment at the Dutch coast. The model used to get these results, however, includes some limitations. The grid over which hydrodynamic and morphodynamic processes are calculated, is fairly gross. The average size of these cells is 30 x 50 m in the nearshore zone. This brings exclusion of processes that otherwise would have influence on the behavior of the nourishment. The small-scale processes (<10 m) are therefore not included as they cannot be described well.

Two processes are important to consider: refraction and diffraction. The steering of waves is crucial in the moment, type and intensity of wave breaking. These processes are not visible in the results, as for every time step in every simulation, the wave direction is uniform, over and around the nourishment location. Curved wave rays were expected to be visible and so should refraction and diffraction be as well.

The model is depth-averaged. Therefore detailed processes of settlement of sediment, the location of disposing sediment in the vertical and the behavior of sediment particles in the water column are still unknown. The vertical position of disposal determines the settling time of sediment, as well as the degree of sediment that is suspended in the water column and sediment that is considered as bed load. Moreover, turbulence is dependent on the degree of suspended load, which gives insight in more ecological effects for the nearshore zone, such as occurrence of sediment plumes. Sediment that is disposed just below the water level is transported by currents right after disposal, which is positive for the redistribution. These elements have not been considered in this research, but are interesting to investigate for small-scale behavior of a continuous nourishment.

Chapter 6: Conclusions & recommendations

The conclusions that are retrieved from this research are given in this chapter. An answer to the research question is given, motivated by the conclusions that are a result from the research parts. The chapter concludes with recommendations for further research and for Engineering & Consultancy firm Sweco NL.

6.1 Conclusion

The aim of this thesis was to gain insight in the behavior of a continuous nourishment in the shallow nearshore zone (MSL 0.0 m – MSL -8.0 m). A study has been performed to define the dominant processes that drive sediment transport around nourishments. Subsequently, research has been executed in three parts to describe the development of a nourishment in time and the interactions with the surrounding coastal domain. At first the optimal depth has been defined. Secondly, the differences between two nourishment volumes have been investigated. At last, the effects of spreading of sediment by applying sediment over multiple locations have been answered.

In general, a continuous nourishment develops best when applied in the surf zone between MSL -3.0 m and MSL -4.0 m, preferably spread over multiple disposal locations, for which the total volume is limited at 100'000 m³/year. These results have shown individually positive behavior regarding longshore redistribution of sediment from the nourishment location. The longshore redistribution of sediment is largest for this configuration.

For practical reasons, the effects of a continuous nourishment in shallower water, between MSL 0.0 m and MSL -2.0 m, have not been investigated. The horizontal distance between these depth contours is small and the distance between the Mean Low Water line and the MSL -2.0 m depth contour is too small (<100 m). The presence of pipelines disposing sediment and water close to the shoreline gives dangerous situations for recreants at the beach. Closure of the beach at locations of pipelines is not efficient, as these pipelines are assumed to be permanently present at that location.

The dominant process that drives sediment transport for a continuous nourishment is wave forcing. The reference situation showed a large transport zone between MSL -1.0 m and MSL -4.0 m, driven by waves. The longshore redistribution of sediment is largest in this transport zone, for supplying at MSL -3.0 m and MSL -4.0 m. The transport magnitude in the zone between the shoreline and MSL -2.0 m decreases, because of the presence of a nourishment: waves break earlier and wave energy is dissipated in front of the nourishment. The decrease is then caused by a shadow-effect of the nourishment. The amount of energy dissipation at the transport zone then decreases and the magnitudes of the longshore current and transport capacity decrease as well.

There are small developments in beach extension towards the location of the nourishment. The decrease in sediment transport between the nourishment and the shoreline creates an increase in accretion and therefore a growing of the bed level between the nourishment and the beach. The application of a nourishment in the transport zone will thus most likely enlarge the beach. The bed level will eventually grow to above MSL and a connection between the beach and the nourishment is generated.

Applying a nourishment at MSL -5.0 m or MSL -6.0 m results in a smaller area of redistributed sediment and is therefore less effective for strengthening the coastline in the short-term. The longshore currents at this depth are significantly smaller and therefore the transport capacity is smaller as well. Although the transport capacity increases due to the supply of sediment, the relative increase in transport capacity is small compared to the supply rate. The initial processes in the nearshore zone therefore predetermine the effective depth to supply sediment. However, the influence of storms on the redistribution of sediment is large. Due to increased wave forcing during storms, sediment is redistributed in cross-shore direction towards the shoreline. Over a longer period of time, this amount of sediment will reach the transport belt, from where it will be redistributed alongshore. The effectivity of nourishments at deeper water on the alongshore redistribution of sediment are then promising.

An increase of the annual nourishment volume at a single supply location is possible. However, the limit is not much larger than the initial applied volume of 100'000 m³/year. A volume of 150'000 m³/year has applied at MSL -3.0 m. The bed level increases to above MSL for a couple of days during a calmer wave climate, which is not desired. The creation of an emerged island in front of the shoreline is not desired, as it is more difficult to be eroded by wave-induced and tide-induced currents. For longer periods of a calm wave climate, the bed level increases even more and eventually remains above MSL. The effectiveness of such a nourishment has then decreased, mainly due to decreased erosion rates.

The spread of sediment shows positive effects in the temporal development of bed level and transport magnitudes. The bed level shows maximum values that are 1.0 m below the maximum values of a single-location nourishment. The transport magnitudes decrease in the nourishment area. In the domain shoreward of the nourishment area, the net transport magnitude is larger than for the situation with a single-location nourishment, because of the shadow-effect. The bed level for a single-cell nourishment is higher, and thus more wave energy is dissipated at this nourishment, causing a decrease in magnitude at the transport belt. The longshore distance of redistributed sediment for the situation of spreading is larger as well. This means that the effectivity is increased when supplying an equal volume proportional to multiple locations. It also gives opportunity to increase the annual nourishment volume to volumes above the 150'000 m³/year.

6.2 Recommendations

A distinction is made between recommendations regarding further research and recommendations regarding the technical feasibility of the concept Zandwindmolen, for which this research has initially been set up.

6.2.1 Recommendations for further research

The model grid used for computing several processes should be refined in order to visualize important local-scale processes, such as refraction and diffraction. In this way, the behavior of the nourishment is monitored on a larger detailed level. This thesis has given insight in the behavior on medium spatial scale, but detailed insight is necessary to optimize the disposal configuration, and to

investigate what happens in the time between disposing sediment in suspension out of the pipeline and the settlement at the bottom.

The computational effort has been a limiting factor for this research. The calculation time required to compute the full period of five years is more than 10 days (240 hours). Therefore, the simulation time has been maximized to a representation of data for the first year only (i.e. 20% of the total time). Recommended is to increase the computational time to five years, in order to study the effects on a longer time scale.

To apply the concept of continuous nourishments, more research is required in maximization of the nourishment volume and in the options of local spreading of disposal locations. It has been proven that spreading optimizes the longshore redistribution of sediment. However, due to the optimization, there are opportunities to increase the annual nourishment volume as well. This is likely an iterative process.

The concept Zandwindmolen should be tested at other coastal stretches along the Dutch coast. The Delfland coastal stretch is a relatively calm and constant part of the Dutch coast where erosion rates are smaller. There are a number of locations where sediment demand is extremely high and therefore more suitable for the concept, for example the northern part of the Holland coast.

Upscaling of disposal locations along a larger coastal stretch is interesting to investigate the long-term behavior of continuous supply of sediment at several locations along the Holland coast simultaneously. As the concept is likely to be feasible at one location, the simultaneous supply at multiple locations brings new optimization tools, such as the required distance between disposal locations.

6.2.2 Recommendations for Engineering & Consultancy firm Sweco NL

Application of a continuous nourishment along the Dutch coastline, derived from the concept Zandwindmolen, is feasible. The results of this thesis have shown that redistribution of sediment is possible if a set of conditions is applied. The initial description stated that a pipeline disposes sediment at a single location in the nearshore zone, from where nature is responsible for the redistribution. The boundary conditions, in particular the annual nourishment volume, are however challenging to execute. The economic annual volume is estimated between 1 and 2 million m³, which is impossible to supply at a small domain as considered in this research. The four locations stated in paragraph 1.2.1 are more suitable for application of this concept. This research has shown that redistribution of sediment is possible as long as the supplied volume is smaller than the annual required volume of sediment.

However, there are opportunities in the execution of the concept for coastal stretches with small required volumes. The configuration of disposal locations over a larger coastal stretch increases the maximum applicable volume of sediment per year. This research has shown that at one location a volume of 100'000 m³ is possible. Spreading the volume over multiple locations at a small domain gives room for an increased nourishment volume. In practice, applying such a disposal setting at multiple locations along the coast, and connecting these sets to the same wind mill, will increase the annual nourishment volume for the whole configuration of disposal locations and thus increase the economic feasibility.

The technical advice to Sweco NL is to continue this research for locations with a small required annual sediment volume with the following starting conditions: a nourishment applied between MSL -3.0 m and MSL -4.0 m, spread over multiple disposal locations close to each other (according to the configuration of locations in research part 3, paragraph 4.3), with an initial annual nourishment volume of 150'000 m³/year. If successful, the annual volume should be increased with steps of 50'000 m³ until one of the evaluation criteria is no longer met. The second part of the continued research should be focused on applying the configuration over a larger coastal stretch, where multiple sets are applied for every, e.g., 3 km. This result will give a solid basis for a complete technical feasibility study for the Zandwindmolen.

Bibliography

- Bosboom, J., & Stive, J. F. (2015). *Coastal Dynamics I* (0.5 ed.). Delft, The Netherlands: Delft Academic Press. Retrieved November 14, 2018
- Cooper, J. A., & Pilkey, O. H. (2004, November). Sea-level rise and shoreline retreat: time to abandon the Bruun Rule. *Global and Planetary Change*, 43(3-4), 157-171. doi:10.1016/j.gloplacha.2004.07.001
- De Bakker, A. T., Tissier, M. F., & Ruessink, B. G. (2014, January 1). Shoreline dissipation of infragravity waves. *Continental Shelf Research*, 72, 73-82. doi:10.1016/j.csr.2013.11.013
- Dekker, S. (2013). *Natúúrlijk suppleren*. Hogeschool van Amsterdam, Civiele Techniek Watermanagement. Amsterdam: Hogeschool van Amsterdam. Retrieved November 12, 2018
- Deltares. (2014). *Manuals*. Retrieved November 26, 2018, from OSS Deltares: https://oss.deltares.nl/web/delft3d/manuals/-/document_library/Hr1g/view_file/458779?_com_liferay_document_library_web_portlet_DLPortlet_INSTANCE_Hr1g_redirect=https%3A%2F%2Foss.deltares.nl%3A443%2Fweb%2Fdelft3d%2Fmanuals%3Fp_p_id%3Dcom_liferay_document_l
- Deltares. (2018). *Mogelijke gevolgen van versnelde zeespiegelstijging voor het Deltaprogramma*. Delft: Deltares. Retrieved August 26, 2019, from <https://www.deltacommissaris.nl/documenten/publicaties/2018/09/18/dp2019-b-rapport-deltares>
- Giardino, A., Santinelli, G., & Vuik, V. (2014). Coastal state indicators to assess the morphological development of the Holland coast due to natural and anthropogenic pressure factors. *Ocean & Coastal Management*, 87, 93-101. doi:10.1016/j.ocecoaman.2013.09.015
- GoSurf Perth. (2016, August 18). *How are waves formed?* Retrieved January 14, 2019, from GoSurf Perth: <https://www.gosurfperth.com/blog/2016/8/18/how-are-waves-formed>
- Hillen, M. M. (2009). *Wave reworking of a delta: Process-based modelling of sediment reworking under wave conditions in the deltaic environment*. Delft University of Technology, Civil Engineering and Geosciences. Delft: TU Delft, Civil Engineering and Geosciences, Hydraulic Engineering. doi:uuid:f1a4983d-acfa-47b5-8579-0a08d4c90dc1
- Holthuijsen, L. H. (2007). *Waves in oceanic and coastal waters* (1st ed.). Cambridge: Cambridge University Press. Retrieved November 27, 2018
- Huisman, B. J. (2019). *On the redistribution and sorting of sand at nourishments: Field evidence and modelling of transport processes and bed composition change*. Delft: Delft University of Technology. doi:10.4233/uuid:a2bbb49d-8642-4a32-b479-4f0091f2d206
- Kennesaw State University. (n.d.). *Waves and Beaches*. Retrieved January 16, 2019, from Oceanography: <http://ksuweb.kennesaw.edu/~jdirnber/oceanography/LecturesOceanogr/LecWaves/LecWaves.html>

Bibliography

- Klein Tank, A., Beersma, J., Bessembinder, J., Van den Hurk, B., Lenderink, G., & , . (2014). *Klimaatscenario's voor Nederland*. De Bilt: KNMI. Retrieved from http://www.klimaatscenario's.nl/images/Brochure_KNMI14_NL.pdf
- Luijendijk, A. P., De Schipper, M. A., & Ranasinghe, R. (2019). Morphodynamic acceleration techniques for multi-timescale predictions of complex sandy interventions. *Journal of Marine Science and Engineering*, 7(3), 23. doi:10.3390/jmse7030078
- Luijendijk, A. P., Ranasinghe, R., De Schipper, M. A., Huisman, B. A., Swinkels, C. M., Walstra, D. J., & Stive, M. J. (2017, January). The initial morphological response of the Sand Engine: A process-based modelling study. *Coastal Engineering*, 119, 1-14. doi:10.1016/j.coastaleng.2016.09.005
- Mulder, J. P., Hommes, S., & Horstman, E. M. (2011, December). Implementation of coastal erosion management in the Netherlands. *Ocean & Coastal Management*, 54(12), 888-897. doi:10.1016/j.ocecoaman.2011.06.009
- Rijkswaterstaat. (n.d.). *Planning en aanpak*. Retrieved December 7, 2018, from Rijkswaterstaat: <https://www.rijkswaterstaat.nl/water/waterbeheer/bescherming-tegen-het-water/maatregelen-om-overstromingen-te-voorkomen/kustonderhoud/planning-en-aanpak.aspx>
- Short, A. D. (2012). *Coastal Processes and Beaches*. Retrieved November 26, 2018, from Nature Education Knowledge: <https://www.nature.com/scitable/knowledge/library/coastal-processes-and-beaches-26276621>
- Stronkhorst, J., Van Rijn, L. C., & De Vroeg, H. (2010). *Technische mogelijkheden voor een dynamische kustuitbreiding: Een voorverkenning t.b.v. het Deltaprogramma*. Delft: Deltares. doi:d3968fe5-5947-445f-99de-adb8a1d192ba
- Texas A&M University at Corpus Christi. (n.d.). *Coastal physical processes*. Retrieved November 19, 2018, from <https://cbi.tamucc.edu/CHRGIS/CHRGIS-Physical-Processes/>
- Tonnon, P. K., Huisman, B. J., Stam, G. N., & Van Rijn, L. C. (2018, January). Numerical modelling of erosion rates, life span and maintenance volumes of mega nourishments. *Coastal Engineering*, 131, 51-69. doi:10.1016/j.coastaleng.2017.10.001
- University of Florida. (2014, February 18). *Index of /adamsp/Outgoing/GLY4734_Spring2014*. Retrieved November 19, 2018, from users.clas.ufl.edu: http://users.clas.ufl.edu/adamsp/Outgoing/GLY4734_Spring2014/S14_NearshoreCirc.pptx.pdf
- Van der Spek, A. J., Cleveringa, J., Van Heteren, S., Van Dam, R. L., Schrijver, B., & , . (1999). *Reconstructie van de ontwikkeling van de Hollandse kust in de laatste 2500 jaar*. Nederlands Instituut voor Toegepaste Geowetenschappen TNO. Utrecht: Rijkswaterstaat, RIKZ. doi:f124e845-089c-4354-bb53-58450cb658f7
- Van Rijn, L. C. (1997). Sediment transport and budget of the central coastal zone of Holland. *Coastal Engineering*, 32(1), 61-90. doi:10.1016/S0378-3839(97)00021-5

List of Figures

FIGURE 1 THE CONCEPT ZANDWINDMOLEN AS HOW IT WORKS. (IMAGE SOURCE: DEKKER (2013))	1
FIGURE 2 VISUALIZATION OF THE PROBLEM ANALYSIS: THE BEHAVIOR OF SEDIMENT PARTICLES AFTER BEING DISPOSED NEAR THE SHORELINE.....	2
FIGURE 3 THE DUTCH COAST SEPARATED IN THREE COASTAL SECTIONS. THE HOLLAND COAST IS LOCATED BETWEEN HOEK VAN HOLLAND AND DEN HELDER, WHERE IJMUIDEN SEPARATES THE NORTHERN PART FROM THE SOUTHERN PART. (IMAGE SOURCE: MULDER, HOMMES, & HORSTMAN (2011))	5
FIGURE 4 THE BEACH SYSTEM AS IS KNOWN FOR THE HOLLAND COAST. THE DEEP WATER LINE IS LOCATED AT THE MSL -20.0 M DEPTH CONTOUR. SEVERAL SAND BARS FUNCTION AS WAVE BREAKER. (IMAGE SOURCE: SHORT (2012))	6
FIGURE 5 DIFFRACTION (LEFT) AND REFRACTION (RIGHT). DIFFRACTION OCCURS DUE TO OBSTACLE IN THE PATH OF THE WAVE. REFRACTION IS CAUSED BY CHANGING ORIENTATION OF DEPTH CONTOURS, AS THE WAVE DIRECTION IS PERPENDICULAR TO THE DEPTH CONTOURS. (IMAGES SOURCE: KENNESAW STATE UNIVERSITY (N.D.))	8
FIGURE 6 UNDERTOW UNDERNEATH WAVES. THE ORBITAL MOTIONS CAUSE THIS RETURN CURRENT. (IMAGE SOURCE: UNIVERSITY OF FLORIDA (2014))	8
FIGURE 7 ORBITAL MOTIONS UNDERNEATH WAVES. IN DEEPER LAYERS, THE EFFECT OF THE WAVES IS NEGLIGIBLY SMALL. THIS LINE IS MARKED AS THE WAVE BASE AND IS EQUAL TO $\frac{1}{2}$ OF THE WAVE LENGTH. (IMAGE SOURCE: GOSURF PERTH (2016))	9
FIGURE 8 PLUNGING WAVE BREAKING IS THE MOST COMMON TYPE OF BREAKING AT THE HOLLAND COAST. A LOT OF WAVE ENERGY IS RELEASED WHICH CAUSES AN INCREASED SEDIMENT TRANSPORT GRADIENT. (IMAGE SOURCE: HOLTHUIJSEN (2007))	9
FIGURE 9 CROSS-SHORE HORIZONTAL PROFILE OF THE LONGSHORE CURRENT IN THE SURF ZONE. PROFILE C IS THE SUM OF THE TIDAL CURRENT (A) AND THE WAVE-INDUCED CURRENT (B). THE TIDAL CURRENT CHANGES DIRECTION FOR FLOOD (LEFT) AND EBB (RIGHT), WHICH CHANGES THE NET DIRECTION AND MAGNITUDE OF THE LONGSHORE CURRENT. (IMAGE SOURCE: BOSBOOM & STIVE (2015))	11
FIGURE 10 THE OCCURRENCE OF EROSION AT THE BEACH. THE RUN-UP (SWASH) BY WAVES GENERATES A RUN-DOWN (BACKWASH) THAT TRANSPORTS SEDIMENT TO THE SURF ZONE. THE NET TRANSPORT DIRECTION IS THEN TO THE NORTH (RIGHT IN THE FIGURE). (IMAGE SOURCE: TEXAS A&M UNIVERSITY AT CORPUS CHRISTI (N.D.))	12
FIGURE 11 VISUALIZATION OF THE EFFECT OF SEA LEVEL RISE ON THE SEDIMENT DEMAND IN THE NEARSHORE ZONE. THE BRUUN RULE IS DEVELOPED TO MOTIVATE THIS. (IMAGE SOURCE: COOPER & PILKEY (2004)).....	13
FIGURE 12 ANNUAL MEASUREMENTS OF THE COASTLINE POSITION FOR THE YEAR 2018. THE MEASUREMENTS ARE RELATIVE TO THE BKL. THE LEFT PART SHOWS THE SOUTHERN HOLLAND COAST BETWEEN HOEK VAN HOLLAND AND IJMUIDEN. THE RIGHT PART SHOWS THE COASTLINE BETWEEN IJMUIDEN AND DEN HELDER. (IMAGE SOURCE: RIKSWATERSTAAT (N.D.))	14
FIGURE 13 MORPHOLOGICAL DEVELOPMENT OF THE SAND ENGINE IN THE FIRST THREE YEARS OF ITS LIFETIME. THE NOURISHMENT IS FLATTENED AT THE SEASIDE, MAINLY DUE TO OBLIQUE WAVE FORCING. (IMAGE SOURCE: TONNON, HUISMAN, STAM, & VAN RIJN (2018)).....	15
FIGURE 14 EXPECTED SEDIMENT VOLUME FOR SEVERAL COASTAL STRETCHES OF THE DUTCH COAST. THE SOUTHERN HOLLAND COAST IS EXPECTED TO HAVE A SHORTAGE OF 2.35 MILLION m^3 PER YEAR FOR THE CASE WITH 80 CM SEA LEVEL RISE IN THE YEAR 2100. FROM THIS VOLUME, 750'000 m^3 IS REQUIRED BETWEEN THE SHORELINE AND THE MSL -8.0 M DEPTH CONTOUR. (IMAGE SOURCE: DEKKER (2013))	17
FIGURE 15 POSSIBLE ACCELERATING SEA LEVEL RISE UP TO THE YEAR 2100. THE WORST-CASE SCENARIO (RCP8.5) PREDICTS A RISE OF OVER 120 CM WITHIN ONE CENTURY, WHICH IS TWICE THE RISING HEIGHT OF THE SECOND SCENARIO (RCP4.5). (IMAGE SOURCE: DELTARES (2018))	17
FIGURE 16 SCHEMATIZATION OF THE PERFORMED STEPS IN THE MOR-MODULE IN DELFT3D. THE MORPHOLOGICAL SCALE FACTOR IS BUILT IN THE STEP FROM 'SEDIMENT TRANSPORT' TO 'BED CHANGE'. (IMAGE SOURCE: HILLEN (2009)).....	24
FIGURE 17 FLOW GRID (BLUE) AND WAVE GRID (GREY). THE WAVE DOMAIN IS MUCH LARGER IN ORDER TO ACCURATELY PREDICT WAVE CHARACTERISTICS FOR THE FLOW DOMAIN.	26
FIGURE 18 AREA OF INTEREST FOR THE RESEARCH. THIS AREA IS BOUNDED BY THE DUNES AND THE 10 M DEPTH CONTOUR, AND THE INITIAL LOCATION OF THE SAND ENGINE IN THE SOUTHWEST AND THE PORT ENTRANCE OF SCHEVENINGEN IN THE NORTHEAST.	27

List of Figures

FIGURE 19 BOUNDARY CONDITIONS FOR SEA03. THE FLUCTUATIONS REPRESENT THE TIDAL CYCLE IN THE NORTH SEA. FOR EVERY BOUNDARY AT SEA, THE VALUES ARE SLIGHTLY DIFFERENT.	28
FIGURE 20 TIME FRAME FOR THE SIMULATIONS. THE DURATION BETWEEN START AND END TIME IS 291 DAYS.	30
FIGURE 21 MORPHODYNAMIC ACCELERATION ON THE WAVE DATA. THE BRUTE FORCE FILTERED AND BRUTE FORCE FILTERED & COMPRESSED HAVE BEEN USED TO REDUCE THE TIME SERIES AND AFTER THAT THE SERIES HAS BEEN COMPRESSED. (IMAGE SOURCE: LUIJENDIJK, DE SCHIPPER, & RANASINGHE (2019)	30
FIGURE 22 WAVE ROSE REPRESENTING THE INPUT WAVE DATA FOR THE FIRST YEAR OF THE MODEL SIMULATION TIME SCALE. AN ANALYSIS OF THIS WAVE DATA IS ELABORATED IN APPENDIX B.2.	31
FIGURE 23 MEAN TOTAL TRANSPORT AFTER 1 YEAR (= TIME-AVERAGED TOTAL TRANSPORT). THE RED ZONE LOCATED AT COORDINATES X,Y = [70,449] REPRESENTS A TRANSPORT BELT WITH SIGNIFICANTLY LARGE TRANSPORT MAGNITUDES.	32
FIGURE 24 RELATION BETWEEN DIFFERENT TIMESCALES IN THE MODEL AND RESULTS. THE REDUCTION OF WAVE DATA AND THE MORPHOLOGICAL ACCELERATION FACTOR LEAD TO AN INCREASE OF COMPUTATION OF 6.27, WHICH IS THE FACTOR FOR MULTIPLYING THE MORPHOLOGICAL TIME IN THE RESULTS.	33
FIGURE 25 DISCHARGES INPUT SCREEN.	34
FIGURE 26 RELATION BETWEEN CONCENTRATION OF SEDIMENT PARTICLES (IN KG/M^3) AND DISCHARGE RATE (IN M^3/S), FOR SEVERAL ANNUAL NOURISHMENT VOLUMES. THE CALCULATION OF THIS GRAPH IS SHOWN IN APPENDIX B.1. THE VARIABLE IS THE ADDED VOLUME OF WATER: MORE WATER DECREASES THE CONCENTRATION AND THUS INCREASES THE DISCHARGE RATE, FOR A CONSTANT SEDIMENT PARTICLE DISCHARGE.	35
FIGURE 27 DISCHARGE LOCATIONS FOR RESEARCH PART 1. THE DISTANCE FROM THE SHORELINE IS ALSO VISUALIZED.	36
FIGURE 28 BED LEVEL AFTER 1 YEAR FOR MSL -3.0 M (LEFT) AND RELATIVE DIFFERENCE TO REFERENCE (RIGHT). THE NOURISHMENTS DEVELOPS AS A BELL-SHAPED EXTENSION OF THE BEACH. THE RELATIVE INCREASE IS AROUND THE NOURISHMENT ONLY, THE DIFFERENCES IN THE REST OF THE DOMAIN ARE MINIMAL.	40
FIGURE 29 MEAN TOTAL TRANSPORT (TIME-AVERAGED TOTAL SEDIMENT TRANSPORT) AFTER 1 YEAR FOR MSL -3.0 M (LEFT) AND RELATIVE DIFFERENCE TO REFERENCE (RIGHT). THE NOURISHMENT CAUSES AN INCREASE IN TRANSPORT JUST DOWNSTREAM IN NORTHEAST DIRECTION. AT THE TRANSPORT ZONE, THE MAGNITUDE DECREASES AS A RESULT OF SHADOWING.	40
FIGURE 30 MEAN TOTAL TRANSPORT ALONG CROSS-SECTION OF NOURISHMENT LOCATION AT 3 M DEPTH, MEASURED FROM THE SHORELINE. THE BLUE PEAK IS LOCATED AT THE NOURISHMENT LOCATION AND SHOWS A SEAWARD SHIFT OF THE TRANSPORT PATTERN.	41
FIGURE 31 TEMPORAL DEVELOPMENT OF BED LEVEL (TOP), MEAN TOTAL TRANSPORT (MIDDLE) AND SIGNIFICANT WAVE HEIGHT (BOTTOM), MEASURED AT THE NOURISHMENT LOCATION. THE BED LEVEL AND TRANSPORT MAGNITUDE INCREASE AS A RESULT OF THE NOURISHMENT. THE WAVE HEIGHT DECREASES DUE TO THE DECREASE IN DEPTH.	42
FIGURE 32 BED LEVEL DEVELOPMENT AFTER 4, 5, 6, AND 7 MONTHS FOR NOURISHING AT 3 M DEPTH. THE STORM CAUSES SIGNIFICANT EROSION OF THE NOURISHMENT AND FLATTENS THE NOURISHMENT OVER A LARGER AREA. APPENDIX D.2 VISUALIZES BOTH BED LEVEL AND MEAN TOTAL TRANSPORT AFTER EACH MONTH.	43
FIGURE 33 BED LEVEL AFTER 1 YEAR FOR MSL -4.0 M (LEFT) AND RELATIVE DIFFERENCE TO REFERENCE (RIGHT). THE NOURISHMENTS DEVELOPS AS AN OVAL-SHAPED ISLAND, CONNECTED TO THE BEACH. THE RELATIVE INCREASE IS AROUND THE NOURISHMENT ONLY, THE DIFFERENCES IN THE REST OF THE DOMAIN ARE MINIMAL.	44
FIGURE 34 MEAN TOTAL TRANSPORT AFTER 1 YEAR FOR MSL -4.0 M (LEFT) AND RELATIVE DIFFERENCE TO REFERENCE (RIGHT). THE NOURISHMENT CAUSES AN INCREASE IN TRANSPORT JUST DOWNSTREAM IN NORTHEAST DIRECTION, ALTHOUGH THIS INCREASE IS NOT SIGNIFICANTLY LARGE. AT THE TRANSPORT ZONE, THE MAGNITUDE DECREASES AS A RESULT OF SHADOWING.	44
FIGURE 35 MEAN TOTAL TRANSPORT ALONG CROSS-SECTION OF NOURISHMENT LOCATION AT 4 M DEPTH, MEASURED FROM THE SHORELINE. THE BLUE PEAKS ARE ALMOST EQUAL IN MAGNITUDE.	45
FIGURE 36 TEMPORAL DEVELOPMENT OF BED LEVEL (TOP), MEAN TOTAL TRANSPORT (MIDDLE) AND SIGNIFICANT WAVE HEIGHT (BOTTOM), MEASURED AT THE NOURISHMENT LOCATION. THE BED LEVEL AND TRANSPORT MAGNITUDE INCREASE AS A RESULT OF THE NOURISHMENT. THE WAVE HEIGHT DECREASES DUE TO THE DECREASE IN DEPTH.	46
FIGURE 37 BED LEVEL DEVELOPMENT AFTER 4, 5, 6, AND 7 MONTHS FOR NOURISHING AT 4 M DEPTH. THE STORM CAUSES SIGNIFICANT EROSION OF THE NOURISHMENT AND FLATTENS THE NOURISHMENT OVER A LARGER AREA. APPENDIX E.2 VISUALIZES BOTH BED LEVEL AND MEAN TOTAL TRANSPORT AFTER EACH MONTH.	47

FIGURE 38 BED LEVEL AFTER 1 YEAR FOR MSL -5.0 M (LEFT) AND RELATIVE DIFFERENCE TO REFERENCE (RIGHT). THE NOURISHMENT DEVELOPS AS A SMALL CIRCULAR ISLAND IN FRONT OF THE SHORELINE. THE DEPTH BETWEEN THE NOURISHMENT AND THE SHORELINE HAS SLIGHTLY DECREASED. A SMALL EXTENSION OF THE BEACH NEAR THE NOURISHMENT IS NOTICED, WHICH CAN MEAN THAT THE BEACH WILL EVENTUALLY BE CONNECTED TO THE NOURISHMENT (E.G. AS A TOMBOLO).	48
FIGURE 39 MEAN TOTAL TRANSPORT AFTER 1 YEAR FOR MSL -5.0 M (LEFT) AND RELATIVE DIFFERENCE TO REFERENCE (RIGHT). THE NOURISHMENT CAUSES AN INCREASE IN TRANSPORT JUST DOWNSTREAM IN NORTHEAST DIRECTION. AT THE TRANSPORT ZONE, THE MAGNITUDE DECREASES AS A RESULT OF SHADOWING.....	48
FIGURE 40 MEAN TOTAL TRANSPORT ALONG CROSS-SECTION OF NOURISHMENT LOCATION AT 5 M DEPTH, MEASURED FROM THE SHORELINE. THE BLUE PEAK AT 100 M IS ALMOST EQUAL TO THE REFERENCE TRANSPORT PEAK, WHILE THE SECOND PEAK AT 300 M IS CAUSED BY THE NOURISHMENT. IT IS LIKELY THAT THE EFFECT OF THE NOURISHMENT ON THE TRANSPORT BELT AT 3 M DEPTH DECREASES WHEN NOURISHING IN DEEPER WATER.....	49
FIGURE 41 TEMPORAL DEVELOPMENT OF BED LEVEL (TOP), MEAN TOTAL TRANSPORT (MIDDLE) AND SIGNIFICANT WAVE HEIGHT (BOTTOM), MEASURED AT THE NOURISHMENT LOCATION. THE BED LEVEL AND TRANSPORT MAGNITUDE INCREASE AS A RESULT OF THE NOURISHMENT. THE WAVE HEIGHT DECREASES DUE TO THE DECREASE IN DEPTH.....	50
FIGURE 42 BED LEVEL DEVELOPMENT AFTER 4, 5, 6, AND 7 MONTHS FOR NOURISHING AT 5 M DEPTH. THE STORM CAUSES SIGNIFICANT EROSION OF THE NOURISHMENT AND FLATTENS THE NOURISHMENT OVER A LARGER AREA. APPENDIX F.2 VISUALIZES BOTH BED LEVEL AND MEAN TOTAL TRANSPORT AFTER EACH MONTH.....	51
FIGURE 43 BED LEVEL AFTER 1 YEAR FOR MSL -6.0 M (LEFT) AND RELATIVE DIFFERENCE TO REFERENCE (RIGHT). THE BED LEVEL DIFFERENCES ARE CENTERED ON THE NOURISHMENT. THE NOURISHMENT SEEMS NOT TO AFFECT THE ZONE BETWEEN THE NOURISHMENT AND THE SHORELINE.....	52
FIGURE 44 MEAN TOTAL TRANSPORT AFTER 1 YEAR FOR MSL -6.0 M (LEFT) AND RELATIVE DIFFERENCE TO REFERENCE (RIGHT). TRANSPORT FROM THE NOURISHMENT IS SMALL COMPARED TO THE MAGNITUDES IN THE TRANSPORT ZONE BETWEEN MSL -1.0 M AND MSL -4.0 M. THE DIFFERENCES WITH THE REFERENCE SITUATION ARE NEGLIGIBLY SMALL.....	52
FIGURE 45 MEAN TOTAL TRANSPORT ALONG CROSS-SECTION OF NOURISHMENT LOCATION AT 6 M DEPTH, MEASURED FROM THE SHORELINE. THE BLUE PEAK AT 100 M IS EQUAL IN MAGNITUDE. A SECOND PEAK AT THE NOURISHMENT LOCATION SHOWS AN INCREASE OF 200%.....	53
FIGURE 46 TEMPORAL DEVELOPMENT OF BED LEVEL (TOP), MEAN TOTAL TRANSPORT (MIDDLE) AND SIGNIFICANT WAVE HEIGHT (BOTTOM), MEASURED AT THE NOURISHMENT LOCATION. THE BED LEVEL AND TRANSPORT MAGNITUDE INCREASE AS A RESULT OF THE NOURISHMENT. THE WAVE HEIGHT DECREASES DUE TO THE DECREASE IN DEPTH.....	54
FIGURE 47 BED LEVEL DEVELOPMENT AFTER 4, 5, 6, AND 7 MONTHS FOR NOURISHING AT 6 M DEPTH. THE STORM CAUSES SIGNIFICANT EROSION OF THE NOURISHMENT AND FLATTENS THE NOURISHMENT TOWARDS THE SHORELINE. APPENDIX G.2 VISUALIZES BOTH BED LEVEL AND MEAN TOTAL TRANSPORT AFTER EACH MONTH.....	55
FIGURE 48 TEMPORAL DEVELOPMENT OF BED LEVEL AND MEAN TOTAL TRANSPORT MAGNITUDE FOR THE FOUR NOURISHMENT DEPTHS.	56
FIGURE 49 MEAN TOTAL TRANSPORT RELATIVE TO REFERENCE SITUATION FOR THE 4 NOURISHMENT DEPTHS.....	58
FIGURE 50 MEAN TOTAL TRANSPORT ALONG CROSS-SECTION OF ALL NOURISHMENT LOCATIONS, MEASURED FROM THE SHORELINE. THE INFLUENCE ON THE TRANSPORT BELT OF THE NOURISHMENT AT 3 M AND 4 M DEPTH IS LARGE. THE MAXIMUM TRANSPORT MAGNITUDE AT THE NOURISHMENT LOCATION DECREASES WITH INCREASING DEPTH.....	59
FIGURE 51 BED LEVEL AFTER 1 YEAR FOR A DISCHARGE OF 150'000 M ³ /YEAR (LEFT) AND RELATIVE DIFFERENCE TO REFERENCE (RIGHT). THE NOURISHMENTS DEVELOPS AS A BELL-SHAPED EXTENSION OF THE BEACH. THE RELATIVE INCREASE IS AROUND THE NOURISHMENT ONLY, THE DIFFERENCES IN THE REST OF THE DOMAIN ARE MINIMAL. A SHALLOW PLUME IS TRAVELLING TO THE SOUTHWEST.....	61
FIGURE 52 MEAN TOTAL TRANSPORT AFTER 1 YEAR FOR A DISCHARGE OF 150'000 M ³ /YEAR (LEFT) AND RELATIVE DIFFERENCE TO REFERENCE (RIGHT). THE NOURISHMENT CAUSES AN INCREASE IN TRANSPORT JUST DOWNSTREAM IN NORTHEAST DIRECTION. AT THE TRANSPORT ZONE, THE MAGNITUDE DECREASES AS A RESULT OF SHADOWING.....	61
FIGURE 53 MEAN TOTAL TRANSPORT ALONG CROSS-SECTION OF NOURISHMENT LOCATION AT 3 M DEPTH WITH INCREASED NOURISHMENT VOLUME, MEASURED FROM THE SHORELINE. THE TRANSPORT PEAK AT 3 M DEPTH IS SIGNIFICANTLY LARGER THAN THE REFERENCE PEAK AT 2 M DEPTH.	62

List of Figures

FIGURE 54 TEMPORAL DEVELOPMENT OF BED LEVEL (TOP), MEAN TOTAL TRANSPORT (MIDDLE) AND SIGNIFICANT WAVE HEIGHT (BOTTOM), MEASURED AT THE NOURISHMENT LOCATION. THE BED LEVEL AND TRANSPORT MAGNITUDE INCREASE AS A RESULT OF THE NOURISHMENT. THE WAVE HEIGHT DECREASES DUE TO THE DECREASE IN DEPTH.....	63
FIGURE 55 BED LEVEL DEVELOPMENT AFTER 4, 5, 6, AND 7 MONTHS FOR NOURISHING AT 3 M DEPTH. THE STORM CAUSES SIGNIFICANT EROSION OF THE NOURISHMENT AND FLATTENS THE NOURISHMENT OVER A LARGER AREA. APPENDIX H.2 VISUALIZES BOTH BED LEVEL AND MEAN TOTAL TRANSPORT AFTER EACH MONTH.....	64
FIGURE 56 TEMPORAL DEVELOPMENT OF BED LEVEL, MEAN TOTAL TRANSPORT MAGNITUDE AND SIGNIFICANT WAVE HEIGHT FOR TWO ANNUAL DISCHARGE VOLUMES AT MSL -3.0 M.....	65
FIGURE 57 DIFFERENCE IN BED LEVEL AND MEAN TOTAL TRANSPORT MAGNITUDE OF NOURISHMENT OF 150'000 M3/YEAR RELATIVE TO 100'000 M3/YR.....	66
FIGURE 58 MEAN TOTAL TRANSPORT ALONG CROSS-SECTION OF FOR THE THREE NOURISHMENT VOLUMES AT 3 M, MEASURED FROM THE SHORELINE: NO VOLUME, 100'000 AND 150'000 M3/YEAR. THE INCREASE OF THE VOLUME LEADS TO A SMALL INCREASE OF TRANSPORT AT THE NOURISHMENT LOCATION AND A DECREASE IN TRANSPORT AT THE TRANSPORT BELT AS A RESULT OF SHADOWING.	67
FIGURE 59 BED LEVEL AFTER 1 YEAR FOR A NOURISHMENT SPREAD OVER 5 CELLS (LEFT) AND RELATIVE DIFFERENCE TO REFERENCE (RIGHT) AROUND 5 M DEPTH. THE NOURISHMENT DEVELOPS SIGNIFICANTLY IN NORTHEAST DIRECTION.....	68
FIGURE 60 MEAN TOTAL TRANSPORT AFTER 1 YEAR FOR A NOURISHMENT SPREAD OVER 5 CELLS (LEFT) AND RELATIVE DIFFERENCE TO REFERENCE (RIGHT). THE EFFECT ON THE TRANSPORT ZONE IS SMALL.....	69
FIGURE 61 TEMPORAL DEVELOPMENT OF THE BED LEVEL, MEASURED AT THE NOURISHMENT LOCATIONS. THE FOUR ADJACENT CELLS (IN THE CORNERS) GIVE THE EFFECTS OF THE NOURISHMENTS IN A RECTANGULAR DOMAIN. THE BED LEVELS IN THE ADJACENT CELLS INCREASE AS WELL DUE TO THE NOURISHMENTS.	70
FIGURE 62 TEMPORAL DEVELOPMENT OF THE MEAN TOTAL TRANSPORT MAGNITUDE, MEASURED AT THE NOURISHMENT LOCATIONS. IN MOST CELLS, THE TRANSPORT MAGNITUDE HAS INCREASED DUE TO THE NOURISHMENT.....	71
FIGURE 63 MEAN TOTAL TRANSPORT ALONG CROSS-SECTION OF NOURISHMENT LOCATION AT 5 M DEPTH WITH SPREADING OVER MULTIPLE CELLS, MEASURED FROM THE SHORELINE. DUE TO THE SPREADING, THE TRANSPORT MAGNITUDE AT THE NOURISHMENT LOCATIONS IS SPREAD AS WELL.	72
FIGURE 64 TEMPORAL DEVELOPMENT OF THE DIFFERENCE IN SIGNIFICANT WAVE HEIGHT BETWEEN THE NOURISHMENT SIMULATION AND THE REFERENCE SIMULATION, MEASURED AT THE NOURISHMENT LOCATIONS. THE WAVE HEIGHT HAS DECREASED DUE TO A DECREASE IN BED LEVEL, EXCEPT FOR THE ADACENT CELL AT THE SEASIDE, WHERE SMALL INCREASES ARE MEASURED.	73
FIGURE 65 TEMPORAL DEVELOPMENT OF BED LEVEL, FOR SINGLE-LOCATION (GREEN) AND 5-CELL NOURISHMENT (BLUE).	74
FIGURE 66 TEMPORAL DEVELOPMENT OF MEAN TOTAL TRANSPORT MAGNITUDE, FOR SINGLE-LOCATION (GREEN) AND 5-CELL NOURISHMENT (BLUE).	75
FIGURE 67 TEMPORAL DEVELOPMENT OF WAVE HEIGHT, FOR SINGLE-LOCATION (GREEN) AND 5-CELL NOURISHMENT (BLUE). THE FIGURES HAVE SWITCHED LAYOUTS FOR CELLS C5, C6, C8, AND C9. THIS IS TO PRESENT THE DIFFERENCES BETTER.....	76
FIGURE 68 DIFFERENCE IN BED LEVEL AND MEAN TOTAL TRANSPORT MAGNITUDE OF 5-CELL NOURISHMENT RELATIVE TO SINGLE-LOCATION NOURISHMENT.	77
FIGURE 69 MEAN TOTAL TRANSPORT ALONG CROSS-SECTION OF NOURISHMENT LOCATION AT 5 M DEPTH WITH SPREADING OVER MULTIPLE CELLS, MEASURED FROM THE SHORELINE. DUE TO THE SPREADING, THE TRANSPORT MAGNITUDE AT THE NOURISHMENT LOCATIONS IS SPREAD AS WELL. THE SINGLE CELL NOURISHMENT SHOWS A SIGNIFICANTLY LARGER PEAK AT THE NOURISHMENT AREA THAN THE 5-CELL NOURISHMENT.	78
FIGURE 70 GRID OF FLOW (BLUE) AND WAVE DOMAIN (GREY). CELLS ARE SMALLER IN SHALLOWER DEPTH.	100
FIGURE 71 GRID OF FLOW DOMAIN. THE CELLS ARE SMALLER IN SHALLOWER DEPTH.	101
FIGURE 72 BATHYMETRY OF FLOW DOMAIN.....	102
FIGURE 73 WAVE ROSE OF THE DATA USED IN THE MODEL SIMULATIONS. THE TWO MAIN WAVE DIRECTIONS ARE SW AND NNW.105	
FIGURE 74 TEMPORAL DEVELOPMENT OF THE WAVES, REPRESENTED BOTH THE WAVE HEIGHT AND THE DIRECTION FROM WHICH THEY PROPAGATE. THE INCOMING WAVES ARE BOUNDED BY THE SHORE-PARALLEL ORIENTATIONS, WHICH ARE THE PURPLE AND BLACK LINES. OUTSIDE THESE LINES, WAVES ARE NUMERICALLY ORIGINATED FROM LAND, WHICH IS NOT POSSIBLE.	106
FIGURE 75 BED LEVEL AT T = 0 AND T = 1 YEAR. THE IRREGULAR PATTERN OF DEPTH CONTOURS HAS BEEN TRANSFORMED TO PARALLEL DEPTH CONTOURS AFTER 1 YEAR.	108

FIGURE 76 MEAN TOTAL TRANSPORT DIRECTION, SPLIT IN ALONGSHORE AND CROSS-SHORE VECTORS, AND THE MAGNITUDE, FOR 1 YEAR. THE LONGSHORE COMPONENT IS SIGNIFICANTLY LARGER THAN THE CROSS-SHORE COMPONENT, WHICH MEANS THAT LONGSHORE TRANSPORT IS DOMINANT.	109
FIGURE 77 MEAN DEPTH-AVERAGED SUSPENDED SEDIMENT TRANSPORT (LEFT) AND MEAN BED LOAD SEDIMENT TRANSPORT (RIGHT). THE SUSPENDED TRANSPORT COMPONENT IS SIGNIFICANTLY LARGER IN THE ZONE OF STRONG TRANSPORT AND COUNTS FOR 85%.	109
FIGURE 78 DIRECTION OF THE MEAN TOTAL TRANSPORT (GREEN) AND THE ALONGSHORE COMPONENT OF THE TRANSPORT (BLUE). THE CROSS-SHORE COMPONENT IS NEGLIGIBLY SMALL, EVEN WHEN INCLUDING THE CELL WIDTH OVER WHICH THE MAGNITUDE AND DIRECTION IS MEASURED.	110
FIGURE 79 CUMULATIVE EROSION (BLUE) AND SEDIMENTATION (RED) AFTER 1 YEAR. THE IRREGULAR PATTERN IS A CONSEQUENCE OF THE FORMING OF PARALLEL DEPTH CONTOURS.	111
FIGURE 80 TEMPORAL DEVELOPMENT OF BED LEVEL AND MEAN TOTAL TRANSPORT, FOR THE SITUATION MSL -3.0 M, VISUALIZED FOR EACH MONTH FOR THE FIRST YEAR.	112
FIGURE 81 BED LEVEL AT T = 0 AND T = 1 YEAR. THE NOURISHMENT DEVELOPS AS A BELL-SHAPED BEACH EXTENSION AND MAINLY SPREADS IN ALONGSHORE DIRECTION.	116
FIGURE 82 CUMULATIVE EROSION (BLUE) AND SEDIMENTATION (RED) AFTER 1 YEAR. AROUND THE NOURISHMENT, ACCRETION OCCURS. JUST UPSTREAM OF THE NOURISHMENT, EROSION IS PRESENT, CAUSED BY INCREASED ENERGY DISSIPATION OF WAVES DUE TO A SUDDEN DECREASE OF DEPTH.	117
FIGURE 83 MEAN TOTAL TRANSPORT DIRECTION, SPLIT IN ALONGSHORE AND CROSS-SHORE VECTORS, AND THE MAGNITUDE, AFTER 1 YEAR. THE TRANSPORT MAGNITUDE HAS INCREASED DOWNSTREAM FROM THE NOURISHMENT LOCATION, AS A RESULT OF THE INCREASED AVAILABLE VOLUME OF SEDIMENT.	117
FIGURE 84 MEAN DEPTH-AVERAGED SUSPENDED SEDIMENT TRANSPORT (LEFT) AND MEAN BED LOAD SEDIMENT TRANSPORT (RIGHT). THE SUSPENDED TRANSPORT COMPONENT IS SIGNIFICANTLY LARGER IN THE ZONE OF STRONG TRANSPORT AND COUNTS FOR ALMOST 90% IN THE STRONG TRANSPORT ZONE.	118
FIGURE 85 DIRECTION OF THE MEAN TOTAL TRANSPORT (GREEN) AND THE ALONGSHORE COMPONENT OF THE TRANSPORT (BLUE). NEAR THE NOURISHMENT, THE CROSS-SHORE COMPONENT INCREASES RELATIVE TO THE ALONGSHORE COMPONENT.	118
FIGURE 86 TEMPORAL DEVELOPMENT OF BED LEVEL AND MEAN TOTAL TRANSPORT, FOR THE SITUATION AT MSL -3.0 M, VISUALIZED FOR EACH MONTH FOR THE FIRST YEAR.	119
FIGURE 87 BED LEVEL AT T = 0 AND T = 1 YEAR. THE NOURISHMENT IS DEVELOPING AS AN OVAL-SHAPED SMALL ISLAND WHICH IS CONNECTED TO THE BEACH.	123
FIGURE 88 CUMULATIVE EROSION (BLUE) AND SEDIMENTATION (RED) AFTER 1 YEAR. AROUND THE NOURISHMENT, ACCRETION OCCURS. JUST UPSTREAM OF THE NOURISHMENT, EROSION IS PRESENT, CAUSED BY INCREASED ENERGY DISSIPATION OF WAVES DUE TO A SUDDEN DECREASE OF DEPTH.	124
FIGURE 89 MEAN TOTAL TRANSPORT DIRECTION, SPLIT IN ALONGSHORE AND CROSS-SHORE VECTORS, AND THE MAGNITUDE, AFTER 1 YEAR. THE MAGNITUDES ARE NOT EXTREMELY LARGE COMPARED TO THE NOURISHMENT AT MSL -3.0 M.	124
FIGURE 90 MEAN DEPTH-AVERAGED SUSPENDED SEDIMENT TRANSPORT (LEFT) AND MEAN BED LOAD SEDIMENT TRANSPORT (RIGHT). THE SUSPENDED TRANSPORT COMPONENT IS SIGNIFICANTLY LARGER IN THE ZONE OF STRONG TRANSPORT AND COUNTS FOR AT LEAST 80% IN THE TRANSPORT ZONE.	125
FIGURE 91 DIRECTION OF THE MEAN TOTAL TRANSPORT (GREEN) AND THE ALONGSHORE COMPONENT OF THE TRANSPORT (BLUE). NEAR THE NOURISHMENT, THE CROSS-SHORE COMPONENT INCREASES RELATIVE TO THE ALONGSHORE COMPONENT. THIS EFFECT IS VISIBLE FURTHER NORTHEAST IN THE DOMAIN.	125
FIGURE 92 TEMPORAL DEVELOPMENT OF BED LEVEL AND MEAN TOTAL TRANSPORT, FOR THE SITUATION AT MSL -4.0 M, VISUALIZED FOR EACH MONTH FOR THE FIRST YEAR.	126
FIGURE 93 BED LEVEL AT T = 0 AND T = 1 YEAR. THE NOURISHMENT DEVELOPS AS A CIRCULAR-SHAPED ISLAND. THE BEACH IS EXTENDING NEAR THE NOURISHMENT, WHICH CAN DEVELOP AS A TOMBOLO (A SAND BAR CONNECTING THE NOURISHMENT AND THE SHORELINE).	130
FIGURE 94 CUMULATIVE EROSION (BLUE) AND SEDIMENTATION (RED) AFTER 1 YEAR. AROUND THE NOURISHMENT, ACCRETION OCCURS. JUST UPSTREAM OF THE NOURISHMENT, EROSION IS PRESENT, CAUSED BY INCREASED ENERGY DISSIPATION OF WAVES DUE TO A SUDDEN DECREASE OF DEPTH. NORTHEAST OF THE NOURISHMENT A LARGE EROSION SPOT IS NOTICED.	131

List of Figures

FIGURE 95 MEAN TOTAL TRANSPORT DIRECTION, SPLIT IN ALONGSHORE AND CROSS-SHORE VECTORS, AND THE MAGNITUDE, AFTER 1 YEAR. THE TRANSPORT MAGNITUDE HAS INCREASED DOWNSTREAM FROM THE NOURISHMENT LOCATION, AS A RESULT OF THE INCREASED AVAILABLE VOLUME OF SEDIMENT.	131
FIGURE 96 MEAN DEPTH-AVERAGED SUSPENDED SEDIMENT TRANSPORT (LEFT) AND MEAN BED LOAD SEDIMENT TRANSPORT (RIGHT). THE SUSPENDED TRANSPORT COMPONENT IS SIGNIFICANTLY LARGER IN THE ZONE OF STRONG TRANSPORT AND COUNTS FOR ALMOST 80% IN THE STRONG TRANSPORT ZONE.	132
FIGURE 97 DIRECTION OF THE MEAN TOTAL TRANSPORT (GREEN) AND THE ALONGSHORE COMPONENT OF THE TRANSPORT (BLUE). NEAR THE NOURISHMENT, THE CROSS-SHORE COMPONENT INCREASES RELATIVE TO THE ALONGSHORE COMPONENT. THIS HAS NO EFFECT ON THE TRANSPORT DIRECTION FURTHER DOWNSTREAM.	132
FIGURE 98 TEMPORAL DEVELOPMENT OF BED LEVEL AND MEAN TOTAL TRANSPORT, FOR THE SITUATION AT MSL -5.0 M, VISUALIZED FOR EACH MONTH FOR THE FIRST YEAR.	133
FIGURE 99 BED LEVEL AT T = 0 AND T = 1 YEAR. THE NOURISHMENT IS A CIRCULAR-SHAPED SUBMERGED ISLAND IN DEEPER WATER. THE DEPTH CONTOURS CURVE AROUND THE NOURISHMENT. BETWEEN THE NOURISHMENT AND THE SHORELINE, THE DEPTH IS FAIRLY UNIFORM TO THE REFERENCE SITUATION.	137
FIGURE 100 CUMULATIVE EROSION (BLUE) AND SEDIMENTATION (RED) AFTER 1 YEAR. AROUND THE NOURISHMENT, ACCRETION OCCURS. BETWEEN THE NOURISHMENT AND THE SHORELINE, SMALL EROSION AND ACCRETION OCCURS IN THE ORDER OF DECIMETERS. NORTHEAST OF THE NOURISHMENT, SIGNIFICANT EROSION OCCURS AS A RESULT OF INCREASED SEDIMENT TRANSPORT TO THE NORTHEAST.	138
FIGURE 101 MEAN TOTAL TRANSPORT DIRECTION, SPLIT IN ALONGSHORE AND CROSS-SHORE VECTORS, AND THE MAGNITUDE, AFTER 1 YEAR. THE TRANSPORT ZONE BETWEEN MSL -1.0 M AND MSL -4.0 M IS HARDLY AFFECTED BY THE NOURISHMENT. A SMALL TRANSPORT MAGNITUDE IS FOUND NEAR THE NOURISHMENT.	138
FIGURE 102 MEAN DEPTH-AVERAGED SUSPENDED SEDIMENT TRANSPORT (LEFT) AND MEAN BED LOAD SEDIMENT TRANSPORT (RIGHT). THE RELATION OF THE MAXIMUM VALUES OF TRANSPORT IS SIMILAR TO THE REFERENCE SITUATION.	139
FIGURE 103 DIRECTION OF THE MEAN TOTAL TRANSPORT (GREEN) AND THE ALONGSHORE COMPONENT OF THE TRANSPORT (BLUE). ALSO FROM THIS FIGURE CAN BE DERIVED THAT THE TRANSPORT MAGNITUDE AND DIRECTION FROM THE NOURISHMENT HARDLY AFFECTS THE TRANSPORT ZONE BETWEEN MSL -1.0 M AND MSL -4.0 M.	139
FIGURE 104 TEMPORAL DEVELOPMENT OF BED LEVEL AND MEAN TOTAL TRANSPORT, FOR THE SITUATION AT MSL -6.0 M, VISUALIZED FOR EACH MONTH FOR THE FIRST YEAR.	140
FIGURE 105 BED LEVEL AT T = 0 AND T = 1 YEAR. THE NOURISHMENT DEVELOPS AS A BELL-SHAPED BEACH EXTENSION AND MAINLY SPREADS IN ALONGSHORE DIRECTION. THE NOURISHMENT ALMOST REACHES THE MEAN WATER LEVEL.	144
FIGURE 106 CUMULATIVE EROSION (BLUE) AND SEDIMENTATION (RED) AFTER 1 YEAR. AROUND THE NOURISHMENT, ACCRETION OCCURS. JUST UPSTREAM OF THE NOURISHMENT, EROSION IS PRESENT, CAUSED BY INCREASED ENERGY DISSIPATION OF WAVES DUE TO A SUDDEN DECREASE OF DEPTH. A SMALL PLUME TOWARDS THE SOUTHWEST IS DEVELOPING DUE TO (PARTIAL) BLOCKAGE OF SEDIMENT IN THE TRANSPORT ZONE.	145
FIGURE 107 MEAN TOTAL TRANSPORT DIRECTION, SPLIT IN ALONGSHORE AND CROSS-SHORE VECTORS, AND THE MAGNITUDE, AFTER 1 YEAR. THE TRANSPORT MAGNITUDE HAS INCREASED DOWNSTREAM FROM THE NOURISHMENT LOCATION, AS A RESULT OF THE INCREASED AVAILABLE VOLUME OF SEDIMENT.	145
FIGURE 108 MEAN DEPTH-AVERAGED SUSPENDED SEDIMENT TRANSPORT (LEFT) AND MEAN BED LOAD SEDIMENT TRANSPORT (RIGHT). THE SUSPENDED TRANSPORT COMPONENT IS SIGNIFICANTLY LARGER IN THE ZONE OF STRONG TRANSPORT AND COUNTS FOR ALMOST 90% IN THE STRONG TRANSPORT ZONE.	146
FIGURE 109 DIRECTION OF THE MEAN TOTAL TRANSPORT (GREEN) AND THE ALONGSHORE COMPONENT OF THE TRANSPORT (BLUE). NEAR THE NOURISHMENT, THE CROSS-SHORE COMPONENT INCREASES RELATIVE TO THE ALONGSHORE COMPONENT.	146
FIGURE 110 TEMPORAL DEVELOPMENT OF BED LEVEL AND MEAN TOTAL TRANSPORT, FOR THE SITUATION WITH AN INCREASED ANNUAL VOLUME, VISUALIZED FOR EACH MONTH FOR THE FIRST YEAR.	147
FIGURE 111 BED LEVEL AT T = 0 AND T = 1 YEAR. THE NOURISHMENT IS SPREAD OVER 5 LOCATIONS, WHICH MAKES THE NOURISHMENT MORE GRADUAL IN THE DOMAIN. THE MAXIMUM HEIGHT IS MUCH LESS. ITS ALONGSHORE SPREAD IS SIMILAR TO THE SINGLE-LOCATION-NOURISHMENT.	151

FIGURE 112 CUMULATIVE EROSION (BLUE) AND SEDIMENTATION (RED) AFTER 1 YEAR. SEDIMENTATION IS VISIBLE NORTHEAST OF THE NOURISHMENT. THE SPREAD OF SEDIMENT IN THIS DIRECTION IS STIMULATED BY THE SUPPLY OF SEDIMENT OVER MULTIPLE LOCATIONS.	152
FIGURE 113 MEAN TOTAL TRANSPORT DIRECTION, SPLIT IN ALONGSHORE AND CROSS-SHORE VECTORS, AND THE MAGNITUDE, AFTER 1 YEAR. THE TRANSPORT MAGNITUDE FROM THE NOURISHMENT IS SMALL COMPARED TO THE SINGLE-LOCATION-NOURISHMENT. THIS IS MAINLY DUE TO THE SPREAD OF SEDIMENT OVER MULTIPLE LOCATIONS. PER CELL, LESS SEDIMENT IS AVAILABLE FOR TRANSPORT.....	152
FIGURE 114 MEAN DEPTH-AVERAGED SUSPENDED SEDIMENT TRANSPORT (LEFT) AND MEAN BED LOAD SEDIMENT TRANSPORT (RIGHT). THE SUSPENDED TRANSPORT COMPONENT IS SIGNIFICANTLY LARGER IN THE ZONE OF STRONG TRANSPORT AND COUNTS FOR ALMOST 90% IN THE STRONG TRANSPORT ZONE.	153
FIGURE 115 DIRECTION OF THE MEAN TOTAL TRANSPORT (GREEN) AND THE ALONGSHORE COMPONENT OF THE TRANSPORT (BLUE). NEAR THE NOURISHMENT, THE CROSS-SHORE COMPONENT INCREASES RELATIVE TO THE ALONGSHORE COMPONENT. THE EFFECT ON THE TRANSPORT ZONE IS NOT SIGNIFICANTLY LARGE.	153
FIGURE 116 TEMPORAL DEVELOPMENT OF BED LEVEL AND MEAN TOTAL TRANSPORT, FOR THE SITUATION WITH AN INCREASED NOURISHMENT AREA, VISUALIZED FOR EACH MONTH FOR THE FIRST YEAR.	154

List of Tables

TABLE 1 MODULES AVAILABLE IN THE DELFT3D SOFTWARE PACKAGE (SOURCE: DELTARES (2014))	24
TABLE 2 BOUNDARY CONDITIONS IN THE MODEL. THE NIEUWE WATERWEG REPRESENTS A DISCHARGE, WHICH IS THE RIVER OUTPUT.	28
TABLE 3 INPUT VALUES FOR MODEL.....	32
TABLE 4 INPUT VALUES FOR SIMULATIONS. SIMULATION 101 REPRESENTS THE REFERENCE SITUATION, WITHOUT A NOURISHMENT..	36
TABLE 5 SEDIMENT REDISTRIBUTION DISTANCE IN ALONGSHORE AND CROSS-SHORE DIRECTION FOR THE 4 NOURISHMENT DEPTHS. THE VALUES ARE RETRIEVED FROM THE BED LEVEL FIGURES IN PARAGRAPHS 4.1.1 TO 4.1.4.	60
TABLE 6 SEDIMENT REDISTRIBUTION DISTANCE IN ALONGSHORE AND CROSS-SHORE DIRECTION FOR THE TWO ANNUAL NOURISHMENT VOLUMES. THE VALUES ARE RETRIEVED FROM PARAGRAPH 4.1.1 AND 4.2.1.	67
TABLE 7 SEDIMENT REDISTRIBUTION DISTANCE IN ALONGSHORE AND CROSS-SHORE DIRECTION FOR THE TWO SPREADING CONFIGURATIONS. THE VALUES ARE RETRIEVED FROM PARAGRAPH 4.1.3 AND 4.3.1.	78
TABLE 8 GENERAL PARAMETERS TO CALCULATE THE REQUIRED DISCHARGE AND CONCENTRATION FOR INPUT.	103
TABLE 9 VALUES FOR DISCHARGE Q AND CONCENTRATION C FOR DIFFERENT VALUES OF WATER VOLUME V_w . THE NOURISHMENT VOLUME IS 100'000 m^3 PER YEAR IN SITU.	104
TABLE 10 INPUT SETTINGS FOR NOURISHMENT AT MSL -3.0 M	116
TABLE 11 INPUT SETTINGS FOR NOURISHMENT AT MSL -4.0 M	123
TABLE 12 INPUT SETTINGS FOR NOURISHMENT AT MSL -5.0 M	130
TABLE 13 INPUT SETTINGS FOR NOURISHMENT AT MSL -6.0 M	137
TABLE 14 INPUT SETTINGS FOR DISCHARGE OF 150'000 m^3 /YEAR	144
TABLE 15 INPUT SETTINGS FOR SPREAD OF NOURISHMENT OVER 5 LOCATIONS.....	151

List of Terms

<i>Accretion</i>	The gain of sediment at a location.
<i>Basiskustlijn</i>	The Dutch coastline position, measured in the year 1990 and currently used as reference measurement for the present coastline position.
<i>Bed load transport</i>	Transport of sediment over the bed, mostly by rolling or jumping. Larger sediment particles are found here.
<i>Bruun Rule</i>	Theory that explains the relation between sea level rise and sediment demand in the nearshore zone, developed by Per Bruun in 1962.
<i>Coastal foundation</i>	The bottom layers of the coastal system.
<i>Coastal system</i>	The area of the coast bounded by the dunes and the deep water line (i.e. 20 m), in which hydrodynamic and morphodynamic processes take place.
<i>Convex</i>	Curved towards the sea.
<i>Cross-shore</i>	Axis perpendicular to the coastline orientation.
<i>Deep water line</i>	The offshore boundary of the coastal area. In the Netherlands, this line is located at MSL -20.0 m.
<i>Delft3D</i>	Numerical modelling tool to simulate hydrodynamic and morphodynamic processes and to predict behavior of regions.
<i>Discharge</i>	A supply of a mixture of water and sediment in the model domain.
<i>Domain</i>	Area of interest.
<i>Dominant (processes, conditions)</i>	“which is more effective than other”.
<i>Dredging</i>	The digging of sediment from the bottom to deepen the waterway or to use the sediment on other locations.
<i>Emission</i>	Exiting of toxic gases by vessels.
<i>Erosion</i>	The loss of sediment at a location.
<i>Europlatform</i>	Measurement platform offshore from the Dutch coast near Rotterdam.
<i>Hollow</i>	Curved towards the land
<i>Hydrodynamic</i>	Motion of water and forces that act on or are a result of water and water motions
<i>Ijmuiden Munitie</i>	Measurement station offshore of the Dutch coast near Ijmuiden.
<i>Stortplaats I</i>	
<i>-Induced</i>	Forced by.
<i>Innovatie Kustlijnzorg</i>	Program of Rijkswaterstaat to improve sustainability of maintenance of the Dutch coastal area.
<i>Longshore</i>	Axis parallel to the coastline orientation.
<i>Maasgeul</i>	Entrance waterway for the Port of Rotterdam.
<i>Mean sea level</i>	Average water level in seas and oceans, without influence of tidal forcing and wave forcing.
<i>Mean total transport</i>	Time-averaged net transport in the net direction.
<i>Morphodynamic</i>	Behavior of sediment particles as a result of hydrodynamics forces and motions.

List of Terms

<i>Morphological scale factor</i>	A function within Delft3D to reduce the computational effort by speeding up the morphodynamic calculations. The factor shows how many morphodynamic calculations steps are performed per hydrodynamic time step.
<i>Nearshore zone</i>	The shallow part of the coast in which hydrodynamics and morphodynamics are actively present. This zone is between the breaker line and the deep water line.
<i>Nieuwe Waterweg Normaal Amsterdams Peil</i>	Main waterway in the Port of Rotterdam. Dutch reference level for water and land, defined at the end of the 19 th century in Amsterdam.
<i>Nourishment</i>	A volume of sediment that is supplied at the coastline, beach or in nearshore zone.
<i>Orbital motions</i>	Motions in the water column right below the surface, forced by waves.
<i>Rijkswaterstaat</i>	Dutch institution that monitors and maintains infrastructure.
<i>Sand Engine</i>	Mega nourishment at the Delfland coast.
<i>Sedimentation</i>	See: accretion
<i>Shoreline</i>	The position of the water line during mean sea level.
<i>Spatio-temporal</i>	Varying in both space and time scale.
<i>Surf zone</i>	The shallow area between the shoreline and the breaker line where sediment transport is largest due to wave breaking.
<i>Suspended sediment transport</i>	Transport of sediment in the water, by currents. Especially light-weighted particles are transported in this way.
<i>Transport capacity</i>	The amount of sediment that is able to be transported by currents.
<i>Transport zone</i>	A longshore zone between MSL -1.0 m and MSL -4.0 m in which large mean total transport magnitudes are measured, due to significant wave forcing. This zone is derived from the numerical results from the reference situation.
<i>Van Rijn 2004 transport formula</i>	Formula used to calculate the volume of sediment that is transported, under a set of hydrodynamic conditions.
<i>Wave base</i>	The depth under which no orbital motions are measured and the effect of waves on currents is negligible.
<i>Zandwindmolen</i>	An innovation that responds to the shift to a more sustainable environment. It is a concept currently being developed in the program IKZ. The concept supplies sediment on the basis of 'zero-emission'.
<i>Zero-emission</i>	Without emitting of toxic gases.

List of Appendices

Appendix	Title	Page
A.1	Grid of FLOW and WAVE Domain	100
A.2	Grid of FLOW Domain	101
A.3	Initial Bathymetry	102
B.1	Calculation of Discharge Rate and Density as Input Values	103
B.2	Wave Data Analysis – Year 1	105
C.1	Reference Situation – Summary	108
C.2	Reference Situation – Monthly Development of Bed Level and Mean Total Transport Magnitude	112
D.1	Nourishment at MSL -3.0 m – Summary	116
D.2	Nourishment at MSL -3.0 m – Monthly Development of Bed Level and Mean Total Transport Magnitude	119
E.1	Nourishment at MSL -4.0 m – Summary	123
E.2	Nourishment at MSL -4.0 m – Monthly Development of Bed Level and Mean Total Transport Magnitude	126
F.1	Nourishment at MSL -5.0 m – Summary	130
F.2	Nourishment at MSL -5.0 m – Monthly Development of Bed Level and Mean Total Transport Magnitude	133
G.1	Nourishment at MSL -6.0 m – Summary	137
G.2	Nourishment at MSL -6.0 m – Monthly Development of Bed Level and Mean Total Transport Magnitude	140
H.1	Discharge of 150'000 m ³ – Summary	144
H.2	Discharge of 150'000 m ³ – Monthly Development of Bed Level and Mean Total Transport Magnitude	147
I.1	Spread over 5 Locations – Summary	151
I.2	Spread over 5 Locations – Monthly Development of Bed Level and Mean Total Transport Magnitude	154

A.1 Grid of FLOW and WAVE domain

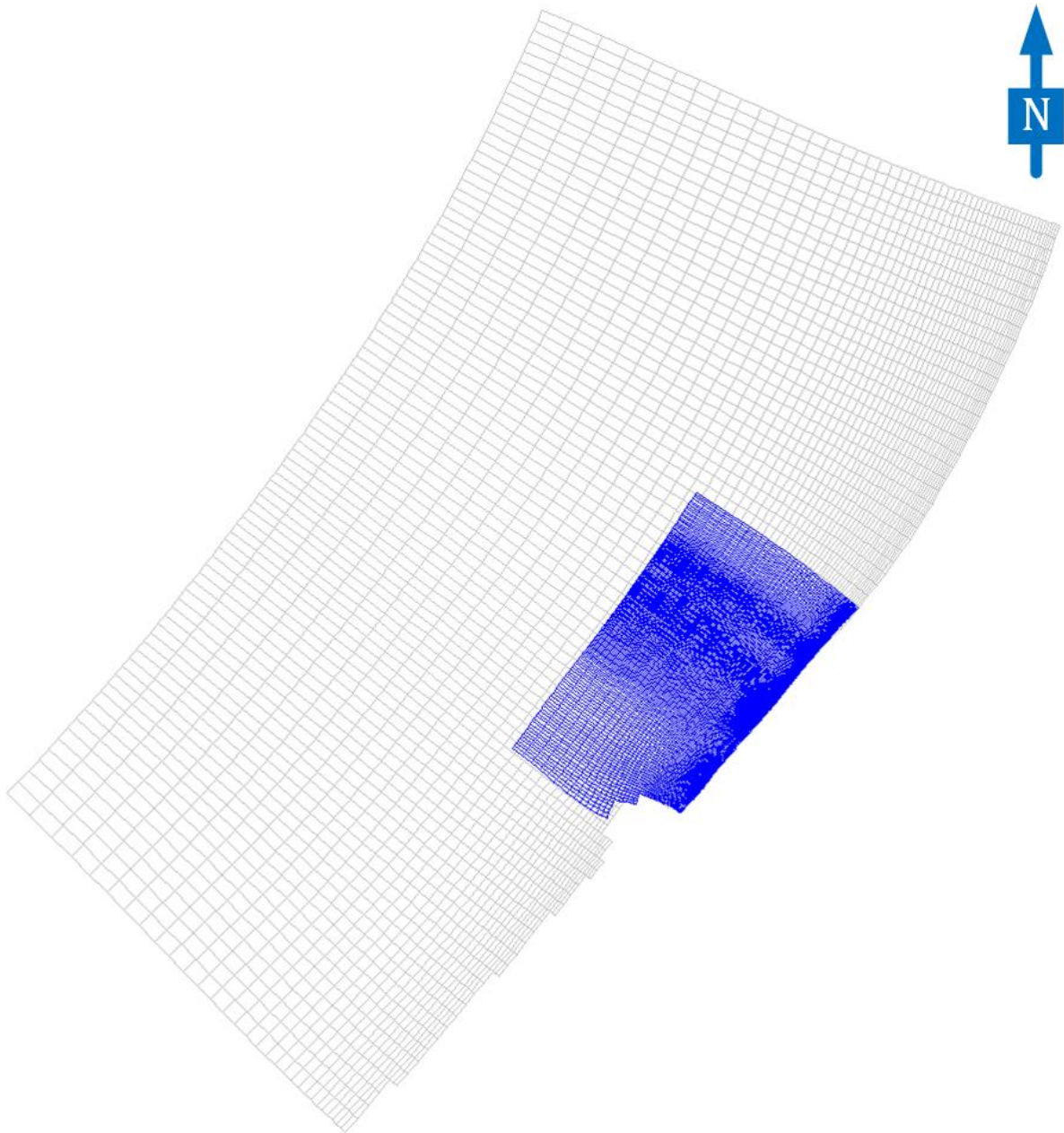


Figure 70 Grid of FLOW (blue) and WAVE domain (grey). Cells are smaller in shallower depth.

A.2 Grid of FLOW domain

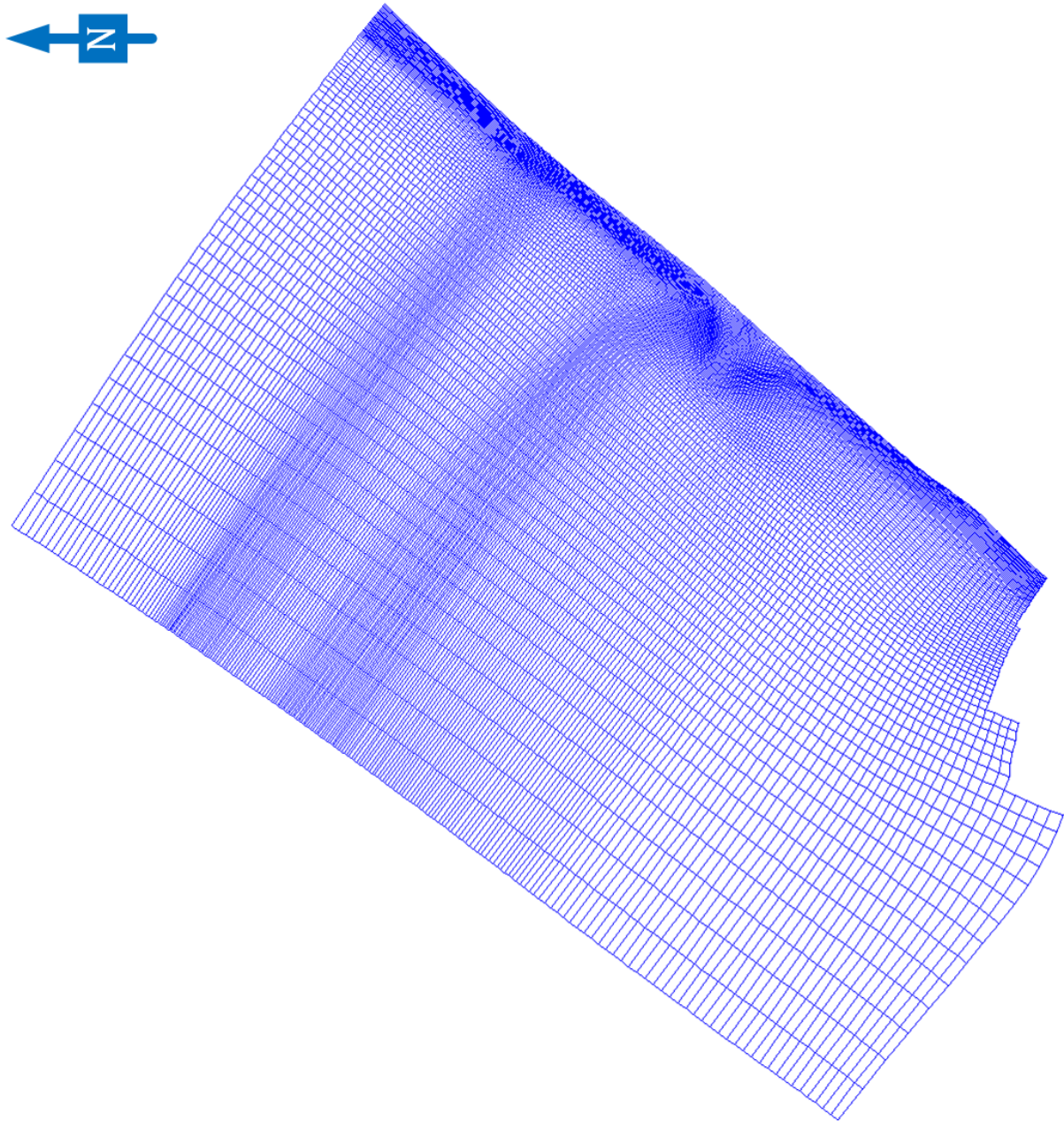


Figure 71 Grid of FLOW domain. The cells are smaller in shallower depth.

A.3 Initial bathymetry

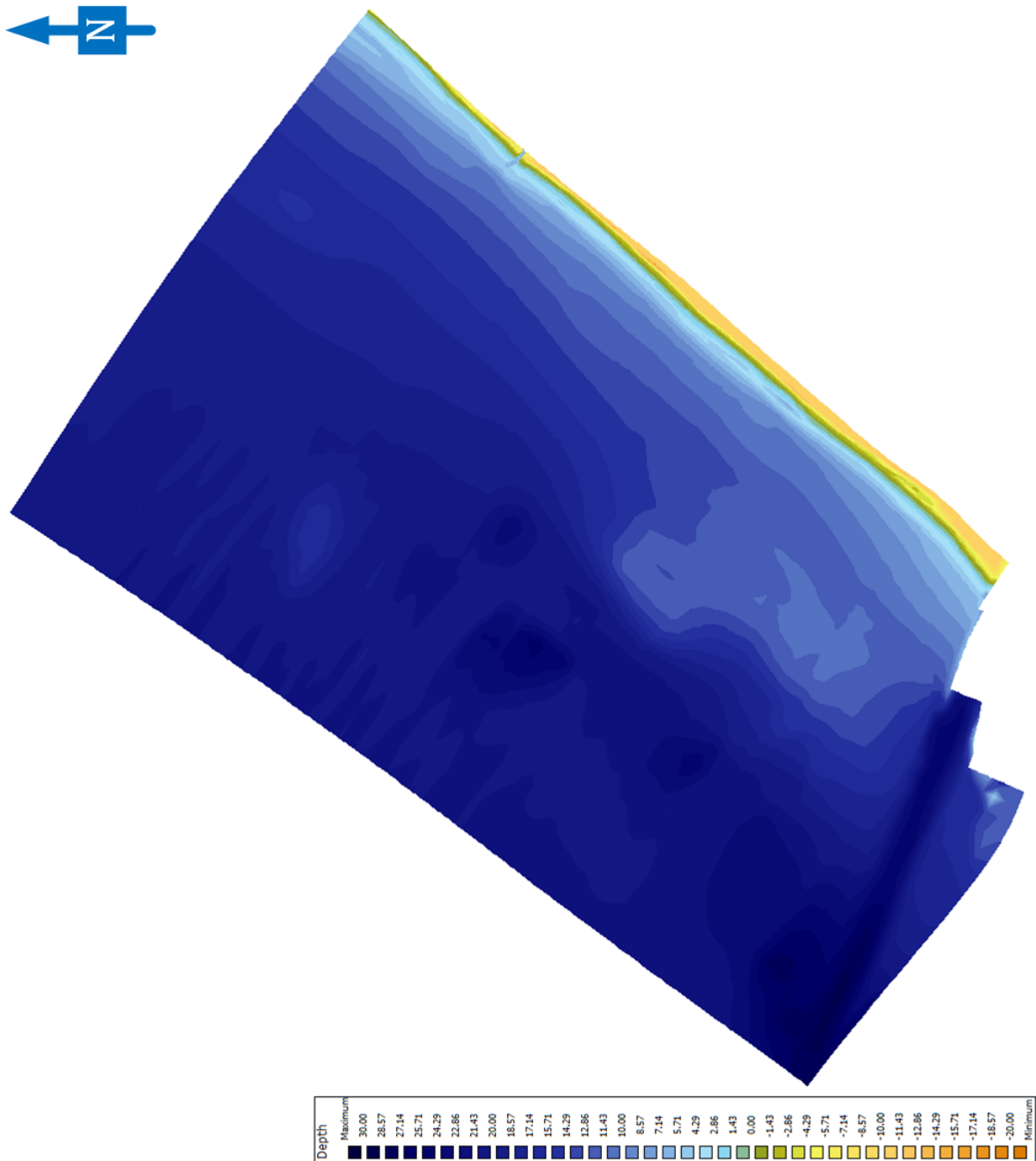


Figure 72 Bathymetry of FLOW domain.

B.1 Calculation of Discharge rate and density as input values

This appendix elaborates the calculation method that lead to the creation of the graph in Figure 26, which represents the relation between the discharge rate Q_{real} [m^3/s] and the concentration of sediment particles in discharge C [kg/m^3]. The relation between the discharge, concentration and input reduction is explained in paragraph 3.5.5.

General parameters

Table 8 General parameters to calculate the required discharge and concentration for input.

Density Sediment particles	ρ_s	2650	kg/m^3
Density Water (sea)	ρ_w	1023	kg/m^3
Porosity	p	0.6	–
Time (Year)	T	365	days

Table 8 shows the general parameters that are used in the calculation of the discharge rate Q_{real} and concentration C .

Nourishment volume, mass and production

The annual nourishment volume is expressed as the in situ volume of sediment including pores: $V_{s,dry}$ [m^3].

To calculate the concentration, one needs the mass of sediment particles in a volume of water. The mass of sediment particles is expressed as: M_s [kg]. The volume of water is expressed as: V_w [m^3]. The relation between the in situ volume of sediment and the mass of sediment particles is:

$$M_s = \rho_s * V_s = \rho_s * \frac{V_{s,dry}}{1 + p}$$

In which the mass is the product of the density and volume of the sediment particles, and the volume is retrieved from the divide from the dry sediment volume including pores and the porosity.

This represents an annual mass of sediment particles. The input is defined as discharge per second. The mass of sediment particles per second is expressed as: $M_{s,sec}$ [kg/s], and is calculated by dividing the annual mass to a mass per second (1 year = 31'536'000 seconds). The mass of sediment particles per second is the product of discharge and concentration that must be used in the model. Then the equation for this mass holds:

$$M_{s,sec} = Q * C$$

In which Q is the discharge rate in m^3/s and C represents the concentration of sediment particles in kg/m^3 . The production $Q * C$ is then given in a mass per time unit, in kg/s .

B.1 Calculation of Discharge rate and density as input values

Relation between discharge, concentration and density

Any combination of Q and C holds, as long as the production remains equal. However, there are practical limitations regarding minimum discharge rates and maximum operational concentrations and density. This step explains the relation between these three parameters, with a single varying parameter called volume of water: V_w .

When the volume of water increases relative to the mass of sediment particles in the water, the concentration and density decrease, and the discharge must increase, in order to remain the production. The mass of water is given as the product of volume and density of water:

$$M_w = \rho_w * V_w$$

The density of the mixture of sediment particles and water is then expressed as:

$$\rho_m = \frac{M_s + M_w}{V_s + V_w}$$

In which ρ_m is the mixture density, M_s and M_w are the masses of sediment and water, and V_s and V_w the volumes of sediment and water.

The concentration C of the sediment particles is expressed as the mass of the particles divided by the sum of the volume of sediment particles and water:

$$C = \frac{M_s}{V_s + V_w}$$

Resulting relation and graph

Table 9 Values for discharge Q and concentration C for different values of water volume V_w . The nourishment volume is 100'000 m^3 per year in situ.

$V_w [m^3]$	$M_w [m^3]$	$\rho_m [kg/m^3]$	$C [kg/m^3]$	$Q [m^3/s]$	$Q_{real} [m^3/s]$
0	0	2650	2650	0.0020	0.00414
50'000	51'150'000	1927	1472	0.0036	0.00746
100'000	102'300'000	1649	1019	0.0052	0.01077
150'000	153'450'000	1502	779	0.0067	0.01408
200'000	204'600'000	1410	631	0.0083	0.01740

The resulting graph in Figure 26 is gained by varying the volume of water, which gives a range of values for the density, the concentration and thus the discharge, as the production is constant. A set of values is collected in Table 9. Every product of Q_{real} and C equals the production that corresponds to an annual nourishment volume of 100'000 m^3 .

The parameter Q_{real} is the discharge rate after including the acceleration factor equal to 2.09 given in paragraph 3.5.4. This is necessary in order to reproduce the correct amount of sediment volume, as the wave data has been reduced.

B.2 Wave data analysis – Year 1

The wave data that is used in the simulations is part of a larger dataset. The visualizations of the simulations show wave data that occurs in the first year. Although standard figures of the entire dataset are published, an analysis has been performed to the wave data that does occur in the first year.

Note: the wave data in this appendix is the input data and is valid at locations far offshore in the WAVE domain. Because of fluctuations in wave propagation, just as refraction, diffraction, and breaking, the wave height and orientation will change in the nearshore zone (between MSL 0.0 m and MSL -8.0 m).

Wave rose: magnitude and direction of all waves

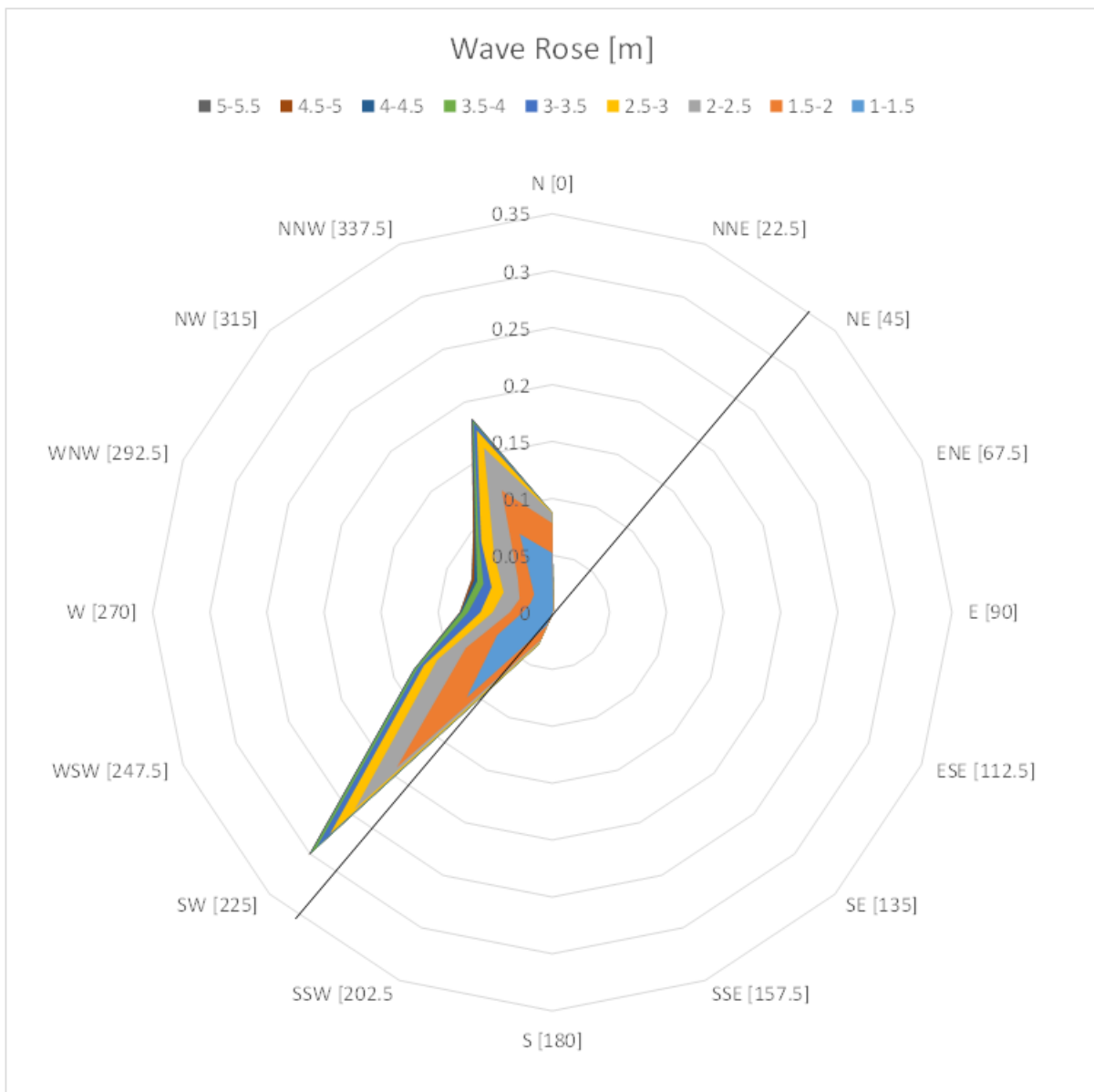


Figure 73 Wave Rose of the data used in the model simulations. The two main wave directions are SW and NNW.

B.2 Wave data analysis – Year 1

Figure 73 represents the wave rose as is used in the simulations. The wave data occurs in the first year, while the dataset represents wave data for five consecutive years. The data is inserted in the model domain at the offshore boundaries of the WAVE domain (see appendix B.1). The wave data has been reduced to wave heights larger than or equal to 1.0 m, as negligible sediment transport is assumed for waves smaller than 1.0 m. The black line in Figure 73 represents the orientation of the Delfland coastal stretch. The coastline has an orientation with a perpendicular of 310 degrees north.

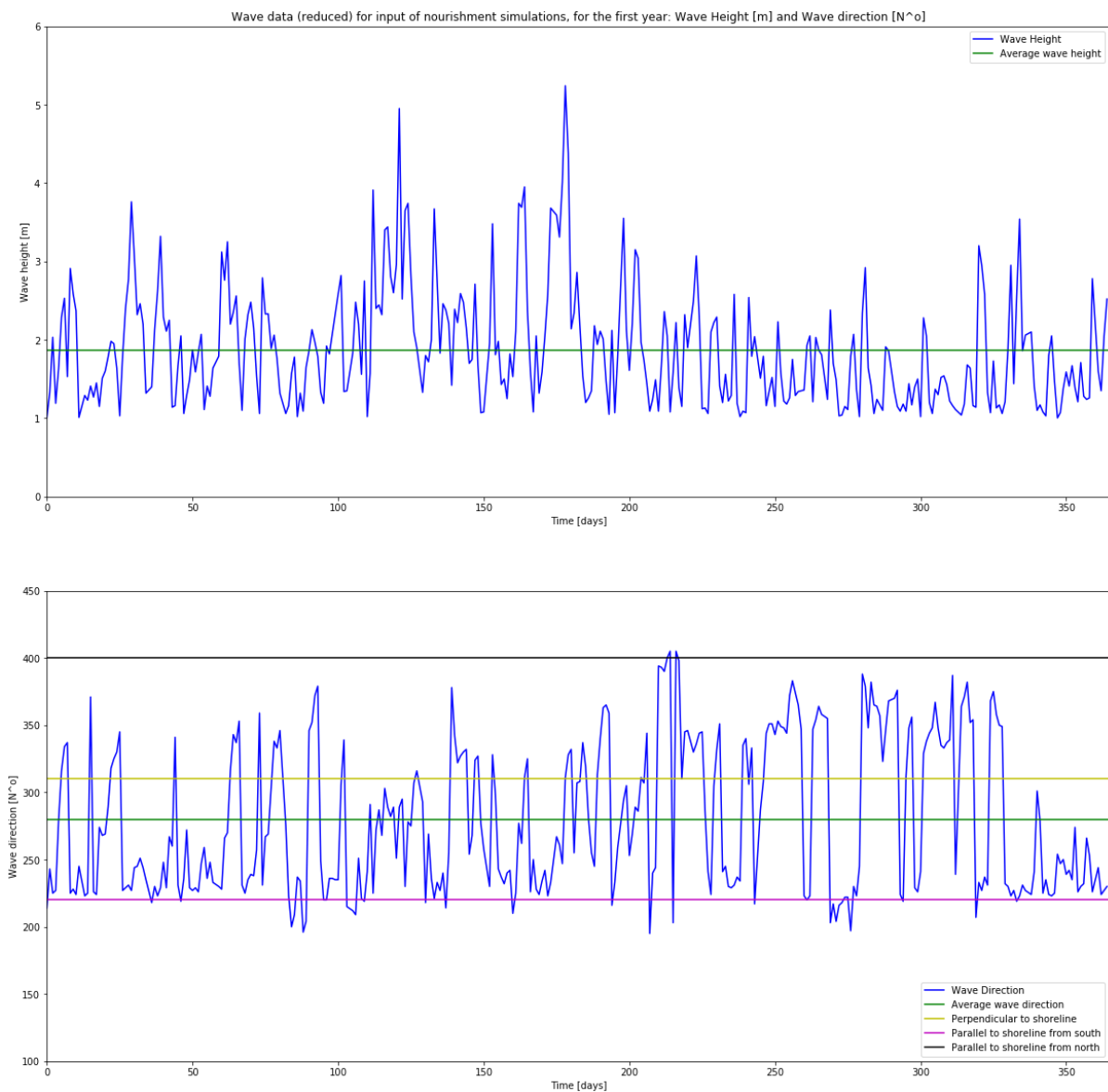


Figure 74 Temporal development of the waves, represented both the wave height and the direction from which they propagate. The incoming waves are bounded by the shore-parallel orientations, which are the purple and black lines. Outside these lines, waves are numerically originated from land, which is not possible.

Figure 74 visualizes the temporal development of the wave height and direction of the first year. The black and purple line represent the northern and southern parallel orientation (in degrees North) of the coastline. Waves outside these limits are approaching the coastline from land, which is

numerically and physically not possible. As these waves are inserted offshore, they will not enter the WAVE and FLOW domain. The yellow line shows the perpendicular of the coastline. The green line represents the mean wave direction.

Dominant wave directions

The two dominant wave directions are southwest (SW) and north-northwest (NNW). Most of the waves come from the southwest, about 30% of all waves. From the north-northwest, around 18% of the waves are approaching. The mean wave direction is at 280 degrees North, which is southward from the perpendicular (i.e. 310 degrees North). The wave height shows a distinction in seasonal variations. During winter time (period between day 100 and 200), the wave heights are larger. There is no clear distinction in wave direction visible between seasonal variations.

The waves from the southwest approach the coastline almost parallel. Due to wave refraction and diffraction, these waves will approach the coastline more perpendicular in the nearshore zone.

Storm climate: the largest waves

Most of the largest waves (> 3.5 m) are approaching from the northwest and west-northwest, almost perpendicular to the coastline (i.e. the green fraction in Figure 73 at orientation WNW). The dominant wave directions, SW and NNW, have a lower fraction of waves in this category and are equal to each other.

Consequence for sediment transport

The mean wave direction is approaching from the southwest and creates a net northward directed longshore current. The net time-averaged strength of this current is partly reduced by the waves from the north-northwest. From this analysis, it can be concluded that the net sediment transport direction is northeast and that in this direction sediment is mostly redistributed. This has also been confirmed in paragraph 2.3.1. However, the presence of larger waves from the north-northwest will cause southward directed sediment transport as well, and thus likely sediment redistribution in both directions.

C.1 Reference simulation – Summary

The reference situation is used to qualitatively and quantitatively define the effects that a nourishment generates in a specific coastal domain. The data is used to calculate the differences in bed level and in mean total transport after 1 year. It is used to analyze the effects of nourishments in time, as a result of wave forcing. In chapter 4, the differences with the several nourishment configurations are visualized and explained. This appendix deals with the observations in the reference simulation only.

C.1.1 Bed level development

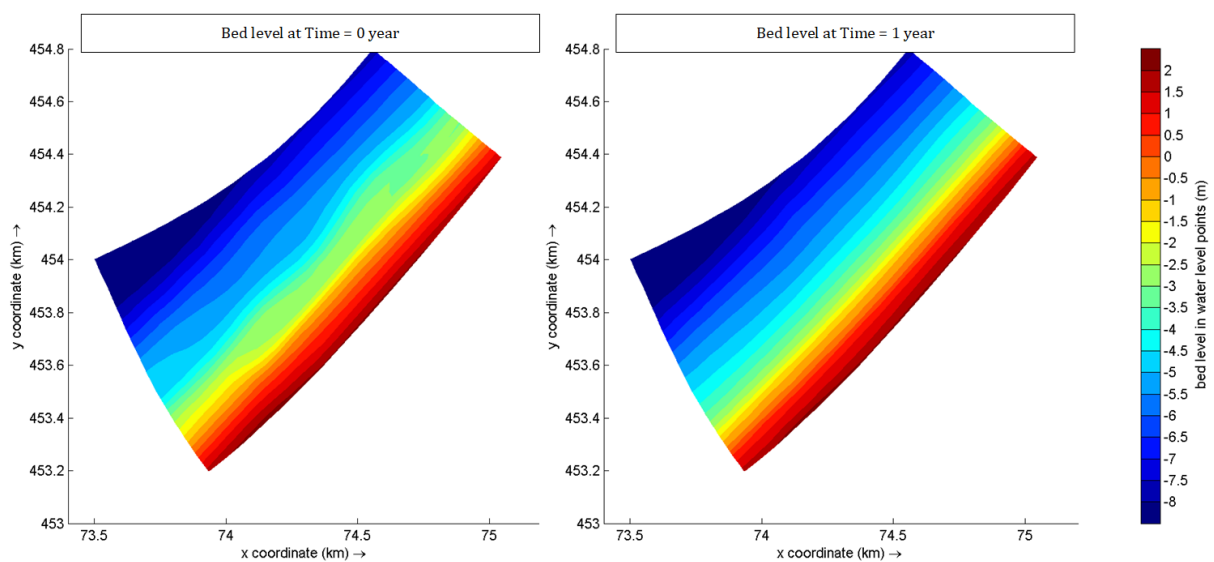


Figure 75 Bed level at $T = 0$ and $T = 1$ year. The irregular pattern of depth contours has been transformed to parallel depth contours after 1 year.

The bed level at the first and last day of the year is shown in Figure 75. The irregular depth contours have transformed to parallel depth contours. This corresponds to the situation at the Delfland coast in real-life. This coastal stretch is fairly uniform. Due to wave forcing and tidal forcing, sand bars emerge and strong longshore currents arise, which generate these parallel depth contours.

C.1.2 Mean total transport development

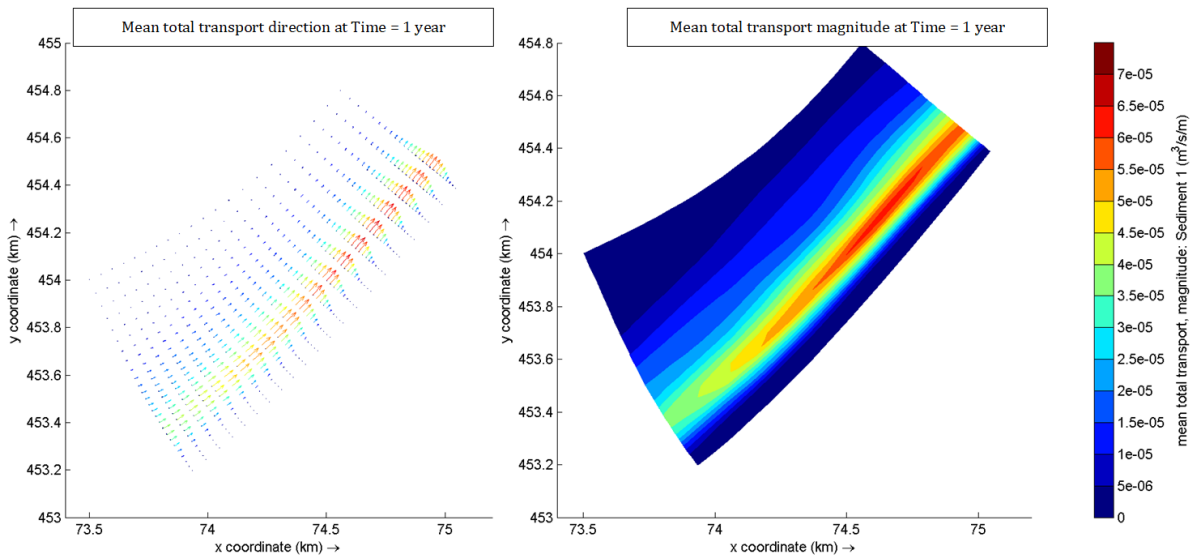


Figure 76 Mean total transport direction, split in alongshore and cross-shore vectors, and the magnitude, for 1 year. The longshore component is significantly larger than the cross-shore component, which means that longshore transport is dominant.

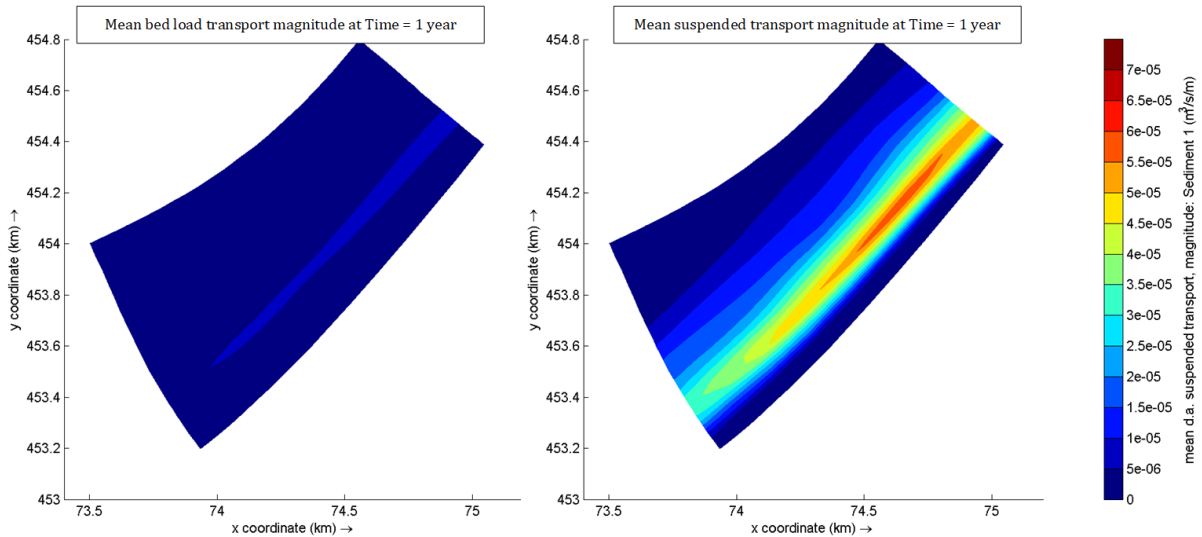


Figure 77 Mean depth-averaged suspended sediment transport (left) and mean bed load sediment transport (right). The suspended transport component is significantly larger in the zone of strong transport and counts for 85%.

Figure 76 visualizes the mean total transport magnitude and direction of 1 year. The longshore component is significantly large relative to the cross-shore component. The magnitude is up to 7×10^{-5} $\text{m}^3/\text{s}/\text{m}$, at a depth between MSL -1.0 m and MSL -4.0 m. By multiplying the magnitude with the cell width over which it is transported, (i.e. 200 m, the average width over which this transport zone exists), the maximum mean total transport magnitude is 7.1 l/s, or 230'000 m^3/year in alongshore

C.1 Reference simulation – Summary

direction. This volume is being transported in a strong longshore transport zone. Outside this zone, the transport magnitudes are much smaller.

The mean total transport magnitude is the sum of mean depth-averaged suspended sediment transport and mean bed load transport. The fraction of these components relative to the total transport component is visualized in Figure 77. The depth-averaged suspended transport component counts for 85% of the mean total transport component and is the predominant contributor to sediment transport in this coastal domain. This is likely to be occurring as a consequence of wave breaking in the strong transport zone, which causes a large rate of turbulence and thus a large volume of sediment in suspension. In deeper water (>5 m), bed load is more dominant as a result of the tidal alongshore current in this part of the nearshore zone. The magnitude, however, is not large enough to increase the mean bed load transport magnitude relative to the suspended transport component.

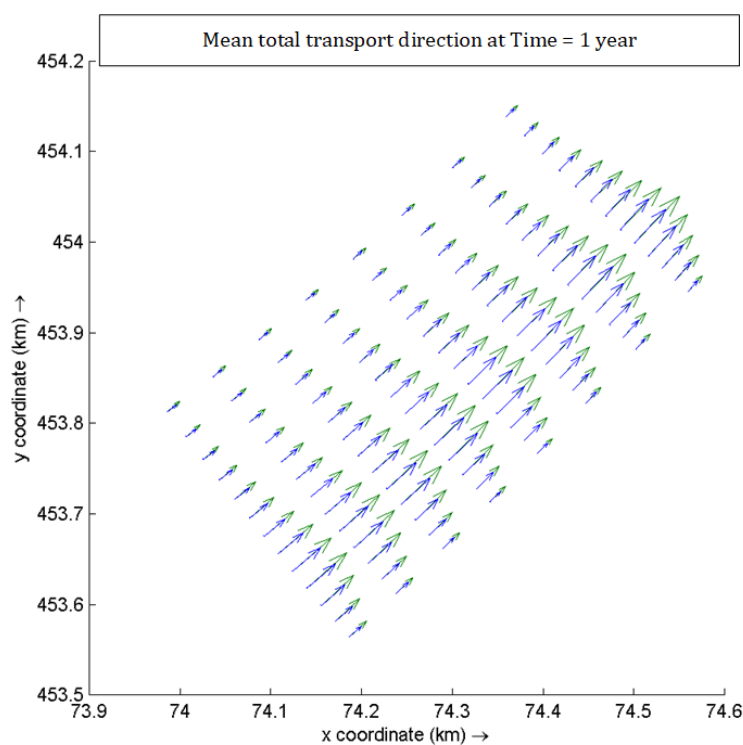


Figure 78 Direction of the mean total transport (green) and the alongshore component of the transport (blue). The cross-shore component is negligibly small, even when including the cell width over which the magnitude and direction is measured.

The directions of the mean total transport components are shoreward (for the cross-shore component) and northeastward (for the alongshore component). The alongshore component is predominantly larger, which results in a net averaged northeast direction. The direction of the net transport is almost parallel to the alongshore component, with a small deviation towards the shoreline. The alongshore magnitude is therefore a reliable indication of the net mean total transport magnitude. This is shown in Figure 78: the vector direction (green) is nearly in the same direction of the alongshore transport component (blue). Although the cell sizes over which they have been calculated is different, the alongshore component is much larger and this difference is negligible.

C.1.3 Cumulative erosion and sedimentation

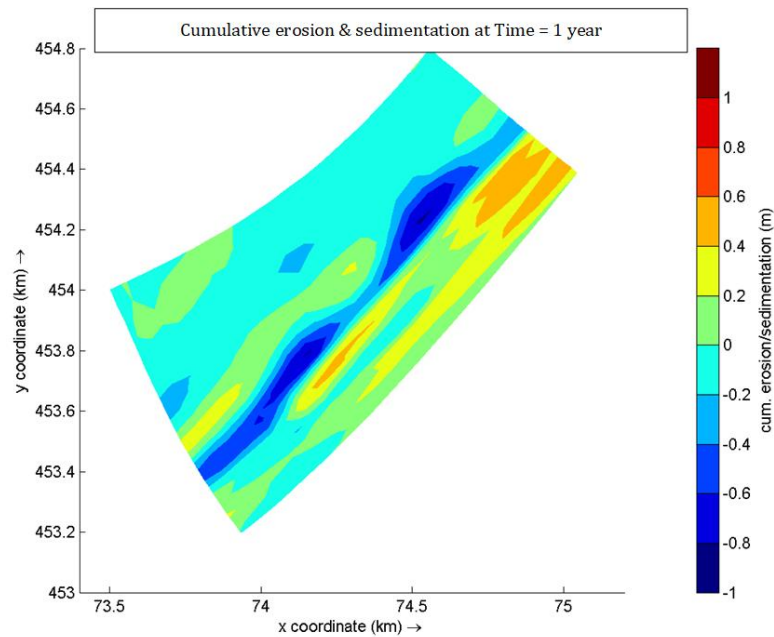
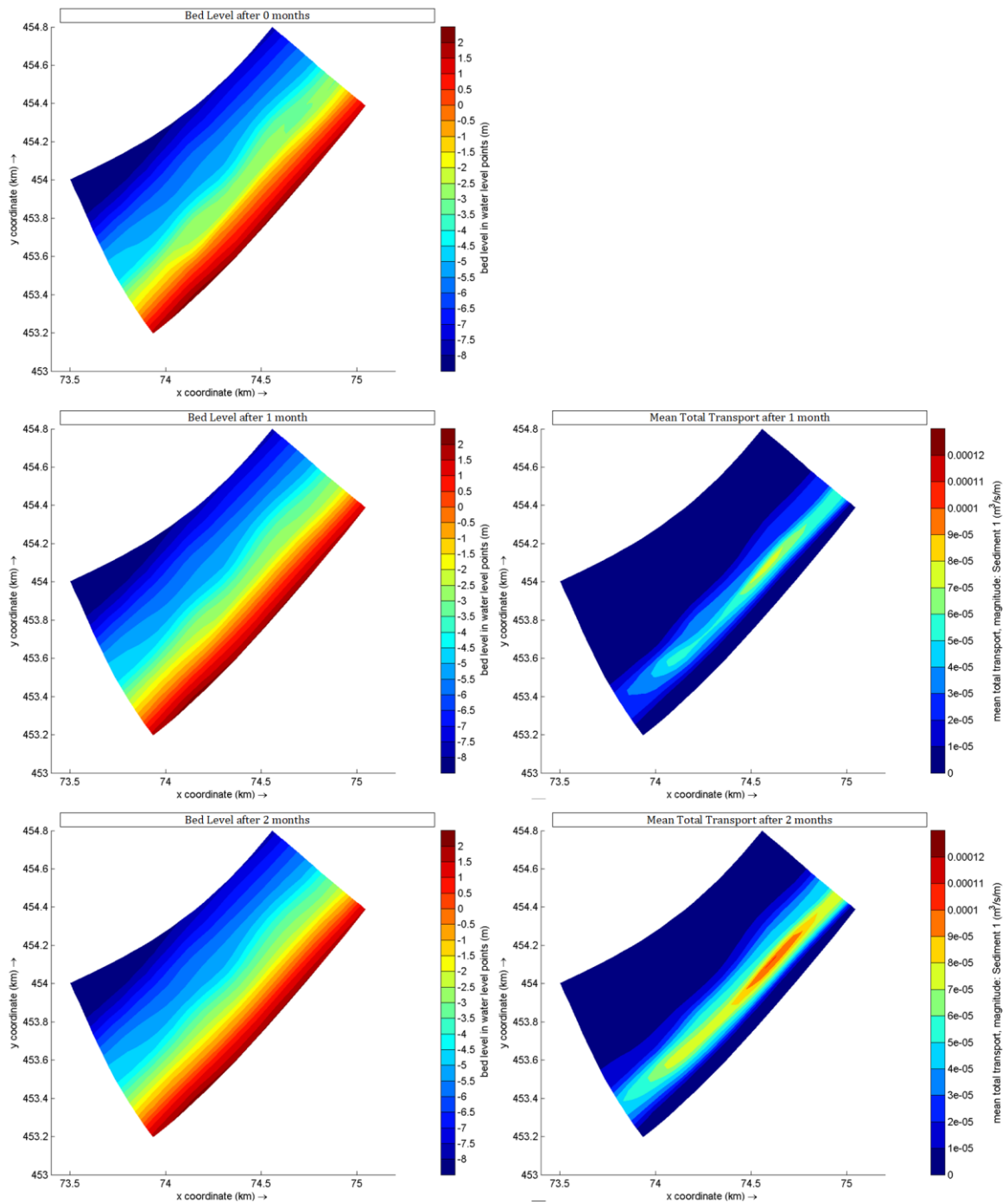


Figure 79 Cumulative erosion (blue) and sedimentation (red) after 1 year. The irregular pattern is a consequence of the forming of parallel depth contours.

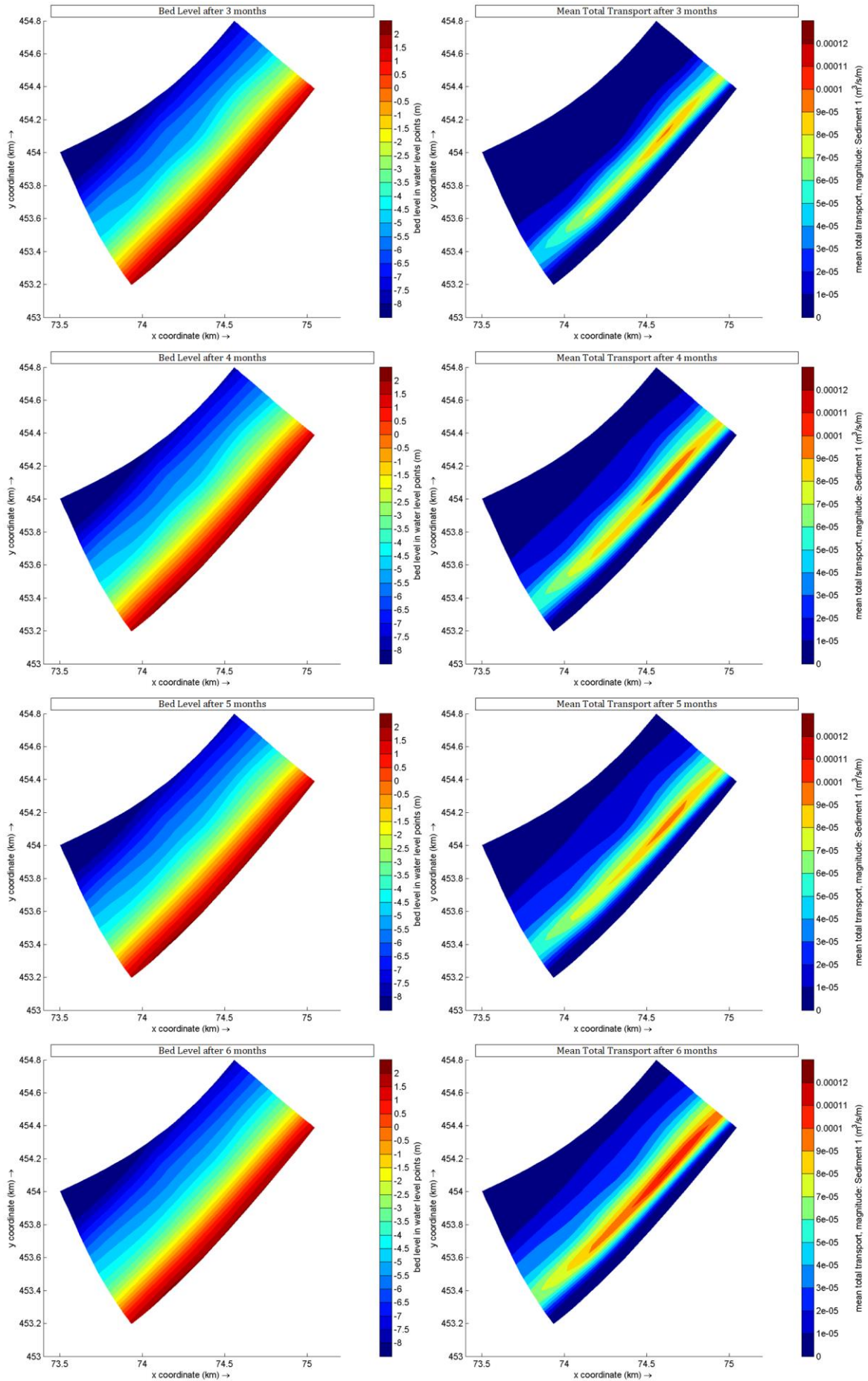
Figure 79 visualizes the cumulative erosion and sedimentation after 1 year in the domain. This graph shows how the coast deals with transport of sediment and where erosion spots are. The data is useful to investigate the occurrence of this erosion pattern in cases with nourishments.

C.2 Reference situation – Monthly development

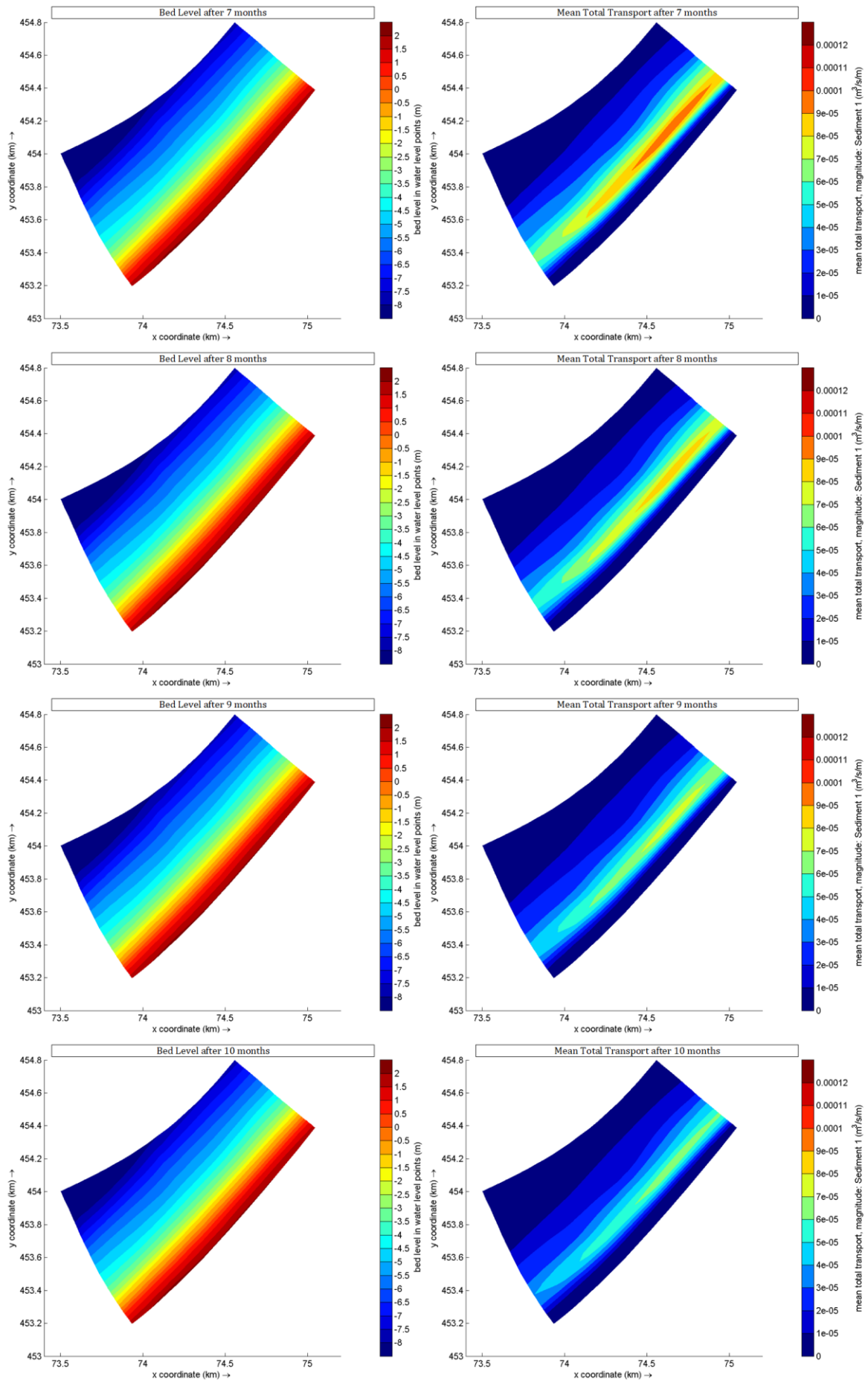
Figure 80 Temporal development of Bed level and Mean Total Transport, for the situation MSL -3.0 m, visualized for each month for the first year.



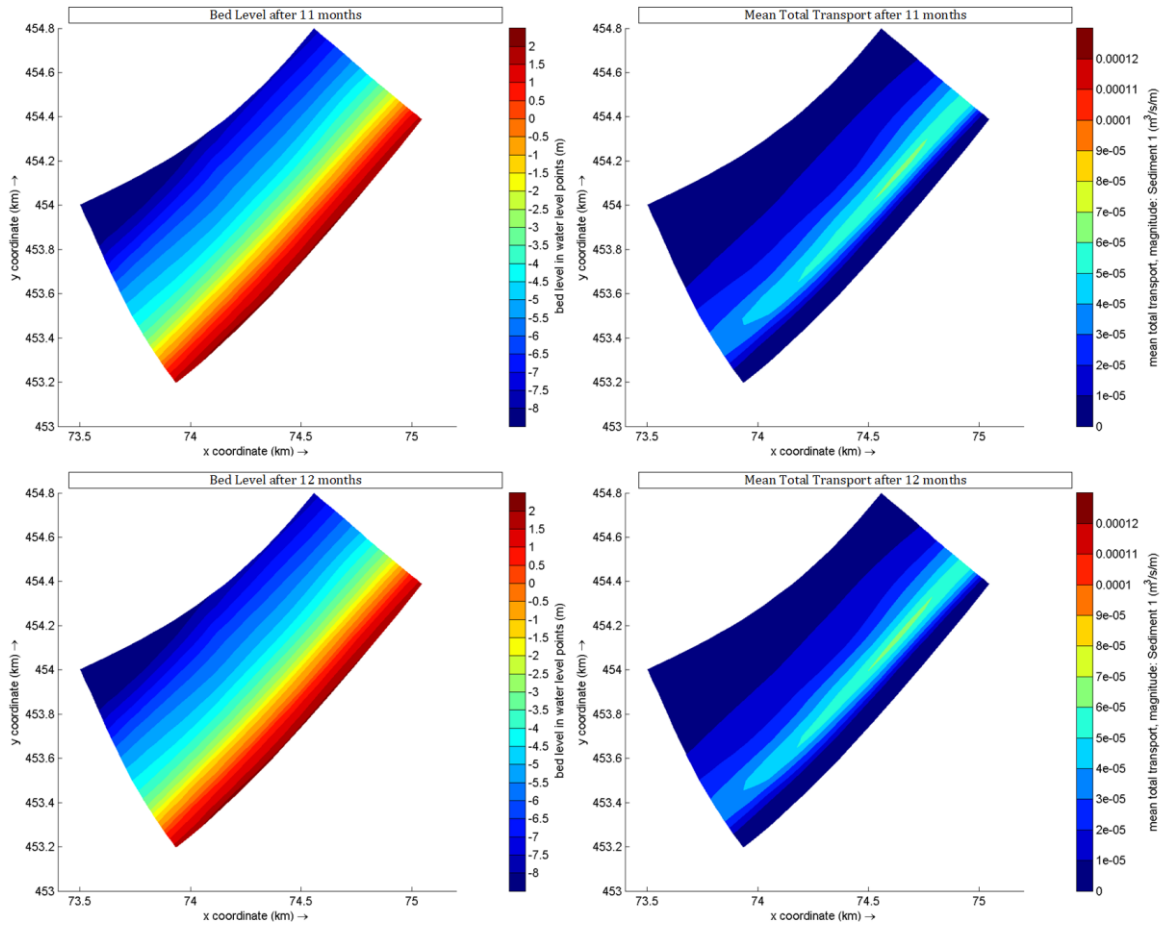
C.2 Reference situation – Monthly development



C.2 Reference situation – Monthly development



C.2 Reference situation – Monthly development



D.1 Nourishment at MSL -3.0 m – Summary

The input settings are given, as well as spatial development of bed level and erosion/sedimentation, and mean total transport.

D.1.1 Input settings

Table 10 Input settings for nourishment at MSL -3.0 m

Depth	3 m
Cell coordinates [M,N]	M,N = 119, 28
Annual volume	100'000 m ³ /year
Discharge input	Flow: Q = 0.02071 m ³ /s Concentration: C = 530 kg/m ³
Simulation time	1 year

D.1.2 Bed level development

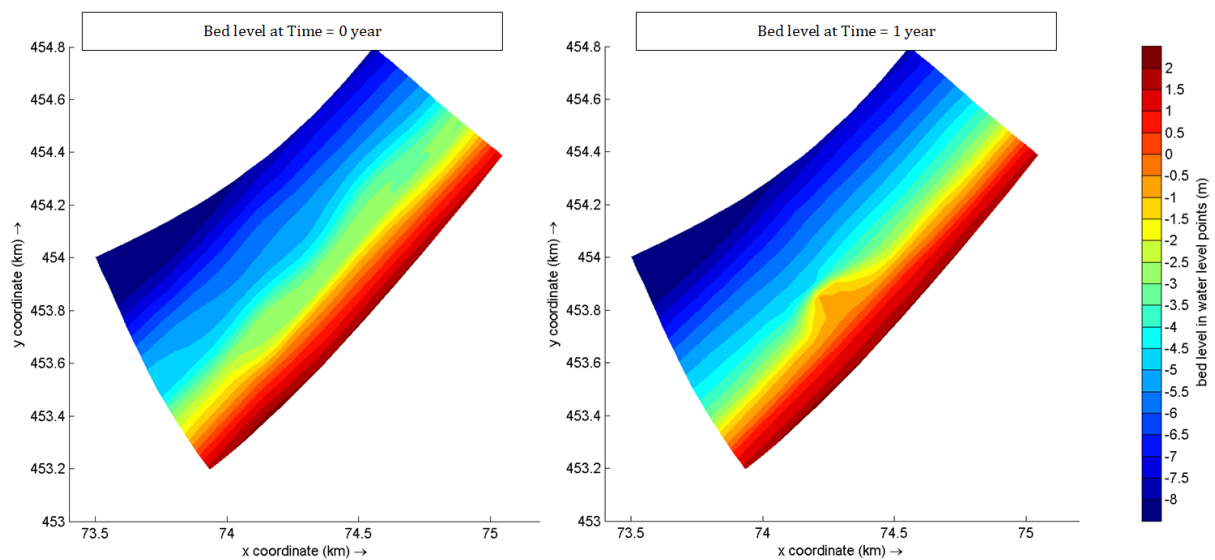


Figure 81 Bed level at $T = 0$ and $T = 1$ year. The nourishment develops as a bell-shaped beach extension and mainly spreads in alongshore direction.

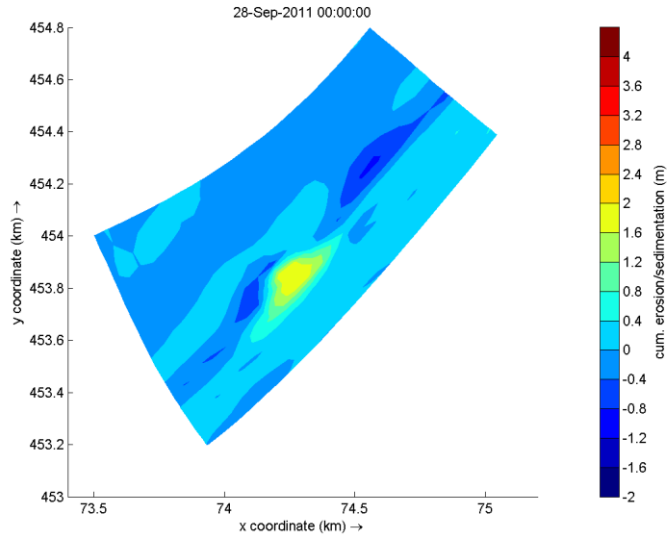


Figure 82 Cumulative erosion (blue) and sedimentation (red) after 1 year. Around the nourishment, accretion occurs. Just upstream of the nourishment, erosion is present, caused by increased energy dissipation of waves due to a sudden decrease of depth.

D.1.3 Mean total transport development

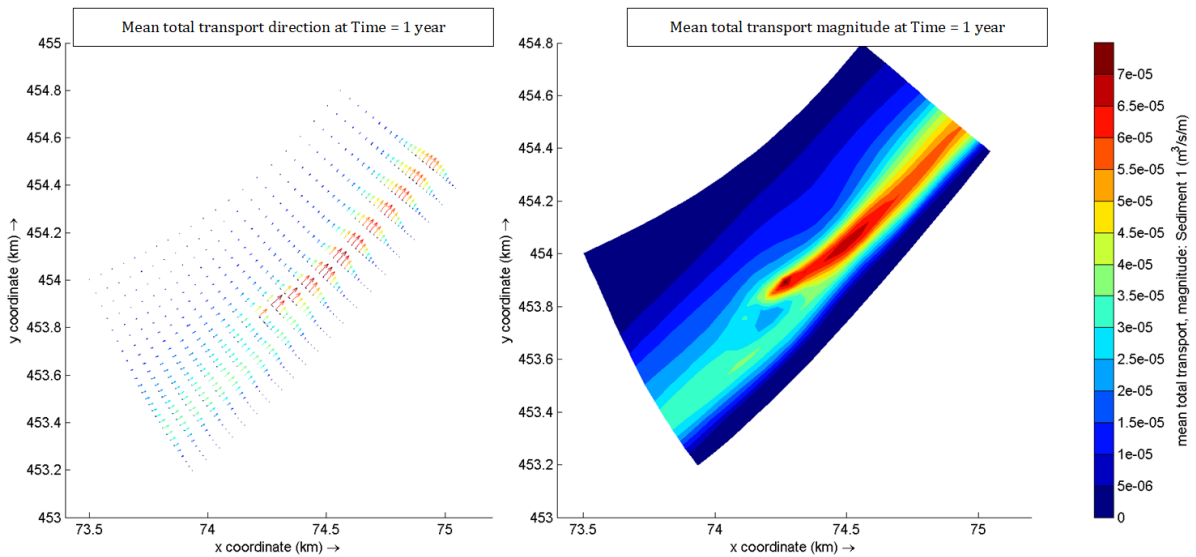


Figure 83 Mean total transport direction, split in alongshore and cross-shore vectors, and the magnitude, after 1 year. The transport magnitude has increased downstream from the nourishment location, as a result of the increased available volume of sediment.

D.1 Nourishment at MSL -3.0 m – Summary

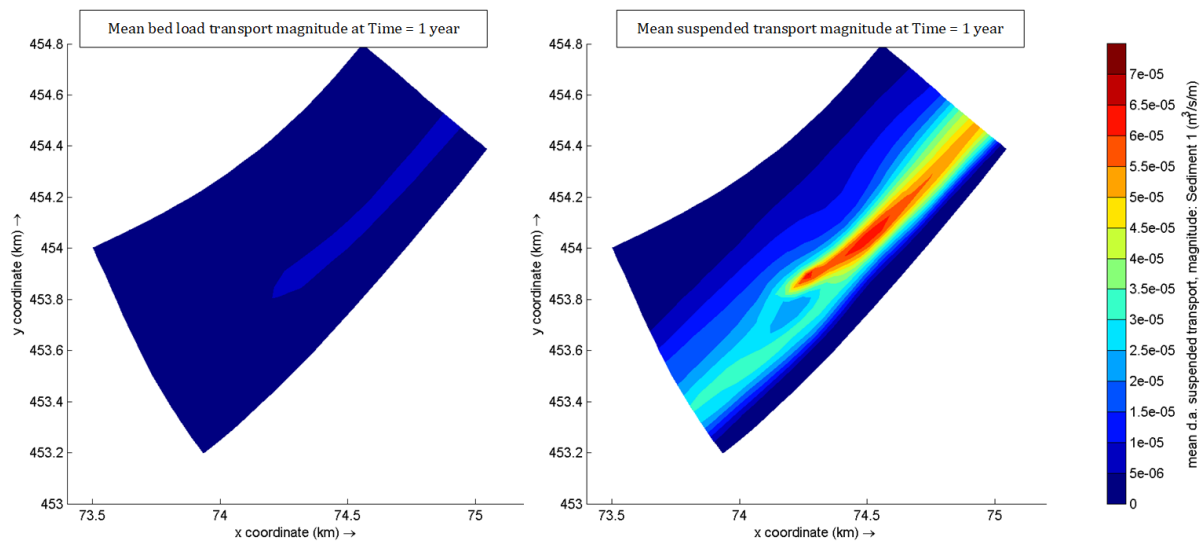


Figure 84 Mean depth-averaged suspended sediment transport (left) and mean bed load sediment transport (right). The suspended transport component is significantly larger in the zone of strong transport and counts for almost 90% in the strong transport zone.

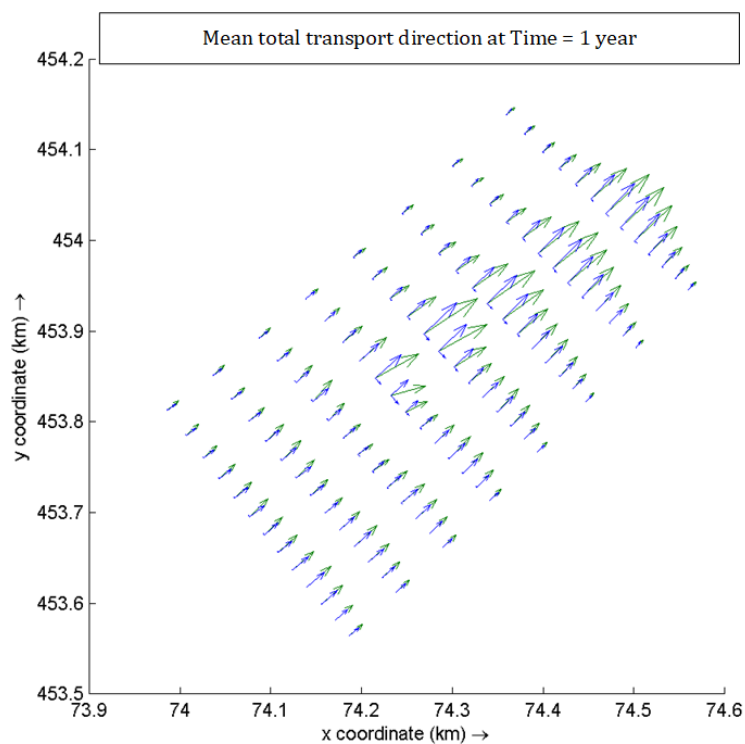
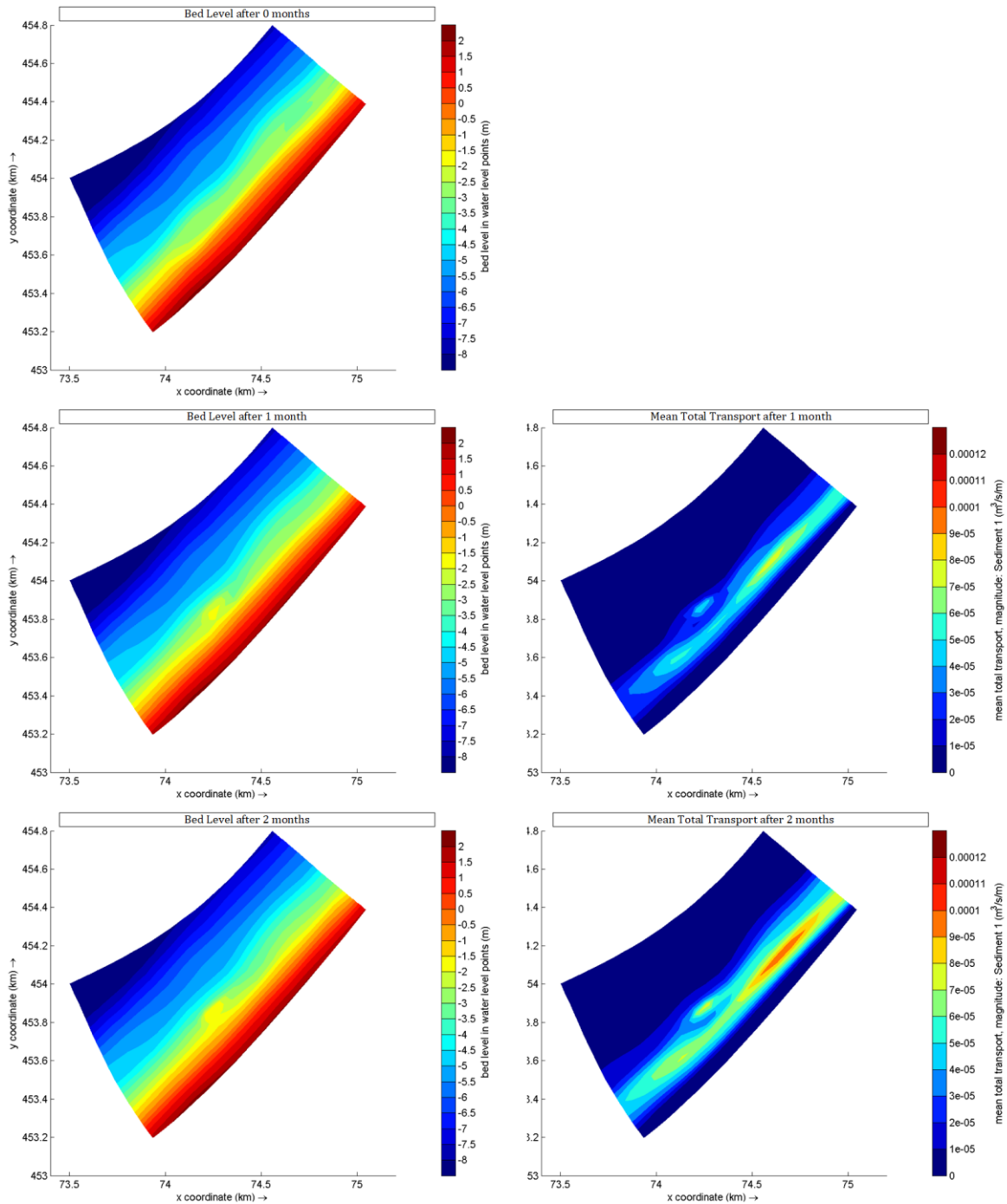


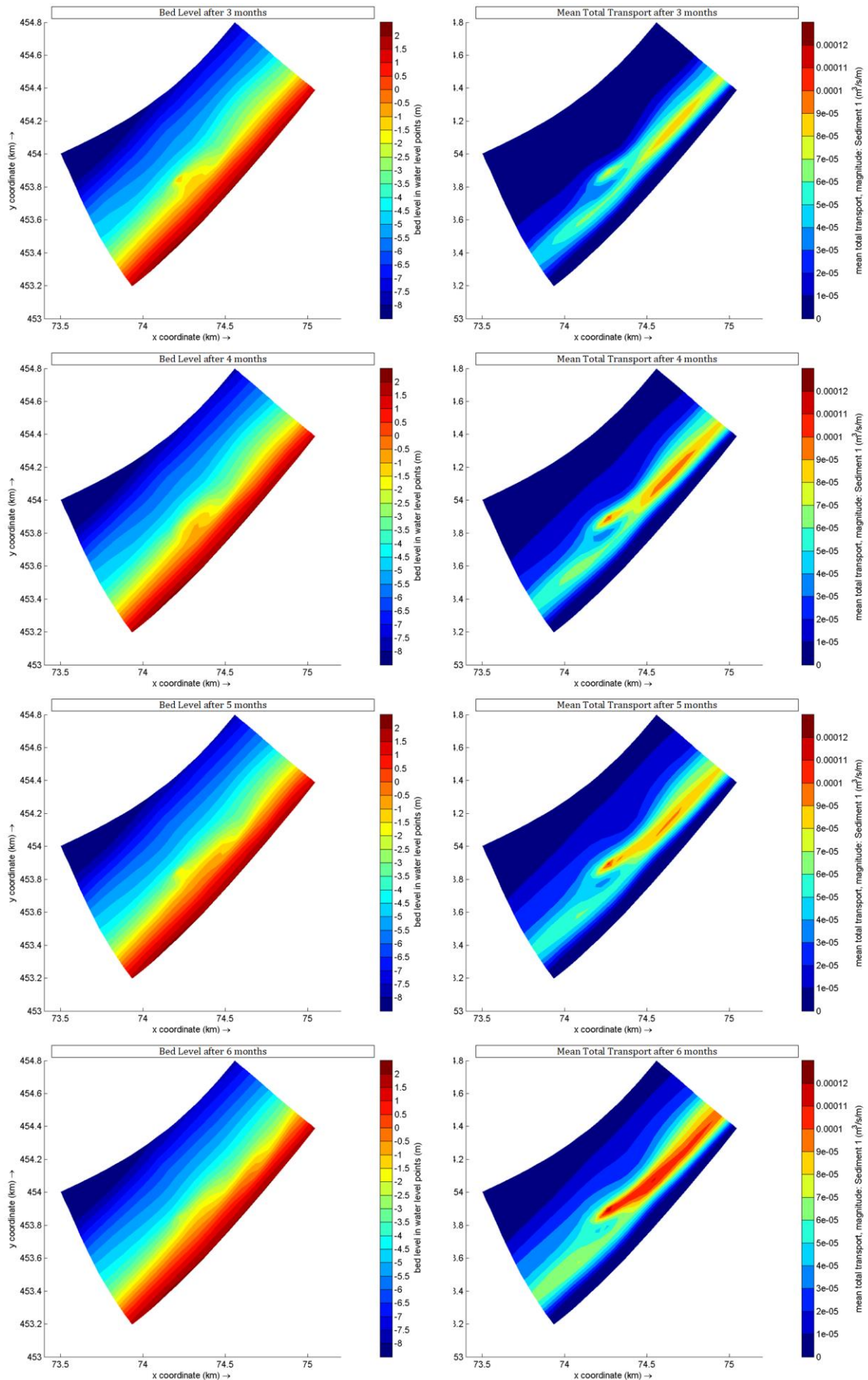
Figure 85 Direction of the mean total transport (green) and the alongshore component of the transport (blue). Near the nourishment, the cross-shore component increases relative to the alongshore component.

D.2 Nourishment at MSL -3.0 m – Monthly development

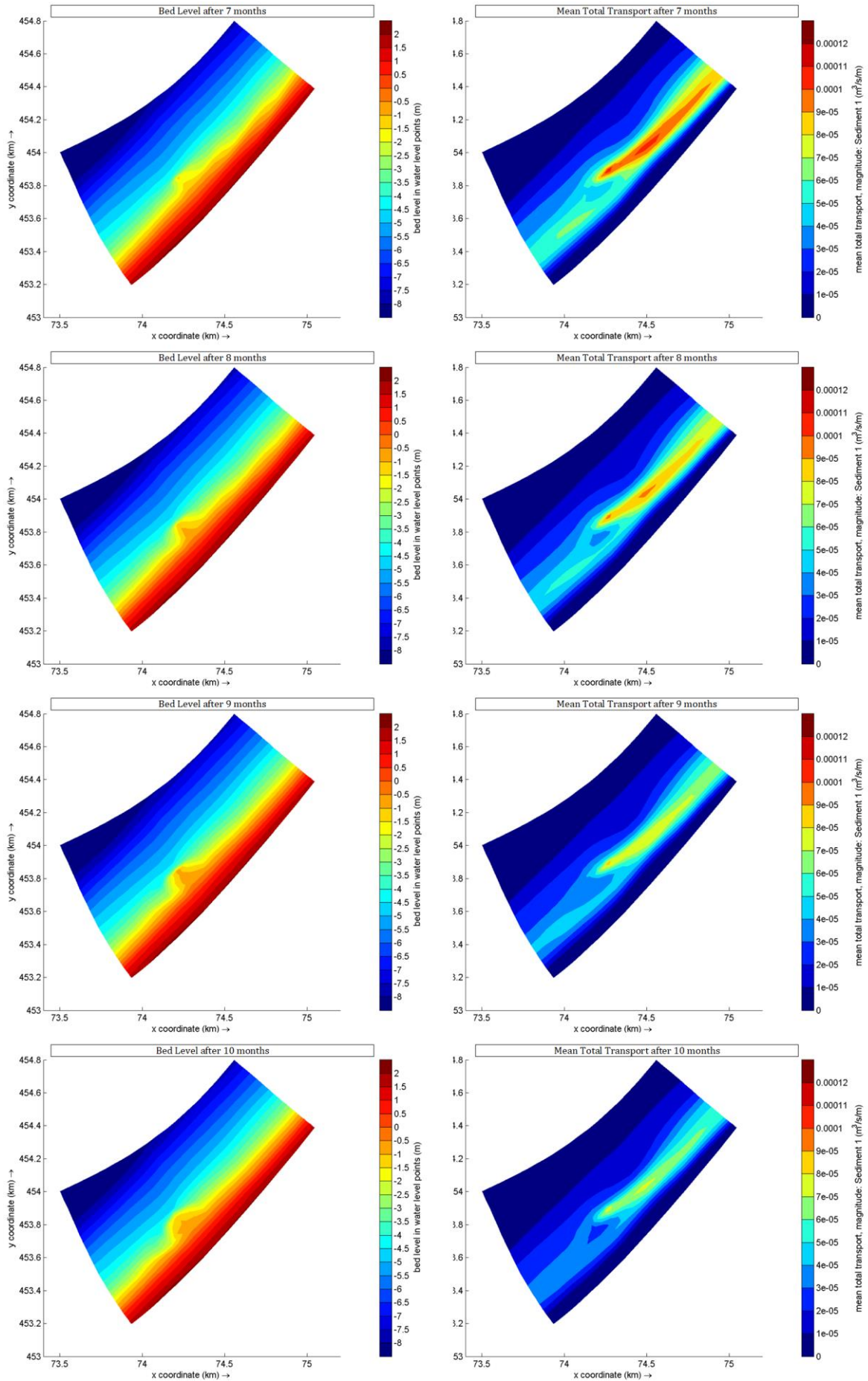
Figure 86 Temporal development of Bed level and Mean Total Transport, for the situation at MSL -3.0 m, visualized for each month for the first year.



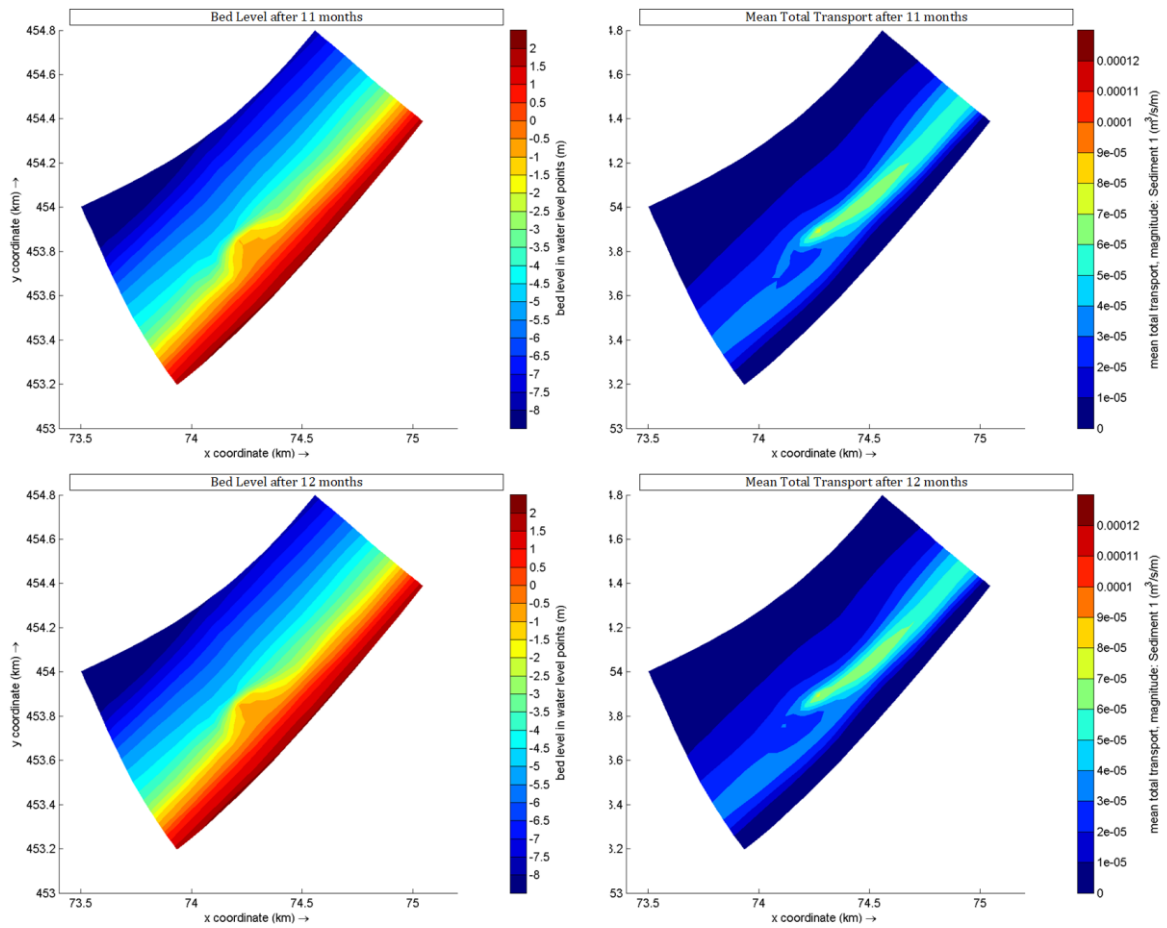
D.2 Nourishment at MSL -3.0 m – Monthly development



D.2 Nourishment at MSL -3.0 m – Monthly development



D.2 Nourishment at MSL -3.0 m – Monthly development



E.1 Nourishment at MSL -4.0 m – Summary

The input settings are given, as well as spatial development of bed level and erosion/sedimentation, and mean total transport.

E.1.1 Input settings

Table 11 Input settings for nourishment at MSL -4.0 m

Depth	4 m
Cell coordinates [M,N]	M,N = 119,30
Annual volume	100'000 m ³ /year
Discharge input	Flow: Q = 0.02071 m ³ /s Concentration: C = 530 kg/m ³
Simulation time	1 year

E.1.2 Bed level development

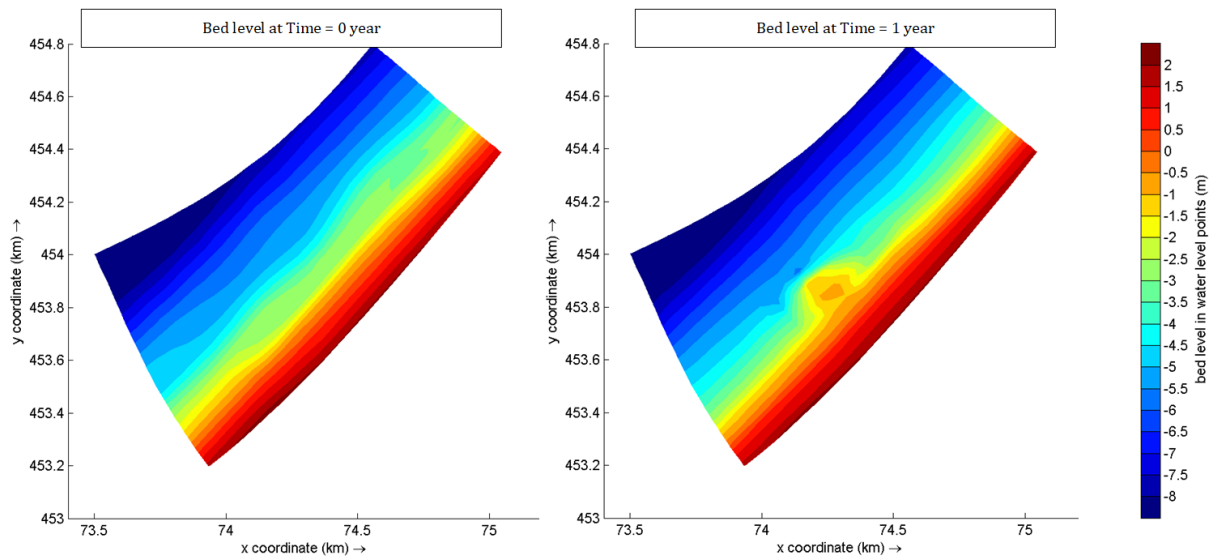


Figure 87 Bed level at T = 0 and T = 1 year. The nourishment is developing as an oval-shaped small island which is connected to the beach.

E.1 Nourishment at MSL -4.0 m – Summary

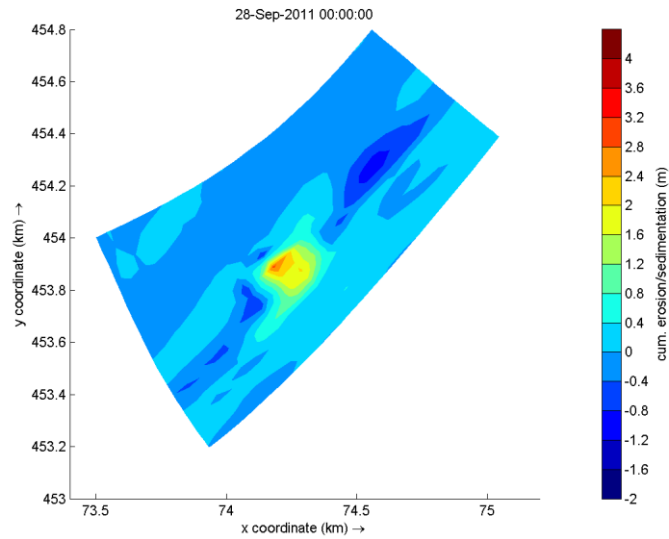


Figure 88 Cumulative erosion (blue) and sedimentation (red) after 1 year. Around the nourishment, accretion occurs. Just upstream of the nourishment, erosion is present, caused by increased energy dissipation of waves due to a sudden decrease of depth.

E.1.3 Mean total transport development

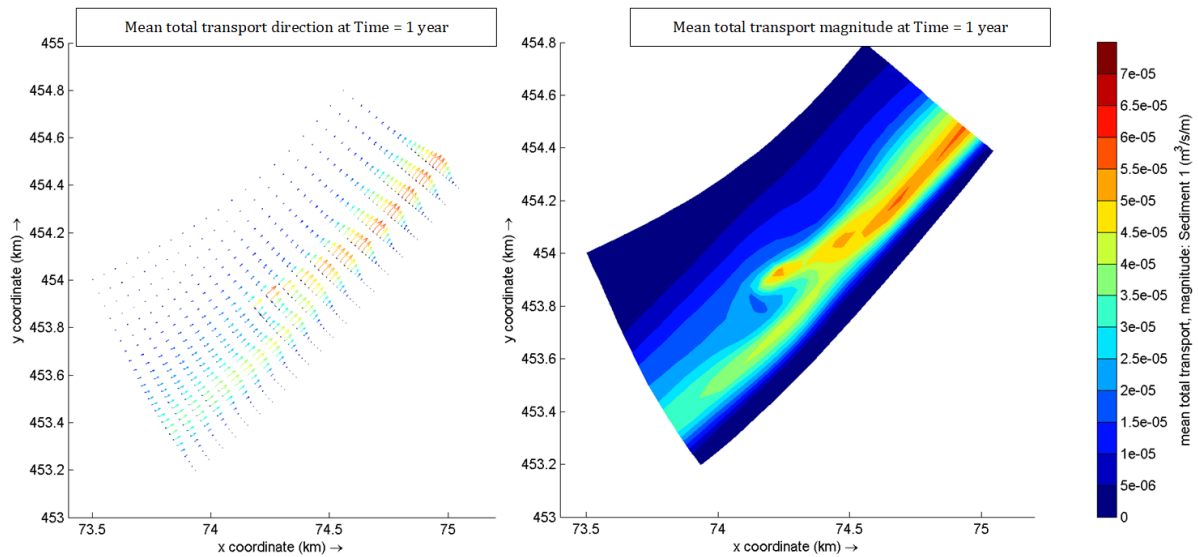


Figure 89 Mean total transport direction, split in alongshore and cross-shore vectors, and the magnitude, after 1 year. The magnitudes are not extremely large compared to the nourishment at MSL -3.0 m.

E.1 Nourishment at MSL -4.0 m – Summary

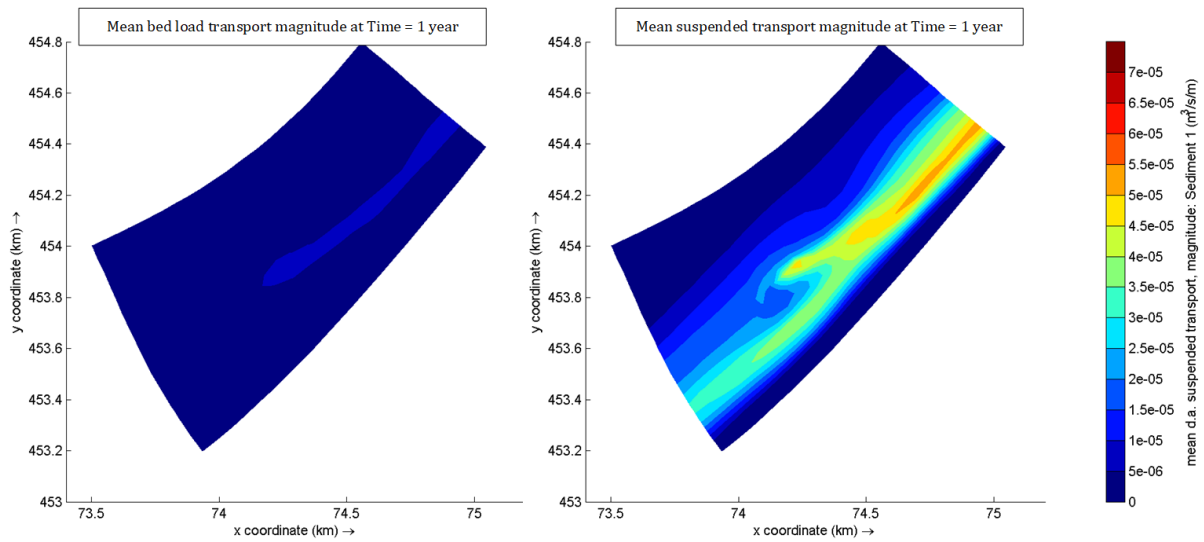


Figure 90 Mean depth-averaged suspended sediment transport (left) and mean bed load sediment transport (right). The suspended transport component is significantly larger in the zone of strong transport and counts for at least 80% in the transport zone.

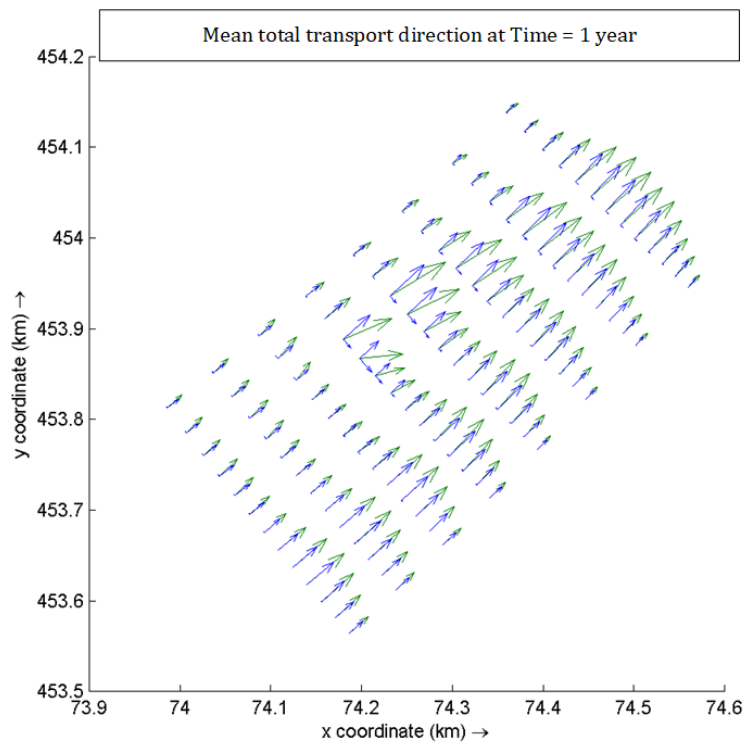
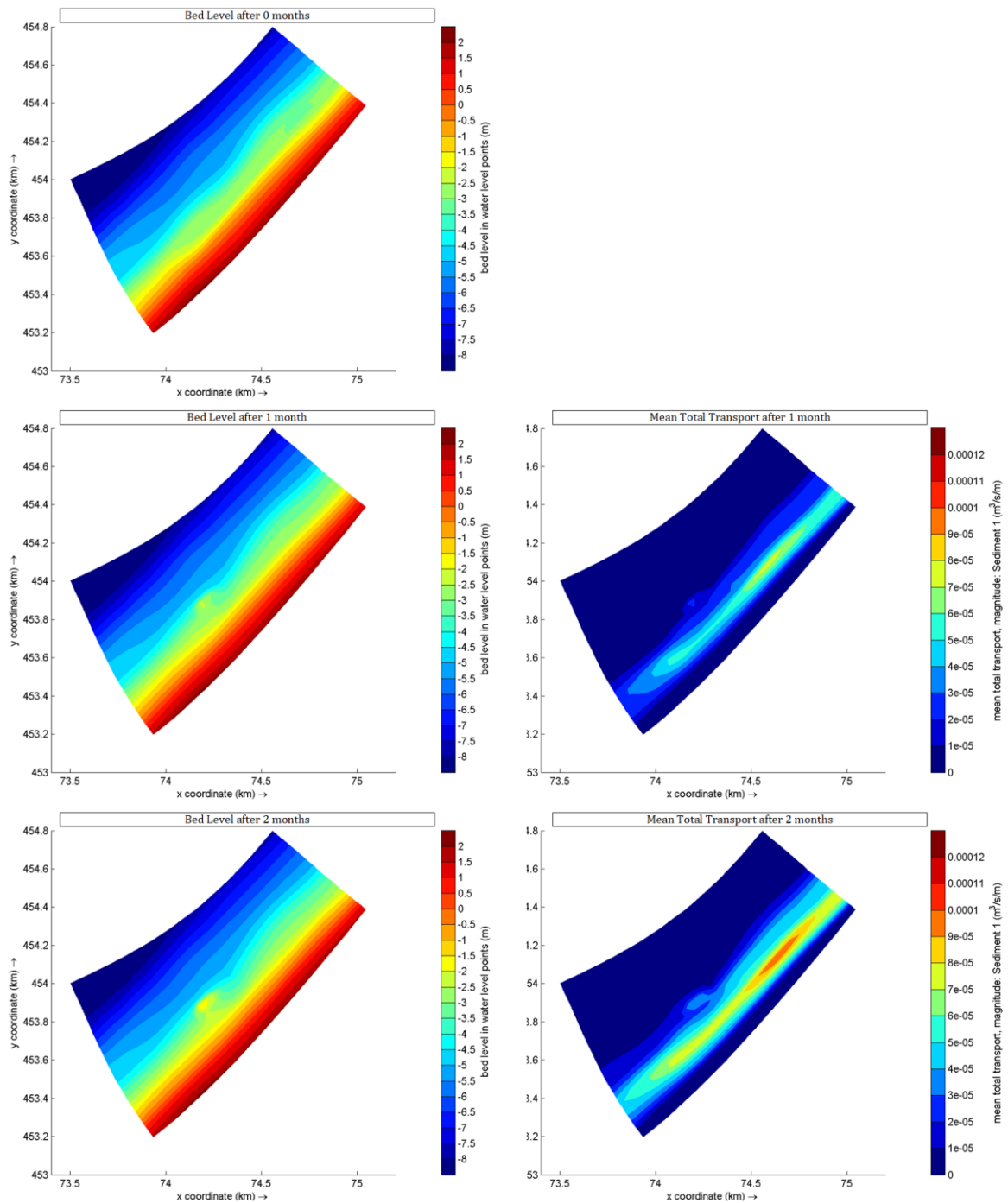


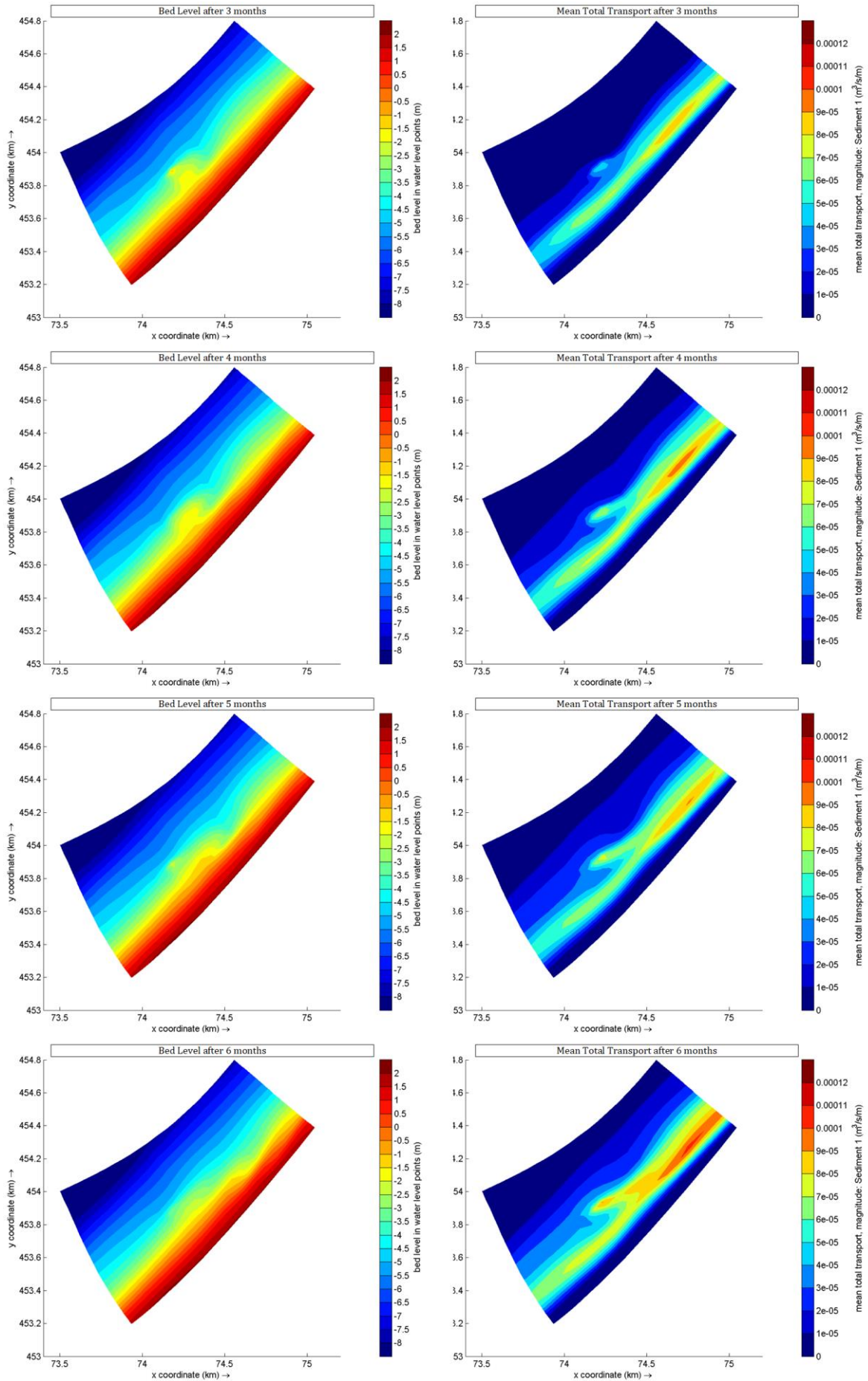
Figure 91 Direction of the mean total transport (green) and the alongshore component of the transport (blue). Near the nourishment, the cross-shore component increases relative to the alongshore component. This effect is visible further northeast in the domain.

E.2 Nourishment at MSL -4.0 m – Monthly development

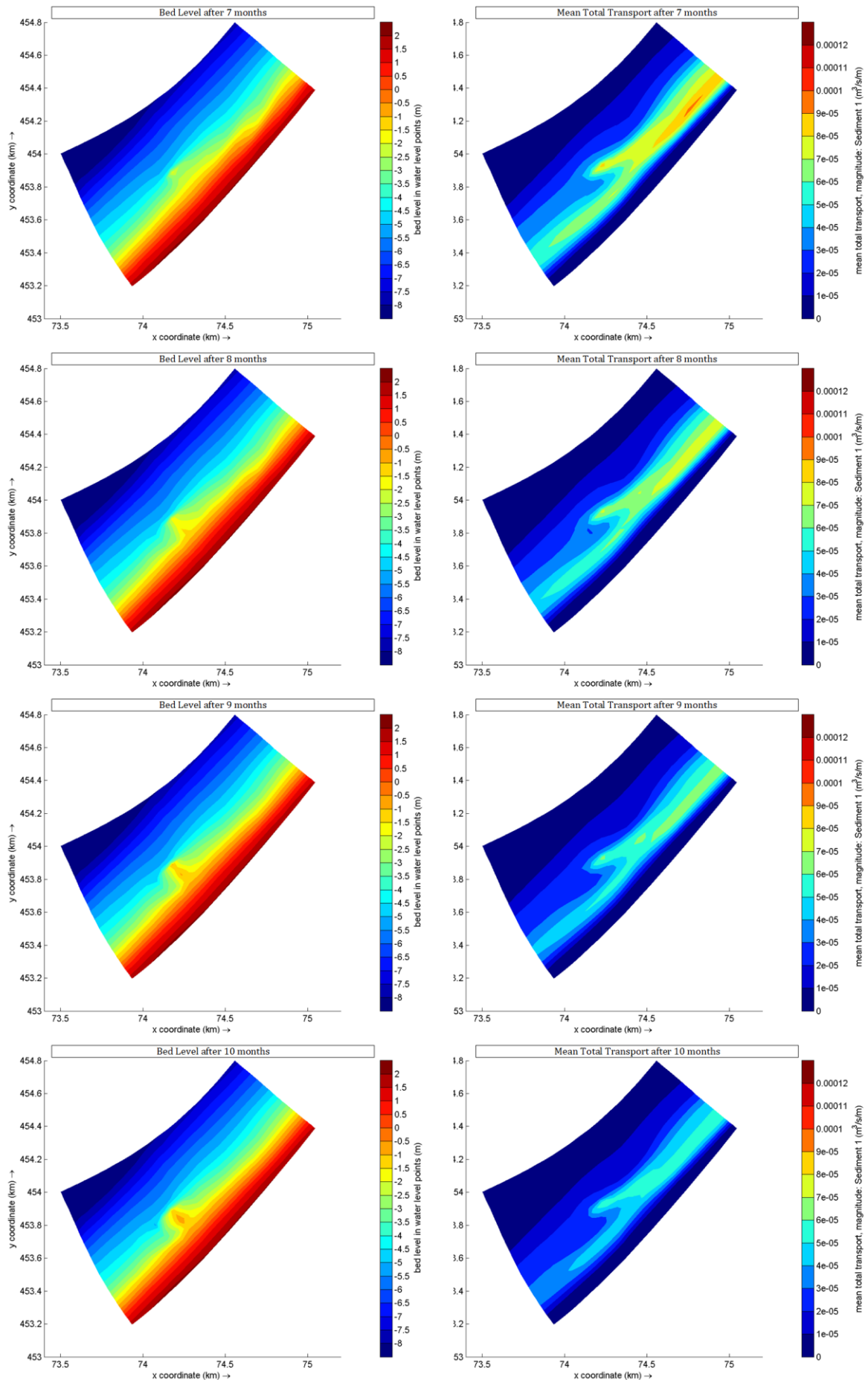
Figure 92 Temporal development of Bed level and Mean Total Transport, for the situation at MSL -4.0 m, visualized for each month for the first year.



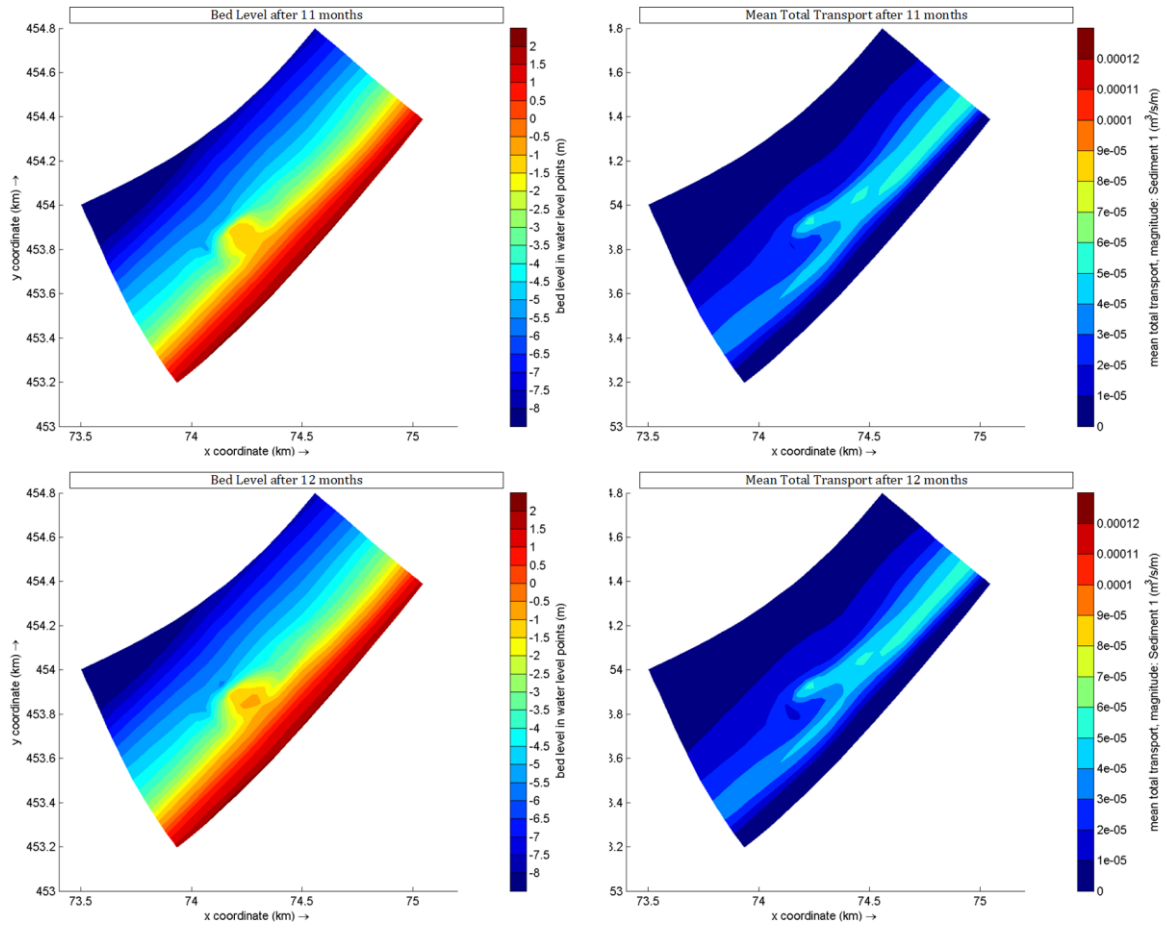
E.2 Nourishment at MSL -4.0 m – Monthly development



E.2 Nourishment at MSL -4.0 m – Monthly development



E.2 Nourishment at MSL -4.0 m – Monthly development



F.1 Nourishment at MSL -5.0 m – Summary

The input settings are given, as well as spatial development of bed level and erosion/sedimentation, and mean total transport.

F.1.1 Input settings

Table 12 Input settings for nourishment at MSL -5.0 m

Depth	5 m
Cell coordinates [M,N]	M,N = 119, 32
Annual volume	100'000 m ³ /year
Discharge input	Flow: Q = 0.02071 m ³ /s Concentration: C = 530 kg/m ³
Simulation time	1 year

F.1.2 Bed level development

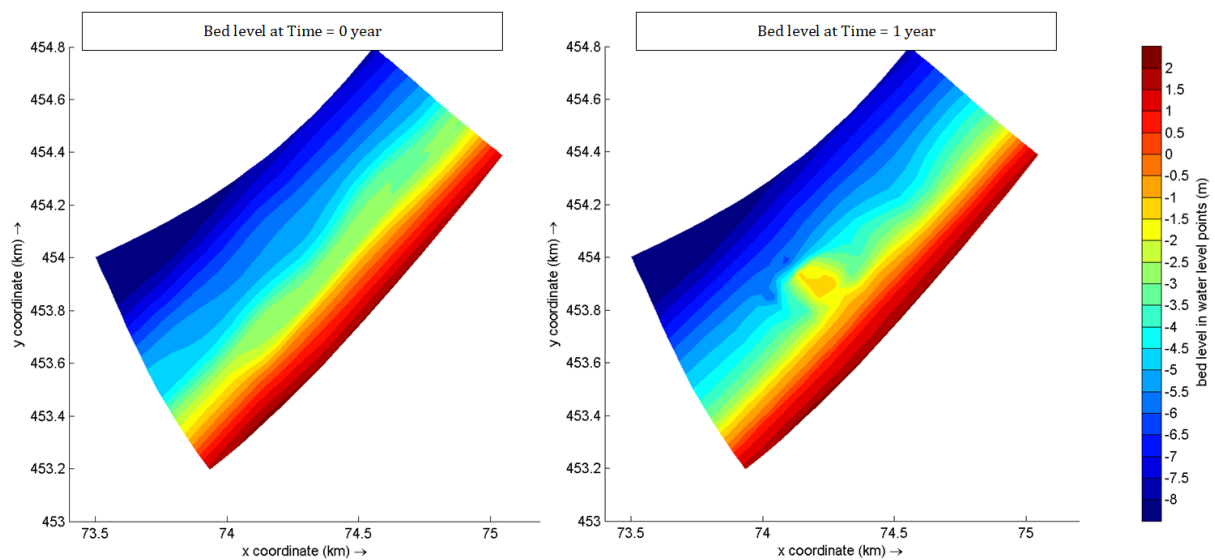


Figure 93 Bed level at $T = 0$ and $T = 1$ year. The nourishment develops as a circular-shaped island. The beach is extending near the nourishment, which can develop as a tombolo (a sand bar connecting the nourishment and the shoreline).

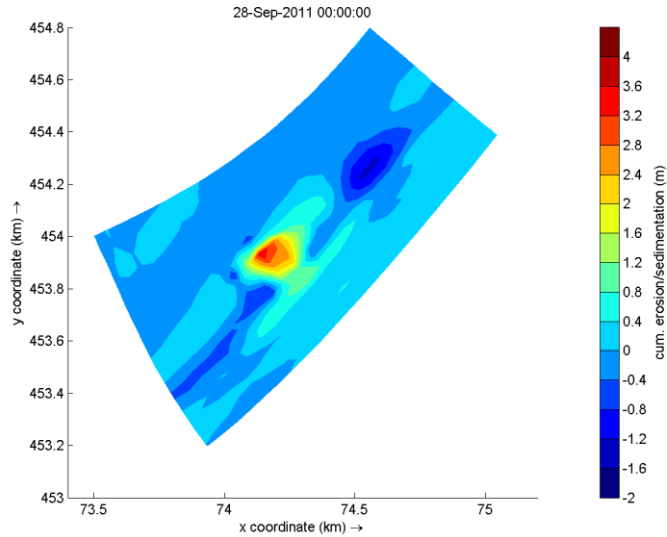


Figure 94 Cumulative erosion (blue) and sedimentation (red) after 1 year. Around the nourishment, accretion occurs. Just upstream of the nourishment, erosion is present, caused by increased energy dissipation of waves due to a sudden decrease of depth. Northeast of the nourishment a large erosion spot is noticed.

F.1.3 Mean total transport development

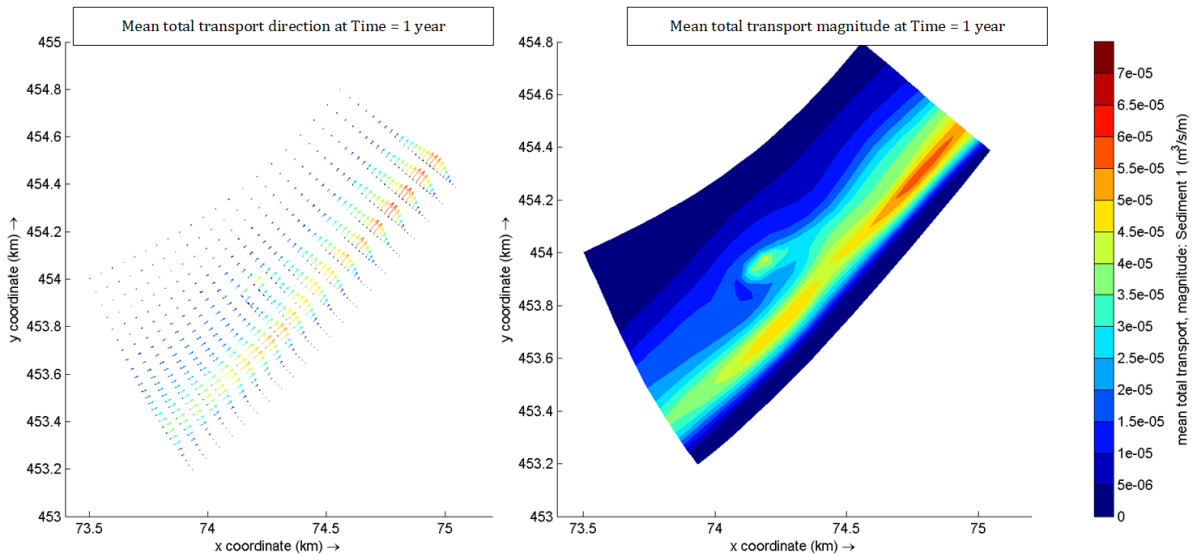


Figure 95 Mean total transport direction, split in alongshore and cross-shore vectors, and the magnitude, after 1 year. The transport magnitude has increased downstream from the nourishment location, as a result of the increased available volume of sediment.

F.1 Nourishment at MSL -5.0 m – Summary

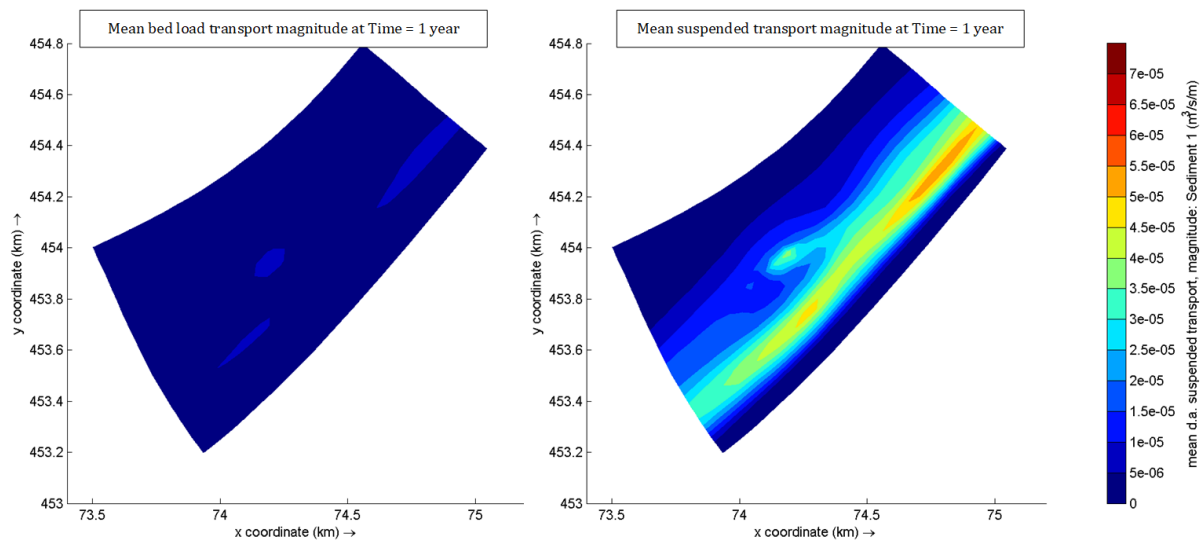


Figure 96 Mean depth-averaged suspended sediment transport (left) and mean bed load sediment transport (right). The suspended transport component is significantly larger in the zone of strong transport and counts for almost 80% in the strong transport zone.

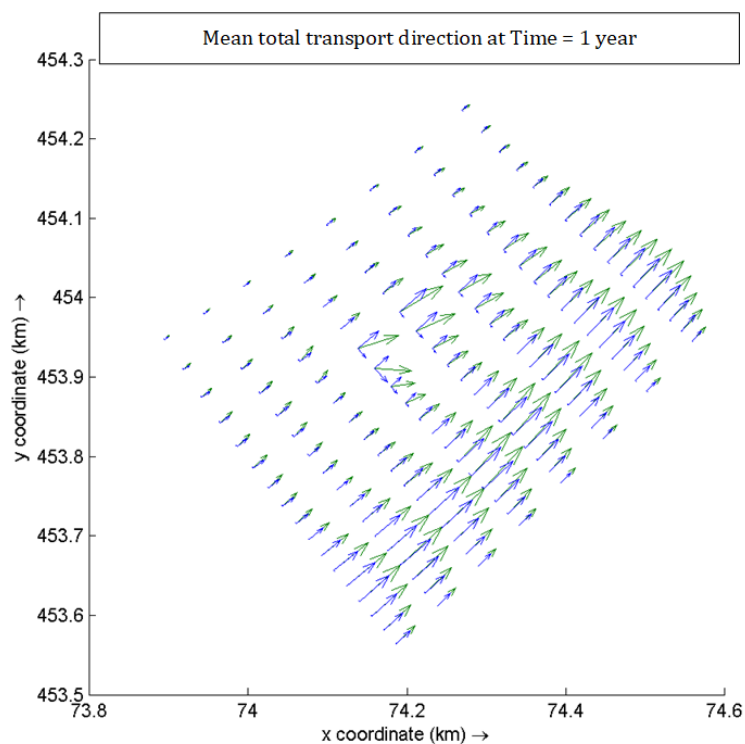
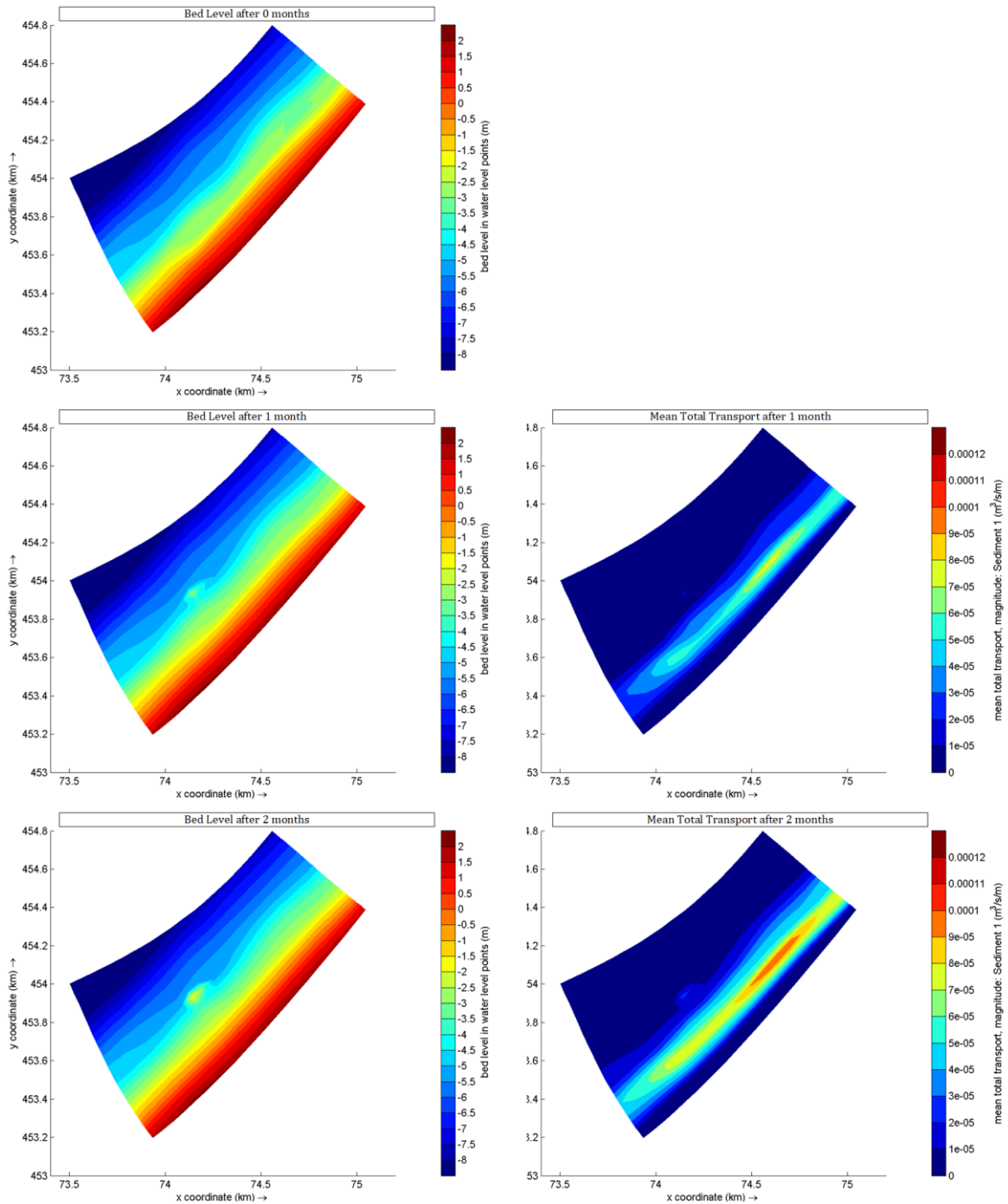


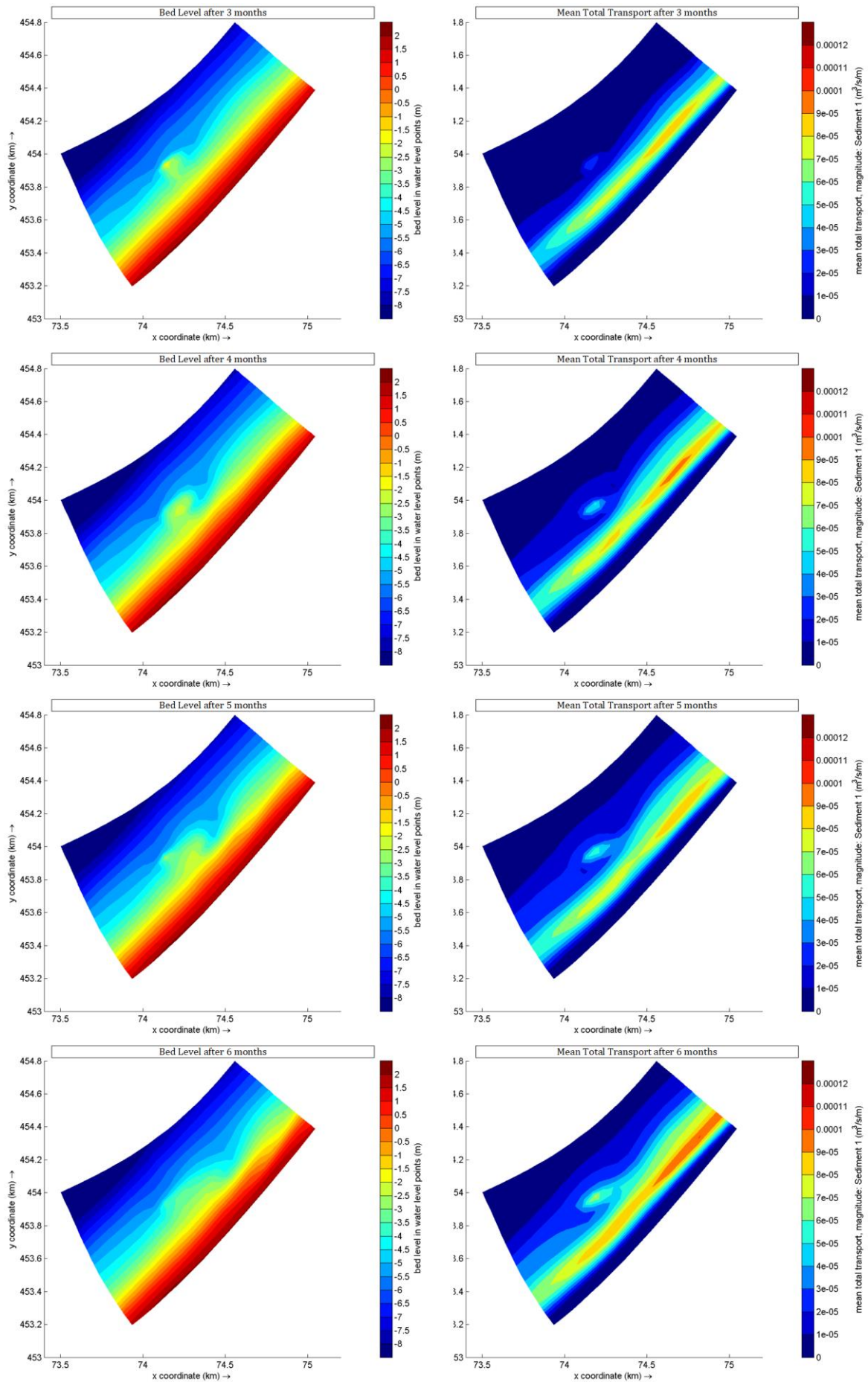
Figure 97 Direction of the mean total transport (green) and the alongshore component of the transport (blue). Near the nourishment, the cross-shore component increases relative to the alongshore component. This has no effect on the transport direction further downstream.

F.2 Nourishment at MSL -5.0 m – Monthly development

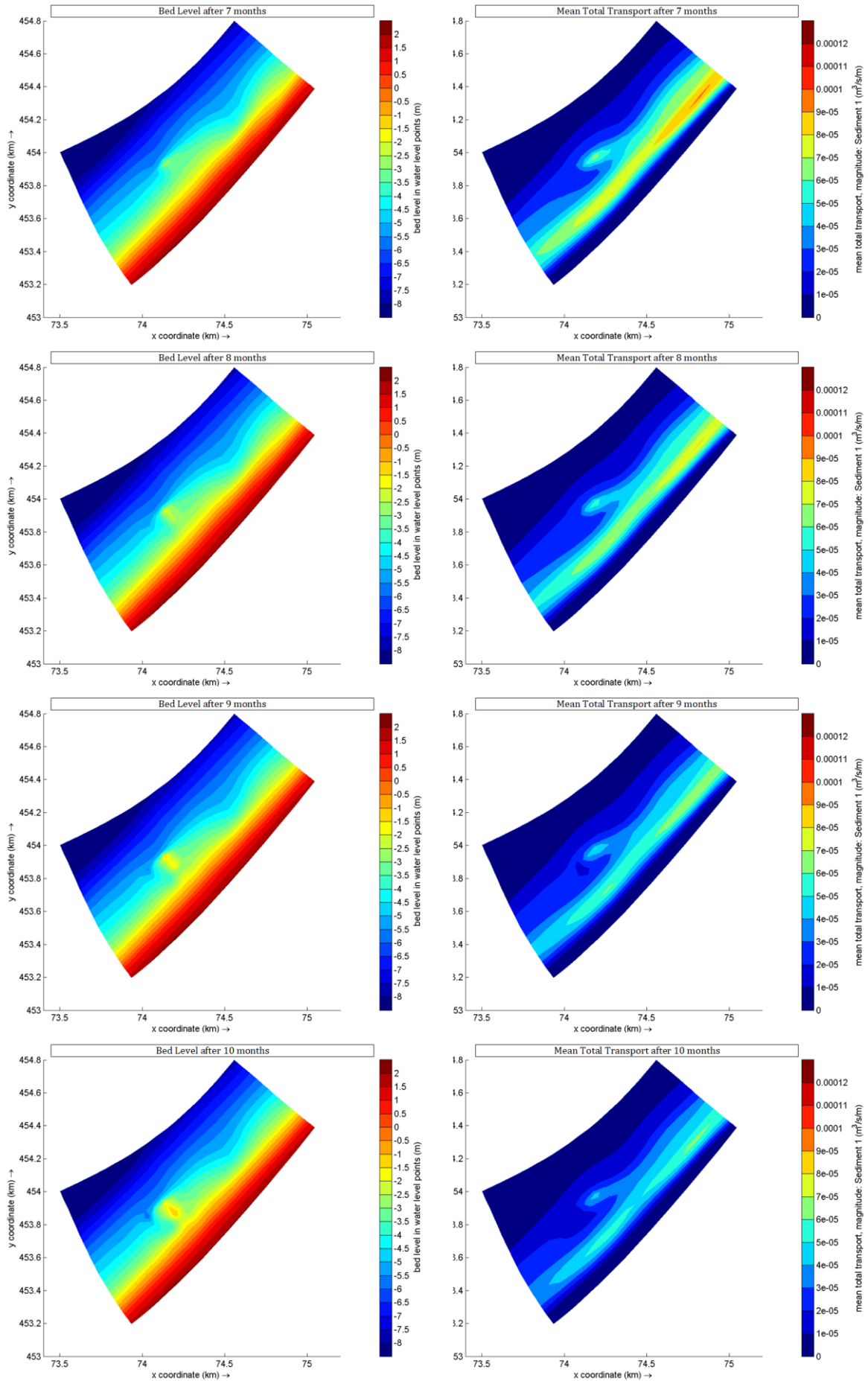
Figure 98 Temporal development of Bed level and Mean Total Transport, for the situation at MSL -5.0 m, visualized for each month for the first year.



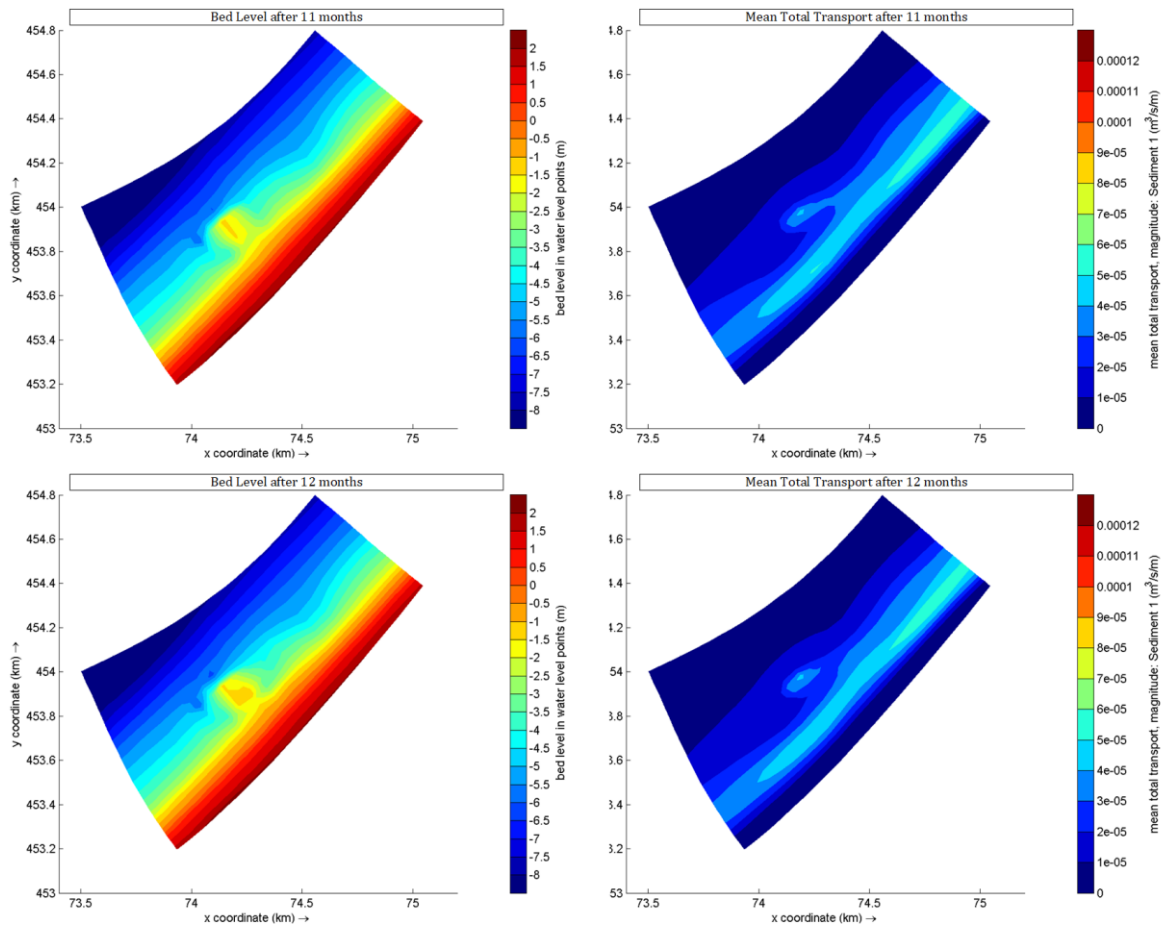
F.2 Nourishment at MSL -5.0 m – Monthly development



F.2 Nourishment at MSL -5.0 m – Monthly development



F.2 Nourishment at MSL -5.0 m – Monthly development



G.1 Nourishment at MSL -6.0 m – Summary

The input settings are given, as well as spatial development of bed level and erosion/sedimentation, and mean total transport.

G.1.1 Input settings

Table 13 Input settings for nourishment at MSL -6.0 m

Depth	6 m
Cell coordinates [M,N]	M,N = 119, 36
Annual volume	100'000 m ³ /year
Discharge input	Flow: Q = 0.02071 m ³ /s Concentration: C = 530 kg/m ³
Simulation time	1 year

G.1.2 Bed level development

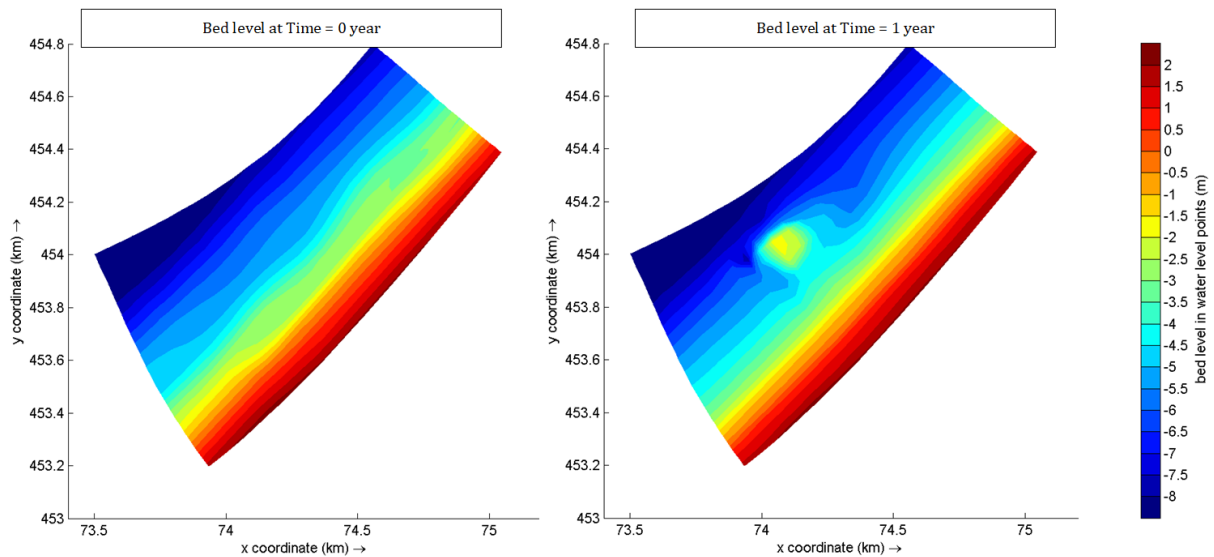


Figure 99 Bed level at $T = 0$ and $T = 1$ year. The nourishment is a circular-shaped submerged island in deeper water. The depth contours curve around the nourishment. Between the nourishment and the shoreline, the depth is fairly uniform to the reference situation.

G.1 Nourishment at MSL -6.0 m – Summary

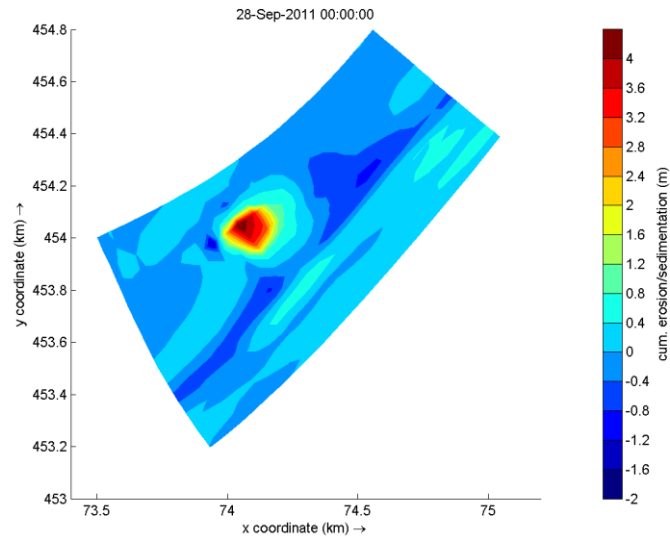


Figure 100 Cumulative erosion (blue) and sedimentation (red) after 1 year. Around the nourishment, accretion occurs. Between the nourishment and the shoreline, small erosion and accretion occurs in the order of decimeters. Northeast of the nourishment, significant erosion occurs as a result of increased sediment transport to the northeast.

G.1.3 Mean total transport development

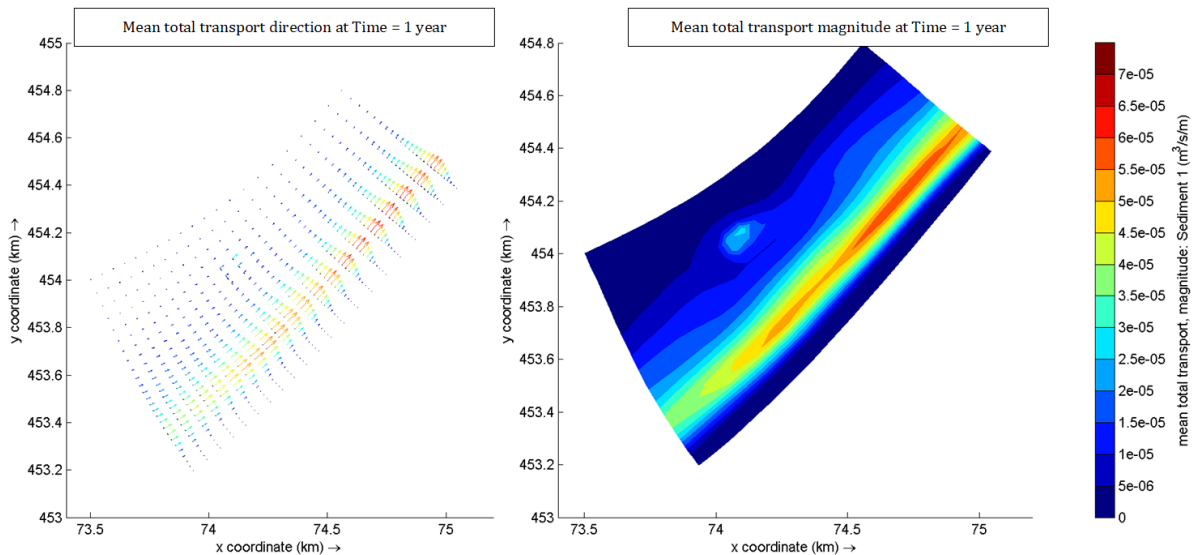


Figure 101 Mean total transport direction, split in alongshore and cross-shore vectors, and the magnitude, after 1 year. The transport zone between MSL -1.0 m and MSL -4.0 m is hardly affected by the nourishment. A small transport magnitude is found near the nourishment.

G.1 Nourishment at MSL -6.0 m – Summary

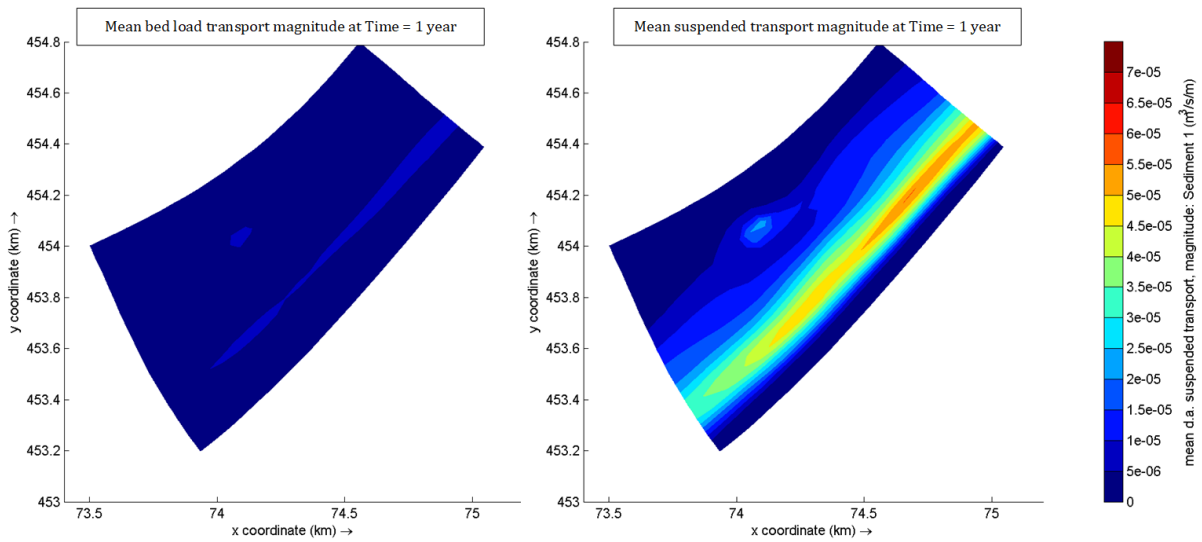


Figure 102 Mean depth-averaged suspended sediment transport (left) and mean bed load sediment transport (right). The relation of the maximum values of transport is similar to the reference situation.

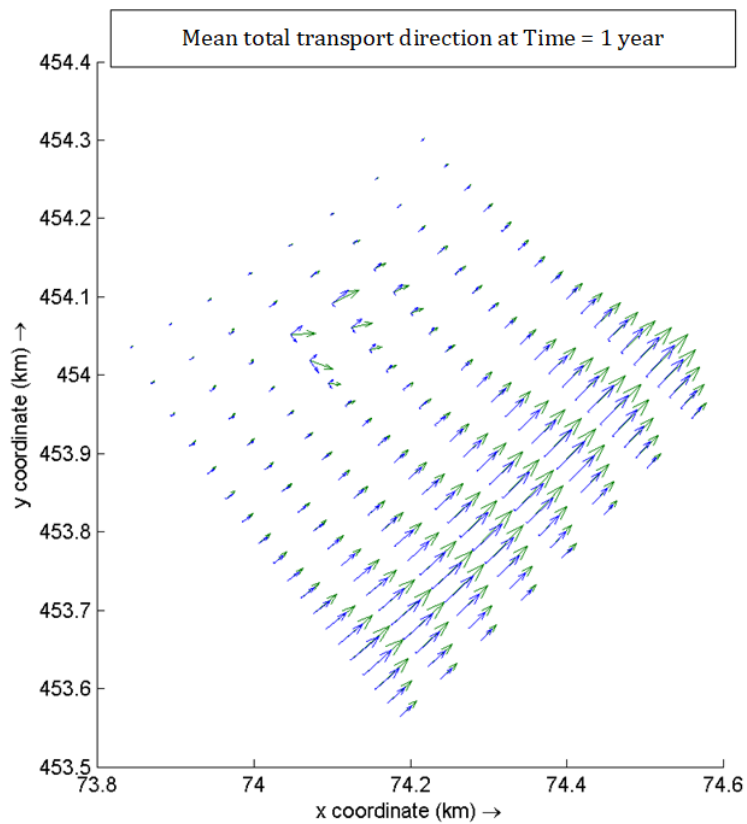
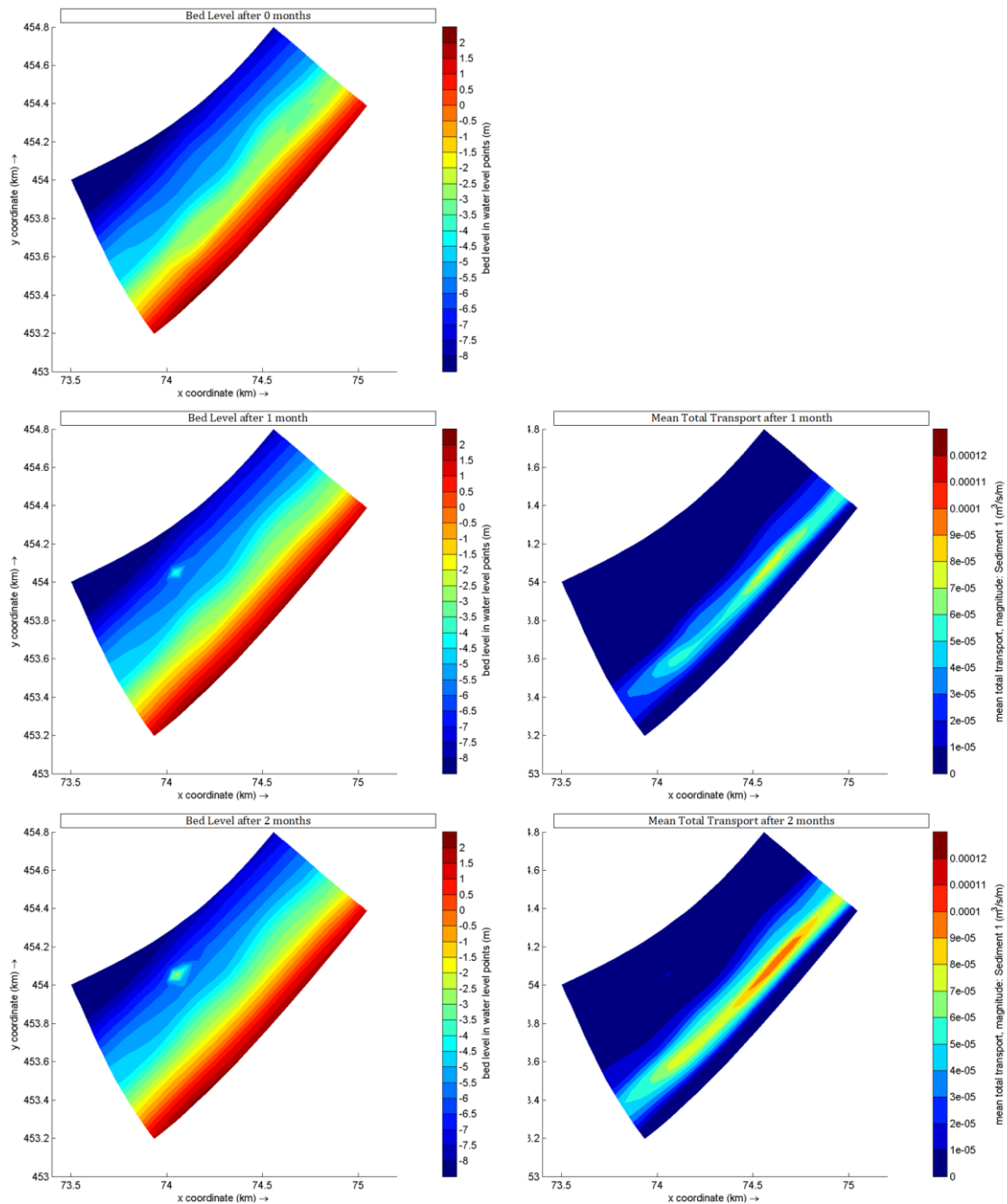


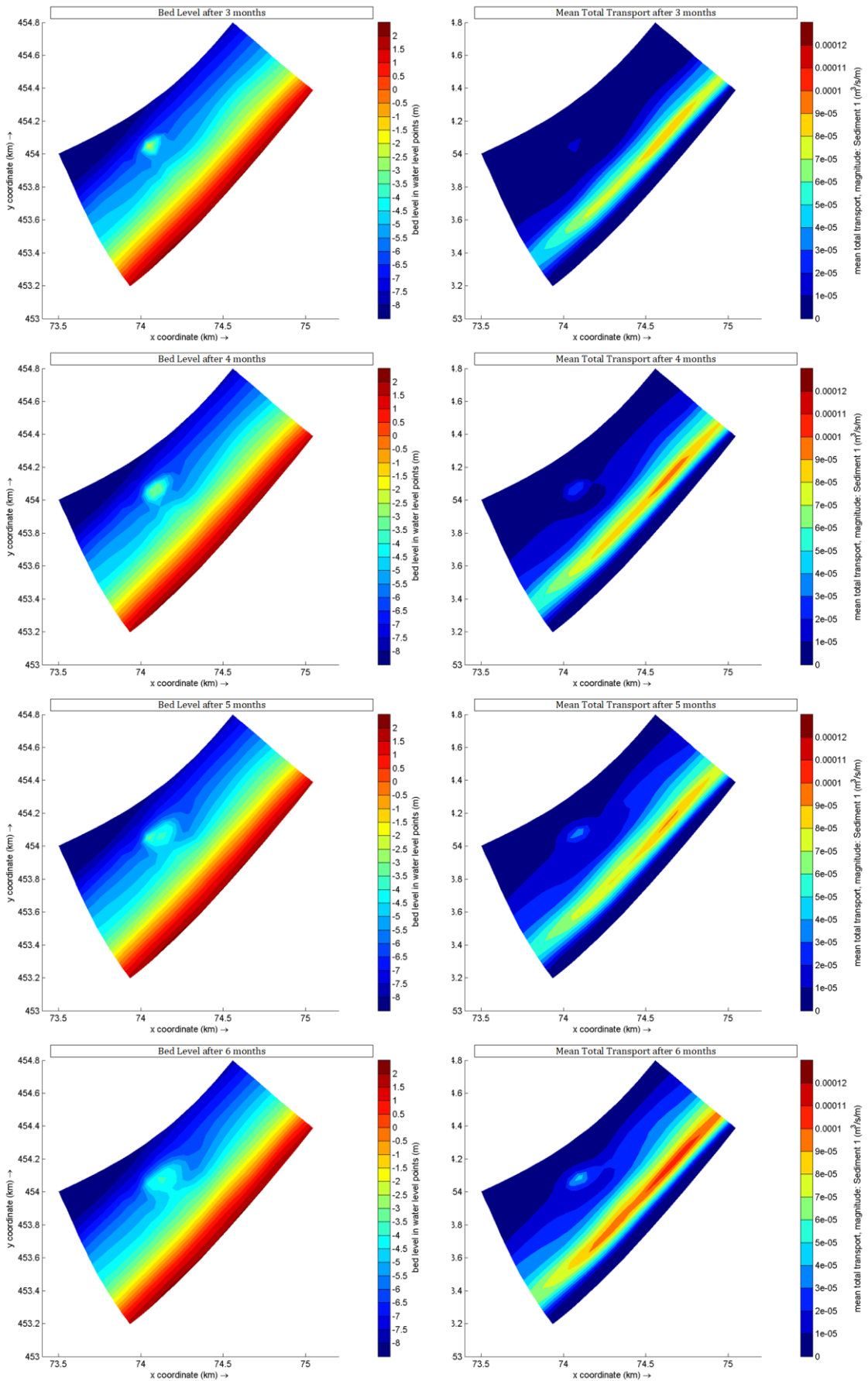
Figure 103 Direction of the mean total transport (green) and the alongshore component of the transport (blue). Also from this figure can be derived that the transport magnitude and direction from the nourishment hardly affects the transport zone between MSL -1.0 m and MSL -4.0 m.

G.2 Nourishment at MSL -6.0 m – Monthly development

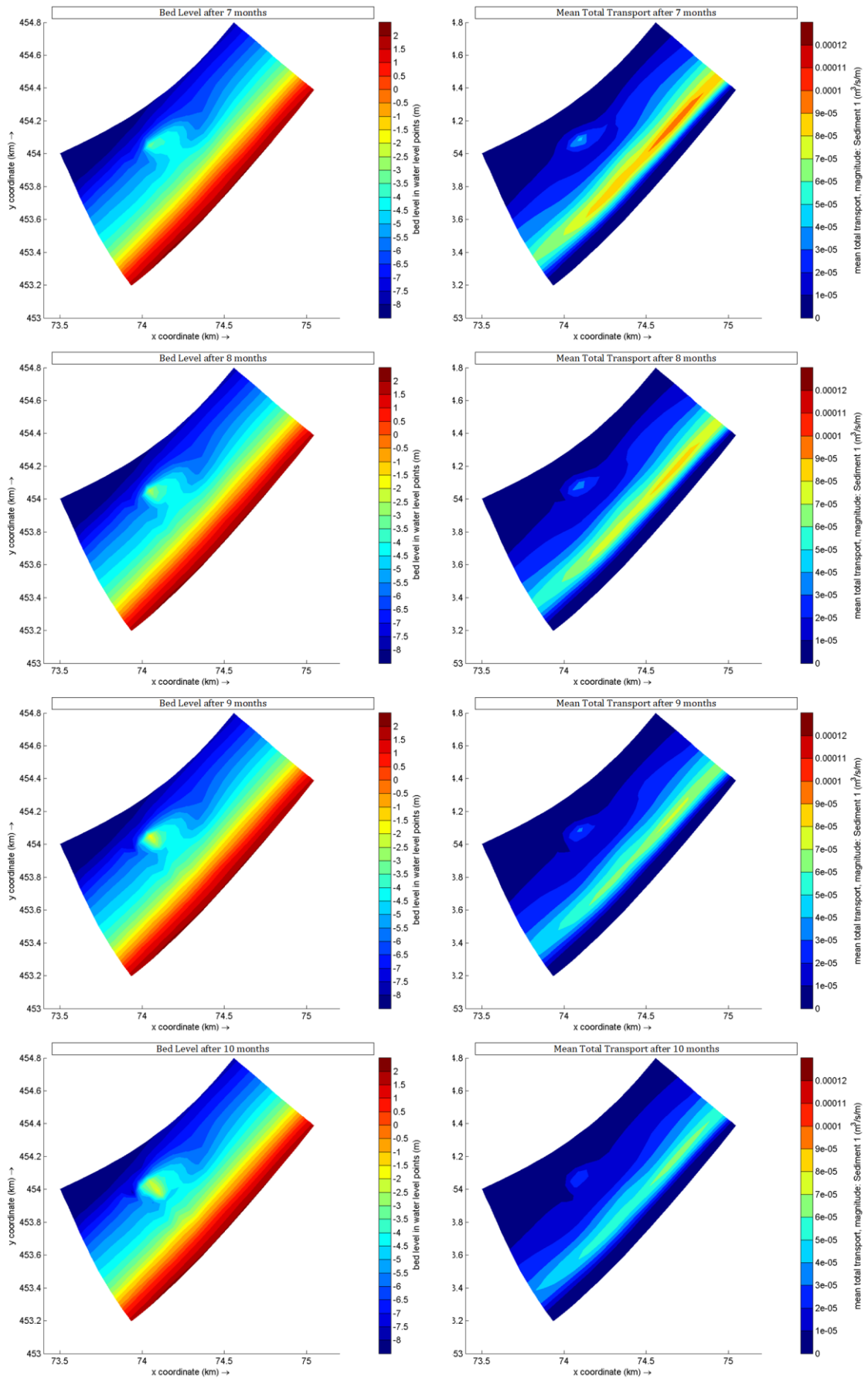
Figure 104 Temporal development of Bed level and Mean Total Transport, for the situation at MSL -6.0 m, visualized for each month for the first year.



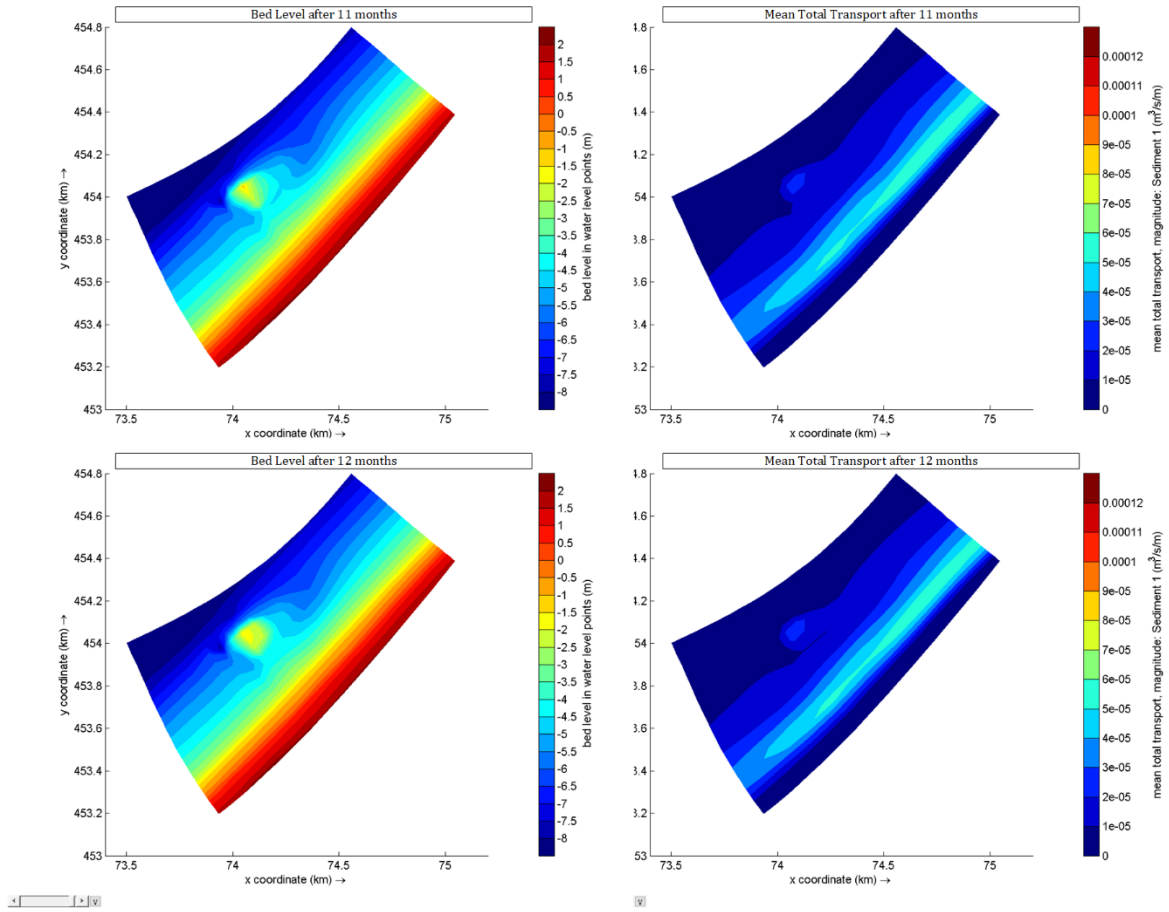
G.2 Nourishment at MSL -6.0 m – Monthly development



G.2 Nourishment at MSL -6.0 m – Monthly development



G.2 Nourishment at MSL -6.0 m – Monthly development



H.1 Discharge of 150'000 m³/year – Summary

The input settings are given, as well as spatial development of bed level and erosion/sedimentation, and mean total transport.

H.1.1 Input settings

Table 14 Input settings for discharge of 150'000 m³/year

Depth	3 m
Cell coordinates [M,N]	M,N = 119, 28
Annual volume	150'000 m ³ /year
Discharge input	Flow: Q = 0.031065 m ³ /s Concentration: C = 530 kg/m ³
Simulation time	1 year

H.1.2 Bed level development

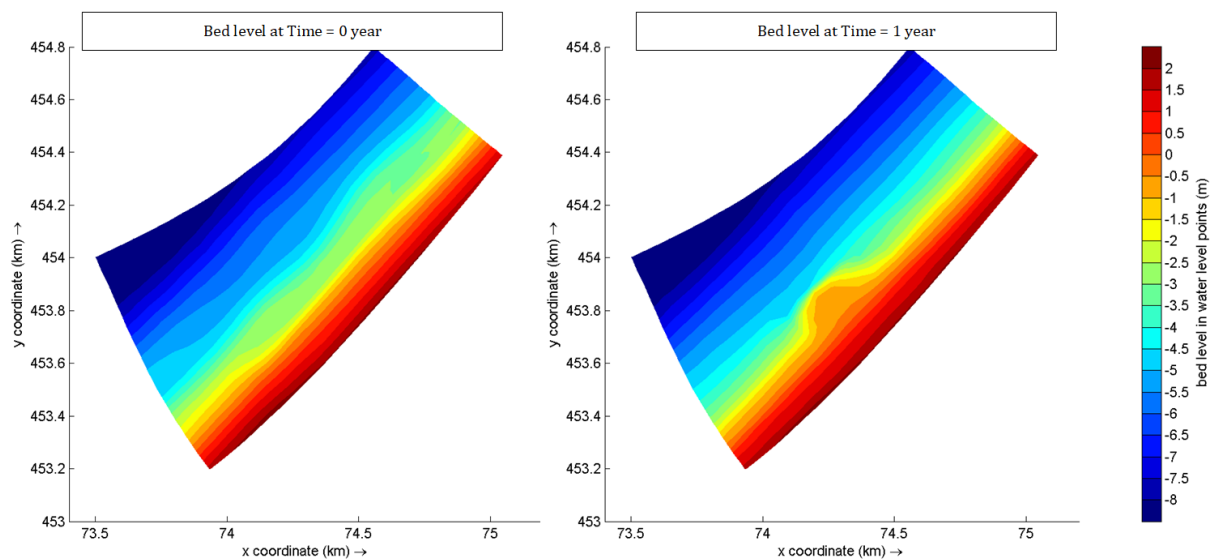


Figure 105 Bed level at T = 0 and T = 1 year. The nourishment develops as a bell-shaped beach extension and mainly spreads in alongshore direction. The nourishment almost reaches the mean water level.

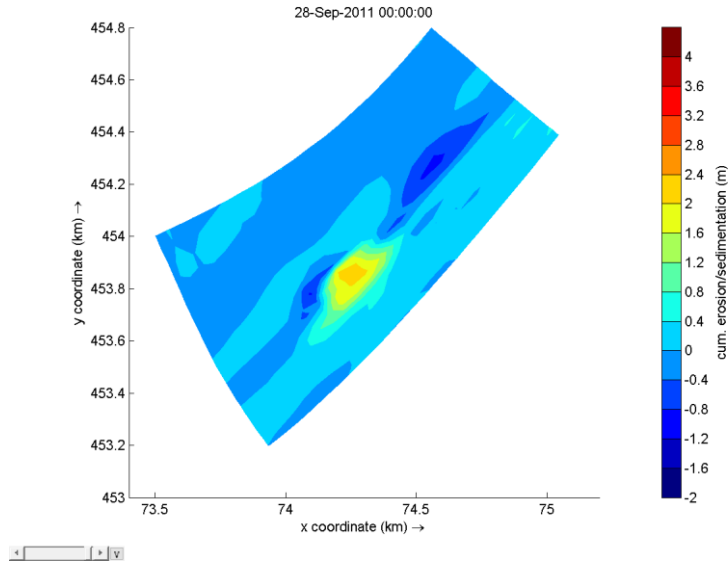


Figure 106 Cumulative erosion (blue) and sedimentation (red) after 1 year. Around the nourishment, accretion occurs. Just upstream of the nourishment, erosion is present, caused by increased energy dissipation of waves due to a sudden decrease of depth. A small plume towards the southwest is developing due to (partial) blockage of sediment in the transport zone.

H.1.3 Mean total transport development

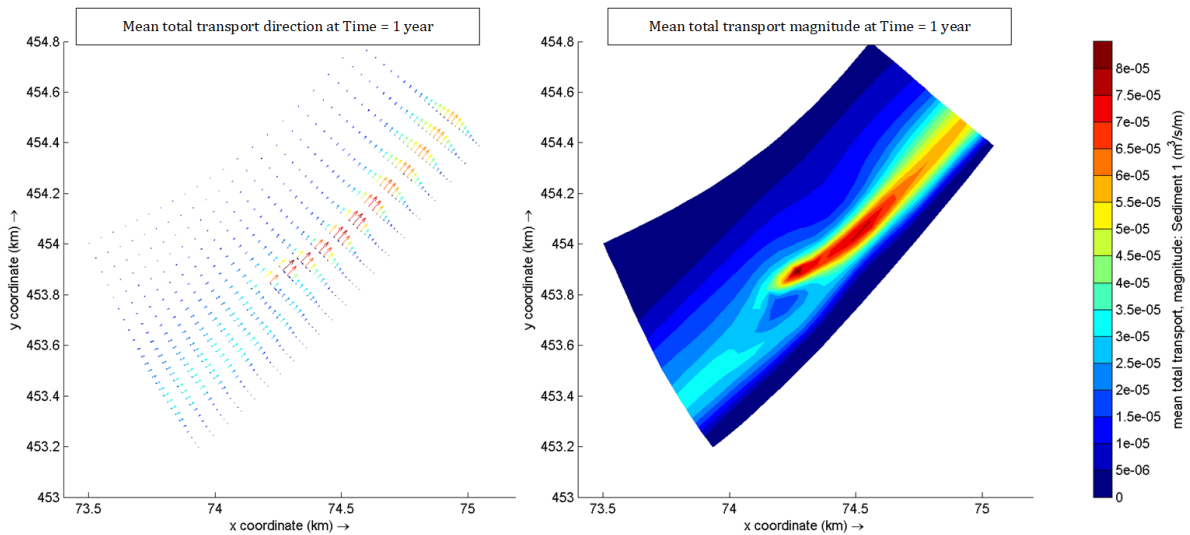


Figure 107 Mean total transport direction, split in alongshore and cross-shore vectors, and the magnitude, after 1 year. The transport magnitude has increased downstream from the nourishment location, as a result of the increased available volume of sediment.

H.1 Discharge of 150'000 m³/year – Summary

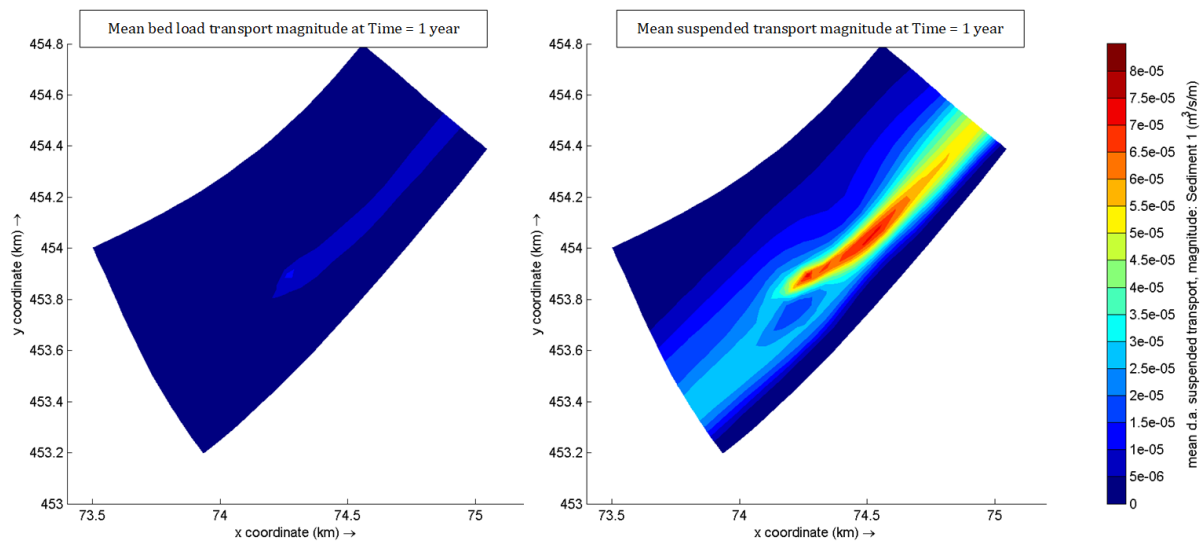


Figure 108 Mean depth-averaged suspended sediment transport (left) and mean bed load sediment transport (right). The suspended transport component is significantly larger in the zone of strong transport and counts for almost 90% in the strong transport zone.

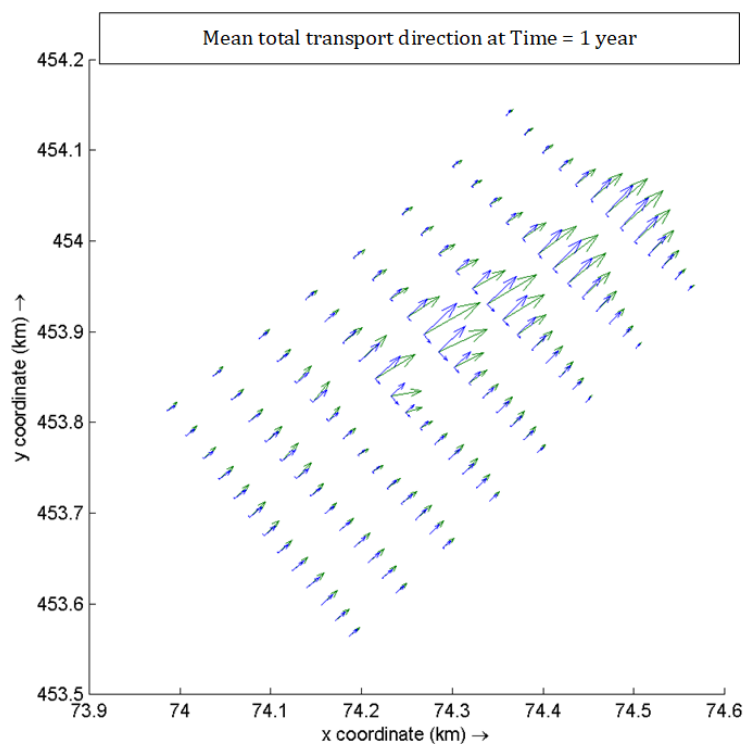
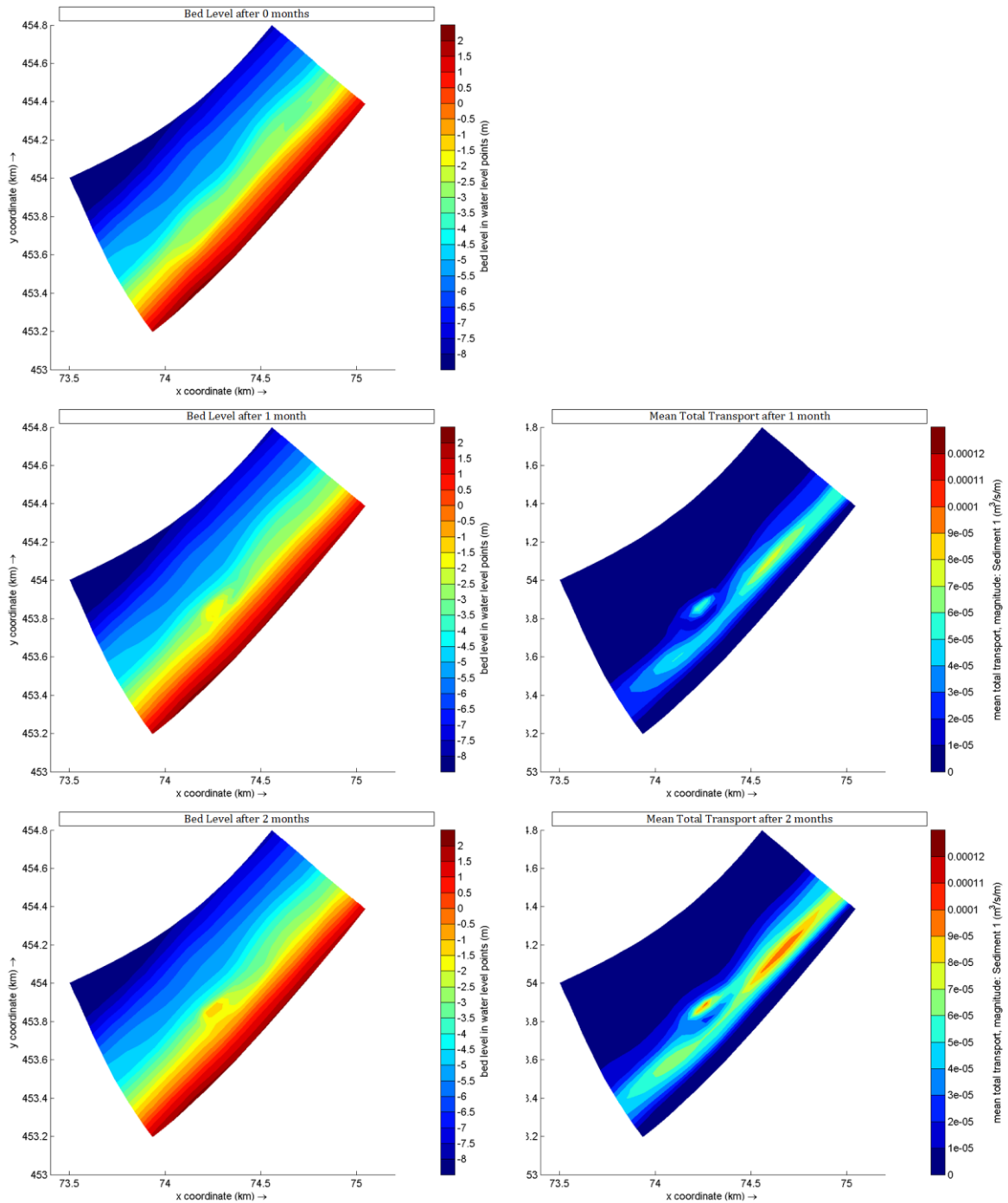


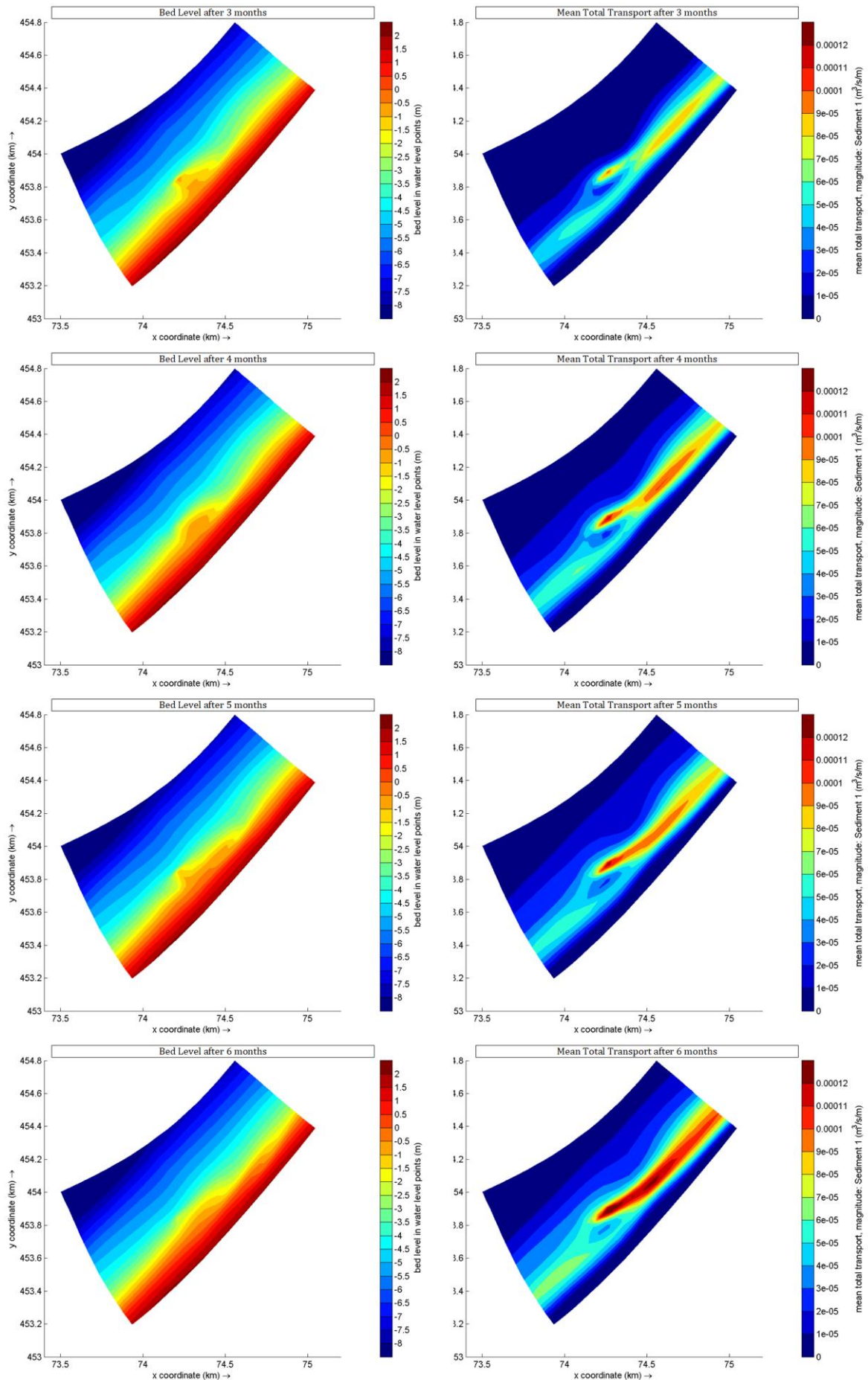
Figure 109 Direction of the mean total transport (green) and the alongshore component of the transport (blue). Near the nourishment, the cross-shore component increases relative to the alongshore component.

H.2 Discharge of 150'000 m³/year – Monthly development

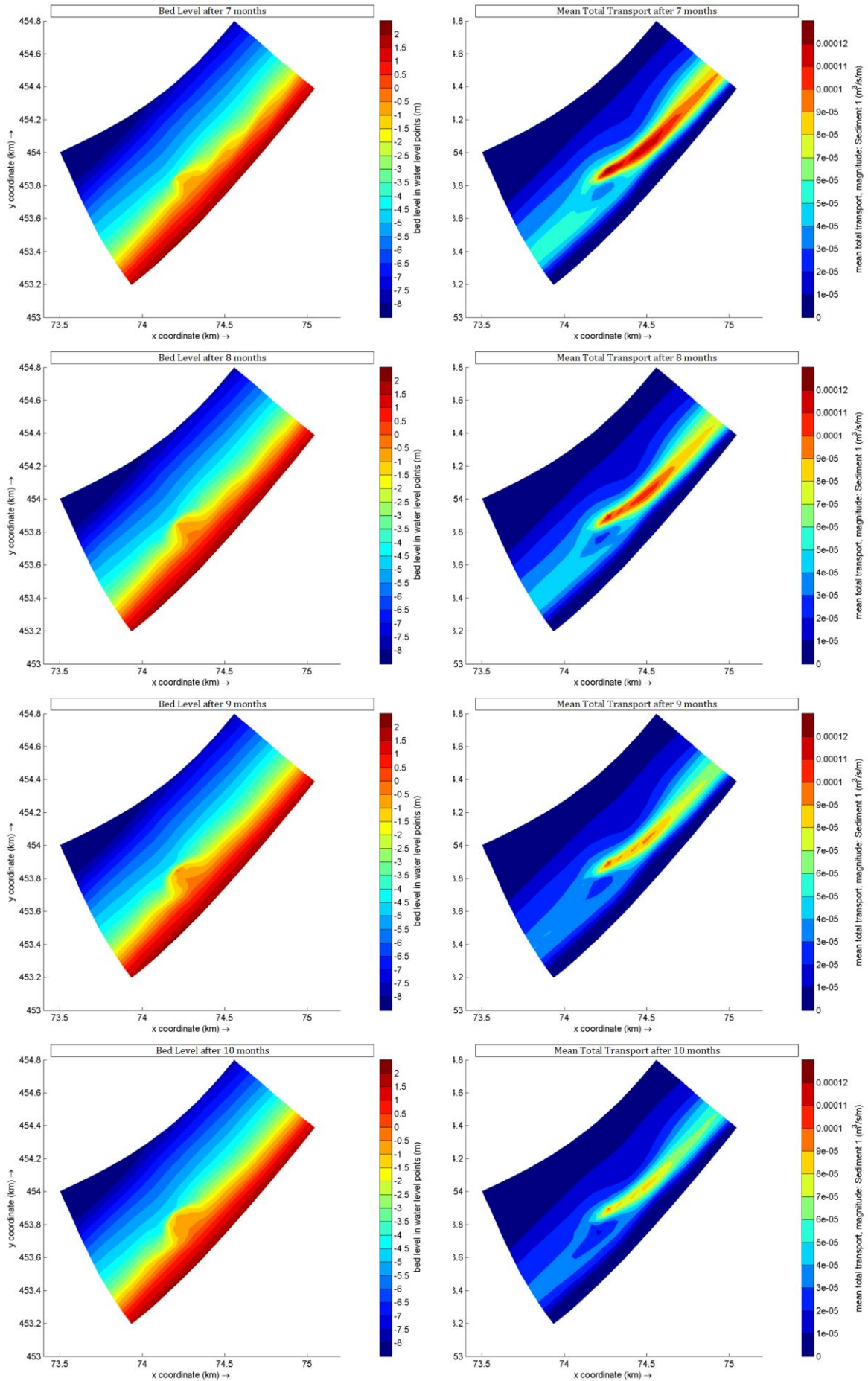
Figure 110 Temporal development of Bed level and Mean Total Transport, for the situation with an increased annual volume, visualized for each month for the first year.



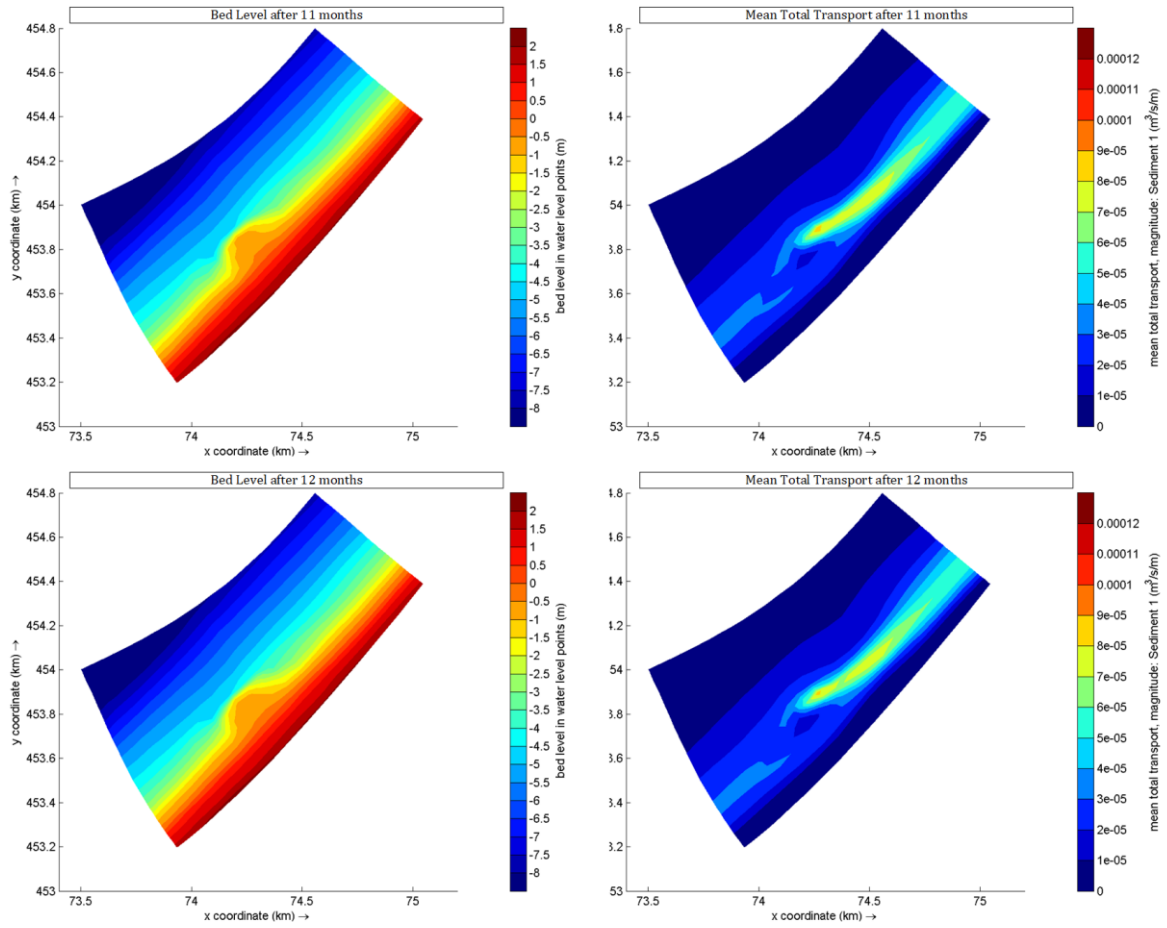
H.2 Discharge of 150'000 m³/year – Monthly development



H.2 Discharge of 150'000 m³/year – Monthly development



H.2 Discharge of 150'000 m³/year – Monthly development



I.1 Spread of nourishment over 5 locations – Summary

The input settings are given, as well as spatial development of bed level and erosion/sedimentation, and mean total transport.

I.1.1 Input settings

Table 15 Input settings for spread of nourishment over 5 locations

Depth	5 m
Cell coordinates [M,N]	M, N = 119, 31 M, N = 119, 32 M, N = 119, 33 M, N = 118, 32 M, N = 120, 32
Annual volume	150'000 m ³ /year
Discharge input	Flow: Q = 0,004142 m ³ /s per cell (0.02071 m ³ /s in total) Concentration: C = 530 kg/m ³
Simulation time	1 year

I.1.2 Bed level development

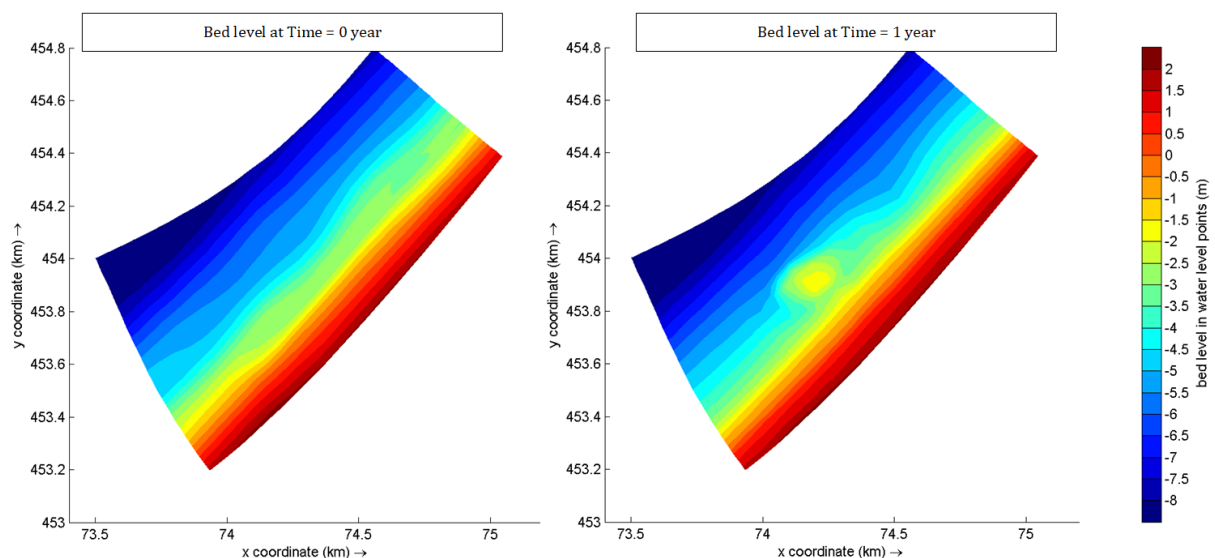


Figure 111 Bed level at T = 0 and T = 1 year. The nourishment is spread over 5 locations, which makes the nourishment more gradual in the domain. The maximum height is much less. Its alongshore spread is similar to the single-location-nourishment.

I.1 Spread of nourishment over 5 locations – Summary

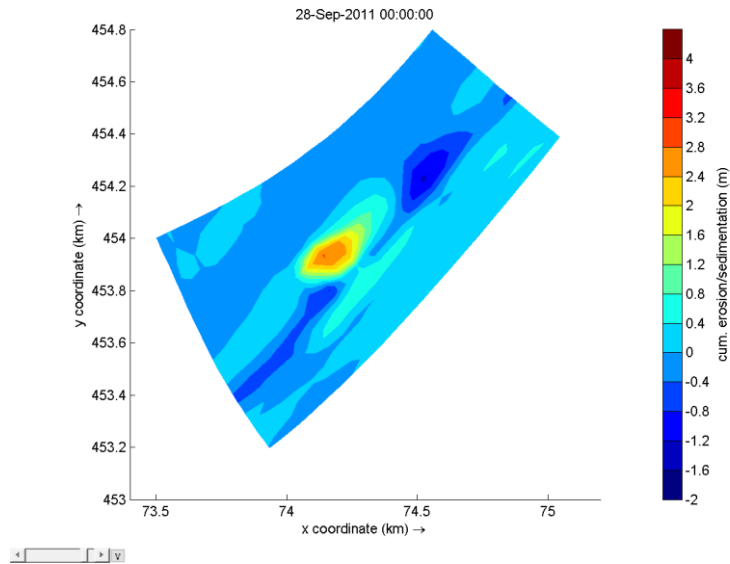


Figure 112 Cumulative erosion (blue) and sedimentation (red) after 1 year. Sedimentation is visible northeast of the nourishment. The spread of sediment in this direction is stimulated by the supply of sediment over multiple locations.

I.1.3 Mean total transport development

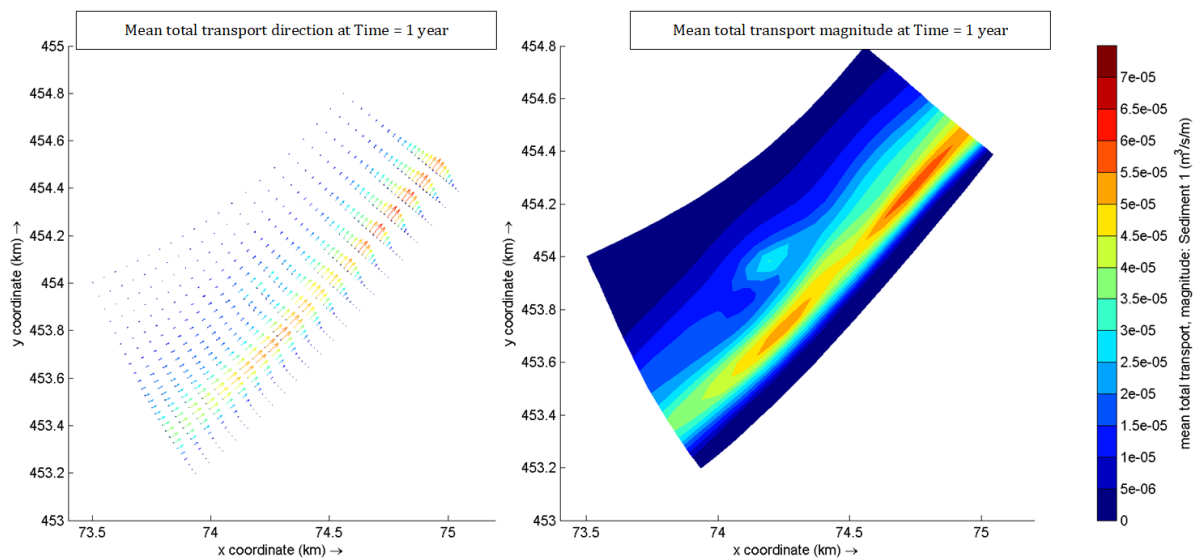


Figure 113 Mean total transport direction, split in alongshore and cross-shore vectors, and the magnitude, after 1 year. The transport magnitude from the nourishment is small compared to the single-location-nourishment. This is mainly due to the spread of sediment over multiple locations. Per cell, less sediment is available for transport.

I.1 Spread of nourishment over 5 locations – Summary

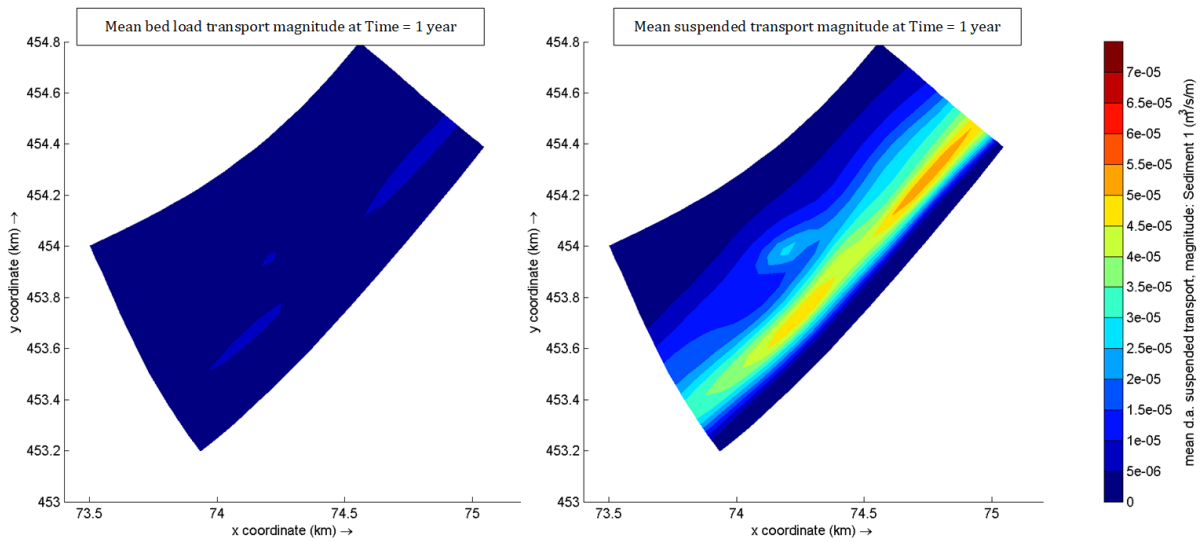


Figure 114 Mean depth-averaged suspended sediment transport (left) and mean bed load sediment transport (right). The suspended transport component is significantly larger in the zone of strong transport and counts for almost 90% in the strong transport zone.

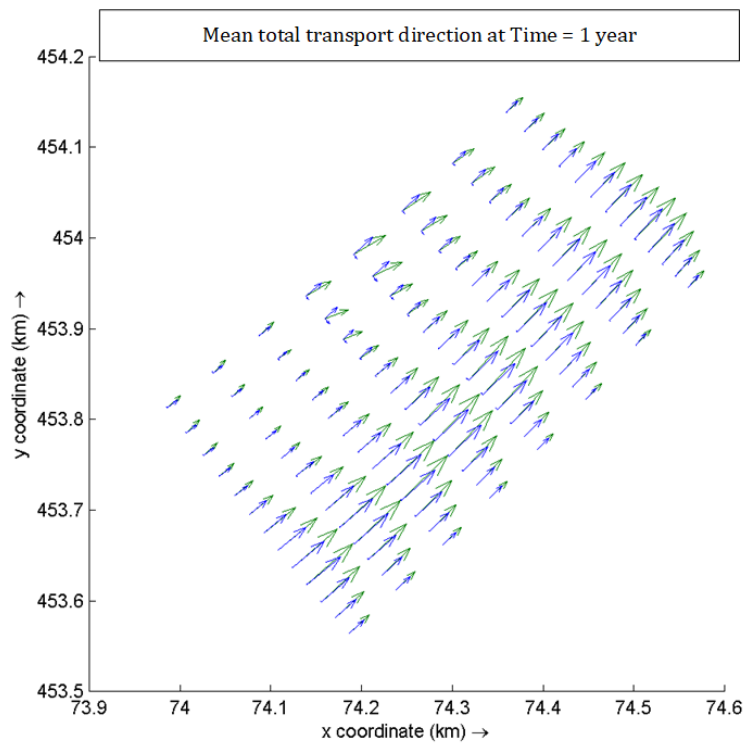
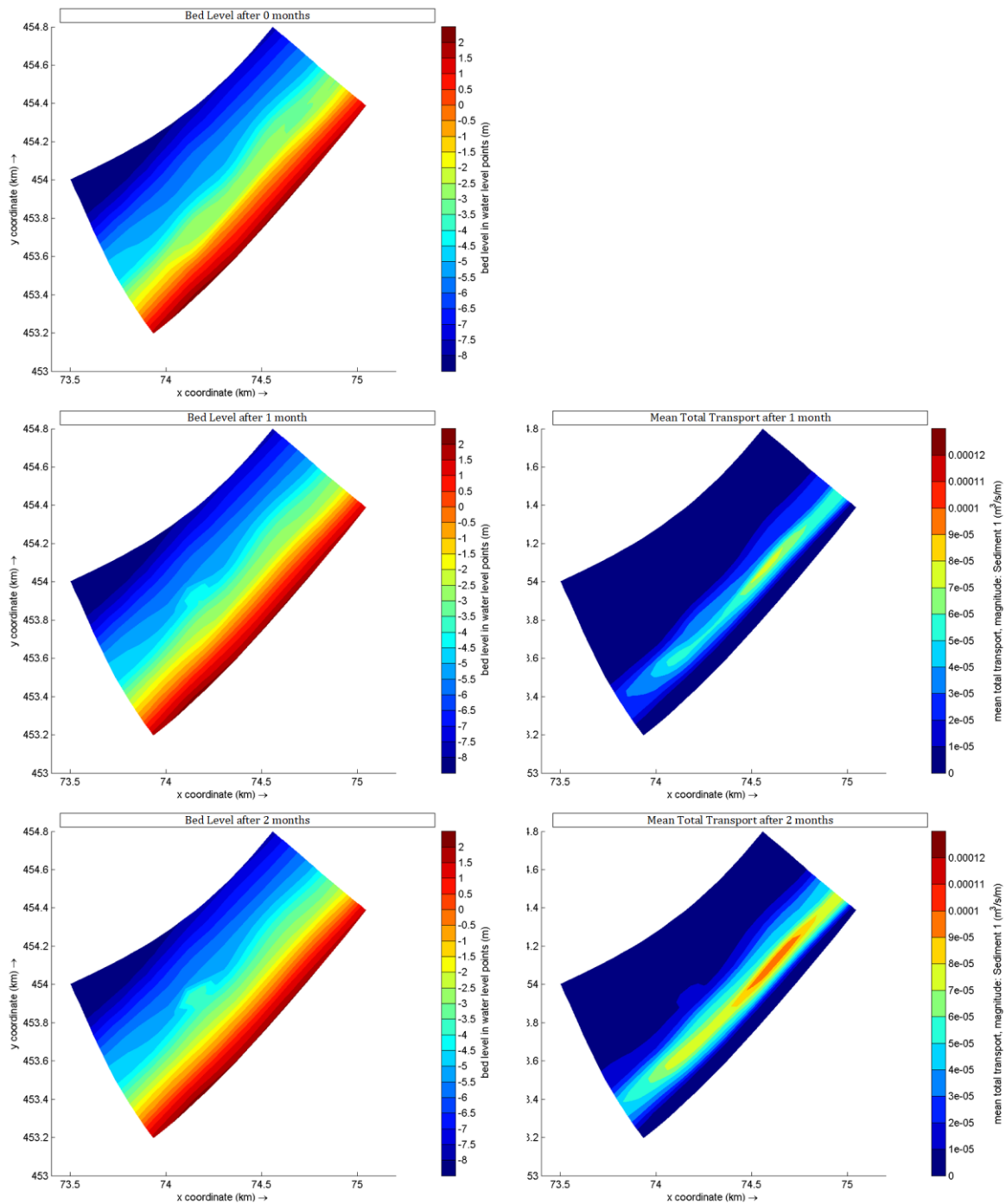


Figure 115 Direction of the mean total transport (green) and the alongshore component of the transport (blue). Near the nourishment, the cross-shore component increases relative to the alongshore component. The effect on the transport zone is not significantly large.

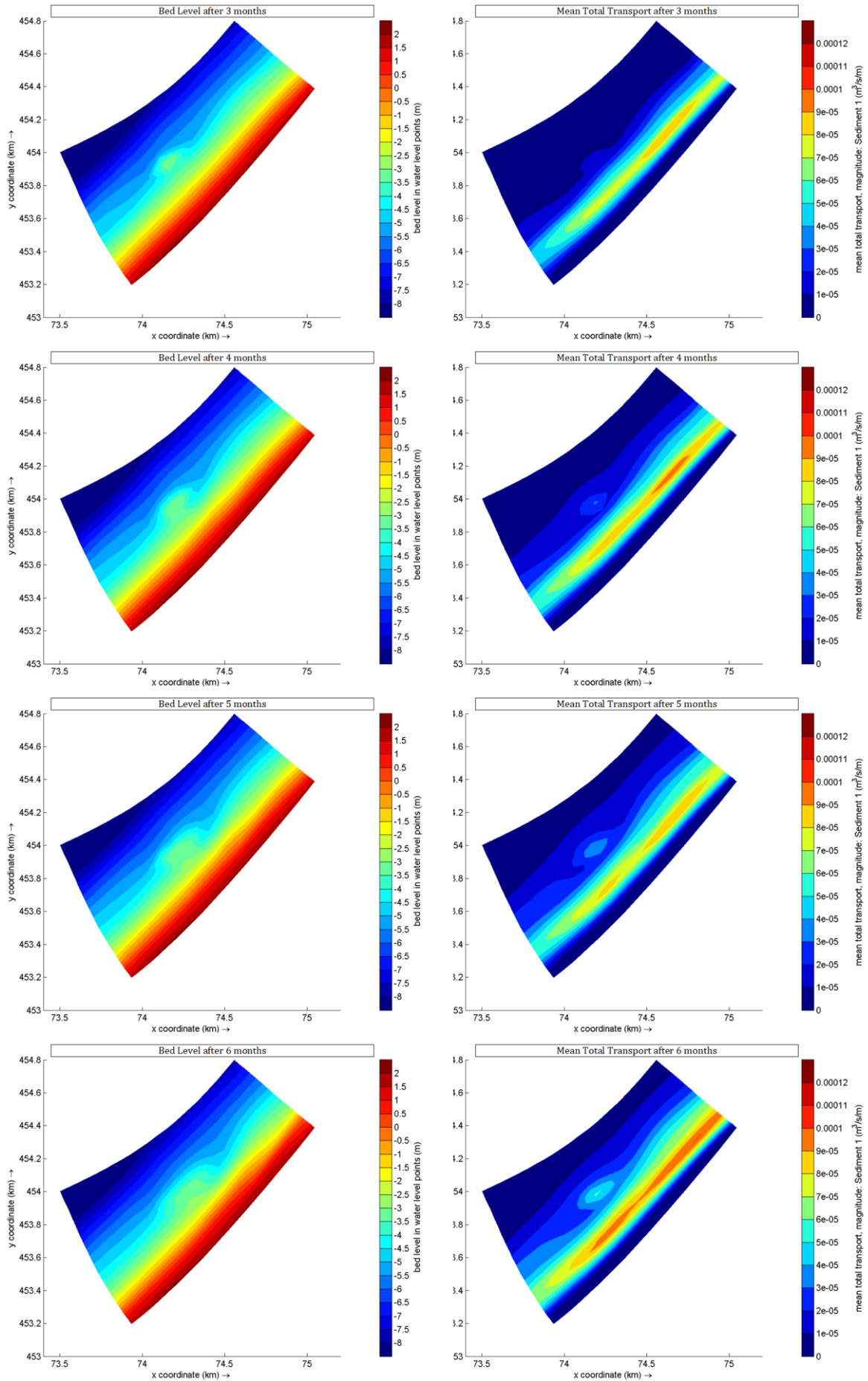
I.2 Spread of nourishment over 5 locations – Monthly development

I.2 Spread of nourishment over 5 locations – Monthly development

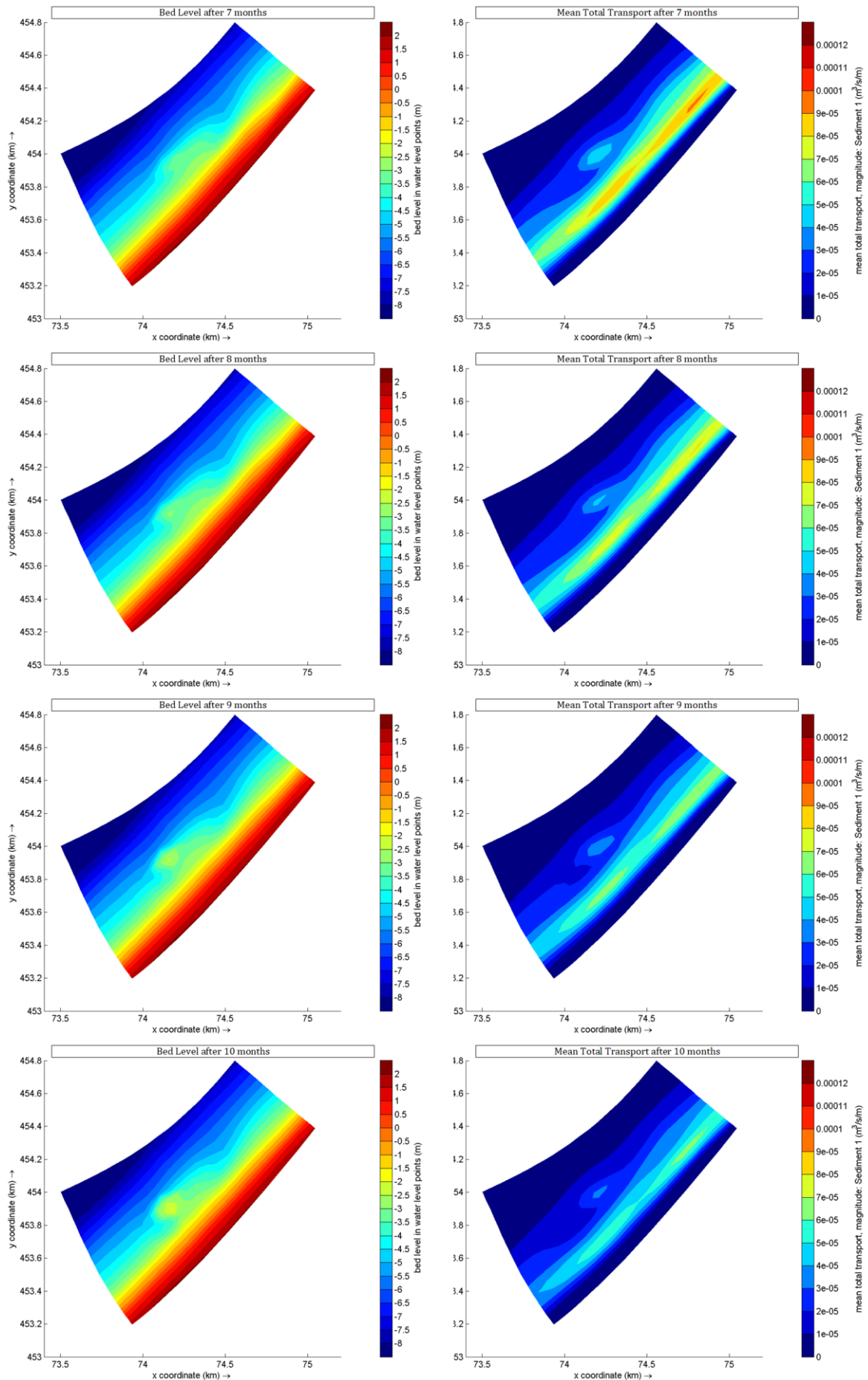
Figure 116 Temporal development of Bed level and Mean Total Transport, for the situation with an increased nourishment area, visualized for each month for the first year.



I.2 Spread of nourishment over 5 locations – Monthly development



1.2 Spread of nourishment over 5 locations – Monthly development



I.2 Spread of nourishment over 5 locations – Monthly development

